Asociación Argentina de Astronomía
Third La Plata International School on Astronomy and Geophysics:
Chaos, diffusion and non–integrability in Hamiltonian Systems
Applications to Astronomy , 2012
P. M. Cincotta, C. M. Giordano & C. Efthymiopoulos, eds.

LECTURE

Canonical perturbation theory, stability and diffusion in Hamiltonian systems: applications in dynamical astronomy

C. Efthymiopoulos[1]

(1) Research Center for Astronomy and Applied Mathematics, Academy of Athens

Abstract. We present some basic methods and techniques of canonical perturbation theory, as well as some of its applications in problems of stability and/or diffusion in dynamical astronomy. The methods presented are: i) the Birkhoff normal form, ii) the Kolmogorov normal form, iii) the resonant normal form, and iv) the hyperbolic normal form used in the computation of invariant manifolds of unstable periodic orbits in the chaotic regime. For each method we give concrete examples presented in some detail in order to facilitate study. In particular, we discuss a step by step implementation of a so-called 'book-keeping' algorithm by which all quantities (i.e. Hamiltonian, generating functions etc.) can be split in groups of terms of similar order of smallness. We explain why the book-keeping schemes presently suggested are particularly suitable in computer-algebraic implementations of normal forms. Also, for each method we explain the pattern by which small divisors are accumulated in the series terms at successive normalization steps, outlining why such accumulation leads to a divergent normalization process in the case of the Birkhoff normal form (both non-resonant or resonant), while it leads to a convergent normalization process in the case of the Kolmogorov normal form or the hyperbolic normal form. After these formal aspects, we present applications of canonical perturbation theory in concrete Hamiltonian dynamical systems appearing in problems of dynamical astronomy. In particular, we explain how resonant normal form theory is connected to the phenomenon of Arnold diffusion, as well as to estimates of the diffusion rate in the action space in systems of three (or more) degrees of freedom. We discuss how is 'book-keeping' implemented in paradigmatic cases, like the treatment of mean motion resonances in solar system dynamics, and the study of orbits in axisymmetric galaxies or in barred-spiral rotating galaxies. Finally, we give an example of implementation of normal form theory in the orbital version of the so-called 'density wave theory' of spiral arms in galaxies.

CONTENTS

1. INTRODUCTION

This is a set of lecture notes on methods and techniques of *canonical perturbation theory*, as well as on the latter's applications in the study of *diffusion processes and chaos* in physical systems related to dynamical astronomy.

The text represents, to a considerable extent, an elaborated transcript of the lectures given by the author during the third La Plata school on Astronomy and Geophysics, in July 2011. However, the structure of the text, and in particular, the sequence of presentation of the topics, has been substantially modified with respect to the structure of the lectures. Also, the text has been enriched by a number of additional topics, reference to which was judged necessary for reasons of completeness.

For a more complete study of the subject, the reader cannot but have recourse to excellent existing textbooks in the literature. As an indicative list of references for one or more of the topics treated below we mention: Ozorio de Almeida (1988), Siegel and Moser (1991), Arnold et al. (1993), Bocaletti and Pucacco (1996), Contopoulos (2002), Morbidelli (2002), and Ferraz-Mello (2007). Quite useful are also reviews and sets of lecture notes as, for example: Delshams and Gutiérrez (1996), Morbidelli and Guzzo (1997), Benettin (1999), Giorgilli and Locatelli (1999), Giorgilli (2002), Cincotta (2002), Chierchia (2008), as well as the review articles included in Benest et al. (2008) and (2010).

My own effort, in writing the present notes, has been to abandon a formal style of presentation in favor of an approach that could be helpful *in practice*. The goal is to show how canonical perturbation theory can be implemented, with much profit, in concrete computations referring to the study of stability, and/or diffusion in systems appearing mainly (but not exclusively) in celestial mechanics, and stellar and galactic dynamics. In fact, with the advent of modern computers (and computer-algebraic techniques), in recent years it has become possible to implement canonical perturbation theory at quite high expansion orders. This fact allows one to sustain that the theory's present usefulness renders it competitive to purely numerical methods, provided that one is able to write a program implementing some perturbative technique of interest at high order in the computer. This topic is discussed also by A. Giorgilli and M. Sansottera in the present volume of proceedings.

On the other hand, the introduction of computer-algebraic methods in the computation of normal forms has rendered clear that, in nearly every form of canonical perturbation theory, a computation can proceed in principle by more than one distinct algorithmic approaches. However, it is a fact that only a subset of such approaches prove to be practical and useful in the applications. Furthermore, a presentation of such practical approaches is often absent in literature reviews of the subject. A well known example refers to the so-called splitting of an analytic Hamiltonian function in parts of 'different order of smallness'. One can show (see Giorgilli (2002), pp.90–91) that the most practical splitting is in powers of a quantity $\sim e^{-\sigma}$, where σ is a positive constant characterizing the analyticity domain of the Hamiltonian in the space of angles. For reasons explained in section 3 below, such a splitting is clearly advantageous (and of nearly exclusive interest in practice) with respect to a more traditional splitting in powers of apparently more 'natural' small parameters, as for example the small parameter ϵ in a Hamiltonian of the form $H = H_0 + \epsilon H_1$, where H_0 is

the integrable part. In fact, the preference to a scheme based on powers of $e^{-\sigma}$, which explicitly appears in the works of Poincaré (1892) and Arnold (1963, see also Arnold et al. (1993)), is not so often discussed in modern references to perturbation theory.

In sections 2 and 3 below, we emphasize the practical aspects of normal form computations by introducing a formal procedure, called 'book-keeping'[1], by which we can systemize the most practical approach to such computations. We give specific examples of the book-keeping process in four different normal form methods: i) the non-resonant normal form of Birkhoff, ii) the normal form of Kolmogorov, employed in the proof of the KAM theorem, iii) the resonant (Birkhoff) normal form used in the study of diffusion along resonances, and iv) the hyperbolic normal form of Moser (1958), by which we can compute unstable periodic orbits and their asymptotic manifolds in the chaotic regime.

In each case, we combine the discussion on 'book-keeping' with a discussion of how *small divisors* are accumulated in the series terms at successive normalization orders, the latter being presently defined as successive orders in a suitably defined 'book-keeping parameter'. This discussion allows to demonstrate in a heuristic way how the pattern of accumulation of small divisors explains the (non-)convergence properties of the various methods, i.e., why the Birkhoff normal form, in both its non-resonant or resonant form, diverges, while the Kolmogorov and the hyperbolic normal forms are convergent within some domain of the phase space.[2].

After discussing the above formal issues, in section 4 we discuss one more issue related to diffusion in the weakly chaotic regime, namely the connection between resonant normal form theory and the example given by Arnold (1964) largely referred to as 'Arnold diffusion'. The main result shown here is that a practical implementation of normal form theory in the computer at a high order allows one to construct a set of good canonical variables (suggested first in the theoretical work of Benettin and Gallavotti (1986)), in which the phenomenon of Arnold diffusion can be visualized in a way particular convenient for quantitative study. In fact, we were recently able to construct such an example (Efthymiopoulos and Harsoula (2012)), briefly presented in the end of section 4. We should emphasize at this point that a study of Arnold diffusion using normal forms proves to be an approach complementary to another approach extensively discussed in the present school, namely the theory of diffusion developed by Chirikov (1979) using tools like the Melnikov - Arnold integral (see the review by Cincotta (2002)). In fact, the combination of the two methods serves as a bridge connecting the 'two sides of the river', i.e. normal form expansions and the use of Arnold-Melnikov techniques. Some discussion of this subject is made in subsection 4.3 below.

The present notes end with a reference to some basic Hamiltonian models encountered in dynamical astronomy, as for example, in the restricted three body problem, in axisymmetric galaxies, and in rotating barred-spiral galaxies. The variety of applications of canonical perturbation theory in dynamical astronomy

---

[1]Term suggested by T. Bountis (private communication).

[2]Quite pedagogic expositions of this subject can be found in various lectures by A. Giorgilli, see reference list.

renders hardly tractable any attempt to review them. Instead, we present below only the Hamiltonian formalisms associated with these specific examples, as well as the way by which book-keeping, and other formal aspects of normal form theory, can be implemented in each case. We hope that the collection of some basic formulae could motivate readers to develop their own implementations of the methods and principles discussed below. This is actually the overall purpose of the present lectures.

Acknowledgements: I am indebted to the head of the 3rd LaPlata school Professor Pablo Cincotta, for his invitation, the fact that he trusted upon me a substantial part of the school's program, and a great hospitality. My thanks go also to Professors Claudia Giordano and J.C. Muzzio. I would like to gratefully acknowledge my interaction over the years with Professor George Contopoulos, who has taught me the importance of focusing on an *application-oriented* approach to canonical perturbation theory, which proves to be quite fruitful in concrete problems encountered in the study of galaxies, the solar system, and plasma physics. Professor Antonio Giorgilli has patiently corrected (and still, occasionally!) many misconceptions of mine regarding how to implement and work out the estimates of normal form theory in Hamiltonian systems. Dr. Kleomenis Tsiganis entrusted me to present some material related to the canonical formalism in problems of solar system dynamics. In my understanding of the material presented in section 4 I benefited a lot from discussions with Profs. Giancarlo Benettin, Claude Froeschlé and Massimiliano Guzzo. Many results reviewed in the same section are the outcome of a joint collaboration with Dr. Maria Harsoula. I am grateful to Nikos Delis, who undertook with dedication the task of reproducing all calculations in the text. Matthaios Katsanikas, Liana Tsigaridi, and Helen Christodoulidi made also useful remarks and corrections.

A final word: These notes are my effort to respond to the many inspiring (and on-going) interactions with a group of very motivated young astronomers that attended the school. I would like to mention in particular the LOC members Luciano Darriba, Nicolás Maffione, Martín Mestre, Octavio Miloni, Rocío Paez and Paula Ronco. Let me hope that the present notes could fulfil in part their expectations for a text providing practical help in their and their colleagues' study of a fascinating subject, namely Hamiltonian dynamical systems as applied to Dynamical Astronomy.

2. A 'WARM-UP' EXAMPLE: THE PERIODICALLY DRIVEN PENDULUM

2.1. Phenomenology

Let us consider a periodically driven pendulum model given by the Hamiltonian

$$H = \frac{p^2}{2} - \omega_0^2(1 + \epsilon(1+p)\cos\omega t)\cos\psi \quad . \tag{1}$$

We postpone until section 5 a detailed discussion of the physical context in which a model like (1) could arise in systems of interest in dynamical astronomy. We

mention only that a model like (1) could represent a simplified version of the local form of Hamiltonian dynamics in cases of *resonances*, as, for example, the mean motion resonances in solar system dynamics or the disc resonances in spiral and barred galaxies.

The model (1) can be considered as a time-dependent system of one degree of freedom (called sometimes 'one and a half' degrees of freedom). In practice, it often proves helpful to eliminate the formal dependence of a Hamiltonian function like (1) on time. When this dependence is through trigonometric terms of the form $\cos[(n_1\omega_1 + n_2\omega_2 + ... + n_m\omega_m)t]$, i.e. with one or more (incommensurable) frequencies $\omega_1, \ldots, \omega_m$, a usual procedure by which we do the formal elimination is to 'upgrade' each of the quantities $\omega_i t$ to an angular variable $\phi_i = \omega_i t$, to which we associate a conjugate 'dummy' action I_i. It is then straightforward to show that Hamilton's equations under the original Hamiltonian $H(\psi, p; \omega_1 t, \omega_2 t, \ldots, \omega_m t)$ are equivalent to Hamilton's equations under a new Hamiltonian, called the extended Hamiltonian:

$$H' = H(\psi, p, \phi_1, \phi_2 \ldots, \phi_m) + \omega_1 I_1 + \ldots + \omega_m I_m \quad . \tag{2}$$

Implementing the above procedure in the Hamiltonian (1) (where we only have one external frequency, i.e. ω), we arrive at the extended hamiltonian:

$$H'(\psi, \phi, p, I) = \frac{p^2}{2} + \omega I - \omega_0^2(1 + \epsilon(1 + p)\cos\phi)\cos\psi \quad . \tag{3}$$

In numerical studies, an advantage of employing the Hamiltonian (3) over (1) is that the energy $E = H'(\psi, \phi, p, I)$ is a preserved quantity along the orbital flow of the hamiltonian (3), while this is not so for the hamiltonian (1). Thus, when we solve numerically the equations of motion under the Hamiltonian (3), we can test the accuracy of numerical integrations by checking how well is the energy E preserved along the numerically computed orbits. This, at the expense of some extra time required to compute the time evolution of the dummy action I.

We proceed now in a rough investigation of the dynamical features of motion under the Hamiltonian (3) via a numerical example. To this end, we first fix numerical values for the frequencies, say, $\omega_0 = 0.2\sqrt{2}$ and $\omega = 1$. The motivation for such choice will be gradually recognized as we proceed.

In order to numerically visualize the properties of motion, a basic first step is to plot *phase portraits*, as we vary the perturbation parameter ϵ. In this it is helpful to introduce a convenient *surface of section*, i.e. a surface crossed by all trajectories. By plotting only the crossing points of the trajectories with the surface of section, we obtain two-dimensional plots easy to visualize and interpret. In systems with a periodic-in-time perturbation, a convenient choice of surface of section stems from noticing that the angle ϕ grows linearly in time (i.e. $\phi = \omega t$, setting $\phi = 0$ at $t = 0$), independently of the time evolution of the remaining variables ψ, p, I. Thus, in a system like (3) we can choose as surface of section the surface given by the condition $\phi mod 2\pi = 0$. Substituting this condition in the Hamiltonian (3), for fixed energy E, we find:

$$E = \frac{p^2}{2} + \omega I - \omega_0^2(1 + \epsilon(1 + p))\cos\psi \quad . \tag{4}$$

This is a condition binding together the variables (ψ, p, I). Solving, for example, for I, we find:

$$I = \frac{1}{\omega}\left(E - \frac{p^2}{2} + \omega_0^2(1+\epsilon(1+p))\cos\psi\right) \quad . \tag{5}$$

Eq.(5) implies that in order to visualize dynamics, it suffices to plot the points (ψ, p) on a two-dimensional plot every time when ϕ becomes equal to a multiple of 2π, since, then, the value of I is specified completely. Equivalently, if we give some initial condition $\psi(0) = \psi_0$, $p(0) = p_0$, and an auxiliary initial condition for the dummy action I, e.g. $I(0) = 0$, we can compute numerically the time evolution $\psi(t), p(t)$ (and $I(t)$), and plot one point on the plane (ψ, p) whenever the time t is equal to a multiple of the perturber's period, i.e. at the times $t_1 = 2\pi/\omega$, $t_2 = 4\pi/\omega$, etc. The set of points $(\psi_i, p_i) = (\psi(t_i), p(t_i))$, $t_i = i(2\pi/\omega)$, $i = 1, 2, ...$ are called surface of section iterates. As a rule, computing a few thousand iterates per trajectory is enough to obtain a clear visual picture of the dynamics.[3]

Figure 1 shows the phase portraits (surfaces of section) of the Hamiltonian model (3) for two different values of ϵ, namely (a) $\epsilon = 0.04$, and (b) $\epsilon = 1$. These are chosen so as to represent two well distinct regimes characterizing hamiltonian dynamics. In particular:

(a) Figure 1a shows a typical phase portrait in the *nearly-integrable*, or *weakly chaotic* case. Its main feature is that the phase space is filled for the most by invariant tori. In fact, we distinguish three types of such tori in Fig.1a: i) librational tori (closed curves), ii) rotational tori (open curves extending from $-\pi < \psi \leq \pi$), and iii) tori around higher order resonances (islands of stability). As we will see, we can establish that the trajectories giving rise to such invariant curves are *quasi-periodic*, i.e. they can be represented by a sum of trigonometric terms with one or more frequencies. Also, these orbits are called regular, i.e. they introduce no chaos, and they have zero Lyapunov characteristic exponents. However, Fig.1a shows also some local chaos around the pendulum separatrix layer. But a main feature of the orbits in the chaotic layer is that these orbits cannot exhibit macroscopic transport beyond a domain confined by the presence of invariant tori. This is a property of systems of at most two degrees of freedom,

---

[3] We note, in passing, that the sequence $(\psi_0, p_0) \to (\psi_1, p_1) \to (\psi_2, p_2) \to \ldots$ can be viewed also as a *mapping*, i.e. the point (ψ_0, p_0) is mapped to (ψ_1, p_1), then (ψ_2, p_2) etc. In fact, in the study of hamiltonian dynamics, we often use as models explicit mappings, like, for example, a 2D mapping of the form

$$\psi_{i+1} = f(\psi_i, p_i), \quad p_{i+1} = g(\psi_i, p_i) \tag{6}$$

where the functions f, g are explicitly given, instead of being computed as the surface of section iterates of some Hamiltonian model. Such is the case of the celebrated Chirikov's (1979) *standard mapping*:

$$\begin{aligned} \psi_{i+1} &= \psi_i + p_i + K\sin\psi_i \quad (mod 2\pi) \\ p_{i+1} &= p_i + K\sin\psi_i \end{aligned} \tag{7}$$

where K is a constant 'non-linearity parameter'. The mapping (7), or variants of it in two or more dimensions, have been used as prototypes for many studies of chaotic diffusion in conservative systems.

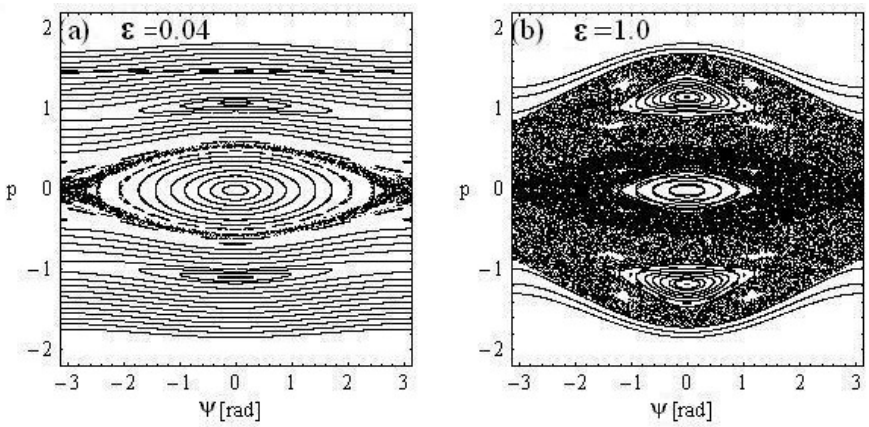

Figure 1. Surfaces of section of the perturbed pendulum model (Hamiltonian (3)) for (a) $\epsilon = 0.04$, and (b) $\epsilon = 1$.

while, as we will see in section 4, in systems of three or more degrees of freedom such transport is allowable via the so-called mechanism of *Arnold diffusion*.

(b) Figure 1b exemplifies the so-called *strong chaos* regime, where most trajectories are chaotic. In the surface of section, chaos shows up as an apparently random distribution of points on the surface, called a 'chaotic layer' or 'chaotic sea'. It should be noted, however, that the motion in a chaotic layer like in Fig.1b has also some underlying structure and obeys laws, which render chaotic motions qualitatively very different from random motions (see Contopoulos (2002)).

In the remaining part of section 2, we will exploit the numerical example of figure 1 as a basis in order to introduce some basic forms and techniques of canonical perturbation theory. Most of the methods presented below deal with a description of the regime of *regular dynamics*. These are useful when the perturbation parameter ϵ is relatively small, for example $\epsilon < 0.1$ in the case of the Hamiltonian (3). Are such perturbation values relevant to the size of various perturbations encountered in systems of interest in dynamical astronomy? We will see that, while we can definitely identify cases of strong chaos in astronomical systems, the case of systems approximated by nearly-integrable (or weakly chaotic) dynamics appears also quite frequently. Table I shows different types of astronomical systems, and the sort of perturbations that can appear in them along with a rough estimate of the expected size of various perturbations. We observe that typical perturbations in dynamical astronomy are in the range $10^{-4} \leq \epsilon \leq 1$. In this regime, most forms of canonical perturbation theory are applicable to some extent. The domain where this is most evident is *solar system dynamics*, which is historically the domain which has lead to most developments in canonical perturbation theory. The importance of nearly-integrable systems in the study of solar system dynamics has been emphasized by H. Poincaré (1892) in his seminal *"Méthodes Nouvelles de la Mécanique Celeste"*. In fact, the study of motions under a Hamiltonian of the form

$$H = H_0 + \epsilon H_1$$

where H_0 is an integrable model and ϵH_1 is a function analytic in ϵ, (i.e. developable as a convergent series in powers of ϵ), is called by Poincaré the "fundamental problem of dynamics".

In subsection 2.10, however, we will see that canonical perturbation theory can be used also with profit in describing even some features of chaotic dynamics, as in Fig.1b. In particular, canonical perturbation theory can be used in order to compute the asymptotic *invariant manifolds* emanating from unstable periodic orbits located in the chaotic subset of the phase space. The invariant manifolds are objects of great complexity, whose form, nevertheless, can be computed by the method of hyperbolic normal forms, discussed first by Moser (1958), and implemented in the canonical framework by Giorgilli (2001). The study of manifold dynamics is a quite modern subject that has led to many applications in celestial mechanics and galactic dynamics (Voglis et al. (2006), Romero-Gomez et al. (2006, 2007), Tsoutsis et al. (2008, 2009)), and even space-flight dynamics (see Perozzi and Ferraz-Mello (2010) and references there in, and Gómez and Barrabés (2011)).

Table 1: Perturbations in astronomical systems

System	Type of perturbation	perturbation value
Earth sattelite dynamics	Earth's oblateness	$\sim 10^{-2}$
Solar system dynamics	Mass of Jupiter	10^{-3}
	Mass of other giant planets	10^{-4}
	Eccentricities	$10^{-2} - 10^{-1}$
	Inclinations	$10^{-2} - 10^{-1}$
Extrasolar planetary systems	Mass of giant planets	$10^{-3} - 10^{-2}$
	Eccentricities	$10^{-1} - 1$
Spiral - Barred galaxies	Spiral perturbation	$10^{-2} - 10^{-1}$
	Bar perturbation	$10^{-1} - 1$
Elliptical galaxies	Ellipticity	~ 0.5, but equipotential surfaces rounder $\sim 0.1 - 0.3$
	Triaxiality	$0.1 - 0.5$
	Ratio of central mass to galaxy mass	$10^{-5} - 10^{-2}$
Charged particle motions in magnetic fields	$B_\perp / B_0$	$10^{-3} - 10^{-1}$

2.2. The concept of normal form

We start our discussion of how to implement canonical perturbation theory in the study of regular motions in a hamiltonian system like (3) by recalling first some basic notions related to the theory of *normal forms* in Hamiltonian systems. This theory will be implemented in the case of the extended Hamiltonian H' of

Eq.(3) (in the sequel, for simplicity we drop the prime symbol and refer to the latter simply as H).

In the context of canonical perturbation theory, a *normal form* can be defined as *a Hamiltonian function yielding a simple-to-analyze dynamics.*

It should be made clear at once that, in the above definition, 'simple-to-analyze' does *not* necessarily mean 'integrable'. In fact, normal forms that are integrable Hamiltonians appear only in particular cases of non-resonant, or at most simply-resonant, models. In general, however, a multiply-resonant normal form is a non-integrable Hamiltonian, and in fact, the dynamics under such a normal form could imply even a large degree of chaos (see section 4). However, normal forms are Hamiltonians having some particular properties to be discussed below, which render their study simpler than the study of the original Hamiltonian from which they arise.

What is precisely the relation between a normal form and the original Hamiltonian of interest? The normal form arises after implementing a *canonical transformation* to the variables appearing in the original Hamiltonian. In the example of the hamiltonian (3), the overall procedure is the following:

i) We are interested in modeling, e.g., the regular trajectories appearing in Fig.1a, by computing one or more normal form models associated with the Hamiltonian (3).

ii) To this end, we introduce, by a suitable method, a canonical transformation allowing to pass from the old canonical variables (ψ, ϕ, p, I) to new canonical variables (ψ', ϕ', p', I').

iii) We substitute this transformation in the original Hamiltonian, and find the form of the Hamiltonian as expressed in the new variables. We then find that, after the substitution, the new Hamiltonian takes typically the form of a sum of two parts

$$\begin{aligned} H_{new}(\psi', \phi', p', I') = \\ H(\psi(\psi', \phi', p', I'), \phi(\psi', \phi', p', I'), p(\psi', \phi', p', I'), I(\psi', \phi', p', I')) \\ = Z(\psi', \phi', p', I') + R(\psi', \phi', p', I') \end{aligned} \tag{8}$$

where the terms $Z(\psi', \phi', p', I')$ and $R(\psi', \phi', p', I')$ are called *normal form* and *remainder* respectively. The normal form term Z is the one whose significance has been discussed already. However, the transformed hamiltonian contains also the remainder term R. This term is important, because it tells us how much the dynamics of the original Hamiltonian really differs from the dynamics of the normal form. In fact, most schemes of perturbation theory are formulated upon the requirement to have proper control over the growth of the *size of the remainder* (see below).

The study of the influence of the remainder on dynamics requires new techniques, going beyond the formal aspects of canonical perturbation theory. A basic example of such techniques is provided by the theory of diffusion developed by Chirikov (1979, see the review by Cincotta (2002) and section 4 below).

We will now examine in detail the technical aspects of how to construct a normal form in practice for the Hamiltonian (3). We first observe that, in order to deal with canonical transformations, we are in need of a formal apparatus performing such transformations in a way convenient to the derivation of a normal form. The technique of *Lie series transformations* is widely used to this

end, and easily transferable to a computer-algebraic program. To this we now turn our attention.

2.3. Canonical transformations by Lie series

The idea of a *Lie series canonical transformation* is very simple: just consider an arbitrary function $\chi(\psi, \phi, p, I)$, and compute the flow produced under Hamilton's equations of motion if, instead of H, χ was supposed to be the Hamiltonian. The equations of motion would then be:

$$\dot{\psi} = \frac{\partial \chi}{\partial p}, \quad \dot{\phi} = \frac{\partial \chi}{\partial I}, \quad \dot{p} = -\frac{\partial \chi}{\partial \psi}, \quad \dot{I} = -\frac{\partial \chi}{\partial \phi} \quad . \tag{9}$$

Let $\psi(t), \phi(t), p(t), I(t)$ be a solution of Eqs.(9) for some choice of initial conditions $\psi(0) = \psi_0$, $\phi(0) = \phi_0$, $p(0) = p_0$, and $I(0) = I_0$. The key remark, now, is the following. For any time t, the mapping of the variables in time, namely

$$(\psi_0, \phi_0, p_0, I_0) \to (\psi_t, \phi_t, p_t, I_t)$$

can be proven to be a canonical transformation (see, for example, Arnold (1978)). In that sense, any arbitrary function $\chi(\psi, \phi, p, I)$ can be thought of as a function which can generate an infinity of different canonical transformations, via its Hamilton equations of motion solved for infinitely many different values of the time t. In fact, from this viewpoint t can be considered as a parameter which defines, according to its value, the whole family of the canonical transformations generated by χ.

How practical is this method in defining canonical transformations? Clearly, for an arbitrary function χ, the task of solving Eqs.(9) for every value of t is hardly tractable. However, we can note that for t small enough, a solution of the initial value problem of Eqs.(9) is always possible via *Taylor series*. This, because by knowing explicitly how the first derivatives $\dot{\psi}, \dot{\phi}, \dot{p}, \dot{I}$ are expressed as functions of the canonical variables (ψ, ϕ, p, I) (via Eqs.(9)), we can find similar expressions for the time derivatives of *all orders*, depending on the same quantities. We have, for example:

$$\begin{aligned} \frac{d^2\psi}{dt^2} &= \frac{d}{dt}\left(\frac{\partial \chi}{\partial p}\right) = \frac{\partial}{\partial \psi}\left(\frac{\partial \chi}{\partial p}\right)\dot{\psi} + \frac{\partial}{\partial \phi}\left(\frac{\partial \chi}{\partial p}\right)\dot{\phi} + \frac{\partial}{\partial p}\left(\frac{\partial \chi}{\partial p}\right)\dot{p} + \frac{\partial}{\partial I}\left(\frac{\partial \chi}{\partial p}\right)\dot{I} \\ &= \frac{\partial^2 \chi}{\partial \psi \partial p}\frac{\partial \chi}{\partial p} + \frac{\partial^2 \chi}{\partial \phi \partial p}\frac{\partial \chi}{\partial I} - \frac{\partial^2 \chi}{\partial^2 p}\frac{\partial \chi}{\partial \psi} - \frac{\partial^2 \chi}{\partial I \partial p}\frac{\partial \chi}{\partial \phi} \quad . \end{aligned} \tag{10}$$

We note that, after all operations, the second derivative $d^2\psi/dt^2$ has been expressed in Eq.(10) in terms of the function $\chi(\psi, \phi, p, I)$ and some partial derivatives of it. This implies that Eq.(10) resumes the form $d^2\psi/dt^2 = F_{\psi,2}(\psi, \phi, p, I)$, i.e. the second derivative $d^2\psi/dt^2$ can be expressed as a function of the canonical variables (ψ, ϕ, p, I). By repeating the above procedure, it is straightforward to see that the same holds true for the derivatives of all orders, i.e. we can derive expressions of the form $d^n\psi/dt^n = F_{\psi,n}(\psi, \phi, p, I)$ for all $n = 1, 2, \ldots$.

Why is this required in practice? If we express the solution $\psi(t)$ as a Taylor series

$$\psi(t) = \psi(0) + \frac{d\psi(0)}{dt}t + \frac{1}{2}\frac{d^2\psi(0)}{dt^2}t^2 + \ldots \tag{11}$$

and substitute in (11) the expressions for all functions $d^n\psi/dt^n$ by their equivalent functions $F_{\psi,n}(\psi,\phi,p,I)$, we find an expression of the form

$$\psi_t = \psi_0 + F_{\psi,1}(\psi_0,\phi_0,p_0,I_0)t + \frac{1}{2}F_{\psi,2}(\psi_0,\phi_0,p_0,I_0)t^2 + \ldots \tag{12}$$

where $\psi_t \equiv \psi(t)$, $\psi_0 \equiv \psi(0)$, etc. This procedure can be repeated for all remaining variables, yielding finally expressions of the form

$$\begin{aligned}
\psi_t &= \psi_0 + F_{\psi,1}(\psi_0,\phi_0,p_0,I_0)t + \frac{1}{2}F_{\psi,2}(\psi_0,\phi_0,p_0,I_0)t^2 + \ldots \\
\phi_t &= \phi_0 + F_{\phi,1}(\psi_0,\phi_0,p_0,I_0)t + \frac{1}{2}F_{\phi,2}(\psi_0,\phi_0,p_0,I_0)t^2 + \ldots \\
p_t &= p_0 + F_{p,1}(\psi_0,\phi_0,p_0,I_0)t + \frac{1}{2}F_{p,2}(\psi_0,\phi_0,p_0,I_0)t^2 + \ldots \\
I_t &= I_0 + F_{I,1}(\psi_0,\phi_0,p_0,I_0)t + \frac{1}{2}F_{I,2}(\psi_0,\phi_0,p_0,I_0)t^2 + \ldots
\end{aligned} \tag{13}$$

Expressions like (13) are called *Lie series*, and they provide a family of formal canonical transformations for any value of the time variable t, which, for this reason, can be considered as a parameter characterizing this family. Of course, in order that the expressions (13) have meaning, the series in the r.h.s. of all equations must be convergent. We will examine the question of convergence in some detail below, but for the moment let us assume that the function χ, and its derivatives, are small enough so that the series (13) are convergent when the time is $t = 1$. We then obtain a *Lie canonical transformation*, from (ψ_0,ϕ_0,p_0,I_0) to (ψ_1,ϕ_1,p_1,I_1), i.e.:

$$\begin{aligned}
\psi_1 &= \psi_0 + F_{\psi,1}(\psi_0,\phi_0,p_0,I_0) + \frac{1}{2}F_{\psi,2}(\psi_0,\phi_0,p_0,I_0) + \ldots \\
\phi_1 &= \phi_0 + F_{\phi,1}(\psi_0,\phi_0,p_0,I_0) + \frac{1}{2}F_{\phi,2}(\psi_0,\phi_0,p_0,I_0) + \ldots \\
p_1 &= p_0 + F_{p,1}(\psi_0,\phi_0,p_0,I_0) + \frac{1}{2}F_{p,2}(\psi_0,\phi_0,p_0,I_0) + \ldots \\
I_1 &= I_0 + F_{I,1}(\psi_0,\phi_0,p_0,I_0) + \frac{1}{2}F_{I,2}(\psi_0,\phi_0,p_0,I_0) + \ldots
\end{aligned} \tag{14}$$

The function χ is called a *Lie generating function*, i.e. it "generates" a canonical transformation via Eqs.(14).

The canonical transformation (13) can be written in a concise form if we introduce the Poisson bracket operator $L_\chi \equiv \{\cdot,\chi\}$, whose action on functions $f(\psi,\phi,p,I)$ is defined by:

$$L_\chi f = \{f,\chi\} = \frac{\partial f}{\partial\psi}\frac{\partial\chi}{\partial p} + \frac{\partial f}{\partial\phi}\frac{\partial\chi}{\partial I} - \frac{\partial f}{\partial p}\frac{\partial\chi}{\partial\psi} - \frac{\partial f}{\partial I}\frac{\partial\chi}{\partial\phi} \quad . \tag{15}$$

The time derivative of any function $f(\psi,\phi,p,I)$ along a hamiltonian flow defined by the function χ is given by:

$$\frac{df}{dt} = \frac{\partial f}{\partial\psi}\dot{\psi} + \frac{\partial f}{\partial\phi}\dot{\phi} + \frac{\partial f}{\partial p}\dot{p} + \frac{\partial f}{\partial I}\dot{I} = \frac{\partial f}{\partial\psi}\frac{\partial\chi}{\partial p} + \frac{\partial f}{\partial\phi}\frac{\partial\chi}{\partial I} - \frac{\partial f}{\partial p}\frac{\partial\chi}{\partial\psi} - \frac{\partial f}{\partial I}\frac{\partial\chi}{\partial\phi}$$

that is

$$\frac{df}{dt} = \{f, \chi\} = L_\chi f \quad . \tag{16}$$

Extending this to higher order derivatives, we have

$$\frac{d^n f}{dt^n} = \{\ldots\{\{f, \chi\}, \chi\}\ldots\chi\} = L_\chi^n f \quad . \tag{17}$$

The Taylor series (13) can now be written as

$$\psi_t = \psi_0 + \frac{d\psi_0}{dt}t + \frac{d^2\psi_0}{dt^2}t^2 + \ldots = \sum_{n=0}^{\infty}\frac{1}{n!}\frac{d^n\psi_0}{dt^n}t^n \quad . \tag{18}$$

However, taking into account that the Taylor expansion of the exponential around the origin is given by

$$\exp(x) = 1 + x + \frac{x^2}{2} + \frac{x^3}{3!} + \ldots = \sum_{n=0}^{\infty}\frac{x^n}{n!}$$

we can see that the Taylor expansion (18) is formally given by the following exponential operator

$$\exp\frac{d}{dt} = 1 + \frac{d}{dt} + \frac{1}{2}\frac{d^2}{dt^2} + \ldots$$

Finally, taking into account Eqs.(16) and (17), we are lead to the formal definition of the *Lie series*

$$\psi_t = \psi_0 + (L_\chi\psi_0)t + \frac{1}{2}(L_\chi^2\psi_0)t^2 + ... \tag{19}$$

Setting, again, in (19) the time as $t = 1$, we define a canonical transformation using Lie series by recasting equations (14) in the form:

$$\psi_1 = \exp(L_\chi)\psi_0, \quad \phi_1 = \exp(L_\chi)\phi_0, \quad p_1 = \exp(L_\chi)p_0, \quad I_1 = \exp(L_\chi)I_0 \quad . \tag{20}$$

We summarize here the following basic properties of Lie series:

i) *Any* arbitrary choice of function χ produces a canonical transformation $(\psi_0, \phi_0, p_0, I_0) \to (\psi_1, \phi_1, p_1, I_1)$ via Eqs.(20). In normal form theory, however, we will see how to make a proper choice of one or more Lie generating functions χ so as to ensure that, after accomplishing a sequence of canonical transformations, the Hamiltonian in the new variables obtains a form representing, indeed, the kind of properties we want it to represent.

ii) The operations involved in Eqs.(20) are just calculations of derivatives. This renders the method quite easy to implement and to adapt to a computer-algebraic program.

iii) The fact that the time derivative of any function f under the Hamiltonian flow of another function χ is given by Eq.(16) implies that:

$$\begin{gathered} f_1(\psi_1, \phi_1, p_1, I_1) = \\ f(\psi(\psi_1, \phi_1, p_1, I_1), \phi(\psi_1, \phi_1, p_1, I_1), p(\psi_1, \phi_1, p_1, I_1), I(\psi_1, \phi_1, p_1, I_1)) \\ = \exp(L_\chi) f(\psi_1, \phi_1, p_1, I_1) \quad . \end{gathered} \tag{21}$$

In other words, in order to find what form does a function f of the canonical variables (ψ, ϕ, p, I) take, if, in the place of (ψ, ϕ, p, I) we substitute the new variables $(\psi_1, \phi_1, p_1, I_1)$, we do not really need to compute the transformation and substitute afterwards in f, we can simply implement the Lie operator $\exp(L_\chi)$ directly on f. This is algebraically very convenient, because it means we never have to make function compositions, which is a cumbersome algebraic procedure, but we only have to deal with computing derivatives of functions, which is always a straightforward procedure.

iv) If χ is a *small* quantity, the Lie series transformation (20) can be considered as a *near-identity* transformation, since, for example,

$$\exp(L_\chi)\psi = \psi + \{\psi, \chi\} + \ldots$$

All the above properties are relevant in the implementation of normal form theory as will be clear by the examples below.

2.4. Application: Birkhoff normal form for rotational tori

We are now ready to see how normal form theory can be implemented in the Hamiltonian (3), in order to help answering some practical questions. The first question that we will address is the following: in the phase portrait of Fig.1a, in the domain beyond the separatrix, we observe the existence of many invariant curves corresponding to rotational tori (roughly at values of p in the domain $|p| > 0.5$). The motion on such tori appears to be *quasi-periodic* [4]. Can we find a useful normal form by which to represent the motions in this domain as quasi-periodic? Even more, can we use normal form theory in order to prove the existence of quasi-periodic motions in the system (3)?

It is always important to recall the following fact: despite that normal form theory is a mathematical theory, our chance to implement it successfully in order to answer such questions depends crucially on our correct understanding of the *physical* properties of the motions we try to represent. In the domain $|p| > 0.5$ of Fig.1a, these motions are rotations, i.e. a test particle (or a real pendulum) subscribes a rotation with a value of the angle ψ monotonically increasing in time (above the separatrix), or decreasing in time (below the separatrix). In fact, it is evident that for p large in measure, the rotational motion of the pendulum approaches more and more uniform rotation. In the phase portrait of Fig.1a, this means that for higher values of p the invariant curves on the top side of the plot take closer and closer the form of straight lines. Thus, it seems reasonable to look for a normal form representing the motions in this domain, constructed in such a way that its lowest order approximation represents uniform rotation.

On the basis of the above argument, let us focus on *one* value of p, to be hereafter denoted p_*, for example $p_* = 2(\sqrt{3} - 1) \simeq 1.46410$, corresponding to the value of the ordinate of a dashed line shown in the upper part of Fig.1a. The reason for choosing a value of this type (which is incommensurable with $\omega = 1$) will become evident in a while. We now clearly see that the dashed line

[4] A dynamical variable $x(t)$ is said to undergo a quasi-periodic time evolution with n incommensurable frequencies $\omega_1, ..., \omega_n$ if its dependence on time is via one or more trigonometric terms of the form $\begin{matrix}\cos\\ \sin\end{matrix}((m_1\omega_1 + m_2\omega_2 + \ldots + m_n\omega_n)t)$, with $m_1, m_2, ..., m_n$ integer.

in Fig.1a intersects some invariant curves in such a way, that the variations of p along one curve above or below the dashed line are relatively small (of order ~ 0.1) around the fixed value $p_* = 1.46410$. Let us then introduce a local action variable I_ψ via

$$I_\psi = p - p_* \tag{22}$$

i.e. by simply shifting the center at $p = p_*$. A change of variables like (22) is a trivial form of canonical transformation, thus it can be substituted in the Hamiltonian function (3). Setting $p = 1.46410 + I_\psi$, and also $\omega_0 = 0.2\sqrt{2}$, $\omega = 1$, $\epsilon = 0.04$, we arrive at the Hamiltonian [5]

$$\begin{aligned} H &= 1.07179 + 1.46410 I_\psi + I + \frac{I_\psi^2}{2} \\ &- 0.08\cos\psi - (0.0078851 + 0.0032 I_\psi)\cos\psi\cos\phi \quad . \end{aligned} \tag{23}$$

The constant 1.07179 in the hamiltonian (23) does not affect the dynamics, thus we will omit it in all subsequent steps. It is interesting to note that, already at this stage, the Hamiltonian (23) provides us with some information about the character of the rotational motion. In fact, if we take Hamilton's equation for $\dot{\psi}$ we find $\dot{\psi} = \partial H/\partial I_\psi = 1.46410 + ...$, where the three dots denote here all remaining terms, whose size, however, is considerably smaller than the size of the first term. We thus see that the Hamiltonian (23) describes rotational motions with an angular frequency that varies in time a little around the value $\omega_* = 1.46410$.

In order to make this statement more precise, we need to characterize quantitatively how does the presence of the terms $-I_\psi^2/2$, $-0.08\cos\psi$ and $-(0.0078851 + 0.0032 I_\psi)\cos\psi\cos\phi$ perturb the motion with respect to a uniform rotation. A quick visual look to Fig.1a shows that the variable I_ψ is expected to hold variations of about ~ 0.2, or $I_\psi^2/2 \sim 0.02$. Thus, the two terms $I_\psi^2/2$ and $0.08\cos\psi$ have a rather comparable size, of the order of a few times 10^{-2}, while the third term can be considered of the same order, or one order of magnitude smaller. For simplicity, we will consider all three terms of similar size [6]. We will introduce a formal notation to account for this consideration: in front of every term in (23), we introduce a factor λ^s, where λ, called hereafter the 'book-keeping parameter', is a constant with numerical value equal to $\lambda = 1$, while s is a positive integer exponent whose value, for every term in (23), is selected so as to

[5] The reader is asked to tolerate the fact that we will continue the example hereafter with numerical coefficients. In fact, this is exactly what happens in practice, i.e., in practical computations we rarely choose to carry along symbols like $\omega_0, \omega, \epsilon$ etc. With a little effort to acquaint him/herself with this notation, the reader will realize that the use of numerical coefficients hereafter renders the example easier to study. Furthermore, there seems to be no better way for one to acquire a 'feeling' of how a method works, than by seeing the real numbers the method produces in a practical example. At any rate, we will truncate all figures at five digits, so as not to produce very lengthy formulae. In the computer, we retain of course many more significant digits.

[6] This is really a convention; with a little a posteriori experience, one understands that a difference of one order of magnitude does not really matter very much in whether or not we should diversify the third term from the first two terms.

reflect our consideration regarding what order of smallness we estimate a term to be of in the Hamiltonian. Thus, considering the leading terms $1.46410 I_\psi$ and I as of order zero, we put λ^0 in front of them. On the other hand, considering the remaining three terms as of a similar order of smallness, i.e. first order, we put a factor λ^1 in front of them. The Hamiltonian now reads:

$$\begin{aligned} H &= \lambda^0 (1.46410 I_\psi + I) \\ &+ \lambda^1 \left(\frac{I_\psi^2}{2} - 0.08 \cos\psi - (0.0078851 + 0.0032 I_\psi) \cos\psi \cos\phi \right) \quad . \end{aligned} \tag{24}$$

Since $\lambda = 1$, nothing has really changed. However, the appearance of the symbol λ allows one to clearly identify one's own perceptions about the 'hierarchy' by which various terms in the Hamiltonian affect the dynamics. These perceptions are not completely objective. Let us discuss some alternative choices with respect to the book-keeping introduced in (24). We could have written:

$$\begin{aligned} H &= \lambda^0 \left(1.46410 I_\psi + I + \frac{I_\psi^2}{2} \right) \\ &- \lambda^1 \left(0.08 \cos\psi + (0.0078851 + 0.0032 I_\psi) \cos\psi \cos\phi \right) \quad . \end{aligned} \tag{25}$$

Such a choice would imply that we consider the free rotator model as the basic approximation, i.e. a model in which the frequency of rotation varies with the action. In fact, this is perfectly true for the pendulum. Thus, one may incorporate this property directly from the start in the 'zeroth-order Hamiltonian', a process which, as we will see, is indispensable in the construction of the so-called Kolmogorov normal form, by which we rigorously show the existence of rotational tori in the Hamiltonian (3). If, on the other hand, we ignore this property at zeroth order, and consider it a higher order effect (like in the book-keeping of Eq.(24)), we will 'recover' the dependence of the frequency on the action I_ψ after working out some steps of perturbation theory. Let us mention still a third option:

$$\begin{aligned} H &= \lambda^0 \left(1.46410 I_\psi + I + \frac{I_\psi^2}{2} - 0.08 \cos\psi \right) \\ &- \lambda^1 (0.0078851 + 0.0032 I_\psi) \cos\psi \cos\phi \quad . \end{aligned} \tag{26}$$

Choosing this book-keeping option is equivalent to saying that, at zero order, we consider the dynamics being that of the pendulum, so that the only perturbing term is provided by the external driving.

It must be emphasized that all these choices are nothing but different representations of what we consider to be the essential dynamics, although, in reality, the true dynamics is one and the same. Thus, in a certain sense a choice of book-keeping is only a representation of *our own* viewpoint of what is a useful basic approximation to the dynamics. This 'freedom' notwithstanding, it should be stressed that having a correct viewpoint guided by physical principles is essential, because the choice of book-keeping affects in a crucial way all subsequent

steps of perturbation theory, thus determining how successful will the approximation prove to be in the end. As we will see, this reflects both in formal, as well as physical properties of the solutions found via any particular perturbative scheme. [7]

We now return to our original book-keeping scheme, i.e. Eq.(24). In this scheme, the zeroth order Hamiltonian is just $H_0 = 1.46410 I_\psi + I$. Thus, under the Hamiltonian flow of H_0, both quantities I_ψ, I are integrals of motion, i.e. one has $\dot{I}_\psi = \dot{I} = 0$, since in the Hamiltonian H_0 both angles ψ, ϕ are ignorable. This property of H_0 suggests looking for the possibility to construct, via a sequence of canonical transformations, a normal form which, in the new variables, is independent of the angles. This guarantees that the new action variables, after the transformation, will be integrals of motion of the normal form canonical flow.

Let us see in detail how to compute the normal form at first order in the book-keeping parameter λ. We implement the following steps[8]:

i) *notation:* We denote by $H^{(0)}$ the original hamiltonian and by $H^{(1)}$ the Hamiltonian after implementing a canonical transformation from the original variables, denoted hereafter by $(\psi^{(0)}, \phi^{(0)}, I_\psi^{(0)}, I^{(0)})$, to new canonical variables, denoted by $(\psi^{(1)}, \phi^{(1)}, I_\psi^{(1)}, I^{(1)})$. Furthermore, we denote by $Z_0 = H_0^{(0)}$ the terms of $H^{(0)}$ of order zero in λ, and by $H_1^{(0)}$ the terms of order one in λ, that is

$$H^{(0)} = Z_0 + \lambda H_1^{(0)} \tag{27}$$

where

$$Z_0 = 1.46410 I_\psi^{(0)} + I^{(0)},$$

$$H_1^{(0)} = \frac{(I_\psi^{(0)})^2}{2} - 0.08 \cos\psi^{(0)} - (0.0078851 + 0.0032 I_\psi^{(0)}) \cos\psi^{(0)} \cos\phi^{(0)} \quad .$$

ii) We look for a Lie generating function bringing the Hamiltonian in normal form up to terms of first order in λ. The generating function, denoted by χ_1, is a function of the *new* canonical variables, i.e. $\chi_1 \equiv \chi_1(\psi^{(1)}, \phi^{(1)}, I_\psi^{(1)}, I^{(1)})$.

---

[7] We will see below that the terms of order zero in λ appear in the so-called 'homological equation', i.e. a partial differential equation by which we compute generating functions in canonical perturbation theory. These terms are also called the 'kernel' of the homological equation, or the 'Hori kernel' (Hori (1966), Deprit (1969), see Ferraz-Mello (2007)). In summary, the choice of Hori kernel implies a choice of basic dynamical model whose qualitative behavior we expect to approximate the true dynamics in the domain of the phase space considered. Four basic choices of possible Hori kernel are: i) the oscillator (e.g., in two degrees of freedom, $\omega I + \omega_* I_\psi$, ii) the rotator ($\omega I + \omega_* I_1 + \beta I_\psi^2/2$), iii) the pendulum (or 'first fundamental resonance model' (Henrard and Lemaitre (1983)) $\omega I + \omega_* I_\psi + \beta I_\psi^2/2 + B\cos(k\psi)$), and iv) the Andoyer Hamiltonian (or 'second fundamental resonance model' (Henrard and Lemaitre 1983), $\omega I + \omega_* I_\psi + \beta I_\psi^2/2 + B I_\psi^{1/2}\cos(k\psi)$). The latter kernel appears quite often in problems or resonance in solar system and in galactic dynamics (see e.g. subsection 5.4).

[8] The reader is prompted not to be discouraged by the apparent complexity of subsequent formulae. But this is really the crucial point of the whole method, so study with paper, pencil, and a lot of patience, is at this point indispensable.

iii) The canonical transformation induced by χ_1 yields the *old* canonical variables *in terms of the new* canonical variables (not the other way around). This is explicitly given by:

$$\begin{aligned} &\psi^{(0)} = \exp(L_{\chi_1})\psi^{(1)}, \quad \phi^{(0)} = \exp(L_{\chi_1})\phi^{(1)}, \\ &I_\psi^{(0)} = \exp(L_{\chi_1})I_\psi^{(1)}, \quad I^{(0)} = \exp(L_{\chi_1})I^{(1)} \ . \end{aligned} \tag{28}$$

We now specify what is an appropriate form χ_1 should have, to render $H^{(1)}$ in normal form up to terms $O(\lambda)$. To accomplish this task, we note that if we knew χ_1, then, according to Eq.(21), the Hamiltonian after the transformation (28) would be given by:

$$H^{(1)}(\psi^{(1)}, \phi^{(1)}, I_\psi^{(1)}, I^{(1)}) = \exp(L_{\chi_1})H^{(0)}(\psi^{(1)}, \phi^{(1)}, I_\psi^{(1)}, I^{(1)}) \ . \tag{29}$$

The lowest order terms of the Lie operation in the r.h.s. of Eq.(29) are:

$$H^{(1)} = \exp(L_{\chi_1})H^{(0)} = H^{(0)} + L_{\chi_1}H^{(0)} + \frac{1}{2}L_{\chi_1}^2 H^{(0)} + ...$$

In view of (27) this takes the form

$$\begin{aligned} H^{(1)} &= Z_0 + \lambda H_1^{(0)} + \{Z_0, \chi_1\} + \lambda\{H_1^{(0)}, \chi_1\} \\ &+ \frac{1}{2}\{\{Z_0, \chi_1\}, \chi_1\} + \lambda\frac{1}{2}\{\{H_1^{(0)}, \chi_1\}, \chi_1\} + ... \end{aligned} \tag{30}$$

The key remark, now, is the following: in the Hamiltonian (27), the 'unwanted' terms (containing angles) are all found in the $H_1^{(0)}$ term. We denote by $h_1^{(0)}$ these terms, and in order to simplify notations, we will drop superscripts from the notation of the canonical variables (ψ, ϕ, I_ψ, I), keeping always in mind that before and after the canonical transformation there is an omitted superscript (0) and (1) respectively in these variables. With these conventions, we have:

$$h_1^{(0)} = -0.08\cos\psi - (0.0078851 + 0.0032 I_\psi)\cos\psi\cos\phi \ .$$

We then note the following: if we choose χ_1 to be a quantity of first order ($O(\lambda)$) in the book-keeping parameter, then, *only the second and third terms in Eq.(30) are of first order in* λ. Indeed, Z_0 is of order zero, while (assuming $\chi_1 = O(\lambda)$)

$$\{Z_0, \chi_1\} + \lambda H_1^{(0)} = O(\lambda),$$

$$\lambda\{H_1^{(0)}, \chi_1\} = O(\lambda^2),$$

$$\frac{1}{2}\{\{Z_0, \chi_1\}, \chi_1\} = O(\lambda^2),$$

$$\lambda\frac{1}{2}\{\{H_1^{(0)}, \chi_1\}, \chi_1\} = O(\lambda^3)$$

etc. We then require that χ_1 be chosen in such a way that the combination of the only two possible terms of order $O(\lambda)$ eliminates the unwanted terms $h_1^{(0)}$ from the new Hamiltonian $H^{(1)}$. That is, we require that χ_1 be such that

$$\lambda(\text{unwanted terms in } H_1^{(0)}) + \{Z_0, \chi_1\} = 0$$

or

$$\{Z_0, \chi_1\} + \lambda h_1^{(0)} = 0 \quad . \tag{31}$$

An equation of the form (31) is called *homological equation*. It is the most basic equation of canonical perturbation theory, since it is the one by which we specify the various generating functions appearing in a theory, like χ_1. Also, we will see that the solution of a homological equation introduces *divisors*, whose accumulation after subsequent steps is responsible for the convergence (or non-convergence) properties of the series under study.

The solution of Eq.(31) is found in a straightforward manner, if we use the exponential notation $\cos\psi = (e^{i\psi} + e^{-i\psi})/2$ (and similarly for $\cos\phi$), in terms of which we have:

$$h_1^{(0)} = -0.04(e^{i\psi} + e^{-i\psi})$$

$$-(0.0019713 + 0.0008I_\psi)(e^{i(\phi+\psi)} + e^{i(\phi-\psi)} + e^{i(-\phi+\psi)} + e^{i(-\phi-\psi)}) \quad .$$

The solution of (31) is then found by noting that a trigonometric term of the form $a(I_\psi, I)e^{i(k_1\psi+k_2\phi)}$, when acted upon by the operator $\{Z_0, \cdot\} = \{\omega_* I_\psi + \omega I, \cdot\}$ (where, in our case, $\omega_* = 1.46410$, $\omega = 1$), yields

$$\begin{aligned} \{Z_0, a(I_\psi, I)e^{i(k_1\psi+k_2\phi)}\} &= \{\omega_* I_\psi + \omega I, a(I_\psi, I)e^{i(k_1\psi+k_2\phi)}\} \\ &= -i(k_1\omega_* + k_2\omega)a(I_\psi, I)e^{i(k_1\psi+k_2\phi)} \quad . \end{aligned} \tag{32}$$

We then readily verify that if $h_1^{(0)}$ is written under the form of a sum of Fourier terms

$$h_1^{(0)} = \sum_{k_1,k_2,|k_1|+|k_2|\neq 0} b_{k_1,k_2}(I_\psi, I)e^{i(k_1\psi+k_2\phi)}$$

the homological equation (31) is satisfied by setting χ_1 equal to:

$$\chi_1 = \lambda \sum_{k_1,k_2,|k_1|+|k_2|\neq 0} \frac{b_{k_1,k_2}(I_\psi, I)}{i(k_1\omega_* + k_2\omega)} e^{i(k_1\psi+k_2\phi)} \quad . \tag{33}$$

In the specific example of $h_1^{(0)}$ given as above, we find:

$$\chi_1 = \lambda i \Bigg(0.027320(e^{i\psi} - e^{-i\psi}) + (0.0008 + 0.00032466I_\psi)(e^{i(\psi+\phi)} - e^{-i(\psi+\phi)})$$

$$+(0.0042475 + 0.0017238I_\psi)(e^{i(\psi-\phi)} - e^{-i(\psi-\phi)}) \Bigg) \quad .$$

We are essentially done. We now only need to find the form of the Hamiltonian in the new canonical variables, by computing

$$H^{(1)} = \exp(L_{\chi_1}) H^{(0)} \quad . \tag{34}$$

Up to second order in λ we find[9]:

$$H^{(1)} = Z_0 + \lambda Z_1 + \lambda^2 H_2^{(1)} + ...$$

where

$$Z_1 = \frac{I_\psi^2}{2}$$

$$\begin{aligned} H_2^{(1)} = & -8.07603\times 10^{-6} - 3.27748\times 10^{-6} I_\psi - 4.43496\times 10^{-6}(e^{i(2\psi+\phi)} + e^{-i(2\psi+\phi)}) \\ & +2.35470\times 10^{-5}(e^{i(2\psi-\phi)} + e^{-i(2\psi-\phi)}) - 6.28249\times 10^{-5}(e^{i\phi} + e^{-i\phi}) \\ & +0.027320 I_\psi (e^{i\psi} + e^{-i\psi}) \\ & +(8 I_\psi + 3.24662 I_\psi^2)\times 10^{-4}(e^{i(\psi+\phi)} + e^{-i(\psi+\phi)}) \\ & +(0.0042475 I_\psi + 0.0017238 I_\psi^2)(e^{i(\psi-\phi)} + e^{-i(\psi-\phi)}) \\ & -(4.03802 + 1.63874 I_\psi)\times 10^{-6}(e^{2i\phi} + e^{-2i\phi}) \quad . \end{aligned}$$

This resumes one complete step of the normalization algorithm.

The following are some remarks regarding the form of the Hamiltonian after the first normalization step:

i) Up to first order, the Hamiltonian $H^{(1)}$ has been 'brought into normal form', i.e. we see the appearance of terms depending only on the actions I_ψ and I.

ii) At second and subsequent orders, on the other hand, the Hamiltonian $H^{(1)}$ contains new terms, depending on the angles. These terms were not present in the initial Hamiltonian, but they were produced by the Lie operation of Eq.(34). In fact, the quantity $R^{(1)} = \lambda^2 H_2^{(1)} + \lambda^3 H_3^{(1)} + ...$ constitutes the *remainder* function at this order of normalization. The appearance of new, 'unwanted', terms, at second and higher orders, implies that, in order to eliminate these terms, we need further canonical transformations. Thus, using a Lie generating function χ_2 (of order $O(\lambda^2)$), we eliminate the unwanted terms of order $O(\lambda^2)$ in the Hamiltonian. This, in turn, generates new unwanted terms to be eliminated at subsequent steps, etc.

iii) Related to the previous remark, we also observe that the action of multiple Poisson brackets in the implementation of the Lie operation of Eq.(34) generates new trigonometric terms, some of which are of *higher Fourier order* than those of the original Hamiltonian. Such are the terms $\exp(i(2\psi \pm \phi))$. This last property is important, because, as shown below, the generation of terms of

[9] Again, possibility to reproduce these results by paper and pencil implies that the method has been understood.

higher and higher Fourier order in the course of normalization implies also the appearance of *new divisors* (of higher order) in the series.[10]

We finally recall again that, despite the absence of superscripts on the canonical variables (ψ, ϕ, I_ψ, I), all variables appearing in the above expressions for $H^{(1)}$ are the new variables, i.e. the one following the Lie series canonical transformation with χ_1.

2.5. General normalization algorithm

So far we demonstrated in detail the computation of a Lie canonical transformation and associated normal form at first order of perturbation theory. We can readily generalize this computation and formulate a recurrent algorithm for Hamiltonian normalization at an arbitrary order r. To this end, we assume that r normalization steps were accomplished, and give the formulae for the $r+1$ step. After r steps, the Hamiltonian has the form:

$$H^{(r)} = Z_0 + \lambda Z_1 + ... + \lambda^r Z_r + \lambda^{r+1} H^{(r)}_{r+1} + \lambda^{r+2} H^{(r)}_{r+2} + \dots \tag{35}$$

The Hamiltonian term $H^{(r)}_{r+1}$ contains some terms that we want to eliminate, denoted by $h^{(r)}_{r+1}$, as well as some terms that we do not want to eliminate, denoted by Z_{r+1} (in the present example, these are the terms containing only the action variables). The question is to specify a generating function, of order $O(\lambda^{r+1})$, which accomplishes the normalizing transformation. As in the case $r = 0$, we observe that in the Lie series $\exp(L_{\chi_{r+1}})H^{(r)}$, the only terms of order λ^{r+1} are $\lambda^{r+1} H^{(r)}_{r+1}$ and $L_{\chi_{r+1}} Z_0$. This implies that the generating function χ_{r+1} can be specified by solving the homological equation:

$$\{Z_0, \chi_{r+1}\} + \lambda^{r+1} h^{(r)}_{r+1} = 0 \quad . \tag{36}$$

This equation can be solved in exactly the same manner as Eq.(33). After the generating function χ_{r+1} has been specified, we can compute the new, transformed Hamiltonian

$$H^{(r+1)} = \exp(L_{\chi_{r+1}}) H^{(r)} \quad . \tag{37}$$

By construction, this is in normal form up to terms of order $r+1$, namely:

$$H^{(r+1)} = Z_0 + \lambda Z_1 + ... + \lambda^r Z_r + \lambda^{r+1} Z_{r+1} + \lambda^{r+2} H^{(r+1)}_{r+2} + \dots \tag{38}$$

This completes the $r+1$ step of the normalization algorithm. The entire recursive algorithm thus takes the following form:

---

[10] On the other hand, in section 3 we will consider cases where Fourier terms of all orders are present in the series from the start. In such cases, however, the analyticity properties of the original Hamiltonian determine the size of its various Fourier terms as a function of the Fourier order in the original Hamiltonian. Then, it turns out that the process of generation of new terms provides again the leading contribution to the growth of the size of the series terms at subsequent normalization steps (see Morbidelli and Giorgilli (1997), and Morbidelli (2002), for a detailed discussion of this process). Thus, despite some formal differences, the outcomes of the normalization of Hamiltonians with either a finite, or a non-finite number of Fourier terms, are not so different in the end. More on this topic is discussed in section 3.

Recursive normalization algorithm with Lie series

Assuming r algorithm steps have been completed:

1) Isolate from the Hamiltonian $H^{(r)}$ (Eq.(35)) the terms in $H^{(r)}_{r+1}$ to be eliminated at the present step, i.e. $h^{(r)}_{r+1}$.

2) Solve the homological equation (36) and define χ_{r+1}.

3) Implement Eq.(37) and compute $H^{(r+1)}$. This contains a normal form part:

$$Z^{(r+1)} = Z_0 + \lambda Z_1 + ... + \lambda^r Z_r + \lambda^{r+1} Z_{r+1}$$

and a remainder part

$$R^{(r+1)} = \lambda^{r+2} H^{(r+1)}_{r+2} + \lambda^{r+3} H^{(r+1)}_{r+3} + \dots$$

The reader is invited to accomplish, for practice, the second normalization step in our example treated in subsection 2.4. We give, for verification, the form of the generating function χ_2:

$$\chi_2 = \lambda^2 i \Bigg(1.12901 \times 10^{-6} (e^{i(2\psi+\phi)} - e^{-i(2\psi+\phi)})$$

$$-1.22119 \times 10^{-5} (e^{i(2\psi-\phi)} - e^{-i(2\psi-\phi)}) + 6.28249 \times 10^{-5} (e^{i\phi} - e^{-i\phi})$$

$$-0.018660 I_\psi (e^{i\psi} - e^{-i\psi})$$

$$-(3.24662 I_\psi + 1.31757 I_\psi^2) \times 10^{-4} (e^{i(\psi+\phi)} - e^{-i(\psi+\phi)})$$

$$-(0.00915214 I_\psi + 0.00371419 I_\psi^2)(e^{i(\psi-\phi)} - e^{-i(\psi-\phi)})$$

$$+(2.01901 + 0.81937 I_\psi) \times 10^{-6} (e^{2i\phi} - e^{-2i\phi}) \Bigg) \quad .$$

The new Hamiltonian, after the second normalization, is given by:

$$H^{(2)} = \exp(L_{\chi_2}) H^{(1)} \quad . \tag{39}$$

Restoring the numerical value of λ, i.e. $\lambda = 1$, the Hamiltonian $H^{(2)}$ is in normal form up to terms of order 2, namely (omitting a constant):

$$H^{(2)} = (1.4641016 - 3.27748 \times 10^{-6}) I_\psi + I + \frac{I_\psi^2}{2} + O(\lambda^3) \quad .$$

We observe that the normalization procedure generated a small frequency correction even to the term linear in the action I_ψ.

On the other hand, the remainder is

$$R^{(2)} = \lambda^3 H^{(2)}_3 + \lambda^4 H^{(2)}_4 + \dots \tag{40}$$

The leading term in the remainder is $H^{(2)}_3$. This contains 75 terms, thus it is unpractical to reproduce here. In fact, beyond the second order, calculations

are all together hard to do without use of a computer-algebraic program. However, we can predict some features of the term $\lambda^3 H_3^{(2)}$. In the series (39), the terms contributing to $H_3^{(2)}$ are just $H_3^{(1)}$ and $\{Z_1, \chi_2\}$. The term $H_3^{(1)}$ can be analyzed itself in terms of Eq.(34), and it is found to contain contributions from $(1/2)\{\{H_1^{(0)}, \chi_1\}, \chi_1\}$, and $(1/6)\{\{\{Z_0, \chi_1\}, \chi_1\}, \chi_1\}$. We thus start seeing, now, that the overall effect of the normalization procedure is to 'propagate' the initial Hamiltonian terms at higher and higher orders via multiple Poisson brackets with one or more of the generating functions χ_1, χ_2, etc. As we have seen already in subsection 2.4, a main effect of this process is the generation of new harmonics, as the normalization proceeds. Namely, taking the Poisson bracket between any two terms of the form $ae^{\pm i(k_1\psi + k_2\phi)}$ and $be^{\pm i(m_1\psi + m_2\phi)}$, with at least one of the coefficients a, or b, depending on the action I_ψ, we find new terms according to

$$\{ae^{\pm i(k_1\psi + k_2\phi)}, be^{\pm i(m_1\psi + m_2\phi)}\} \rightarrow \text{New Fourier terms } \; e^{\pm i((k_1 \pm m_1)\psi + (k_2 \pm m_2)\phi)} \quad .$$

Since two out of the four possible (plus or minus) combinations of the expressions $|k_1 \pm m_1| + |k_2 \pm m_2|$ are larger from both $|k_1| + |k_2|$, and $|m_1| + |m_2|$, we see that the result of the Poisson brackets acting via the Lie operator is to generate new Fourier harmonics, of higher and higher order, at consecutive normalization steps. Thus, for example, we can check that the term $H_3^{(2)}$ contains harmonics beyond the order 3, namely the harmonics:

$$H_3^{(2)} \rightarrow e^{i(2\psi \pm 2\phi)}, \; e^{i(\psi \pm 3\phi)}, \; e^{i(3\psi \pm 2\phi)} \quad .$$

In subsection 2.7 we analyze how the appearance of harmonics of increasing order affects the *convergence properties* of the whole normalization process presently examined. We will see that these harmonics result in the appearance of new divisors, which, in turn, affect the growth rate of the series terms at successive normalization steps.

2.6. Practical benefits from the normal form computation

The practical question now is: what is our benefit from computing a normal form as above? In particular, can we advance our understanding of the dynamics by a normal form computation in a system like (3) with respect to a purely numerical investigation of the orbits?

Two main ways to benefit from computing a normal form are related to explicitly computing the *normalizing transformation* by which we pass from the old to the new canonical variables, and vice versa. Consider first the transformation yielding the old variables in terms of the new variables. After r normalization steps, this is given by a *composition of Lie series*:

$$\begin{aligned} \psi &= \exp(L_{\chi_r}) \exp(L_{\chi_{r-1}}) ... \exp(L_{\chi_1}) \psi^{(r)} \\ \phi &= \exp(L_{\chi_r}) \exp(L_{\chi_{r-1}}) ... \exp(L_{\chi_1}) \phi^{(r)} \\ I_\psi &= \exp(L_{\chi_r}) \exp(L_{\chi_{r-1}}) ... \exp(L_{\chi_1}) I_\psi^{(r)} \\ I &= \exp(L_{\chi_r}) \exp(L_{\chi_{r-1}}) ... \exp(L_{\chi_1}) I_\psi^{(r)} \quad . \end{aligned} \tag{41}$$

The net result of Eqs.(41) is to find series expressions of the form

$$\begin{aligned} \psi &= F_\psi(\psi^{(r)}, \phi^{(r)}, I_\psi^{(r)}, I^{(r)}) \\ \phi &= F_\phi(\psi^{(r)}, \phi^{(r)}, I_\psi^{(r)}, I^{(r)}) \\ I_\psi &= F_{I_\psi}(\psi^{(r)}, \phi^{(r)}, I_\psi, I^{(r)}) \\ I &= F_I(\psi^{(r)}, \phi^{(r)}, I_\psi^{(r)}, I^{(r)}) \end{aligned} \tag{42}$$

in which the old canonical functions are expressed in terms of the new canonical variables[11]. However, in our example of subsections 2.4 and 2.5, after a normal form has been computed, the time evolution of the new canonical variables under the normal form dynamics alone (i.e. ignoring the effect of the remainder) can itself be easily computed. In fact, since our normal form depends only on the actions $I_\psi^{(r)}, I^{(r)}$, both $I_\psi^{(r)}$ and $I^{(r)}$ are *integrals* of the normal form dynamics. This also determines the frequencies by which the angles $\psi^{(r)}$ and $\phi^{(r)}$ evolve. In summary, we have the following time evolution of all new canonical variables:

$$\begin{aligned} I_\psi^{(r)}(t) &= I_{\psi,0}^{(r)} \\ I^{(r)}(t) &= I_0^{(r)} \\ \psi^{(r)}(t) &= \left(\psi_0^{(r)} + \left. \frac{\partial Z^{(r)}}{\partial I_\psi^{(r)}} \right|_{I_{\psi,0}^{(r)}, I_0^{(r)}} \right) t \\ \phi^{(r)}(t) &= \left(\phi_0^{(r)} + \left. \frac{\partial Z^{(r)}}{\partial I^{(r)}} \right|_{I_{\psi,0}^{(r)}, I_0^{(r)}} \right) t \end{aligned} \tag{43}$$

where the constants $(\psi_0^{(r)}, \phi_0^{(r)}, I_{\psi,0}^{(r)}, I_0^{(r)})$ mark the initial conditions of an orbit computed in the new variables. Since in a numerical calculation we can usually know the initial conditions only in the old variables $\psi_0, \phi_0, I_{\psi,0}, I_0$, we need also the inverse canonical transformation (from old to new variables) to compute the constants $(\psi_0^{(r)}, \phi_0^{(r)}, I_{\psi,0}^{(r)}, I_0^{(r)})$. It is easy to verify that the latter is given by:

$$\begin{aligned} \psi^{(r)} &= \exp(-L_{\chi_1}) \exp(-L_{\chi_2}) ... \exp(-L_{\chi_r}) \psi \\ \phi^{(r)} &= \exp(-L_{\chi_1}) \exp(-L_{\chi_2}) ... \exp(-L_{\chi_r}) \phi \\ I_\psi^{(r)} &= \exp(-L_{\chi_1}) \exp(-L_{\chi_2}) ... \exp(-L_{\chi_r}) I_\psi \\ I^{(r)} &= \exp(-L_{\chi_1}) \exp(-L_{\chi_2}) ... \exp(-L_{\chi_r}) I \quad . \end{aligned} \tag{44}$$

Substituting the values of the initial conditions $(\psi_0, \phi_0, I_{\psi,0}, I_0)$ in Eqs.(44) we then find the constants $(\psi_0^{(r)}, \phi_0^{(r)}, I_{\psi,0}^{(r)}, I_0^{(r)})$, and, thereby, the whole time evolution of an orbit in the new variables via Eqs.(43). But then, substituting the

[11] Of course, in the computer we can only store a finite truncation of such series.

expressions for $\psi^{(r)}(t)$, $\phi^{(r)}(t)$, $I_\psi^{(r)}(t)$, and $I^{(r)}(t)$ in the transformation (41), we can obtain an analytical formula for $\psi(t)$, $\phi(t)$, $I_\psi(t)$, and $I(t)$, i.e. for the time evolution of the old variables as well. That is, using the normal form we can obtain an analytical *quasi-periodic representation of the time evolution of all canonical variables for regular orbits.*

What is the precision level of such a representation? This is of the same order as the difference between the normal form dynamics and the true dynamics, implying that *the precision level of normal form calculations is of the order of the size of the remainder* $R^{(r)}$. In a realistic computation, aimed, for example to represent the orbit of a planet or an asteroid in the solar system, or the motion of a satellite around a planet, the size of the remainder can be used in the above sense in order to estimate the timescale up to which a normal form computation yields a useful prediction. This timescale is essentially given by the inverse of the size of the remainder function.

The second way in which Eqs.(41) are useful regards the possibility to parametrically represent the invariant surfaces on which lie the regular orbits, i.e., in our example, the rotational tori on which the orbits evolve quasi-periodically. In fact, the parametrization is provided, precisely, by Eqs.(41). This is trivial to see, since the values of $I_\psi^{(r)}$ and $I^{(r)}$, which are integrals of motion, can be replaced by the constants $(I_{\psi,0}^{(r)}, I_0^{(r)})$, which act as labels for invariant tori. After this replacement, all the old variables $(\psi_0, \phi_0, I_{\psi,0}, I_0)$ are given by equations depending on two parameters, namely $\psi^{(r)}$ and $\phi^{(r)}$. Thus, we have the definition of a surface topologically equivalent to a two-torus, which we can actually explicitly compute by taking many values of both angles $\psi^{(r)}$ and $\phi^{(r)}$ in the interval $[0, 2\pi)$.

Let us see the above properties in practice, by explicitly performing the associated calculations in our working example of subsections 2.4 and 2.5, up to a normalization order $r = 2$. Since χ_1 and χ_2 are given, it is straightforward to compute the transformations (41), expanding both exponentials up to order 2 in the book-keeping parameter λ. Recalling that $\chi_1 = O(\lambda)$ and $\chi_2 = O(\lambda^2)$, we have:

$$\exp(L_{\chi_2})\exp(L_{\chi_1}) = (1 + L_{\chi_2} + \frac{1}{2}L_{\chi_2}^2 + ...)(1 + L_{\chi_1} + \frac{1}{2}L_{\chi_1}^2 + ...)$$

$$= 1 + L_{\chi_1} + \frac{1}{2}L_{\chi_1}^2 + L_{\chi_2} + O(\lambda^3) \quad .$$

Passing from exponentials back to trigonometric expressions, and setting $\lambda = 1$, we then find (using the expressions found in previous pages for χ_1 and χ_2):

$$\psi = \psi^{(2)} + 0.0373205\sin(\psi^{(2)}) + 1.11928 \times 10^{-6}\sin(2\psi^{(2)})$$

$$+0.01486\left(1 + I_\psi^{(2)}\right)\sin(\psi^{(2)} - \phi^{(2)}) - 1.63874 \times 10^{-6}\sin(2\phi^{(2)})$$

$$+5.27027 \times 10^{-4} I_\psi^{(2)}\sin(\psi^{(2)} + \phi^{(2)}) + 2.97135 \times 10^{-6}\sin(2\psi^{(2)} - 2\phi^{(2)})$$

$$+1.05405 \times 10^{-7}\sin(2\psi^{(2)} + 2\phi^{(2)}) + \ldots$$

$$I_\psi = 1.51629 \times 10^{-5} + 1.00001 I_\psi^{(2)} + \left(0.054641 - 0.0.037320 I_\psi^{(2)}\right) \cos(\psi^{(2)})$$
$$+1.11928 \times 10^{-4} \cos(\phi^{(2)}) + \left(5.51603 + 2.23856 I_\psi^{(2)}\right) \times 10^{-6} \cos(2\phi^{(2)})$$
$$+ \left(0.00849504 - 0.014857 I_\psi^{(2)} - 0.0074284 (I_\psi^{(2)})^2\right) \cos(\psi^{(2)} - \phi^{(2)})$$
$$-4.88476 \times 10^{-5} \cos(2\psi^{(2)} - \phi^{(2)})$$
$$+ \left(0.0016 - 2.63513 \times 10^{-4} (I_\psi^{(2)})^2\right) \cos(\psi^{(2)} + \phi^{(2)})$$
$$+4.51602 \times 10^{-6} \cos(2\psi^{(2)} + \phi^{(2)}) + \ldots$$

We also have

$$\phi = \phi^{(2)} \quad ,$$

i.e. the angle ϕ obeys the identity transformation. This is a particular feature of Hamiltonian systems like (3), i.e. where some angles (and their conjugate dummy actions) were artificially introduced to account for the time-dependent trigonometric terms. In fact, we observe that the dummy action I does not appear in any of the above expressions, or the expressions found for the Lie generating functions χ_r.

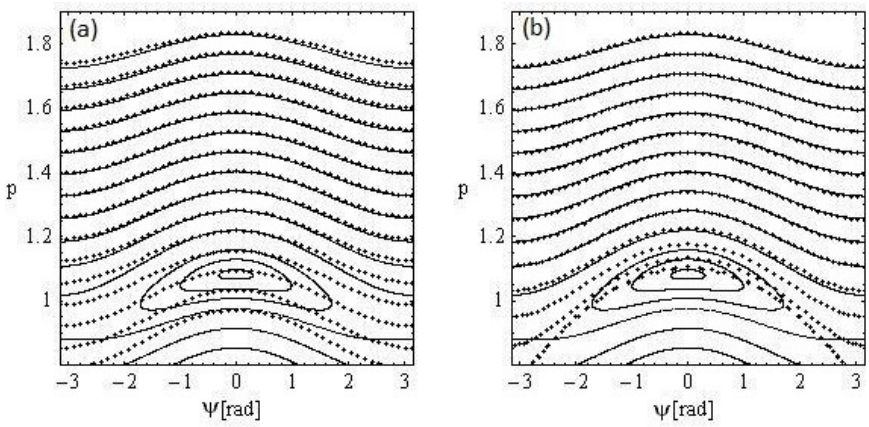

Figure 2. Numerical (solid) and theoretical (dotted) invariant curves after a hamiltonian normalization (see text) up to the maximum normalization order $r_{max} = 2$ (left panel), or $r_{max} = 8$ (right panel). There are 15 theoretical invariant curves shown, corresponding to the constant 'label' values of $I_\psi^{(2)}$ (in panel (a), or $I_\psi^{(8)}$, respectively, in panel (b)) given by $I_\psi^{(2)} = 0.065n - 0.008$, $n = -9, -8, \ldots, 5$.

How well can the above transformations account for a precise analytical description of motions on rotational tori? Figure 2 shows a comparison between the theoretical invariant curves arising from the above expressions and the true invariant curves corresponding to the intersection of the rotational invariant tori

in the domain $0.5 \leq p \leq 1.3$, with the surface of section $\phi(mod 2\pi) = 0$. The theoretical invariant curves are computed as follows: due to the surface of section condition, we first set $\phi^{(2)} = \phi = 0$. Then, we are left with expressions yielding ψ and I_ψ each in terms of $\psi^{(2)}$ and $I_\psi^{(2)}$. However, $I_\psi^{(2)}$ is an integral under the normal form dynamics. Thus, each (constant) value of $I_\psi^{(2)}$ represents a label value for one rotational torus. In particular, the value $I_\psi^{(2)} = 0$ represents a torus around the value $p = p_* = 1.46410$ in the original variables. By fixing a value for $I_\psi^{(2)}$, and giving several values to $\psi^{(2)}$ in the interval $0 \leq \psi^{(2)} < 2\pi$, we compute both ψ and I_ψ (and hence $p = p_* + I_\psi$) via the transformation equations. This yields theoretical invariant curves that can be compared to the numerical invariant curves on the surface of section.

Figure 2a shows this comparison using the normal form computation up to second order in λ, for which the explicit parametric formulae corresponding to invariant curves are given above. The theoretical invariant curves are shown by thick dotted lines, superposed to the true invariant curves. We see that, already at this order of approximation, the theoretical invariant curves explain the shape of the true invariant curves in a domain above $p = 1.2$, although they have visible differences from them (of order 10^{-2}). The approximation becomes worse as we approach closer to the separatrix of an island of stability located in the lower part of the figure. In fact, we observe that the theoretical invariant curves cannot represent the shape of the invariant curves in *resonant domains*, i.e. where islands of stability are formed. This is due to the fact that the basic frequencies ω_* and ω employed in the current normal form construction are non resonant. We will see, however (subsection 2.9) that it is possible to make a so-called resonant normal form construction, accounting locally for the dynamics within resonant domains of the model (3) that give rise to island chains as the one shown in Fig.2.

On the other hand, far from resonant domains the local approximation by the theoretical invariant curves becomes better, at least for low orders, as we increase the order of normalization. Thus, Fig.2b shows the comparison between theoretical and numerical invariant curves when the maximum normalization order is equal to $r = 8$. We now see that in the domain $p > 1.2$ the theoretical invariant curves nearly coincide with the true ones, as there are no visible differences in the scale of Fig.2b. In fact, the accuracy of the approximation at this order can be checked to be of the order of 10^{-4}, and the same result is reached by checking the time variations of the quantity $I_\psi^{(8)}(t)$, which is an integral of the normal form dynamics, when computed along the numerical orbits lying on some invariant curves of Fig.2.

2.7. (Non-)Convergence properties. Small divisors

So far, we have seen that a normal form computation already at an order as low as two may provide a useful practical representation of the regular motions of a system under study. Furthermore, calculations like the one of Fig.2 yield the impression that by going to higher and higher normalization order, we can approximate regular motions up to any desired level of accuracy. However, one can see that by the method of Birkhoff normalization exposed in subsections

2.4 and 2.5, this is *not* possible, i.e., there is a *finite precision level* reached at an optimal order, beyond which the above method does not converge. This is because the normalization algorithm of subsection 2.5 leads to a sequence of remainder values, as a function of the normalization order r, which is not a convergent, but only an *asymptotic* sequence.

Let $||R^{(r)}||_{W^{(r)}}$ denote a suitably defined norm for the remainder series $R^{(r)}$ at the r-th normalization step, that gives the size of the remainder in a subdomain $W^{(r)}$ of the phase space contained in the domain of analyticity of the function $R^{(r)}$.[12] Our statement on non-convergence of the Birkhoff normalization process can be formulated as follows:

i) If the initial Hamiltonian is an analytic function in an open domain $W^{(0)}$ of the phase space, then, for arbitrarily high normalization order r, there is a domain $W^{(r)}$, which is a restriction of the initial analyticity domain $W^{(0)}$, in which the remainder $R^{(r)}$ is an analytic function with bounded norm, i.e. $||R^{(r)}||_{W^{(r)}} < \infty$.

ii) The sequence $||R^{(r)}||_{W^{(r)}}$, for $r = 1, 2, 3, \ldots$ has an asymptotic behavior. Thus, initially (at low orders) $||R^{(r)}||_{W^{(r)}}$ decreases as r increases, up to an optimal order r_{opt} at which $||R^{(r_{opt})}||_{W^{(r_{opt})}}$ becomes minimum. Then, for $r > r_{opt}$, we find that $||R^{(r)}||_{W^{(r)}}$ increases with r, and we have $||R^{(r)}||_{W^{(r)}} \to \infty$ as $r \to \infty$.

iii) *Exponential stability:* under particular assumptions for the original Hamiltonian, we find that the optimal remainder is exponentially small in a small parameter μ, namely

$$||R^{(r_{opt})}||_{W^{(r_{opt})}} \sim \exp\left(-\left(\frac{\mu_0}{\mu}\right)^b\right) \tag{45}$$

where μ_0 and b are positive constants and μ is a parameter related to small quantities appearing in the problem under study. Thus, in the Hamiltonian (3) we can construct exponential estimates where μ coincides with ϵ, but also, for fixed ϵ and p_*, estimates where μ gives the distance from p_* (e.g. coinciding with the variable I_ψ).

Let us make some additional comments on statements (i) to (iii) above.

Regarding (i), a common misunderstanding is that by computing normal forms at higher and higher order r, there is a finite order r beyond which the Hamiltonian $H^{(r)} = Z^{(r)} + R^{(r)}$ becomes a divergent series for any possible datum

[12] The author recognizes that too much is said at this point in only one sentence, without detailed explanation. But my purpose is to avoid at this point a detailed reference on how we deal with domains and norms in the functional space of interest in normal form theory, because such reference would distract us considerably from the main line of thought, concerning the practical implementation of normal forms in concrete problems. But we will return to the technical aspects on this issue in subsections 3.3 and 4.2, giving, in 4.2, a more precise definition of the so-called *Fourier-weighted norm*, convenient in the study of the analyticity properties of the various functions appearing in the implementation of normal form theory.

in the phase space. In fact, we can show that for an arbitrarily high value of r, there is always a certain domain $W^{(r)}$ where we have convergence of $H^{(r)}$. However, our interest is in characterizing particular orbits lying in a certain domain of the phase space, denoted, say, by W_{orbits}, whose size depends only on the initial conditions and the time evolution of the orbits themselves, and not on the normal form that we compute for their study. On the other hand, as r increases, the analyticity domain $W^{(r)}$ of the normal form series becomes smaller and smaller. Thus, there comes a critical order r_c, beyond which the domain W_{orbits} is no longer included in $W^{(r)}$. Then, further normalization becomes pointless. It is in this sense that we speak about "the divergence of the Birkhoff series". [13]

(ii) Not every form of perturbation theory leads to a divergent sequence of remainders. In fact, by changing our normalization strategy we can be lead to a convergent normalization. This is exactly the case, for example, of the so-called Kolmogorov algorithm, examined in subsection 2.8, which leads to a normal form allowing to prove the existence of particular solutions lying on invariant tori. However, we will see also that such a normal form implies that the dynamics, in general, is non-integrable in any open domain around one KAM torus. Thus, the convergence in that case is achieved at the cost of giving up the effort to construct local integrals of motion valid in open domains of the action space.

(iii) The fact that we can have an exponentially small remainder implies that in a Hamiltonian of the form $H = H_0 + \epsilon H_1$ the effect of the perturbation term ϵH_1 should not be considered as entirely destroying the regular character of motions due to H_0. In fact, the largest part of the perturbation only causes *deformation effects*, i.e. it deforms the orbits (and the invariant tori) with respect to the orbits (or tori) in the system with Hamiltonian H_0, and only an

---

[13] This is not the whole story. The way by which we restrict domains as we move forward at successive normalization steps depends itself crucially on the way by which we have chosen to construct the normal form, and, in particular, on the choice of 'Hori kernel' (see footnote 7). In fact, if the function Z_0 playing the role of Hori kernel depends on the action variables by terms of order higher than linear, the way by which we restrict domains is dictated by the requirement to avoid *resonances* in the action space. As an example, if, in the Hamiltonian (3) we chose to include $I_\psi^2/2$ in Z_0, i.e. to follow the book-keeping of Eq.(25), then, it is easy to check that the resulting homological equations appearing in the construction of the Birkhoff normal form are equations of the form

$$\{\omega_* I_\psi + \omega I + \frac{I_\psi^2}{2}, \chi_r\} + h_r^{(r-1)} = 0$$

for some functions $h_r^{(r-1)}$ determined along the normalization process. But then, it is easy to check that χ_r contains divisors of the form $k_1(\omega_* + I_\psi) + k_2\omega$, i.e. linearly depending on the action I_ψ. Assuming, now, that trigonometric terms $\exp(i(k_1\phi_1 + k_2\phi_2))$ of *all* possible wave vectors (k_1, k_2) are generated as we proceed in successive normalization steps (or, as in other models examined in section 3, that they are present already from the start) we can see that a construction of this form cannot be defined in any *open interval* of values of the action I_ψ on the real axis. This is because there is a dense set of values $I_\psi = -\omega_* - (k_2/k_1)\omega$ for which some divisor in the series, at some order, will become *equal to zero exactly*. Thus, with such a normalization scheme, we can only proceed by 1) an algorithm eliminating only a finite number of harmonics at every step, and 2) excluding particular values of the action I_ψ (and some interval around them) from the domain in I_ψ where the series can be valid.

exponentially small part is responsible for long term effects on the stability of orbits. This fact becomes particularly relevant when we examine the speed of diffusion in multidimensional systems, i.e. the phenomenon of Arnold diffusion (section 4).

The asymptotic properties of the normalization process can be seen in our perturbed pendulum example in the following way: After r normalization steps, we find that the remainder function has the following structure:

$$R^{(r)} = H^{(r)}_{r+1} + H^{(r)}_{r+2} + \ldots \tag{46}$$
$$= \sum_{s=r+1}^{\infty} \left(\sum_{\substack{|k_1|+|k_2|\leq 2s-1 \\ k_1,k_2}} \left(b^{(s)}_{k_1,k_2,0} + b^{(s)}_{k_1,k_2,1} I_\psi + \ldots + b^{(s)}_{k_1,k_2,r} (I_\psi)^r \right) e^{i(k_1\psi + k_2\phi)} \right)$$

with real coefficients $b^{(s)}_{k_1,k_2,n}$. We recall again that I_ψ in this expression means the *transformed* action variable $I^{(r)}_\psi$, after r consecutive Lie transformations. Also, the fact that with increasing s we also have an increasing maximum Fourier order $|k_1| + |k_2| \leq 2s - 1$ has been explained in the previous subsection, i.e. the higher order harmonics are generated by the action of repeated Poisson brackets via the Lie operation defining $H^{(r)}$.

If, now, we consider a domain in action space centered around the value $p = p_*$ (which is the origin of our construction), we can estimate the size of the remainder in the interval $-\Delta I_\psi \leq I_\psi \leq \Delta I_\psi$ by taking, e.g., a so-called *majorant series*, i.e. a series in which we take the absolute sum of all terms in Eq.(46), namely:

$$||R^{(r)}||_{\Delta I_\psi} = \tag{47}$$
$$\sum_{s=r+1}^{\infty} \left(\sum_{\substack{|k_1|+|k_2|\leq 2s-1 \\ k_1,k_2}} \left(|b^{(s)}_{k_1,k_2,0}| + |b^{(s)}_{k_1,k_2,1}| \Delta I_\psi + \ldots + |b^{(s)}_{k_1,k_2,r}| (\Delta I_\psi)^r \right) \right) .$$

In the computer we cannot store infinitely many remainder terms, thus we have to rely on a finite truncation of the sum (47) at a maximum order s_{max}:

$$||R^{(r)}||_{\Delta I_\psi, \leq s_{max}} = \tag{48}$$
$$\sum_{s=r+1}^{s_{max}} \left(\sum_{\substack{|k_1|+|k_2|\leq 2s-1 \\ k_1,k_2}} \left(|b^{(s)}_{k_1,k_2,0}| + |b^{(s)}_{k_1,k_2,1}| \Delta I_\psi + \ldots + |b^{(s)}_{k_1,k_2,r}| (\Delta I_\psi)^r \right) \right)$$

checking numerically that s_{max} is sufficiently large for the quantity $||R^{(r)}||_{\Delta I_\psi, \leq s_{max}}$ to have practically reached the remainder's limiting value (which corresponds to $s_{max} \to \infty$).

The computation of the quantity $||R^{(r)}||_{\Delta I_\psi, \leq s_{max}}$ allows us to test the convergence properties of the adopted Birkhoff normalization. Namely, by computing the value of $||R^{(r)}||_{\Delta I_\psi, \leq s_{max}}$ as a function of the normalization order r, we can check up to what order $||R^{(r)}||_{\Delta I_\psi, \leq s_{max}}$ keeps decreasing with r. In a

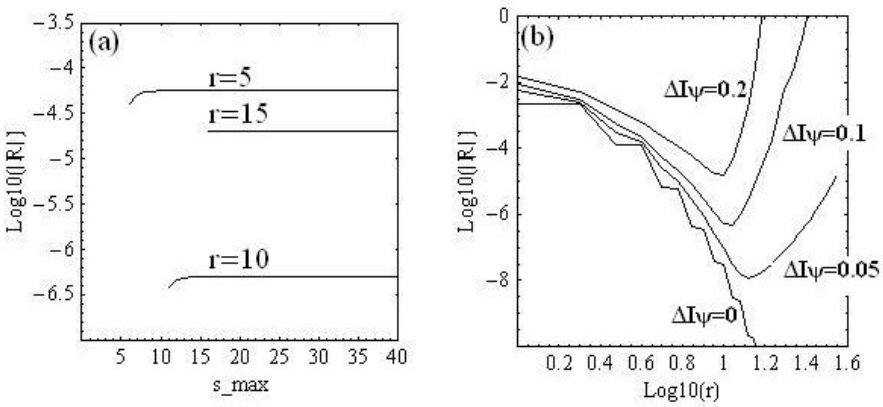

Figure 3. (a) The numerically computed value of the remainder $||R^{(r)}||_{\Delta I_\psi, \leq s_{max}}$ (Eq.(48)), as a function of the truncation order s_{max}, for the Birkhoff normal form computation of subsections 2.4 and 2.5, for $\Delta I_\psi = 0.1$, and for three different normalization orders, namely $r = 5$, $r = 10$, $r = 15$. The fact that in all three cases $||R^{(r)}||_{\Delta I_\psi, \leq s_{max}}$ stabilizes to a final value as s_{max} increases indicates that the remainder series is absolutely convergent in the domain considered. (b) The quantity $||R^{(r)}||_{\Delta I_\psi, \leq 40}$ for four different values of ΔI_ψ, namely $\Delta I_\psi = 0$, $\Delta I_\psi = 0.05$, $\Delta I_\psi = 0.1$, and $\Delta I_\psi = 0.2$ (curves from bottom to top respectively).

convergent process, we should have $||R^{(r)}||_{\Delta I_\psi, \leq s_{max}} \to 0$ as $r \to \infty$. In reality, however, we find that $||R^{(r)}||_{\Delta I_\psi, \leq s_{max}}$ reaches a minimum at a finite order r.

Figure 3 shows such a numerical test, which illustrates the asymptotic behavior of the remainder for the Birkhoff normal form calculation of our example of subsections 2.4 and 2.5. In producing this figure, we have used a computer program in fortran[14] which computes normal forms up to a high order. We set the maximum truncation order as $s_{max} = 40$, and proceed up to the maximum normalization order $r_{max} = 35$. Figure 3a shows a numerical probe of the convergence of the remainder function in a domain indicated in the figure caption. We set $\Delta I_\psi = 0.1$, and, for different normalization orders r, we compute the truncated remainder at various truncation orders s_{max} in the range $r < s_{max} \leq 40$. The figure shows the value of $||R^{(r)}||_{\Delta I_\psi, \leq s_{max}}$, in the examples of three different normalization orders, namely $r = 5$, $r = 10$, and $r = 15$, as a function of the truncation order s_{max}. Clearly, we see that in all three cases the value of $||R^{(r)}||_{\Delta I_\psi, \leq s_{max}}$ stabilizes as s_{max} increases, indicating the absolute convergence of the remainder function in the domain considered. However, we also observe that the value of $||R^{(r)}||_{\Delta I_\psi, \leq s_{max}}$ for both $r = 5$ and $r = 15$ is *higher* than its value for $r = 10$. This fact implies that the value of the remainder becomes minimum for some normalization order between $r = 5$ and $r = 15$. This is clearly shown in Fig.3b, showing the evolution of the quantity $||R^{(r)}||_{\Delta I_\psi, \leq 40}$, as a function of r, in four different cases, namely $\Delta I_\psi = 0$, $\Delta I_\psi = 0.05$, $\Delta I_\psi = 0.1$, and

[14] All the programs used by the author for this tutorial are freely available upon request.

$\Delta I_\psi = 0.2$. Except for the first case, where we have not reached a minimum of $||R^{(r)}||_{\Delta I_\psi, \leq 40}$ up to $r = 35$, in all other cases we find that the minimum occurs at an order within the range considered in Fig.3b. In the case $\Delta I_\psi = 0.1$ (referring to Fig.3a), the optimal normalization order, as indicated by the corresponding minimum in Fig.3b, is $r = 11$ ($\log_{10}(r) = 1.04$). Furthermore, we observe that the optimal normalization order decreases as ΔI_ψ increases, while the optimal remainder value $||R^{(r_{opt})}||_{\Delta I_\psi, \leq 40}$ increases with increasing ΔI_ψ. Despite this increase, however, for $\Delta I_\psi = 0.2$ we still have a rather small optimal remainder value, of order $\sim 10^{-5}$, which indicates that the so-computed normal form still approximates reasonably well the true dynamics.

We now focus on the following basic question: what is the cause of the asymptotic behavior of the remainder shown in figure 3? We can see that, despite the fact that in every normalization step we eliminate from the Hamiltonian terms of higher and higher book-keeping order, the process becomes divergent due to the presence in the series of *small divisors*, and, in particular, due to the fact that these divisors exhibit a bad *accumulation* in the denominators of the series terms.

We recall that small divisors appear in the series due to the solution of the homological equation (36) for all generating functions χ_1, χ_2, etc. More precisely, if the terms to be eliminated at the r-th normalization step (denoted by $h_r^{(r-1)}$) are written in the form of a sum of Fourier terms

$$h_r^{(r-1)} = \sum_{k_1,k_2 \notin \mathcal{M}} b_{k_1,k_2}^{(r-1)}(I_\psi, I) e^{i(k_1\psi + k_2\phi)} \tag{49}$$

the homological equation (36) (written for the order r rather than $r+1$) is satisfied by setting χ_r equal to:

$$\chi_r = \lambda^r \sum_{k_1,k_2 \notin \mathcal{M}} \frac{b_{k_1,k_2}^{(r-1)}(I_\psi, I)}{i(k_1\omega_* + k_2\omega)} e^{i(k_1\psi + k_2\phi)} \quad . \tag{50}$$

Equation (50) contains divisors of the form $k_1\omega_* + k_2\omega$. Notice that in Eqs.(49) and (50), we have changed the way by which we denote those wavenumbers (k_1, k_2) which are excluded from the sum in the r.h.s. Namely, instead of writing $|k_1| + |k_2| \neq 0$ (as in Eq.(33)), we use a new symbol, $\mathcal{M}$, to denote the set of all excluded wavenumbers. This set is called the *resonant module*. In most forms of perturbation theory, the resonant module is determined by the requirement that no extremely small divisors, or divisors equal to zero exactly, appear in the solution (50). In fact, if ω_* and ω are incommensurable, the only possibility for $k_1\omega_* + k_2\omega = 0$ is provided by both k_1 and k_2 being equal to zero. Thus, if we choose the resonant module by the requirement to exclude the appearance of only zero divisors, the resonant module is:

$$\mathcal{M} = \{k_1, k_2 : |k_1| + |k_2| = 0\} \quad .$$

However, we will see below (subsection 2.9) that in the theory of *resonant normal forms* the so-arising resonant module necessarily contains also non-zero wavevectors (k_1, k_2).

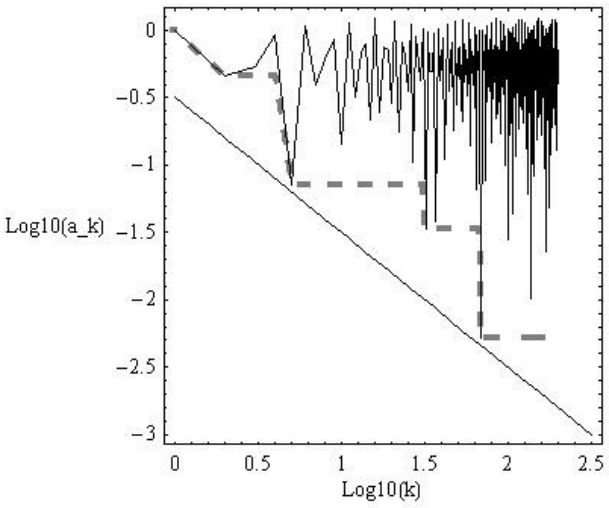

Figure 4. The minimum divisor a_k (Eq.(51) as a function of the order k of the divisor in our numerical example (solid curve). The gray dashed curve shows the minimum divisor that appears up to the order k. The straight line represents a low 'diophantine' bound for small divisors explained in subsection 2.8 (see Eq.(62)).

It is possible to see now that, even after the choice of a resonant module, we are always left in a series with non-zero, but quite small divisors. These divisors exist as a consequence of the fact that even incommensurable frequencies form ratios which are close to rational numbers. Let us exemplify this with the frequencies used in our numerical example, namely $\omega_* = 2(\sqrt{3}-1) = 1.4641016151377546...$, $\omega = 1$. We define $k = |k_1| + |k_2|$ as the *order* of the divisor $k_1\omega_* + k_2\omega$. Furthermore, we define the minimum of all divisors at a given order by:

$$a_k = \min\{|k_1\omega_* + k_2\omega| : |k_1| + |k_2| = k) \quad . \tag{51}$$

Figure 4 shows a_k as a function of k for the numerical frequencies of our example. We observe that at most orders k the smallest possible divisor a_k has relatively large size (above 10^{-1}, and most of them close to 1). However, there are particular orders at which quite small divisors appear. For example:

$$\text{order 5: } |2\omega_* - 3\omega| = 7.179677 \times 10^{-2}$$

$$\text{order 32: } |13\omega_* - 19\omega| = 3.332099 \times 10^{-2}$$

$$\text{order 69: } |28\omega_* - 41\omega| = 5.154776 \times 10^{-3} \quad .$$

These divisors form sharp reversed spikes in the curve a_k of Fig.4. What are the important effects they introduce? Let us consider, for example, the case of the divisor $a_{32} = 3.332099 \times 10^{-2}$. In our example, we have seen that at

the r-th normalization step the harmonics appearing in the Hamiltonian can be up to order $k = 2r - 1$. Thus, a term of the form $\exp(i(k_1\psi + k_2\phi))$ with $|k_1| + |k_2| = 32$ can only appear after the normalization order $r = 17$. However, once it appears, it generates a divisor a_{32} which could be as small as 3.3×10^{-2} in the series, via the solution of Eq.(50) for χ_{17}. The key point now is that this divisor *repeats appearing* at all subsequent normalization steps $r = 18$, $r = 19$, ..., thus generating a *sequence* of terms containing powers of this divisor, i.e. a_{32}, $(a_{32})^2$, ... [15]

By carefully studying our examples so far, it is easy to see that this repetition is a consequence of our chosen normalization scheme. To show this, let us consider a sequence of this type, which starts being formed after the normalization order $r = 17$. Due to Eq.(50), some term in χ_{17} acquires a divisor a_{32}. We introduce a heuristic (although rather unusual) notation to indicate this:

$$\chi_{17} \to \lambda^{17} \frac{e^{i32\Phi}}{a_{32}} \quad .$$

The above notation means: in χ_{17}, which has a book-keeping parameter λ^{17} in front, there are terms of Fourier order 32 containing small divisors bounded from below by a_{32}.

Let us now check how this divisor propagates at subsequent orders. The Hamiltonian normalization at $r = 17$ yields

$$H^{(17)} = \exp(L_{\chi_{17}}) H^{(16)} = H^{(16)} + \{H^{(16)}, \chi_{17}\} + ...$$

The Hamiltonian $H^{(16)}$ is in normal form up to order $O(\lambda^{16})$. Thus, at its lowest two orders we have

$$H^{(16)} = Z_0 + \lambda Z_1 + ...$$

Isolate now, in $H^{(17)}$, the following term, arising from the Poisson bracket $\{H^{(16)}, \chi_{17}\}$:

$$\{H^{(16)}, \chi_{17}\} \to \{\lambda Z_1, \chi_{17}\} = \left\{ \lambda \frac{I_\psi^2}{2}, \chi_{17} \right\} \to \left\{ \lambda \frac{I_\psi^2}{2}, \lambda^{17} \frac{e^{i32\Phi}}{a_{32}} \right\} \quad .$$

The last Poisson bracket produces a term whose size is rather easy to estimate, just thinking in the way by which the Poisson bracket derivatives act on the various parts of it. We have

$$\{ \frac{I_\psi^2}{2}, e^{i(k_1\psi + k_2\phi)} \} = -ik_1 I_\psi e^{i(k_1\psi + k_2\phi)} \quad .$$

---

[15] It is important to recall that, depending on the initial Hamiltonian model, a Fourier term $\exp(i(k_1\psi + k_2\phi))$ with the particular combination of wavenumbers (k_1, k_2) producing the smallest possible divisor at order 17 (i.e. in our example $\exp(\pm i(13\psi - 19\phi))$) may or may not have been generated in the normalized Hamiltonian. Thus, a correct reading of all estimates using divisors discussed hereafter is that these are *lower bound* estimates on the size of divisors, or upper bound estimates on the size of the various terms appearing in the series.

The wavenumber k_1 satisfies $|k_1| \leq 2r-1$, and typically we have the estimate that $|k_1|$ grows linearly with r, or $|k_1| = O(r)$. Thus we can write

$$\left\{ \lambda \frac{I_\psi^2}{2}, \lambda^{17} \frac{e^{i32\Phi}}{a_{32}} \right\} \to \lambda^{18} I_\psi \frac{O(17) e^{i32\Phi}}{a_{32}} \quad .$$

The key remark is that after all the operations, the new Hamiltonian contains the *same* Fourier term as before, but with a different coefficient. That is, by accomplishing one normalization step, besides the generation of new terms of higher and higher harmonics, we also have repetitions of terms of the same harmonics.

However, consider now the next normalization step. The term $\lambda^{18} I_\psi O(17)$ $e^{i32\Phi}/a_{32}$ is part of $h_{18}^{(17)}$, i.e. part of the Hamiltonian to be now normalized. The normalization will be done by the generating function χ_{18}. The crucial remark is, that due again to Eq.(50), the generating function χ_{18} will acquire a second divisor a_{32}, namely:

$$\chi_{18} \to \lambda^{18} \frac{I_\psi O(17) e^{i32\Phi}}{(a_{32})^2} \quad .$$

The same effect appears, now, at all subsequent normalization steps. As a result, after n steps the generating function χ_{17+n} contains a term with n divisors equal to a_{32}, i.e.:

$$\chi_{17+n} \to \lambda^{17+n} \frac{(I_\psi)^n 17^n e^{i32\Phi}}{(a_{32})^{n+1}}$$

Let us generalize: if a new small divisor appears at the normalization order $2r_0 - 1$, the associated term in the generating function produces a sequence of terms at subsequent steps, with coefficients growing *geometrically*:

$$\lambda^{r_0} \frac{1}{a_{2r_0-1}} \to \lambda^{r_0+1} \frac{I_\psi r_0}{a_{2r_0-1}^2} \to \lambda^{r_0+2} \frac{I_\psi^2 r_0^2}{a_{2r_0-1}^3} \ldots \tag{52}$$

The geometric ratio is just $I_\psi r_0/a_{2r_0-1}$, thus, the domain in action space where we expect the geometric progress to be convergent is given by requiring that $|I_\psi r_0/a_{2r_0-1}| < 1$ or:

$$|I_\psi| < a_{2r_0-1}/r_0 \quad . \tag{53}$$

But according to Fig.(4), as we move on to higher and higher order normalization steps, there are particular orders $r_0, r_0', r_0'', \ldots$ where new, smaller and smaller divisors, appear, and we have

$$a_{2r_0-1}/r_0 > a_{2r_0'-1}/r_0' > a_{2r_0''-1}/r_0'' > \ldots \tag{54}$$

Thus, we conclude that with the appearance of every new divisor, the normalization generates a new geometric sequence of terms *of smaller and smaller domain of convergence*. This ensures that the domain of convergence shrinks to zero as $r \to \infty$.

We have not yet answered why at the optimal normalization order we have an exponentially small estimate (Eq.(45)) for the size of the remainder. However, a heuristic derivation of such estimates can be given in more general models than the one considered up to now. Such a derivation will be made in section 4 (see subsection 4.2 and the Appendix).

2.8. Kolmogorov normal form and the existence of invariant tori

Let us summarize progress so far: we were able to employ a normalization algorithm in order to represent the rotational motions in the perturbed pendulum model (3) via normal forms. This renders possible a number of practical applications stemming from the analytic representation of the regular orbits in terms of series. However, we have seen also that the above normalization process is divergent, a fact implying that we can only reduce the size of the remainder to a finite (albeit, possibly, quite small) optimal lower bound. In many applications, this is sufficient, since we are interested just in approximating the true dynamics by some version of normal form dynamics. However, this type of approach leaves unanswered a question of central interest: can we *prove* that quasi-periodic motions exist? In other words, can we devise a *convergent* normalization algorithm, by which to determine unambiguously the existence of quasi-periodic trajectories moving on invariant tori?

A positive answer to this question is provided by the celebrated Kolmogorov (1954) - Arnold (1963) - Moser (1962) theorem (KAM), which proves the existence of a large set of invariant tori in nearly-integrable Hamiltonian systems satisfying some so-called *analyticity* and *non-degeneracy* conditions.

In the present section we present the normalization algorithm due to Kolmogorov, following a Lie series approach. Also, as in Giorgilli and Locatelli (1997), in our demonstration example we employ a *linear* scheme in which the normalization progresses, as usually, in ascending powers of λ. However, later in this subsection we explain also the so-called *quadratic* scheme, in which the normalization proceeds in groups of terms of book keeping order λ, then λ^2 and λ^3 in one step, then λ^4 to λ^7 in one step, etc. We also discuss why the two schemes are essentially equivalent as far as the accumulation of small divisors in the series terms is concerned. In fact, such accumulation leads to a so-called *quadratic convergence* of the Kolmogorov normal form. Finally, we discuss some practical advantages of Kolmogorov's algorithm with respect to Birkhoff's algorithm regarding the accuracy of computation of particular quasi-periodic solutions in the system (3).

We start with the basic idea of Kolmogorov's scheme, which is simple and drastic: so far, our normalization strategy has been to try to eliminate all terms depending on the angles from the Hamiltonian (3), or its transformed forms $H^{(1)}$, $H^{(2)}$ etc., hoping to give the Hamiltonian a form as close as possible to integrable. Clearly, however, the Hamiltonian (3) is not integrable. Thus, our effort resulted in a bad accumulation of divisors, which eventually causes the series to diverge. In Kolmogorov's scheme, instead, we abandon from the start the process of eliminating from the Hamiltonian *all* the terms depending on the angles. Instead, we only eliminate *a small subset* of terms depending on the angles, which, as shown below, are selected to be the terms preventing to establish the existence, under the Hamiltonian flow, of *a particular equilibrium solution* corresponding to motion on a torus with frequencies selected in advance. Thus, the Kolmogorov normal form continues to represent a non-integrable Hamiltonian, like the original one, which, however possesses a particular equilibrium solution corresponding to a torus.

To fix ideas, let us return to our usual example of the Hamiltonian (3). The first step in Kolmogorov's algorithm is the same as what we have done so far, i.e., to consider a fixed action value p_* and expand the Hamiltonian around it. This leads to the Hamiltonian (23). For reasons that will soon become clear, we now choose to change our book-keeping according to

$$\begin{aligned} H &= H_0 + \lambda H_1 = 1.46410 I_\psi + I + \frac{I_\psi^2}{2} \\ &- \lambda \left(0.08 \cos\psi + (0.0078851 + 0.0032 I_\psi) \cos\psi \cos\phi\right) \quad . \end{aligned} \tag{55}$$

We observe that the term H_0 has no dependence on the angles, while the term H_1 has such a dependence, and this is in terms which are either constant or linear in the actions. We now give the following definition:

Let $\mathbf{\Omega}$ be a $n-$dimensional frequency vector. A Hamiltonian function of the form

$$K = \mathbf{\Omega} \cdot \mathbf{I} + Z(\mathbf{I}) + H_1(\mathbf{I}, \phi) \tag{56}$$

where $(\mathbf{I}, \phi)$ are $n-$dimensional action-angle variables, is said to be 'in Kolmogorov normal form' if the functions $Z(\mathbf{I})$, $H_1(\mathbf{I}, \phi)$ are *at least quadratic* in the actions $\mathbf{I}$.

According to this definition, the Hamiltonian (55) is not in Kolmogorov normal form, since H_1 contains terms independent of the actions and linear in the action I_ψ.

Two points must be stressed:

i) A Hamiltonian like (56) is in general non-integrable, since it exhibits a non-linear coupling of the action - angle variables.

ii) However, the fact that Z and H_1 have quadratic (or higher order) dependence on the actions implies that the Hamiltonian K has a particular fixed point solution, i.e. the fixed point $\mathbf{I} = 0$. Indeed, taking into account the quadratic dependence we find immediately that Hamilton's equations for K read:

$$\begin{aligned} \dot{\phi} &= \frac{\partial K}{\partial \mathbf{I}} = \mathbf{\Omega} + O(\mathbf{I}) \\ \dot{\mathbf{I}} &= -\frac{\partial K}{\partial \phi} = O(\mathbf{I^2}) \quad . \end{aligned} \tag{57}$$

Thus, if we set $\mathbf{I} = 0$, we find $\dot{\mathbf{I}} = 0$, hence $\mathbf{I}(t) = 0$ at all times t. Furthermore, $\dot{\phi} = \mathbf{\Omega}$ yielding $\phi = \mathbf{\Omega} t + \phi_0$. Thus, in a Hamiltonian of the form (56) we have an invariant torus solution, with fixed frequencies $\mathbf{\Omega}$.

In summary, the Kolmogorov normal form is, in general, a non-integrable Hamiltonian which, however, is guaranteed to possess *one* solution lying on an invariant torus with fixed frequencies.

A Kolmogorov normalization algorithm is an algorithm intending to bring a particular Hamiltonian function in Kolmogorov normal form. For this to be possible, the original Hamiltonian must fulfil particular *analyticity* and *non-degeneracy* conditions. These conditions will be explained in section 3 below, where we give the general algorithm of computation of the Kolmogorov normal

form. Here, instead, we implement Kolmogorov's algorithm in the specific example of the Hamiltonian (55), showing the steps in some detail so as to facilitate further study of the general algorithm.

Starting from the Hamiltonian (55), in the first normalization step the aim is to bring the Hamiltonian in Kolmogorov normal form up to terms of degree 1 in the book-keeping parameter λ. One step is subdivided in the following three substeps:

Substep 1: Eliminate from $H^{(0)}$ all the $O(\lambda)$ terms depending on the angles and independent of the actions, using a generating function $\chi_{1,0}$. Compute the transformed Hamiltonian $H^{(1,0)} = \exp(L_{\chi 1,0})H^{(0)}$.

Substep 2: Eliminate from $H^{(1,0)}$ all the $O(\lambda)$ terms linear in the actions and independent of the angles, using a generating function $\chi_{1,c}$. Compute the transformed Hamiltonian $H^{(1,c)} = \exp(L_{\chi 1,c})H^{(1,0)}$.

Substep 3: Eliminate from $H^{(1,c)}$ all the $O(\lambda)$ terms linear in the actions and depending of the angles, using a generating function $\chi_{1,1}$. Compute the transformed Hamiltonian $H^{(1)} = \exp(L_{\chi 1,1})H^{(1,c)}$.

Let us implement these steps one by one:

i) Substep 1: elimination of $O(\lambda)$ terms independent of the actions and depending on the angles. These are:

$$h_{1,0}^{(0)} = -0.04\left(e^{i\psi} + e^{-i\psi}\right) - 0.0019712\left(e^{i(\psi+\phi)} + e^{-i(\psi+\phi)} + e^{i(\psi-\phi)} + e^{-i(\psi-\phi)}\right) .$$

It is easy to see that the generating function $\chi_{1,0}$ must be determined by the same homological equation as in Eq.(31). In fact, if we assume $\chi_{1,0}$ to be a $O(\lambda)$ quantity, then, in the transformed Hamiltonian $H^{(1,0)} = \exp(L_{\chi_{1,0}})H^{(0)}$, the terms of order $O(\lambda)$ are[16]:

$$H_1^{(1,0)} = H_1^{(0)} + \left\{\omega_* I_\psi + \omega I + \frac{I_\psi^2}{2}, \chi_{1,0}\right\} \quad .$$

We observe that, due to the different book-keeping that we adopted in Eq.(55), compared to Eq.(24), we have now the presence of the term I_ψ^2 in the Poisson bracket contributing to $O(\lambda)$ terms. However, determining $\chi_{1,0}$ by the usual homological equation:

$$\{\omega_* I_\psi + \omega I, \chi_{1,0}\} + \lambda h_{1,0}^{(0)} = 0 \tag{58}$$

has no consequences, since the extra Poisson bracket $\{I_\psi^2, \chi_{1,0}\}$ only generates a term of order $O(\lambda)$ which is *linear* in the actions, and such terms are to be eliminated at substep 3.

[16]Sufficient familiarity with the notation is assumed by now, so that the meaning of various subscripts or superscripts in all expressions below should be straightforward.

In conclusion:

$$\chi_{1,0} = \lambda i \Bigg[0.027321 \left(e^{i\psi} - e^{-i\psi} \right)$$

$$+0.0008 \left(e^{i(\psi+\phi)} - e^{-i(\psi+\phi)} \right) + 0.0042475 \left(e^{i(\psi-\phi)} - e^{-i(\psi-\phi)} \right) \Bigg] \ .$$

Up to terms $O(\lambda^2)$, the Hamiltonian $H^{(1,0)} = \exp(L_{\chi_{1,0}}) H^{(0)}$ is given by:

$$H^{(1,0)} = 1.46410 I_\psi + I + \frac{I_\psi^2}{2}$$

$$+\lambda I_\psi \Bigg[0.027321 \left(e^{i\psi} + e^{-i\psi} \right) + 0.0034475 \left(e^{i(\psi-\phi)} + e^{-i(\psi-\phi)} \right) \Bigg]$$

$$+\lambda^2 \Bigg[7.57016 \times 10^{-4} + 9.41880 \times 10^{-5} \left(e^{i\phi} + e^{-i\phi} \right)$$

$$+3.72565 \times 10^{-4} \left(e^{2i\psi} + e^{-2i\psi} \right) - 6.4 \times 10^{-7} \left(e^{2i\phi} + e^{-2i\phi} \right)$$

$$+9.41880 \times 10^{-5} \left(e^{i(2\psi-\phi)} + e^{-i(2\psi-\phi)} \right)$$

$$-3.2 \times 10^{-7} \left(e^{i(2\psi+2\phi)} + e^{-i(2\psi+2\phi)} \right) + 5.6227 \times 10^{-6} \left(e^{i(2\psi-2\phi)} + e^{-i(2\psi-2\phi)} \right) \ .$$

Substep 2: we observe that in $H^{(1,0)}$ there are no $O(\lambda)$ terms linear in the actions and independent of the angles. We thus have to postpone until second order our discussion of how such terms are eliminated.

Substep 3: elimination of the $O(\lambda)$ terms in $H^{(1,0)}$ linear in the actions and depending on the angles. These are:

$$h_{1,1}^{(1,0)} = I_\psi \Bigg[0.027321 \left(e^{i\psi} + e^{-i\psi} \right) + 0.0034475 \left(e^{i(\psi-\phi)} + e^{-i(\psi-\phi)} \right) \Bigg] \ .$$

Again, we use the same type of homological equation to determine the generating function $\chi_{1,1}$:

$$\{ \omega_* I_\psi + \omega I, \chi_{1,1} \} + \lambda h_{1,1}^{(1,0)} = 0 \ . \tag{59}$$

A similar question as before arises: in computing $H^{(1)} = \exp(L_{\chi_{1,1}}) H^{(1,0)}$, how do we deal with the non-elimination of $O(\lambda)$ terms generated by the Poisson bracket $\{ I_\psi^2, \chi_{1,1} \}$? However, since $\chi_{1,1}$ is linear in the actions, it follows that the terms under question are *quadratic* in the actions. According to the Kolmogorov scheme, such terms are not to be normalized, thus their presence in the Hamiltonian after normalization is consistent with the algorithm. [17]

[17] This last remark sounds like a detail, but in the author's opinion, it shows one of the most beautiful aspects of canonical perturbation theory, namely the fact that the physical principles

In summary:

$$\chi_{1,1} = \lambda I_\psi i \Bigg[-0.018660 \left(e^{i\psi} - e^{-i\psi} \right) - 0.0074284 \left(e^{i(\psi-\phi)} - e^{-i(\psi-\phi)} \right) \Bigg]$$

and the final Hamiltonian $H^{(1)} = \exp(L_{\chi_{1,1}}) H^{(1,0)}$ up to terms of second degree is given by:

$$H^{(1)} = 1.46410 I_\psi + I + \frac{I_\psi^2}{2}$$

$$-\lambda I_\psi^2 \Bigg[0.018660 \left(e^{i\psi} + e^{-i\psi} \right) + 0.0074284 \left(e^{i(\psi-\phi)} + e^{-i(\psi-\phi)} \right) \Bigg]$$

$$+\lambda^2 \Bigg[7.57016 \times 10^{-4} - 0.0010708 I_\psi + 0.0012102 I_\psi^2$$

$$+ \left(3.72565 + 1.74103 I_\psi^2 \right) \times 10^{-4} \left(e^{2i\psi} + e^{-2i\psi} \right) - 3.2 \times 10^{-7} \left(e^{i(2\psi+2\phi)} + e^{-i(2\psi+2\phi)} \right)$$

$$+ \left(9.41880 \times 10^{-5} - 2.67279 \times 10^{-4} I_\psi + 4.15846 \times 10^{-4} I_\psi^2 \right) \left(e^{i\phi} + e^{-i\phi} \right)$$

$$+ \left(5.6227 \times 10^{-6} + 2.75904 \times 10^{-5} I_\psi^2 \right) \left(e^{i(2\psi-2\phi)} + e^{-i(2\psi-2\phi)} \right)$$

$$+ \left(9.41880 \times 10^{-5} + 1.38615 \times 10^{-4} I_\psi^2 \right) \left(e^{i(2\psi-\phi)} + e^{-i(2\psi-\phi)} \right)$$

$$-6.4 \times 10^{-7} \left(e^{2i\phi} + e^{-2i\phi} \right) \Bigg] \quad .$$

We observe that the Hamiltonian $H^{(1)}$ is in Kolmogorov normal form up to order $O(\lambda)$, since all terms at this order depend quadratically on the action I_ψ. However, the $O(\lambda^2)$ part contains now terms to be normalized. In particular, we see a term $-0.0010708 I_\psi$ which is independent of the angles. As shown below, such terms are eliminated by a rather unusual form of generating function. Such elimination guarantees that the torus solution found after the Kolmogorov normalization corresponds to the fixed frequencies selected in the start, i.e. in our case $\omega_* = 2(\sqrt{3} - 1)$ and $\omega = 1$.

We give now in detail the three sub-steps for the normalization of $H^{(1)}$:

'guide' our choice of normalization scheme and determine for the most even the formal aspects of normalization algorithms. One example was already pointed out in subsection 2.4, regarding the choice of 'Hori kernel' (see footnote 7). Here, the main advance due to Kolmogorov, is to understand, precisely, that the presence of terms depending on the angles, but quadratic in the actions, does not influence the presence of a torus solution, despite the fact that it is a resignation from our requirement to produce an integrable approximation to the original Hamiltonian.

Substep 1: elimination of the $O(\lambda^2)$ terms independent of the actions and depending on the angles. These are:

$$h^{(1)}_{2,0} = 3.72565 \times 10^{-4} \left(e^{2i\psi} + e^{-2i\psi}\right)$$

$$-3.2 \times 10^{-7} \left(e^{i(2\psi+2\phi)} + e^{-i(2\psi+2\phi)}\right) + 9.41880 \times 10^{-5} \left(e^{i\phi} + e^{-i\phi}\right)$$

$$+5.6227 \times 10^{-6} \left(e^{i(2\psi-2\phi)} + e^{-i(2\psi-2\phi)}\right) + 9.41880 \times 10^{-5} \left(e^{i(2\psi-\phi)} + e^{-i(2\psi-\phi)}\right)$$

$$-6.4 \times 10^{-7} \left(e^{2i\phi} - e^{-2i\phi}\right) \quad .$$

Hence

$$\chi_{2,0} = \lambda^2 i \Bigg[- 1.27233 \times 10^{-4} \left(e^{2i\psi} - e^{-2i\psi}\right)$$

$$+6.49324 \times 10^{-8} \left(e^{i(2\psi+2\phi)} - e^{-i(2\psi+2\phi)}\right) - 9.41880 \times 10^{-5} \left(e^{i\phi} - e^{-i\phi}\right)$$

$$-6.05762 \times 10^{-6} \left(e^{i(2\psi-2\phi)} - e^{-i(2\psi-2\phi)}\right) - 4.88476 \times 10^{-5} \left(e^{i(2\psi-\phi)} - e^{-i(2\psi-\phi)}\right)$$

$$+3.2 \times 10^{-7} \left(e^{2i\phi} - e^{-2i\phi}\right) \Bigg] \quad .$$

The Hamiltonian $H^{(2,0)} = \exp(L_{\chi_{2,0}}) H^{(1)}$ is in normal form up to terms of order $O(\lambda)$, while at order $O(\lambda^2)$ we have:

$$H^{(2,0)}_2 = \lambda^2 \Bigg[7.57016 \times 10^{-4} - 0.0010708 I_\psi + 0.0012102 I_\psi^2$$

$$+ \left(-2.54467 I_\psi + 1.74103 I_\psi^2\right) \times 10^{-4} \left(e^{2i\psi} + e^{-2i\psi}\right)$$

$$+1.29865 \times 10^{-7} I_\psi \left(e^{i(2\psi+2\phi)} + e^{-i(2\psi+2\phi)}\right)$$

$$+ \left(-2.67279 I_\psi + 4.15846 I_\psi^2\right) \times 10^{-4} \left(e^{i\phi} + e^{-i\phi}\right)$$

$$+ \left(-1.21152 I_\psi + 2.75904 I_\psi^2\right) \times 10^{-5} \left(e^{i(2\psi-2\phi)} + e^{-i(2\psi-2\phi)}\right)$$

$$+ \left(-9.76951 \times 10^{-5} I_\psi + 1.38615 \times 10^{-4} I_\psi^2\right) \left(e^{i(2\psi-\phi)} + e^{-i(2\psi-\phi)}\right) \Bigg] \quad .$$

Substep 2: elimination of the $O(\lambda^2)$ terms linear in the actions and independent of the angles.

There is just one such term, $-0.0010708 I_\psi$. This term would be impossible to

eliminate by a generating function $\chi_{2,c}$ defined by the usual form of homological equation, i.e. an equation of the form

$$\{\omega_* I_\psi + \omega I, \chi_{2,c}\} - \lambda^2 0.0010708 I_\psi = 0$$

because looking for a solution of the above equation in the form of Eq.(50) would require division by a *zero* divisor (since $k_1 = k_2 = 0$). However, precisely at this point *we now exploit the fact that* Z_0 *contains a non-vanishing quadratic part* $I_\psi^2/2$. We set

$$\chi_{2,c} = X_{2,c}\psi \tag{60}$$

where $X_{2,c}$ is a *constant*, and observe that, through the Lie operation $H^{(2,c)} = \exp(L_{\chi_{2,c}})H^{(2,0)}$, $\chi_{2,c}$ generates a term linear in the actions and independent of the angles via the Poisson bracket

$$\exp(L_{\chi_{2,c}})H^{(2,0)} \to L_{\chi_{2,c}}H^{(2,0)} \to \{Z_0, \chi_{2,c}\}$$

$$\to \left\{\frac{I_\psi^2}{2}, X_{2,c}\psi\right\} = -X_{2,c}I_\psi \quad .$$

In order to eliminate the term $-\lambda^2 0.0010708 I_\psi$ from $H^{(2,0)}$, we then simply set $X_{2,c} = -\lambda^2 0.0010708$. [18]

In summary

$$\chi_{c,2} = -\lambda^2 0.0010708\psi \quad .$$

The transformed Hamiltonian is

$$H^{(c,2)} = \exp(L_{\chi_{2,c}})H^{(2,0)} \quad .$$

We can check that $H^{(2,c)}$ does not differ from $H^{(2,0)}$ up to terms $O(\lambda^2)$, apart from the elimination of the term $-\lambda^2 0.0010708 I_\psi$. On the other hand, differences between $H^{(2,c)}$ and $H^{(2,0)}$ exist at all subsequent orders. Finally, it is

[18] We see now the reason for keeping the term $I_\psi^2/2$ in the Z_0 part of the Hamiltonian in the choice of book-keeping. This term is used in sub-step 2 of Kolmogorov's algorithm. In fact, the requirement that the original Hamiltonian *posess* a non-vanishing quadratic part proves here to be crucial for the algorithm to proceed. Recalling that the quadratic term was produced after substituting in the original Hamiltonian (3) the expression $p = p_* + I_\psi$ and expanding, we can restate this condition as the requirement that $\partial^2 H_0(p)/\partial p^2 \neq 0$, where , in the original Hamiltonian, we have just $H_0 = p^2/2 + I$. However, under more general Hamiltonian functions of more than one degrees of freedom, the condition, as shown in section 3, can be formulated as the requirement that the determinant of the Hessian matrix of the unperturbed Hamiltonian with respect to the action variables be different from zero, namely $det(\partial^2 H_0/\partial \mathbf{p}^2) \neq 0$. We have, here, one more example of how a formal aspect of perturbation theory is guided by a physical principle. From the physical point of view, a condition of the form $det(\partial^2 H_0/\partial \mathbf{p}^2) \neq 0$ is called a 'twist condition', i.e. it says that the frequencies on different tori should be different, changing with the values of the actions which label the tori. In the Kolmogorov normal form, however, this condition is used in order that it becomes possible to define the generating functions $\chi_c^{(r)}$ by which we eliminate terms linear in the angles and independent of the actions. A posteriori, it can be seen that by this elimination we ensure, precisely, that in our construction of a torus solution, we do not change frequencies with respect to our initial choice, in which the frequencies depended only on the choice of some label values $\mathbf{p}_*$.

straightforward to see that the linear dependence of $\chi_{2,c}$ in the angles produces no terms in $H^{(2,c)}$ which are not trigonometric in the angles.

Substep 3: elimination of the $O(\lambda^2)$ terms linear in the actions and depending on the angles.

These are

$$h_{2,1}^{(2,c)} = I_\psi \Bigg[-2.54467 \times 10^{-4} \left(e^{2i\psi} + e^{-2i\psi}\right)$$
$$+1.29865 \times 10^{-7} \left(e^{i(2\psi+2\phi)} + e^{-i(2\psi+2\phi)}\right) - 2.67279 \times 10^{-4} \left(e^{i\phi} + e^{-i\phi}\right)$$
$$-1.21152\times10^{-5} \left(e^{i(2\psi-2\phi)} + e^{-i(2\psi-2\phi)}\right) - 9.76951\times10^{-5} \left(e^{i(2\psi-\phi)} + e^{-i(2\psi-\phi)}\right) \Bigg] .$$

These terms can be eliminated by a generating function $\chi_{2,1}$, defined by the usual homological equation. Hence

$$\chi_{2,1} = \lambda^2 I_\psi i \Bigg[8.6902 \times 10^{-5} \left(e^{2i\psi} - e^{-2i\psi}\right)$$
$$-2.63513 \times 10^{-8} \left(e^{i(2\psi+2\phi)} - e^{-i(2\psi+2\phi)}\right) + 2.67279 \times 10^{-4} \left(e^{i\phi} - e^{-i\phi}\right)$$
$$+1.30524\times10^{-5} \left(e^{i(2\psi-2\phi)} - e^{-i(2\psi-2\phi)}\right) + 5.06664\times10^{-5} \left(e^{i(2\psi-\phi)} - e^{-i(2\psi-\phi)}\right) \Bigg] .$$

Finally, computing $H^{(2)} = \exp(L_{\chi_{2,1}}) H^{(2,c)}$, the Hamiltonian is brought to Kolmogorov normal form up to order $O(\lambda^2)$, i.e.:

$$H^{(2)} = 1.46410 I_\psi + I + \frac{I_\psi^2}{2} + \lambda Z_1 + \lambda^2 Z_2 + \lambda^3 H_3^{(2)} + \lambda^4 H_4^{(2)} + \dots \qquad (61)$$

where (apart from a constant)

$$Z_1 = -\lambda I_\psi^2 \left[0.018660 \left(e^{i\psi} + e^{-i\psi}\right) + 0.0074284 \left(e^{i(\psi-\phi)} + e^{-i(\psi-\phi)}\right) \right]$$

$$Z_2 = \lambda^2 I_\psi^2 \Bigg[0.0012102 + 3.47907 \times 10^{-4} \left(e^{2i\psi} + e^{-2i\psi}\right)$$
$$+4.15846 \times 10^{-4} \left(e^{i\phi} + e^{-i\phi}\right) + 2.39948 \times 10^{-4} \left(e^{i(2\psi-\phi)} + e^{-i(2\psi-\phi)}\right)$$
$$+5.36951 \times 10^{-5} \left(e^{i(2\psi-2\phi)} + e^{-i(2\psi-2\phi)}\right)$$
$$-5.27027 \times 10^{-8} \left(e^{i(2\psi+2\phi)} + e^{-i(2\psi+2\phi)}\right) \Bigg] .$$

This accomplishes the normalization at order $r = 2$ following Kolmogorov's algorithm for the Hamiltonian (55).

Accumulation of divisors and convergence. After having examined the formal aspects of Kolmogorov's algorithm, we can now ask the same question as in subsection 2.6, namely what are the benefits from computing a Kolmogorov normal form as above. In particular, in what aspects should the above presented algorithm be considered as preferential over the algorithm presented in subsections 2.4 and 2.5?

A basic answer to this question is the following: one can prove that the Kolmogorov normalization is *convergent* in an open domain around the solution of interest, i.e. around $I_\psi = 0$. This implies that in the limit of the normalization process, the final Hamiltonian $H^{(\infty)}$ is entirely in Kolmogorov normal form, while the remainder shrinks to zero. Thus, by this method we can *prove the theorem of Kolmogorov* about the existence of invariant tori in a Hamiltonian system like (3).

Are there not small divisors in this case? In fact, the solution to the homological equations defining the generating functions $\chi_{r,0}$ and $\chi_{r,1}$ for $r = 1, 2, \ldots$ introduce precisely the same divisors as in the normalization scheme of subsections 2.4 and 2.5. However, we can demonstrate that by eliminating only some terms depending on the angles, in the Kolmogorov construction we avoid the generation of any divergent sequence due to a bad *accumulation* of divisors. For example, let us consider the sequence of Eq.(52), which leads to the asymptotic behavior of the series considered in subsections 2.4. and 2.5. In this sequence we have a *growing power* of the variable I_ψ, namely a sequence introduces terms $O(I_\psi) \rightarrow O(I_\psi^2) \rightarrow O(I_\psi^3) \rightarrow \ldots$, due to repeated Poisson brackets of some generating function terms with the Hamiltonian term $I_\psi^2/2$. However, in the Kolmogorov normal form *we stop normalizing such terms, precisely, at the point when a term acquires a factor* $O(I_\psi^2)$. In this way, we do not allow such dangerous sequences to propagate in the series.

We are still left with having to demonstrate that there are no other types of dangerous sequences appearing in the Kolmogorov series. The simplest demonstration relies on the employment of the so-called *quadratic scheme*, which leads to the same accumulation of divisors as in the linear scheme developed above.

In order to understand the quadratic scheme, referring to our usual example, consider again the three sub-steps eliminating unwanted terms at order $O(\lambda^2)$. At sub-step 1, we can now remark the following: instead of considering a generating function $\chi_{2,0}$, eliminating the $O(\lambda^2)$ terms depending on the angles and independent of the actions, we could have considered a generating function of the form $\chi_{2+3,0}$, eliminating *simultaneously* the terms $O(\lambda^2)$ and $O(\lambda^3)$ depending on the angles and independent of the actions. Using the "heuristic" notation of subsection 2.7, the corresponding generating function would be of the form:

$$\chi_{2+3,0} \rightarrow C \left(\lambda^2 \frac{e^{iK_2\Phi}}{a_2} + \lambda^3 \frac{e^{iK_3\Phi}}{a_3} \right)$$

where C is a factor coming from the normalization procedure up to that point, and the relevant values for the integers K_2, K_3 and divisors a_2, a_3 will be dis-

cussed below. We can see now that the operation $\exp(L_{\chi_{2+3,0}})H^{(1)})$ will not generate new terms at orders $O(\lambda^2)$ and $O(\lambda^3)$ which are depending on the angles and independent of the actions. To see this, we only have in fact to consider Poisson brackets of $\chi_{2+3,0}$ with terms up to order λ in $H^{(1)}$. We have:

$$H^{(1)} = Z_0 + \lambda Z_1 \to \omega_* I_\psi + \omega I + \frac{I_\psi^2}{2} + \lambda I_\psi^2 e^{iK_1\Phi} + \dots$$

The Poisson bracket $\{\omega_* I_\psi + \omega I, \chi_{2+3,0}\}$ eliminates the unwanted terms of $H^{(1)}$ depending on the angles and independent of the actions. On the other hand

$$\left\{ \frac{I_\psi^2}{2} + \lambda I_\psi^2 e^{iK_1\Phi}, \chi_{2+3,0} \right\} \to$$

$$\left\{ \frac{I_\psi^2}{2} + \lambda I_\psi^2 e^{iK_1\Phi}, \lambda^2 \frac{e^{iK_2\Phi}}{a_2} + \lambda^3 \frac{e^{iK_3\Phi}}{a_3} \right\} \to$$

$$C\Bigg[- i\lambda^2 K_2 I_\psi \frac{e^{iK_2\Phi}}{a_2} - i\lambda^3 I_\psi \left(\frac{K_3 e^{iK_3\Phi}}{a_3} + \frac{2K_2 e^{i(K_1+K_2)\Phi}}{a_2} \right)$$

$$-2i\lambda^4 K_3 I_\psi \frac{e^{i(K_1+K_3)\Phi}}{a_3} \Bigg] \quad .$$

In conclusion, after computing $H^{(2+3,0)} = \exp(L_{\chi_{2+3,0}})H^{(1)}$ we are left with only terms linear in the actions in $H^{(2+3,0)}$.

In precisely the same way, we can see that the operation $H^{(2+3,c)} = \exp(L_{\chi_{2+3,c}})\, H^{(2+3,0)}$ leaves no terms of order $O(\lambda^2)$ and $O(\lambda^3)$ in $H^{(2+3,c)}$ which are linear in the actions and independent of the angles, and, finally, that the operation $H^{(2+3)} = \exp(L_{\chi_{2+3,1}})\, H^{(2+3,c)}$ leaves no terms of order $O(\lambda^2)$ and $O(\lambda^3)$ in $H^{(2+3)}$ which are linear in the actions and depending on the angles.

In summary, we conclude that, when implementing Kolmogorov's algorithm, the unwanted terms of orders $O(\lambda^2)$ and $O(\lambda^3)$ can be normalized as a group in one step, divided in the usual three sub-steps referred to as above.

In exactly the same way, we can show that the terms $O(\lambda^4)$, $O(\lambda^5)$, $O(\lambda^6)$, $O(\lambda^7)$ can be normalized as a group in one step (divided in the usual three sub-steps), then $O(\lambda^8), \dots, O(\lambda^{15})$ in one step, etc. This particular way of grouping terms which are to be normalized at successive steps is called a quadratic method.

Let us now examine, with the help of the quadratic scheme, why, despite the accumulation of divisors, the Kolmogorov normalization leads to a convergent series. To this end, we will assume that the divisors appearing in the series satisfy a so-called *diophantine condition*, namely, that there are positive constants γ, τ such that for all wavevectors $\mathbf{k}$ one has:

$$|\mathbf{k} \cdot \omega| > \frac{\gamma}{|k|^\tau} \quad . \tag{62}$$

A condition like (62) implies that at any order $|k|$ there is a lower bound on the smallness of all divisors of the order $|k|$, so that very small divisors can only

appear at very high orders. A diophantine condition of the form (62) is satisfied for a subset of large measure in the set of incommensurable frequencies (ω_*, ω), and it is satisfied also in our numerical example, as shown by the straight line plot in Fig.(4) which corresponds to a lower bound to the divisor values given by a power law of the form (62) for $\gamma = 0.223$, $\tau = 1.02$.

In order, now, to establish a bound for the size of the sequence of terms yielding the worst possible accumulation of divisors in the quadratic scheme, recall (from above) that the Lie operation of $\chi_{2+3,0}$ on $H^{(1)}$ generated, at orders $O(\lambda^2)$ and $O(\lambda^3)$, various terms linear in the actions and depending on the angles. Since higher order divisors appear at higher book-keeping orders, we have $K_3 > K_2$, $a_3 < a_2$. Thus, the terms of largest size linear in the actions are $C\lambda^3 K_3 I_\psi e^{iK_3\Phi}/a_3$. Thus

$$\chi_{2+3,1} \to C\lambda^3 K_3 I_\psi e^{iK_3\Phi}/(a_3)^2 \quad .$$

We can now see that, after the operation $H^{(2+3)} = \exp(L_{\chi_{2+3,1}})H^{(2+3,c)}$, the above term generates in $H^{(2+3)}$ a term of order $O(\lambda^6)$, linear in the actions and depending on the angles

$$\exp(L_{\chi_{2+3,1}})H^{(2+3,c)} \to \frac{1}{2}\left\{\{\omega_* I_\psi + \omega I + ..., \chi_{2+3,1}\}, \chi_{2+3,1}\right\}$$

$$\to \lambda^6 C^2 (K_3)^2 I_\psi e^{iK_6\Phi}/(a_3)^2 \quad .$$

Similar terms are generated by the repeated Poisson brackets of $\chi_{2+3,0}$. For example:

$$\exp(L_{\chi_{2+3,0}})H^{(1)} \to \frac{1}{2}\left\{\{\lambda Z_1, \chi_{2+3,0}\}, \chi_{2+3,0}\right\}$$

$$\to \frac{1}{2}\left\{\{\lambda (I_\psi)^2 e^{ik_1\Phi}, \chi_{2+3,0}\}, \chi_{2+3,0}\right\} \to \lambda^7 C^2 (K_3)^2 e^{iK_7\Phi}/(a_3)^2 \quad .$$

But, now, this last term must be eliminated in the normalization of $H^{(2+3)}$ using the generating function $\chi_{4+5+6+7,0}$, which thus acquires a divisor a_7, i.e.:

$$\chi_{4+5+6+7,0} \to \lambda^7 \frac{C^2 (K_3)^2 e^{iK_7\Phi}}{(a_3)^2 a_7} \quad .$$

Similarly, the term $\lambda^6 (K_3)^2 I_\psi e^{iK_6\Phi}/(a_3)^2$ in the previous example must be normalized by the generating function $\chi_{4+5+6+7,1}$. Thus:

$$\chi_{4+5+6+7,1} \to \lambda^6 \frac{C^2 (K_3)^2 I_\psi e^{iK_6\Phi}}{(a_3)^2 a_6} \quad .$$

Carefully examining the above formulae, the main effect of the quadratic scheme can now be stated: [19] *in every normalization step, the worst possible accumulation of divisors is given by the square of the worst possible divisor product of the*

[19] In fact, we have exactly the same effect in the linear scheme as well (see Giorgilli and Locatelli (1997,1999), at the end of the steps 1,2,4,8, etc. of that scheme.

previous step times a new divisor equal to the smallest possible in the current group. Namely we have (taking, as an example, the accumulation of divisors in the generating functions $\chi_{1,0}$, $\chi_{2+3,0}$, etc.):

$$\chi_{1,0} \quad \rightarrow \text{ worst possible factor } \frac{\lambda\mu}{a_1}$$

$$\chi_{2+3,0} \quad \rightarrow \text{ worst possible factor } \frac{\lambda^3\mu^3(K_1)^2}{(a_1)^2 a_3}$$

$$\chi_{4+5+6+7,0} \rightarrow \text{ worst possible factor } \frac{\lambda^7\mu^7(K_1)^4(K_3)^2}{(a_1)^4(a_3)^2 a_7}$$

$$\chi_{8+9+\ldots+15,0} \rightarrow \text{ worst possible factor } \frac{\lambda^{15}\mu^{15}(K_1)^8(K_3)^4(K_7)^2}{(a_1)^8(a_3)^4(a_7)^2 a_{15}}$$

$$\ldots$$

where μ is the largest possible numerical coefficient of all Fourier terms in $h^{(0)}_{1,0}$ (in our numerical example, $\mu = 0.04$).

It is possible to see now, that a sequence of worst possible factors as the above *is bounded by a geometric progress.* To see this, we recall that i) $a_{r_1} > a_{r_2}$ if $r_1 < r_2$, ii) the maximum Fourier order K_r of a term at book-keeping order r is $K_r = K'r - 1$, where, in our example, we have $K' = 2$, iii) $K_r > 1$ for all r, and iv) $\mu < 1$. Taking into account the latter relations we deduce that the fastest growing sequence of terms at successive normalization steps in the above example is bounded by the sequence

$$\frac{2K'\mu}{a_2} \rightarrow \frac{((2K')^2 \cdot (4K'))\mu^2}{(a_2)^2 a_4} \rightarrow \frac{((2K')^4 \cdot (4K')^2 \cdot (8K'))\mu^4}{(a_2)^4 (a_4)^2 a_8} \rightarrow \ldots$$

Taking finally into account the diophantine inequality (62), after q normalization steps (by the quadratic scheme), the q-th term of the above sequence reads

$$B_q = \mu^{r_q} \left(\frac{K'^{(1+\tau)}}{\gamma} \right)^{L_q} \cdot 2^{P_q} \tag{63}$$

where

$$r_q = 2^{q-1}, \qquad L_q = \sum_{j=1}^{q} 2^{j-1}, \qquad P_q = \sum_{j=1}^{q} j(2^{q-j}) \quad .$$

It is now a simple exercise to show that [20]

$$B_q < \left(\frac{\gamma}{4K'^{(\tau+1)}} \right) \left(\frac{16K'^{(2\tau+2)}\mu}{\gamma^2} \right)^{r_q} \tag{64}$$

---

[20] Prove and use the equalities $L_q = 2^q - 1$ and $P_q = 2^{q+1} - 2$.

i.e. *the fastest growing sequence of terms in Kolmogorov's algorithm is bounded by a geometric progress*. But for μ sufficiently small, the geometric ratio becomes smaller than unity. We thus demonstrate that for sufficiently small μ, the Kolmogorov normalization is convergent, and this ensures the existence of a torus solution with the given diophantine frequencies. [21]

It should be emphasized that the quadratic scheme used above is not indispensable in proving that the worst accumulation of divisors in the Kolmogorov scheme is bounded by a geometric progress. If we work, instead, with a 'classical', i.e. order by order, elimination of terms, book-keeping scheme, we can still recover essentially the same accumulation of divisors as in Eq.(63) (see Giorgilli and Locatelli (1997, 1999)). In fact, in numerical computations it turns out that the classical scheme performs somewhat better in establishing limits of applicability of the Kolmogorov construction in concrete physical systems (see, for example, Giorgilli et al. (2009), or Sansottera et al. (2011) and references there in).

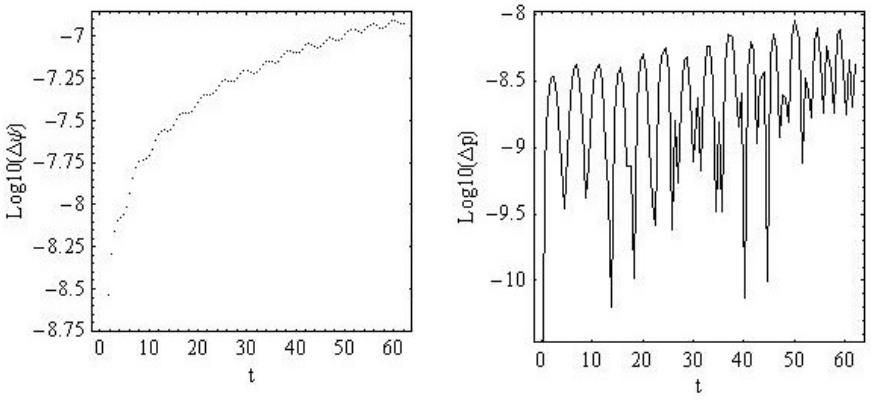

Figure 5. Time evolution of the absolute error between a theoretical calculation of the time evolution of the variables $\psi(t)$ (left) and $p(t)$ (right) using the Kolmogorov normal form up to normalization order $r = 10$, and the corresponding numerical orbit with initial conditions $\psi = 0$, $p = 1.529162868490481$, up to $t = 60$.

We note finally, that the fact that Kolmogorov's scheme is convergent, has the practical benefit that we can use it in order to obtain very accurate ana-

[21] How small should μ be? If we make the calculation in our example, setting $K' = 2$, $\gamma = 0.223$, $\tau = 1.02$, we find $\mu < 1.9 \times 10^{-4}$, while numerically we found that there are invariant tori for μ more than two orders of magnitude larger, i.e. $\mu = 0.04$. However, the source of the discrepancy is the use of unrealistic upper bound limits in the above estimates, while a 'computer-assisted' calculation of the Kolmogorov series up to a high order is likely to yield a much better estimate of the maximum value of μ for which the series converge. This subject has a long history. In one of the first applications of KAM theory by purely analytical means, M. Hénon (1966) showed that in the restricted three body problem we have KAM stable motions if $\mu < 10^{-300}$. However, in recent years there have been quite realistic computer-assisted implementations (or even proofs, using interval arithmetics, of the KAM stability in dynamical systems (see Celletti et al. (2000)), for perturbation parameter values up to 92% of the value for which the existence of a KAM torus is established by numerical means.

lytical expressions for quasi-periodic trajectories using the Lie-transformations from the new to the old canonical variables of the problem under study. The transformations are given by equations quite similar to Eqs.(41). For example, we have:

$$\psi = \exp(L_{\chi_{r,1}}) \exp(L_{\chi_{r,c}}) \exp(L_{\chi_{r,0}}) \ldots \exp(L_{\chi_{1,1}}) \exp(L_{\chi_{1,c}}) \exp(L_{\chi_{1,0}}) \psi^{(r)} \tag{65}$$

and similarly for all other variables. Furthermore, for the torus solution, we simply substitute in the end $I_\psi^{(r)}(t) = 0$, and $\psi^{(r)}(t) = \omega_* t$ or $\phi^{(r)}(t) = \omega t$. We can then compute theoretically the time evolution of the old variables by the above expressions. Figure (5) shows an example of the error, i.e., the difference between theoretical and numerical calculation for a torus solution in the example treated in the present subsection, and a computation of the Kolmogorov normal form up to order 10 in the book-keeping parameter. The numerical trajectory is found by integrating the original equations of motions with initial conditions obtained by setting $t = 0$ in the above expressions, when the normalization was implemented up to the order $r = 10$. We observe that the error in the computation of the action variable is of the order of 10^{-8}, while in the angles there is a cumulative error of order 10^{-7} at the time $t = 60$, implying a frequency error of the order, again, 10^{-8}. But the error can be reduced to an arbitrarily small amount by normalizing to higher orders r.

2.9. Resonant normal form

So far, we focused on constructing normal forms in the Hamiltonian model (3) around some action value p_* ($p_* = 2(\sqrt{3} - 1)$ in our example) such that the resulting frequency is incommensurable with the perturber's frequency ω. It is immediately clear that the fact that the two frequencies satisfy no resonance condition of the form

$$k_1 \omega_* + k_2 \omega = 0 \tag{66}$$

was essential so far in our success in constructing a normal form, since it ensures that we never encounter in the series (e.g. in the solution (50) of the homological equation) a divisor equal to zero *exactly*. However, such divisors could appear for other choices of p_*. For example, if we choose $p_* = 1$, we have $\omega_* = 1$, thus $\omega_* - \omega = 0$, which is a resonance condition of the form (66), for a particular vector of wavenumbers, denoted hereafter as $\mathbf{k^{(1)}} \equiv (k_1^{(1)}, k_2^{(2)}) = (1, -1)$, or multiples of it.[22] If we choose $p_* = 1$ in the Birkhoff normal form construction

[22] In the case of wavenumbers, the use of the superscript (1) has a completely different meaning than in the notation introduced so far for the series. Namely, (1) means 'the first resonance condition'. We will see (section 4) that when we have more than two frequencies, there are cases where we can define more than one linearly independent resonance conditions, the maximum number being equal to the number of frequencies considered minus one. For example, if we have three frequencies $(\omega_1, \omega_2, \omega_3)$, we can have cases with i) no resonance condition (e.g.: $\omega_1 = 1$, $\omega_2 = \sqrt{2}$, $\omega_3 = \sqrt{3}$), ii) one resonance condition (='simply resonant', e.g.: $\omega_1 = 1$, $\omega_2 = \sqrt{2}$, $\omega_3 = 2 + 2\sqrt{2}$, whence $2\omega_1 + 2\omega_2 - \omega_3 = 0$, implying that we have a unique resonant vector $(k_1^{(1)}, k_2^{(1)}, k_3^{(1)}) = (2, 2, -1)$), iii) two independent resonance conditions (='doubly resonant', e.g.: $\omega_1 = 0.4, \omega_2 = 0.2, \omega_3 = 1$, whence $\omega_1 - 2\omega_2 = 0$ but also $2\omega_1 + \omega_2 - \omega_3 = 0$, implying that we have two independent resonant vectors $(k_1^{(1)}, k_2^{(1)}, k_3^{(1)}) = (1, -2, 0)$ and $(k_1^{(2)}, k_2^{(2)}, k_3^{(2)}) =$

of subsections 2.4 and 2.5, we can immediately see that the construction cannot proceed even at order $O(\lambda)$. This, because we can note, for example, that in the expression for the unwanted terms $h_1^{(0)}$, there is a term $e^{i(\psi-\phi)}$ whose elimination, according to Eq.(33), would require a divisor equal to zero exactly. Furthermore, as we have seen, even if the original Hamiltonian contains a finite number of harmonics, the implementation of the normal form algorithm leads to the generation of new ones as we proceed. Thus, it is always possible that we will encounter such a zero divisor at some subsequent normalization step.

What is the physical effect of the so-called 'resonant terms' $e^{i(\psi-\phi)}$, or $e^{-i(\psi-\phi)}$ (or simply $\cos(\psi-\phi)$) in the original Hamiltonian? Returning to the phase portraits of Fig.1, we see that, around $p = p_* = 1$, a conspicuous *island of stability* is formed. In fact, at the center of the island lies a stable periodic orbit, whose fundamental frequency is equal to $\omega = \omega_* = 1$. As shown in Fig.1b, the stability of this orbit is preserved when ϵ is as high as $\epsilon = 1$, and this fact implies the presence of an island of stability around it even when most other invariant curves have been destroyed and replaced by chaotic orbits.

Another relevant remark is that, within resonant domains, the phase portrait takes locally the form of a perturbed pendulum phase portrait, while the limits of the resonant domain (the so-called 'separatrix width', in analogy with the pendulum case), grow with ϵ, at least for small ϵ, up to a point when the separatrix-like chaotic layer formed in the domain around these limits prevails the dynamics. Figure 6 shows these effects. The left column shows a detail of the surface of section computed as in Fig.1, i.e. by numerical orbits, for (a) $\epsilon = 0.04$ and (c) $\epsilon = 0.16$. In fact, a rough estimate shows that by quadrupling the perturbation, the island size grows by a factor ~ 2, i.e. the *square root* of the growth factor of the perturbation.

All these features can be explained by a particular form of normal form theory, called a *resonant normal form*.[23] We will give below a detailed numerical example of how to construct a resonant normal form. However, we can see immediately the outcome of this analysis, shown in the right column of Fig.6, which shows a theoretical phase portrait obtained by a resonant normal form calculation up to order 4, as explained below. We see that the resonant normal form construction: i) explains the fact that the phase portrait in the neighborhood of a resonance has the pendulum form, ii) can predict the size of the resonant domain, and iii) gives a separatrix-like representation for the *shape* of the thin chaotic layer, which is formed in reality by the orbits as computed in

---

$(2, 1, -1)$. In the latter case we can actually form an infinity of different couples of resonant vectors, by taking linear combinations of $\mathbf{k^{(1)}}$ and $\mathbf{k^{(2)}}$ defined as above).

[23] Historically, the implementation of a resonant normal form in the computer preceded that of a non-resonant one. The work of Gustavson (1966) refers to the Hénon - Heiles Hamiltonian, which is a model of the 1:1 resonance. However, the work of Gustavson was itself preceded by the development of a 'direct' method of computation of resonant integrals by Contopoulos (1963) and Contopoulos and Moutsoulas (1965). In the direct method, we perform no canonical transformations, but simply a computation of a formal series defined so as to have vanishing Poisson bracket with the Hamiltonian. The non-resonant case (Whittaker (1916), Cherry (1924), Contopoulos (1960)) is known in galactic dynamics as the 'third integral', i.e. an approximate integral beyond the two exact ones for axisymmetric galaxies, i.e. the energy and the component of the angular momentum along the axis of symmetry.

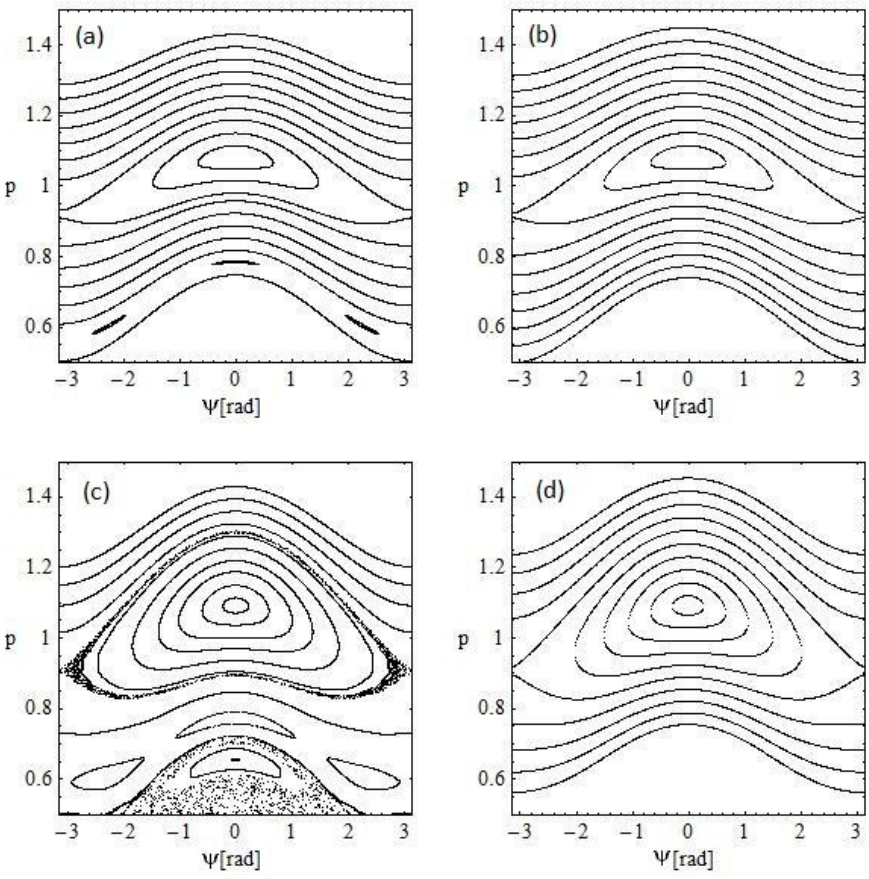

Figure 6. (a) The phase portrait of the model (3) in the 1:1 resonance, for $\epsilon = 0.04$ as computed by numerical integration of orbits, and (b) its theoretical representation by the invariant curves computed via a resonant normal form (see text). (c) and (d) Same as in (a) and (b) respectively, but for $\epsilon = 0.16$. We note that i) the size of the resonant domain has nearly doubled by changing the perturbation by a factor 4, and ii) the theoretical computation yields invariant curves even in a domain where the true dynamics yields a thin chaotic separatrix-like layer.

the full Hamiltonian (3).

The present calculation concerns the model (3), which is of two degrees of freedom. In section 3 we will see that resonant normal form theory can be used in order to describe a new phenomenon taking place within the chaotic layers of resonances in the weakly chaotic regime, namely *Arnold diffusion*. The latter originates from the topological possibility (in three or more degrees of freedom) of having chaotic motions in phase space directions normal to the planes defined by the separatrix-like resonant chaotic layers (while such motions are not possible in systems of two degrees of freedom). In that case, we will see that the *remainder* of the resonant normal form construction accounts for the speed

by which diffusion takes place. A quantitative theory of diffusion in systems of three or more degrees of freedom was developed by Chirikov (1979). This is further reviewed in Cincotta (2002) with a focus on applications in dynamical astronomy. The relation between Chirikov's theory and the outcome of resonant normal form theory is briefly discussed in subsection 4.3.

We now pass to examining the process by which we construct a resonant normal form in the example as above. Essentially, nothing changes with respect to the general normalization algorithm presented in subsection 2.5, apart from recalling that the resonant module (subsection 2.7) contains now wave vectors different from $(k_1, k_2) = 0$. In fact, if we simply define the resonant module to be the set of all wave vectors with associated divisors equal to zero exactly, we can have a consistent normal form algorithm covering all cases, i.e. non-resonant, or resonant of any multiplicity. We thus define:

$$\mathcal{M} = \{\mathbf{k} \equiv (k_1, k_2) : k_1\omega_* + k_2\omega = 0\} \tag{67}$$

and have the following general normalization algorithm:

Recursive normalization algorithm covering all types of resonant conditions

Assuming r algorithm steps have been completed, the Hamiltonian has the form:

$$H^{(r)} = Z_0 + \lambda Z_1 + ... + \lambda^r Z_r + \lambda^{r+1} H^{(r)}_{r+1} + \lambda^{r+2} H^{(r)}_{r+2} + \dots$$

where all Z terms are in normal form, while the remaining terms define the remainder $R^{(r)}$. Then:

1) Isolate from the Hamiltonian $H^{(r)}$ the terms in $H^{(r)}_{r+1}$ to be eliminated at the present step, denoted by $h^{(r)}_{r+1}$. To define these terms, write $H^{(r)}_{r+1}$ as:

$$H^{(r)}_{r+1} = \sum_{k_1,k_2} b^{(r)}_{r+1,k_1,k_2}(\mathbf{I}) e^{i(k_1\psi + k_2\phi)}$$

and choose

$$h^{(r)}_{r+1} = \sum_{k_1,k_2 \notin \mathcal{M}} b^{(r)}_{r+1,(k_1,k_2)}(\mathbf{I}) e^{i(k_1\psi + k_2\phi)}$$

where $\mathcal{M}$ is defined as in Eq.(67).

2) Solve the homological equation

$$\{Z_0, \chi_{r+1}\} + \lambda^{r+1} h^{(r)}_{r+1} = 0$$

and define χ_{r+1}.

3) Compute $H^{(r+1)} = \exp(L_{\chi_{r+1}}) H^{(r)}$. This contains a normal form part:

$$Z^{(r+1)} = Z_0 + \lambda Z_1 + ... + \lambda^r Z_r + \lambda^{r+1} Z_{r+1}$$

and a remainder part

$$R^{(r+1)} = \lambda^{r+2} H^{(r+1)}_{r+2} + \lambda^{r+3} H^{(r+1)}_{r+3} + \dots$$

This completes one full step of the general normalization algorithm.

Let us implement this algorithm in the 1:1 resonant case of the model (3). First, we prepare our Hamiltonian to be in the right form for implementing the algorithm, i.e., as in subsection 2.4, we first set $p = p_* + I_\psi$ in (3) with $p_* = 1$, expand, introduce a book-keeping, and turn trigonometric functions to exponentials. Then (apart from a constant):

$$H^{(0)} = I_\psi + I$$

$$+\lambda\left[\frac{I_\psi^2}{2} - 0.04\left(e^{i\psi} + e^{-i\psi}\right)\right.$$

$$\left.-(0.0016 + 0.0008I_\psi)\left(e^{i(\psi+\phi)} + e^{-i(\psi+\phi)} + e^{i(\psi-\phi)} + e^{-i(\psi-\phi)}\right)\right] .$$

Now, we isolate the terms to be normalized at order 1. We observe that the terms $e^{\pm i(\psi-\phi)}$ yield $(k_1, k_2) = (\pm 1, \mp 1)$, which belong to the resonant module $\mathcal{M}$. Thus, they are not to be normalized. In fact, the other term with the same property is $I_\psi^2/2$, whose 'wave vector' is just $(k_1, k_2) = (0, 0)$. In summary:

$$h_1^{(0)} = -0.04\left(e^{i\psi} + e^{-i\psi}\right) - (0.0016 + 0.0008I_\psi)\left(e^{i(\psi+\phi)} + e^{-i(\psi+\phi)}\right)$$

leading to

$$\chi_1 = \lambda i\left[0.04\left(e^{i\psi} - e^{-i\psi}\right) + (0.0008 + 0.0004I_\psi)\left(e^{i(\psi+\phi)} - e^{-i(\psi+\phi)}\right)\right] .$$

After performing $H^{(1)} = \exp(L_{\chi_1})H^{(0)}$ we find, up to second order:

$$H^{(1)} = I_\psi + I + \lambda\frac{I_\psi^2}{2} - \lambda(0.0016 + 0.0008I_\psi)\left(e^{i(\psi-\phi)} + e^{-i(\psi-\phi)}\right)$$

$$+\lambda^2\left[-1.28\times10^{-6} - 6.4\times10^{-7}I_\psi + 0.04I_\psi\left(e^{i\psi} + e^{-i\psi}\right) - 5.6\times10^{-5}\left(e^{i\phi} + e^{-i\phi}\right)\right.$$

$$- \left(1.28\times10^{-6} + 6.4\times10^{-7}I_\psi\right)\left(e^{2i\phi} + e^{-2i\phi}\right)$$

$$+ \left(0.0008I_\psi + 0.0004I_\psi^2\right)\left(e^{i(\psi+\phi)} + e^{-i(\psi+\phi)}\right)$$

$$\left.-8\times10^{-6}\left(e^{i(2\psi+\phi)} + e^{-i(2\psi+\phi)}\right) - 3.2\times10^{-5}\left(e^{i(2\psi-\phi)} + e^{-i(2\psi-\phi)}\right)\right] .$$

This accomplishes the first step of the resonant normalization process. Clearly, in the second step, the only term to survive in the Hamiltonian (apart from a constant) is $-6.4\times10^{-7}I_\psi$. Thus, omitting the details on the form of χ_2, the

Hamiltonian $H^{(2)} = \exp(L_{\chi_2})H^{(1)}$, which is in normal form up to terms $O(\lambda^2)$, is given by

$$H^{(2)} = I_\psi + I + \lambda\frac{I_\psi^2}{2}$$

$$-\lambda(0.0016 + 0.0008I_\psi)\left(e^{i(\psi-\phi)} + e^{-i(\psi-\phi)}\right) - \lambda^2(6.4\times 10^{-7}I_\psi) + O(\lambda^3) + ...$$

Considering the normal form terms only, setting $\lambda = 1$, ignoring the small linear correction in I_ψ, and passing back to trigonometric functions, we find:

$$Z^{(2)} = I_\psi + I + \frac{I_\psi^2}{2} - (0.0032 + 0.0016I_\psi)\cos(\psi - \phi) \quad . \tag{68}$$

It is now straightforward to see that a Hamiltonian like (68) induces the pendulum dynamics, leading to phase portraits like in Fig.6. The clearest way to see this is by transforming the Hamiltonian (68) to one in *resonant canonical variables* (called sometimes 'fast' and 'slow' variables). For a general resonant wave vector $\mathbf{k^{(1)}}$, the procedure to find the resonant variables is as follows:

i) Define an integer vector $\mathbf{m}$ by the condition

$$\mathbf{m}\cdot\mathbf{k^{(1)}} = 0 \quad . \tag{69}$$

ii) Write:

$$\begin{aligned} I_\psi &= k_1^{(1)}I_R + m_1 I_F \qquad & \phi_R &= k_1^{(1)}\psi + k_2^{(1)}\phi \\ I &= k_2^{(1)}I_R + m_2 I_F \qquad & \phi_F &= m_1\psi + m_2\phi \end{aligned} \tag{70}$$

and solve to get I_ψ, I in terms of I_R, I_F. We note that Eq.(70) defines a canonical transformation, since it arises from the generating function $S(\psi,\phi,I_R,I_F) = (k_1^{(1)}\psi + k_2^{(1)}\phi)I_R + (m_1\psi + m_2\phi)I_F$.

iii) Substitute Eq.(70) in the resonant normal form (Eq.(68) in our example). Then, ϕ_F becomes an ignorable variable, implying I_F is an integral of motion of the normal form dynamics. Then, the remaining pair of variables yields the pendulum dynamics.

Let us implement these steps, concerning the resonant normal form $Z^{(2)}$ given in (68). We have:

$$(k_1^{(1)}, k_2^{(1)}) = (1,-1) \qquad \text{implying} \qquad (m_1, m_2) = (1,1) \quad .$$

Then

$$I_\psi = I_R + I_F, \quad I = -I_R + I_F, \quad \phi_R = \psi - \phi \quad \phi_F = \psi + \phi \quad .$$

Thus, substituting the above expressions into $Z^{(2)}$ we find the form of the resonant Hamiltonian in the resonant canonical variables:

$$Z_{res} = 2I_F + \frac{I_F^2}{2} + I_F I_R + \frac{I_R^2}{2} - (0.0032 + 0.0016(I_R + I_F))\cos(\phi_R) \quad . \tag{71}$$

It is now already clear that, since ϕ_F is ignorable, the variable I_F is an integral of the Hamiltonian flow of Z_{res}. Thus, it can be viewed as a parameter of a one-dimensional pendulum-like Hamiltonian system. In fact, in systems like (3), since I is a dummy action, we can exploit the freedom to assign arbitrary values to I in order to render the value of I_F equal to any convenient value. Since $I_F = (I_\psi + I)/2$, setting, for any initial condition for I_ψ, a corresponding value $I = -I_\psi$, we find $I_F = 0$, and this value is preserved along the flow of Z_{res}. Thus, without loss of generality we can recast Z_{res} as:

$$Z_{res} = \frac{I_R^2}{2} - (0.0032 + 0.0016 I_R)\cos(\phi_R) \quad . \tag{72}$$

We observe that, up to second order, and except for a small correction, this resonant normal form is what we would have found if we only kept the resonant terms in the expression of the original Hamiltonian, but as a function of the new, instead of old, resonant canonical variables. Leaving ϵ as a parameter, we find the following expression for the resonant normal form in this approximation:

$$Z_{res} \approx \frac{I_R^2}{2} - \epsilon\,(0.08 + 0.04 I_R)\cos(\phi_R) \quad . \tag{73}$$

The so-called *separatrix width*, which determines the size of the resonance, can be estimated as follows. The unstable equilibrium point of Z_{res} is at $I_R = 0$, $\phi_R = \pm\pi$. Substituting these values in (73) we find the energy value at the unstable equilibrium, which is equal to the (constant) energy value along the whole separatrix, i.e.$E_{sep} = 0.08\epsilon$. The separatrix half-width, now, corresponds to the value of $I_{R,sep}$ at $\phi_R = 0$ along the separatrix. We have

$$E_{sep} = \frac{I_{R,sep}^2}{2} - \epsilon\,(0.08 + 0.04 I_{R,sep}) \quad .$$

Solving this equation, we find the values $I^+_{R,sep}$ and $I^-_{R,sep}$, in the upper and lower separatrix branch, where the separatrix intersects the axis $\phi_R = 0$. The difference between these two values defines the separatrix width:

$$\Delta I_{R,sep} = \sqrt{(0.08\epsilon)^2 + 1.28\epsilon} \simeq 0.8\sqrt{2\epsilon} \quad . \tag{74}$$

We obtain a basic result, namely that the resonance width scales as the square root of the perturbation parameter ϵ. This is exemplified by a comparison of the top and bottom row of figure 6, where we see that, by increasing the perturbation by a factor 4, the island of the 1:1 resonance has increased in size by a factor ~ 2.

Staying in the same figure, in order to obtain the theoretical invariant curves shown in panels (b) and (d), we work as follows: Starting from a resonant normal form like (71), we fix different values of the *normal form energy* E, and compute many pairs of values (ϕ_R, I_R) along the curves of constant energy $Z_{res}(\phi_R, I_R) = E$. We also know that $I_F = 0$, and for this value we have $I_R = I_\psi$. Also, $\phi_R = \psi - \phi$, thus, on the surface of section $\phi = 0$ we have $\phi_R = \psi$. This allows to obtain a set of pairs of values (ψ, I_ψ) representing the constant energy level curves of Z_{res}. Now, it must be recalled that the variables (ψ, I_ψ) here

referred to are the *new* canonical variables, after the composition of Lie series with all generating functions χ_1, χ_2, etc. However, using Eqs.(41), from each pair of values of the new canonical variables we can compute a corresponding pair of values of the old canonical variables. Obtaining many such pairs gives the set of invariant curves shown in Figs.6b,d. In particular, we observe that the theoretical separatrix shows a deformation in its top part towards higher values of p. This is an effect due to the canonical transformations (41), while in the new variables the whole portrait at the resonance looks very symmetric around the axis $I_\psi^{(r)} = 0$, for any $r \geq 2$.

Resonant construction for librational motions

An interesting remark, at this point, is that the resonant construction described so far can be applied in the same way in the case of the main separatrix domain of the pendulum, which corresponds to librational motions. In fact, this can be considered as a case of resonance around the action value $p_* = 0$, or $\omega_* = 0$. This corresponds to the resonant wave vector $(k^{(1)}, k^{(2)}) = (1, 0)$, yielding a normal vector $\mathbf{m} = (0, 1)$. We then readily find that the resonant module is simply $\mathcal{M} = \{\mathbf{k} : k_2 = 0\}$. This means to keep in the normal form all trigonometric terms of the form $e^{ik_1\psi}$, i.e. we eliminate all terms containing the angle ϕ. Also, using Eq.(70), in this case we find $I_R = I_\psi$, and $\phi_R = \psi$. The reader can easily fill in now the details for the computation of the corresponding resonant normal form associated with librational motions. The final result, up to fourth order, apart from a constant, and after setting $\lambda = 1$ is:

$$Z_{lib}^{(4)} = I + 5.12 \times 10^{-6} I_\psi + (1 + 7.68 \times 10^{-6}) \frac{I_\psi^2}{2}$$

$$-0.0799999 \cos\psi - (1.28 + 2.56 I_\psi + 1.28 I_\psi^2) \times 10^{-6} \cos(2\psi) + 1.024 \times 10^{-7} \cos(3\psi) \ .$$

A comparison of the theoretical (with the above formula) versus numerical phase portraits in the libration domain is left as an exercise.

2.10. Hyperbolic normal form and the computation of invariant manifolds

So far, we have explored the possibilities offered by canonical perturbation theory in order to find useful representations for regular orbits in various cases of interest related either to non-resonant or to resonant dynamics. In subsection 2.2, however, it was mentioned that normal form theory can be useful even in representing some features of *chaotic dynamics*, and, in particular, in the computation of the invariant manifolds emanating from unstable periodic orbits in a chaotic domain like the extended chaotic domain of Fig.1b. We now turn our attention to this subject, which, as discussed in the introduction, has lead to a number of quite interesting modern applications.

We recall first the notion of an unstable periodic orbit, and of its asymptotic invariant manifolds. Let $(\psi(t), \phi(t), I_\psi(t), I(t))$ be an orbit of the system (3). This is called *periodic* if there is a time $t = T$ (the period) at which the orbit

closes in itself, i.e.

$$\Big(\psi(t+T), \phi(t+T), I_\psi(t+T), I(t+T)\Big) = \Big(\psi(t)(mod 2\pi), \phi(t)(mod 2\pi), I_\psi(t), I(t)\Big) \ .$$

Since in our example the angle ϕ evolves linearly with frequency equal to $\omega = 1$, it follows that the only possible periods for periodic orbits in the system (3) are $T = 2\pi$ or multiples of it. We now focus on a particular periodic orbit, denoted P, whose limit, for $\epsilon = 0$, is the unstable equilibrium point at $\psi_P = \pi$ (or $-\pi$), and $p_P = 0$. This equilibrium point continues as a periodic orbit, for values of ϵ different from zero.

Fixing a value of ϵ (say $\epsilon = 1$, as in Fig.1b), how can we locate the initial condition for this periodic orbit on the surface of section of Fig.1b? We recall that such a surface of section can be thought of as providing a mapping of the form (6), where the functions $f(\psi, p)$ and $g(\psi, p)$ are provided just by the numerical computation of the image (ψ', p'), on the surface of section, of some initial point (ψ, p). Now, assume that the point (ψ, p) is the initial condition of a periodic orbit. Then, at return on the section after one period we have $\psi' = \psi$, $p' = p$, or

$$F(\psi, p) = f(\psi, p) - \psi = 0, \qquad G(\psi, p) = g(\psi, p) - p = 0 \ . \tag{75}$$

We now see that the initial condition of the periodic orbit is the solution to a 2×2 set of algebraic equations, namely $F(\psi, p) = 0$, $G(\psi, p) = 0$. In the absence of a trivial solution, we can rely on a numerical method for the solution of this set of equations, as, for example, Newton's method.[24]

---

[24] Newton's method is an iterative method for finding the roots of a set of algebraic equations. In this method, we start with an initial guess (in our case (ψ_0, p_0) on the surface of section), and compute iteratively better approximations (ψ_1, p_1), (ψ_2, p_2), ... to a root of the system of equations $F(\psi, p) = 0$, $G(\psi, p) = 0$. Let (ψ_n, p_n) be the n-th iterate of the method. We compute the next iterate by:

$$\begin{pmatrix} \psi_{n+1} \\ p_{n+1} \end{pmatrix} = \begin{pmatrix} \psi_n \\ p_n \end{pmatrix} + \begin{pmatrix} \frac{\partial F}{\partial \psi_n} & \frac{\partial F}{\partial p_n} \\ \frac{\partial G}{\partial \psi_n} & \frac{\partial G}{\partial p_n} \end{pmatrix}^{-1} \cdot \begin{pmatrix} F(\psi_n, p_n) \\ G(\psi_n, p_n) \end{pmatrix} \ . \tag{76}$$

In practice, we need a numerical procedure for finding the values of both $F(\psi_n, p_n)$, $G(\psi_n, p_n)$, and all their partial derivatives. This can be as follows: given a point (ψ_n, p_n) on the surface of section, we compute its image (ψ'_n, p'_n) under the Poincaré surface of section mapping. This yields numerical values for the functions $f(\psi_n, p_n) = \psi'_n$ and $g(\psi_n, p_n) = p'_n$, and hence, $F(\psi_n, p_n) = f(\psi_n, p_n) - \psi_n$, $G(\psi_n, p_n) = g(\psi_n, p_n) - p_n$. In the same way, we compute the surface of section images of four neighboring initial conditions, i.e. $(\psi_n + h, p_n)$, $(\psi_n - h, p_n)$, $(\psi_n, p_n + h)$, $(\psi_n, p_n - h)$ for some small number h. This yields numerical values for the functions f and g with all four combinations of arguments. Then we can approximate partial derivatives e.g. as:

$$\frac{\partial f}{\partial \psi_n} = \frac{f(\psi_n + h, p_n) - f(\psi_n - h, p_n)}{2h} + O(h^2) \ ,$$

and similarly for $\partial f/\partial p_n$, $\partial g/\partial \psi_n$, $\partial g/\partial p_n$. Steps of order $h = 10^{-5}$ to $h = 10^{-7}$ give optimal results. The error in the computation can always be controlled by computing the determinant $(\partial f/\partial \psi_n)(\partial g/\partial p_n) - (\partial f/\partial p_n)(\partial g/\partial \psi_n)$ which is theoretically equal to 1. Finally, we form the

Implementing Newton's method in our system (3), for $\epsilon = 1$, we find that the periodic orbit is located at $\psi_P = \pi$, $p_P = -0.0073246492486565$, with an uncertainty in the last digit.

In order to check the *stability* of this orbit, we compute the so-called monodromy (or Floquet) matrix, which is the matrix of the linearized mapping equations computed at the point (ψ_P, p_P), namely

$$M = \begin{pmatrix} a & b \\ c & d \end{pmatrix} = \left. \begin{pmatrix} \frac{\partial f}{\partial \psi} & \frac{\partial f}{\partial p} \\ \frac{\partial g}{\partial \psi} & \frac{\partial g}{\partial p} \end{pmatrix} \right|_{\psi=\psi_P, p=p_P} \quad . \tag{77}$$

The stability is characterized by the eigenvalues of the monodromy matrix, given by the solution of the characteristic polynomial $\Lambda^2 - (a+d)\Lambda + (ad - bc) = 0$. By the symplectic condition, we have $ad - bc = 1$, thus

$$\Lambda_{1,2} = \frac{(a+d) \pm \sqrt{(a+d)^2 - 4}}{2} \quad . \tag{78}$$

In the case of unstable periodic orbits, we have two real and reciprocal eigenvalues $\Lambda_1 \Lambda_2 = 1$. The condition for instability, thus, is given by $|a + d| > 2$. Without loss of generality, assume $|\Lambda_1| > 1$ and $|\Lambda_2| < 1$. The eigenvector of M corresponding to the eigenvalue L_1 defines an *unstable eigen-direction* of the linearized mapping around (ψ_P, p_P), while the eigenvector corresponding to Λ_2 defines a *stable* eigen-direction respectively. These directions are easily found by taking the definition of an eigenvector, namely a vector which, acted upon by M, yields a multiple of itself by a factor equal to the eigenvalue. Implementing this definition, if $(\Delta\psi, \Delta p)$ denotes, say, the unstable eigenvector, we have:

$$\begin{pmatrix} a & b \\ c & d \end{pmatrix} \begin{pmatrix} \Delta\psi \\ \Delta p \end{pmatrix} = \Lambda_1 \begin{pmatrix} \Delta\psi \\ \Delta p \end{pmatrix} \quad .$$

The above condition yields two linearly dependent equations, thus we may chose any of them to define the direction of the unstable eigenvector, i.e.

$$\frac{\Delta p}{\Delta \psi} = \frac{\Lambda_1 - a}{b} = \frac{c}{\Lambda_1 - d} \quad . \tag{79}$$

Consider now a small segment of length ΔS on the surface of section along, say, the unstable eigen-direction, starting from the periodic orbit P (Figure 8), and compute the successive images of this segment under the surface of section mapping. By this process we obtain numerically the intersection (with the surface of section) of the *unstable manifold* of the periodic orbit P. In Figs.8a,b, the

---

matrix

$$\begin{pmatrix} \frac{\partial F}{\partial \psi_n} & \frac{\partial F}{\partial p_n} \\ \frac{\partial G}{\partial \psi_n} & \frac{\partial G}{\partial p_n} \end{pmatrix} = \begin{pmatrix} \frac{\partial f}{\partial \psi_n} & \frac{\partial f}{\partial p_n} \\ \frac{\partial g}{\partial \psi_n} & \frac{\partial g}{\partial p_n} \end{pmatrix} - \begin{pmatrix} 1 & 0 \\ 0 & 1 \end{pmatrix} \quad .$$

The method is successful if the sequence of successive iterates $(\psi_n, p_n) \to (\psi_{n+1}, p_{n+1})$ converges. Numerically, we stop when differences between successive iterates become smaller than a prescribed precision level (which can be very small, say 10^{-14}).

unstable manifold (denoted by W_u) is shown as a thin curve starting from the left point P (which is the same as the right point, modulo 2π). This curve has the form of a straight line close to P, but exhibits a number of oscillations as it approaches the right point P. In the same way, we can compute the stable manifold W_s emanating from the right point P, also shown by a thin curve (in our example the two curves are symmetric with respect to the axis $\psi = 0$, due to a corresponding symmetry in the Hamiltonian (3)). In the case of the stable manifold, we integrate backwards in time all initial conditions on the initial segment ΔS, until finding the pre-image of this segment on the surface of section. We observe that the stable manifold also develops oscillations as it approaches the left point P.

The following are now some more precise definitions. Let

$$\mathcal{D}_P = \left\{ \left(\psi_P(t), \phi_P(t), I_{\psi,P}(t), I_P(t) \right), 0 \leq t \leq T \right\}$$

be the set of all points of the periodic orbit P parametrized by the time t, and $\mathbf{q} = (\psi, \phi, I_\psi, I)$ a randomly chosen point in phase space. We define the distance of an arbitrary point $\mathbf{q}$ of the phase space from the periodic orbit as:

$$d(\mathbf{q}, P) = \min \{ dist(\mathbf{q}, \mathbf{q}_P) \text{ for all } \mathbf{q}_P \in \mathcal{D}_P \}$$

where $dist()$ means the Euclidean distance. Let now $\mathbf{q}_0$ be a particular initial condition at $t = 0$, and let $\mathbf{q}(t; \mathbf{q}_0)$ denote the orbit resulting from that initial condition. The unstable manifold of P is defined as:

$$W_u^P = \left\{ \mathbf{q}_0 : \lim_{t \to -\infty} d(\mathbf{q}(t; \mathbf{q}_0), P) = 0 \right\} \quad . \tag{80}$$

In words, the unstable manifold W_u^P is the set of all initial conditions in the phase space leading to orbits which tend asymptotically to the periodic orbit P when integrated in the backward sense of time. This, in fact, implies that these orbits recede (on average) from the periodic orbit in the forward sense of time.

Similarly, we define the stable manifold of P by:

$$W_s^P = \left\{ \mathbf{q}_0 : \lim_{t \to \infty} d(\mathbf{q}(t; \mathbf{q}_0), P) = 0 \right\} \quad . \tag{81}$$

In words, it is the set of all initial conditions whose resulting orbits tend asymptotically to the periodic orbit P in the forward sense of time.

The following are some basic properties of W_u and W_s:

i) Both sets are *invariant* under the Hamiltonian flow, i.e. any initial condition on W_u^P leads to an orbit lying always on W_u^P (and similarly for W_s^P).

ii) The unstable (or stable) invariant manifold cannot intersect itself at any of its points. In fact, a simple argument shows that such intersections are inconsistent with causality.

iii) In contrast to (ii), the unstable and stable manifolds may intersect each other. Such intersections are called *homoclinic points*, and their resulting orbits are called homoclinic orbits. Such is the example of the homoclinic point H in figure 8 (see below).

iv) As a consequence of the so-called Grobman (1959) and Hartman (1960) theorem, the unstable manifold W_u^P is tangent to the unstable manifold of the linearized flow around P. In fact, it is this property which allows us to approximate numerically the computation of the invariant manifolds, by taking the successive images of small straight segments along one of the eigendirections close to P.

The study of the asymptotic manifolds of unstable periodic orbits in a chaotic domain is a key element for understanding the structure and mechanisms of chaos in dynamical systems. This key role was already emphasized by Poincaré, who, on the basis of theoretical arguments, predicted the complexity induced in the behavior of chaotic orbits in the phase space due to the manifold dynamics. Various laws characterizing, in particular, the *lobes* and *recurrences* of the invariant manifolds are given in Contopoulos and Polymilis (1993).

We now show that, despite their complexity, the invariant manifolds are objects possible to compute, up to some extent, via an appropriate form of canonical perturbation theory. The resulting normal form, called a *hyperbolic normal form*, was first studied by Moser (1958), while its implementation via canonical transformations was first discussed by Giorgilli (2001).

We give below a specific example of computation of a hyperbolic normal form, and discuss the kind of phenomena whose study becomes possible by using such a normal form.

The idea of a hyperbolic normal form is simple: close to any unstable periodic orbit, we wish to pass from old to new canonical variables $(\psi, \phi, p, I) \rightarrow (\xi, \phi', \eta, I')$, so that the Hamiltonian in the new variables takes locally the form:

$$Z_h = \omega I' + \nu \xi \eta + Z(I', \xi\eta) \tag{82}$$

where ν is a real constant. In a Hamiltonian like (82), the point $\xi = \eta = 0$ corresponds to a periodic orbit, since, from Hamilton's equation we find $\dot{\xi} = \dot{\eta} = 0 = \dot{I'} = 0$, while $\phi' = \phi'_0 + (\omega + \partial Z(I', 0)\partial I')t$. This implies a periodic orbit, with frequency $\omega' = (\omega + \partial Z(I', 0)\partial I')$. In a system like (3), where the action I is dummy, we find that I' does not appear in the hyperbolic normal form, thus, the periodic solution $\xi = \eta = 0$ has a frequency equal to ω always.

By linearizing Hamilton's equations of motion near this solution, we find that it is always unstable. In fact, we can easily show that the linearized equations of motion for small variations $\delta\xi, \delta\eta$ around $\xi = 0, \eta = 0$ are

$$\dot{\delta\xi} = (\nu + \nu_1(I'))\delta\xi, \qquad \dot{\delta\eta} = -(\nu + \nu_1(I'))\delta\eta$$

where $\nu_1(I') = \partial Z(I', \xi\eta = 0)/\partial(\xi\eta)$. The solutions are $\delta\xi(t) = \delta\xi_0 e^{(\nu+\nu_1)t}$, $\delta\eta(t) = \delta\eta_0 e^{-(\nu+\nu_1)t}$. After one period $T = 2\pi/\omega$ we have $\delta\xi(T) = \Lambda_1 \delta\xi_0$, $\delta\eta(T) = \Lambda_2 \delta\xi_0$, where $\Lambda_{1,2} = e^{\pm 2\pi(\nu+\nu_1)/\omega}$. Thus, the two eigendirections of the linearized flow correspond to setting $\delta\xi_0 = 0$, or $\delta\eta_0 = 0$, i.e. they coincide with the axes $\xi = 0$, or $\eta = 0$. These axes are invariant under the flow of (82) and, therefore, *they constitute the unstable and stable manifold of the associated periodic orbit* P.

In summary: if we succeed in finding a canonical transformation of the form

$$\begin{aligned} \psi &= \Phi_\psi(\xi, \phi', \eta, I') \\ \phi &= \Phi_\phi(\xi, \phi', \eta, I') \\ p &= \Phi_p(\xi, \phi', \eta, I') \\ I &= \Phi_I(\xi, \phi', \eta, I') \end{aligned} \tag{83}$$

in which the Hamiltonian in the neighborhood of an unstable periodic orbit takes the form (82), then, the expressions i) $\xi = \eta = 0$, and ii) $\xi = 0$ or $\eta = 0$ yield the position of the periodic orbit, and ii) the form of its invariant manifolds in the variables (ξ, ϕ', η, I'). Furthermore, iii) the expressions $\Lambda_{1,2} = e^{\pm 2\pi(\nu+\nu_1)/\omega}$ yield the eigenvalues of the unstable periodic orbit.

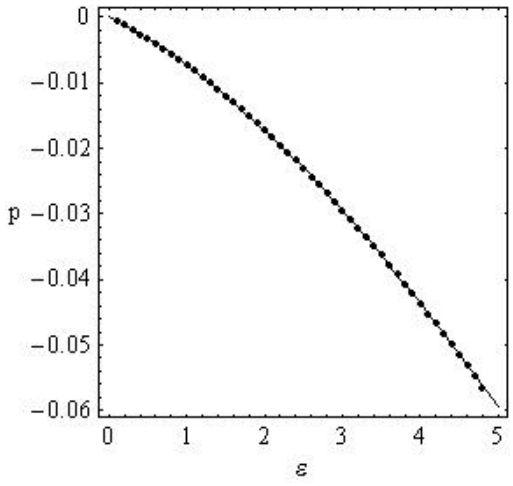

Figure 7. The characteristic curve (value of the fixed point variable p_P on the surface of section) for the main unstable periodic orbit as a function of ϵ. The dots correspond to a purely numerical calculation using Newton's method. The solid curve shows the theoretical calculation using a hyperbolic normal form (similar to formula (96) in text, but for a normalization up to the fifteenth order).

A key point is, now, the following: after we explicitly compute the canonical transformations (83), we can use Eqs.(83) in order to *compute analytically the periodic orbit and its asymptotic invariant manifolds in the original canonical variables as well.* Such a computation, whose details will be presented below, is shown in figures 7 and 8. Figure 7 shows the so-called *characteristic curve* of the main unstable periodic orbit of the system (3), i.e. the orbit which is the continuation, for $\epsilon \neq 0$, of the unstable equilibrium point $(\psi = \pm\pi, p = 0)$ which exists for $\epsilon = 0$. The characteristic curve is a curve yielding the value of the initial conditions on a surface of section, as a function of ϵ, for which the resulting orbit is the periodic one. In our case, we always have $\psi_P = 0$, while p_P varies with ϵ. The dotted curve shows $p_P(\epsilon)$ as computed by a purely numerical process, i.e., implementing Newton's root-finding method, while the solid curve yields $p_P(\epsilon)$ as computed by a hyperbolic normal form at the normalization order

$r = 15$ (see below). The agreement is excellent, and we always recover 8-9 digits of the numerical calculation in this approximation, even for values of ϵ much larger than unity.

How is this computation possible? Returning to Eqs.(83), we simply set $\xi = \eta = 0$, while I', which is an integral of the Hamiltonian flow of (82), can be replaced by a constant label value $I' = c$. [25] Finally, knowing the frequency ω' by which ϕ' evolves, we can set $\phi' = \omega' t + \phi'_0$. Substituting these expressions in the transformation equations (83), we are lead to:

$$\begin{aligned} \psi_P(t) &= \Phi_\psi(0, \omega' t + \phi'_0, 0, c) \\ \phi_P(t) &= \Phi_\phi(0, \omega' t + \phi'_0, 0, c) \\ p_P(t) &= \Phi_p(0, \omega' t + \phi'_0, 0, c) \\ I_P(t) &= \Phi_I(0, \omega' t + \phi'_0, 0, c) \quad . \end{aligned} \tag{84}$$

The set of Eqs.(84) yields now an *analytic representation of the periodic orbit* P in the whole time interval $0 \leq t \leq 2\pi/\omega'$. In fact, by the form of the hyperbolic normal form and its normalizing transformations, we find that Eqs.(84) provide a formula for the periodic orbit in terms of a Fourier series, which allows us to find not only its initial conditions on a surface of section, but also the whole time evolution of the set of canonical variables along P.

Similar principles apply to the computation of the invariant manifolds of P. In this case, we first fix a surface of section by setting, say, $\phi' = 0$. Then, assuming, without loss of generality, that the unstable manifold corresponds to setting $\eta = 0$, we find a parametric form for all canonical variables as a function of ξ along the asymptotic curve of the unstable manifold on the surface of section:

$$\psi_{P,u}(\xi) = \Phi_\psi(\xi, 0, 0, c), \quad p_{P,u}(\xi) = \Phi_p(\xi, 0, 0, c) \quad . \tag{85}$$

Due to Eq.(85), ξ can be considered as a *length parameter* along the asymptotic curve of the unstable manifold W_u. Numerically, this allows to compute the asymptotic curve W_u on the surface of section by giving different values to ξ. Such a computation is shown with a thick curve in Fig.8a. We observe that the theoretical curve W_u agrees well with the numerical one up to a certain distance corresponding to $\xi \sim 1$, whereby the theoretical curve starts deviating from the true asymptotic curve W_u. This is because, as we will see, the hyperbolic normal form has a *finite domain of convergence* around P. Thus, by using a finite truncation of the series (83) (representing the normalizing canonical transformations), deviations occur at points beyond the domain of convergence of the hyperbolic normal form.

Similar arguments (and results, as shown in Fig.8) are found for the stable manifold of P. In that case, we substitute $\xi = 0$ in the transformation equations, and employ η as a parameter, namely:

$$\psi_{P,s}(\eta) = \Phi_\psi(0, 0, \eta, c), \quad p_{P,s}(\eta) = \Phi_p(0, 0, \eta, c) \quad . \tag{86}$$

---

[25] In fact, if I is a dummy action, its near identity transformation I' does not appear in the Eqs.(83).

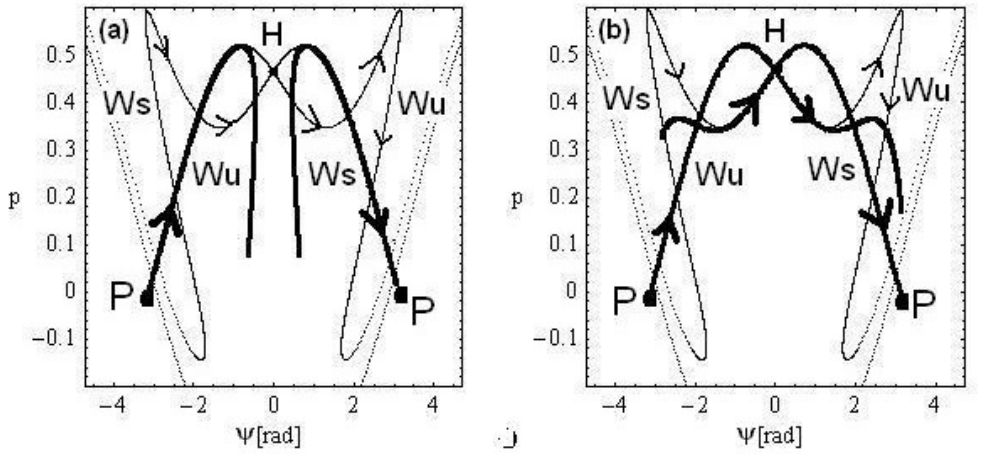

Figure 8. The thin dotted lines show the unstable (W_u) and stable ((W_s) manifolds emanating from the main unstable periodic orbit (P) in the model (3), for $\epsilon = 1$, after a purely numerical computation (mapping for 8 iterations of 1000 points along an initial segment of length $ds = 10^{-3}$ taken along the unstable and stable eigen-directions respectively. In (a), the thick lines show a theoretical computation of the invariant manifolds using a hyperbolic normal form at the normalization order $r = 15$ (see text). Both theoretical curves W_u and W_s deviate from the true manifolds before reaching the first homoclinic point (H). (b) Same as in (a), but now the theoretical manifolds are computed using the analytic continuation technique suggested in Ozorio de Almeida and Viera (1997). The theoretical curves cross each other at the first homoclinic point, thus, this point can be computed by series expansions.

In figure 8 we see that the domains of convergence of the hyperbolic normal form are small enough so that the two theoretical curves W_u and W_s have no intersection. This implies that we cannot use this computation in order to specify analytically the position of a *homoclinic* point, like H in figure 8. However, in recent years, Ozorio de Almeida and co-workers (Da Silva Ritter et al. (1987), Viera and Ozorio de Almeida (1996), Ozorio de Almeida and Viera (1997)) have considered an extension of the original theory of Moser, which allows to extend considerably the domain of validity of the hyperbolic normal form construction, and to compute homoclinic intersections and even some lobes formed by the asymptotic manifolds in the vicinity of P. Essentially, the technique relies on i) using first the usual construction in order to compute a finite segment of, say, W_u within the domain of convergence of the hyperbolic normal form, and ii) analytically continue this part up to one or more images of it, using *the original Hamiltonian as a Lie generating function*. That is, if $\mathbf{q}$ is a point computed on the invariant manifold, we compute its image via

$$\mathbf{q}' = \exp(t_n L_H) \exp(t_{n-1} L_H) \ldots \exp(t_1 L_H) \mathbf{q} \tag{87}$$

where $t_n + t_{n-1} + \ldots + t_1 = T$, while the times are chosen so as to always lead to a mapping within the analyticity domain of the corresponding Lie series in a complex time domain. Figure 8b shows such a result. Computing a Lie series via (87) with $t_1 = t_2 = t_3 = t_4 = \pi/2$, the thick lines show the theoretical

computation of the images (for the unstable manifold), or pre-images (for the stable manifold), for which we put a minus sign in front of all times t_1 to t_4) of the thick lines shown in panel (a), after (or before) one period. We now see that the resulting series represent the true invariant manifolds over a considerably larger extent, thus, allowing to compute theoretically the position of the homoclinic point H. [26]

We now present in detail the steps leading to the previous results, i.e. a practical example of the calculation of a hyperbolic normal form.

i) *Hamiltonian expansion.* Starting from the Hamiltonian (3), in the neighborhood of P (see phase portraits in Fig.1) it is convenient to expand the Hamiltonian around the value $\psi_0 = \pi$ (or, equivalently, $-\pi$), which corresponds to the position of the unstable equilibrium when $\epsilon = 0$. Setting $\psi = \pi + u$, we then find (up to fourth order): [27]

$$H = \frac{p^2}{2} + I - 0.08\left(1 + 0.5\epsilon(1+p)(e^{i\phi} + e^{-i\phi})\right)\left(-1 + \frac{u^2}{2} - \frac{u^4}{24} - ...\right) \quad (88)$$

The hyperbolic character of motion in the neighborhood of the unstable equilibrium is manifested by the combination of terms:

$$H = I + \frac{p^2}{2} - 0.08\frac{u^2}{2} + ... \quad (89)$$

The constant ν appearing in Eq.(82) is related to the constant 0.08 appearing in Eq.(89) via $\nu^2 = 0.08$. In fact, if we write the hyperbolic part of the Hamiltonian as $H_h = p^2/2 - \nu^2 u^2/2$, it is possible to bring H_h in hyperbolic normal form, by introducing a linear canonical transformation:

$$p = \frac{\sqrt{\nu}(\xi + \eta)}{\sqrt{2}}, \quad u = \frac{(\xi - \eta)}{\sqrt{2\nu}} \quad (90)$$

where ξ and η are the new canonical position and momentum respectively. Then H_h acquires the desired form, i.e. $H_h = \nu\xi\eta$.

Substituting the transformation (90) in the Hamiltonian (88) we find

$$H = I + 0.282843\xi\eta - 0.041667\xi\eta^3 + 0.0625\xi^2\eta^2 - 0.041667\xi^3\eta + 0.010417\xi^4$$

$$+\epsilon\Big[0.08 + 0.030085\eta - 0.070711\eta^2 - 0.026591\eta^3 + 0.010417\eta^4$$

[26] The reader may wonder why there should be interest in knowing the position of homoclinic points like H. The role of homoclinic points, as well as of their resulting (as initial conditions) homoclinic orbits, in the problem of the so-called *structure of chaos* in Hamiltonian systems cannot be overemphasized. In fact, the homoclinic points form the basis upon which we understand the structure of the *homoclinic tangle*, which is the main local source of chaos close to unstable periodic orbits (see Contopoulos (2002), for a review of the concept and consequences of homoclinic chaos).

[27] In this example we keep ϵ as a parameter, without substituting its numerical value. This is needed in the calculation of the position of the periodic orbit P as a function of ϵ, used in Fig.7.

$$+0.030085\xi + 0.14142\xi\eta + 0.0265915\xi\eta^2 - 0.041667\xi\eta^3$$
$$-0.070711\xi^2 + 0.026591\xi^2\eta + 0.0625\xi^2\eta^2 - 0.026591\xi^3$$
$$-0.041667\xi^3\eta + 0.010417\xi^4 + ...\Bigg] \left(\frac{e^{i\phi} + e^{-i\phi}}{2}\right) \quad .$$

As always, we now have to introduce some book-keeping. In the present case, it is crucial to recognize that the quantities ξ, η themselves can be considered as small quantities describing the neighborhood of a hyperbolic point. However, we want to retain a book-keeping factor λ^0 for the lowest order term $\xi\eta$, since, as we will see, this term appears in the homological equation defining the Lie generating functions in the present case. We thus follow the rule that monomial terms containing a product $\xi^{s_1}\eta^{s_2}$ acquire a book-keeping factor $\lambda^{s_1+s_2-2}$ in front. [28] Finally, we add a book-keeping factor λ to all the terms that are multiplied by ϵ.

In summary, up to $O(\lambda^2)$ the Hamiltonian before any normalization reads:

$$H^{(0)} = I + 0.282843\xi\eta$$
$$+\lambda\epsilon\Big[0.04 + 0.0150424(\xi+\eta) - 0.0353553(\xi^2+\eta^2) + 0.0707107\xi\eta\Big](e^{i\phi} + e^{-i\phi})$$
$$+\lambda^2\Big[0.0104167(\xi^4+\eta^4) - 0.0416667(\xi\eta^3 + \xi^3\eta) + 0.0625\xi^2\eta^2$$
$$+0.0132957\epsilon(\xi^2\eta + \xi\eta^2 - \xi^3 - \eta^3)(e^{i\phi} + e^{-i\phi})\Big] + \dots$$

According to the definition of the hyperbolic normal form (Eq.(82)), at first order we want to eliminate i) terms depending on the angle ϕ, or, ii) terms independent of ϕ but depending on a product $\xi^{s_1}\eta^{s_2}$ with $s_1 \neq s_2$. These are

$$h_1^{(0)} = \epsilon\Big[0.04 + 0.0150424(\xi+\eta) - 0.0353553(\xi^2+\eta^2) + 0.0707107\xi\eta\Big](e^{i\phi} + e^{-i\phi}) \; .$$

---

[28] This, by the way, is precisely the optimal book-keeping scheme in computing normal forms for polynomial Hamiltonians in general. In the case of elliptic equilibria, in particular, assuming that the lowest order term in the Hamiltonian is the harmonic oscillator model

$$H = \frac{p^2}{2} + \frac{\omega_0^2\psi^2}{2}$$

we introduce complex canonical variables via a linear canonical transformation quite similar to (90), namely

$$p = \frac{\sqrt{\omega_0}(iQ+P)}{\sqrt{2}}, \quad \psi = \frac{(Q+iP)}{\sqrt{2\omega_0}} \quad . \tag{91}$$

The zeroth order Hamiltonian takes the form $H = i\omega_0 QP$. Then, we normalize all monomial terms of the form $Q^{s_1}P^{s_2}$ giving rise to non-zero divisors. This is the way to normalize, for example, the Hamiltonian of the Hénon-Heiles (1964) model. The variables Q, P have a particular importance in quantum mechanics, where Q is called the creation operator, while iP is the annihilation operator.

In order to define the generating function χ_1 performing the first order normalization, we now see that we need a homological equation different from what we have seen so far, namely:

$$\{I + 0.282843\xi\eta, \chi_1\} + \lambda h^{(0)} = 0 \quad . \tag{92}$$

The solution of equation (92) is found by noticing that the action of the operator $\{\omega I + \nu\xi\eta, \cdot\}$ on monomials of the form $\xi^{s_1}\eta^{s_2}a(I)e^{ik_2\phi}$ yields

$$\left\{\omega I + \nu\xi\eta, \xi^{s_1}\eta^{s_2}a(I)e^{ik_2\phi}\right\} = -[(s_1 - s_2)\nu + i\omega k_2]\xi^{s_1}\eta^{s_2}a(I)e^{ik_2\phi} \quad .$$

Thus, if we write $h_1^{(0)}$ as

$$h_1^{(0)} = \sum_{(s_1,s_2,k_2)\notin\mathcal{M}} b_{s_1,s_2,k_2}(I)\xi^{s_1}\eta^{s_2}e^{ik_2\phi}$$

where the resonant module in this case is defined as:

$$\mathcal{M} = \{(s_1, s_2, k_2) : s_1 = s_2 \text{ and } k_2 = 0\} \tag{93}$$

then, the solution of the homological equation (92) is

$$\chi_1 = \sum_{(s_1,s_2,k_2)\notin\mathcal{M}} \frac{b_{s_1,s_2,k_2}(I)}{(s_1 - s_2)\nu + i\omega k_2}\xi^{s_1}\eta^{s_2}e^{ik_2\phi} \quad . \tag{94}$$

In fact, since I is a dummy action, it does not appear in any of the coefficients b_{s_1,s_2,k_2}. But the main observation, regarding Eq.(94), is that *the divisors are complex numbers with a modulus bounded from below by a positive constant*, i.e. we have:

$$\begin{aligned} |\nu(s_1 - s_2) + ik_2\omega| &= \sqrt{(s_1 - s_2)^2\nu^2 + k_2^2\omega^2} \geq \min(|\nu|, |\omega|) \\ &\quad \text{for all } (s_1, s_2, k_2) \notin \mathcal{M} \quad . \end{aligned} \tag{95}$$

This last bound constitutes the most relevant fact about the construction of hyperbolic normal forms, because it implies that this construction is convergent. In fact, the sequences of repetitions of divisors encountered in subsection 2.5 appear here also in a quite similar manner, as the reader may readily verify by trying to reconstruct the 'most dangerous' sequence of terms produced by successive Poisson brackets. However, the fact that divisors are bounded from below by a positive constant implies that the radius of convergence remains finite as the normalization order tends to infinity.

Returning to the numerical example, after performing the computations in (94) the generating function χ_1 reads:

$$\chi_1 = \lambda\epsilon i\Bigg[\Bigg(- 0.04 + (0.00393948 - 0.0139282i)\xi - (0.00393948 + 0.0139282i)\eta$$

$$-(0.0151515 - 0.0267843i)\xi^2 + (0.0151515 + 0.0267843i)\eta^2 - 0.070711\xi\eta\Big)e^{i\phi}$$

$$+\Big(0.04 + (0.00393948 + 0.0139282i)\xi - (0.00393948 - 0.0139282i)\eta$$

$$-(0.0151515 + 0.0267843i)\xi^2 + (0.0151515 - 0.0267843i)\eta^2 + 0.070711\xi\eta\Big)e^{-i\phi}\Big]$$

The normalized Hamiltonian, after computing $H^{(1)} = \exp(L_{\chi_1})H^{(0)}$ is in normal form up to terms of $O(\lambda)$. In fact, we find that there are no new normal form terms at this order, but such terms appear at order λ^2. The reader is invited to make the computation at order 2, which finally yields $H^{(2)} = \exp(L_{\chi_2})H^{(1)}$, in normal form up to order two. We give the final result for verification. Apart from a constant, we have

$$H^{(2)} = I + 0.282843\eta\xi + \lambda^2(0.0625\xi^2\eta^2 - \epsilon^2 0.0042855\xi\eta) + O(\lambda^3) + \ldots$$

Let us also give the analytic expressions for the periodic orbit, up to order $O(\lambda^2)$, found by exploiting the normalizing transformations of the hyperbolic normal form. The old canonical variables (ξ, η) are computed in terms of the new canonical variables $(\xi^{(2)}, \eta^{(2)})$ following:

$$\xi = \exp(L_{\chi_2})\exp(L_{\chi_1})\xi^{(2)}$$

$$\eta = \exp(L_{\chi_2})\exp(L_{\chi_1})\eta^{(2)} \quad .$$

This yields functions (up to order $O(\lambda^2)$ $\xi = \Phi_\xi(\xi^{(2)}, \phi^{(2)}, \eta^{(2)})$, and $\eta = \Phi_\eta(\xi^{(2)}, \phi^{(2)}, \eta^{(2)})$. By virtue of the fact that I is a dummy action, we have $\phi^{(2)} = \phi = \omega t = t$, while, for the periodic orbit we set $\xi^{(2)} = \eta^{(2)} = 0$. With these substitutions, we find

$$\xi_P(t) = \Phi_\xi(0, t, 0), \quad \eta_P(t) = \Phi_\eta(0, t, 0) \quad .$$

Finally, we substitute the expressions for $\xi_P(t)$ and $\eta_P(t)$ in the linear canonical transformation (90), in order to find analytic expressions for the periodic orbit in the original variables $p, \psi = \pi + u$. Switching back to trigonometric functions, and setting $\lambda = 1$, we finally find:

$$\begin{aligned} \psi_P(t) &= \pi + 0.0740741\epsilon \sin t - 0.000726216\epsilon^2 \sin(2t) \\ p_P(t) &= -0.00592593\epsilon \cos t - 0.00145243\epsilon^2 \cos(2t) \quad . \end{aligned} \tag{96}$$

The position of the periodic orbit on the surface of section can be found now by setting $t = 0$ in Eqs.(96). In the actual computation of figures 7 and 8, we compute all expansions up to $O(\lambda^{15})$, after expanding also $\cos\psi$ in the original Hamiltonian up to the same order.

3. CONSEQUENCES OF ANALYTICITY

3.1. Book-keeping in models with infinitely many Fourier harmonics

So far, we have examined some basic methods of canonical perturbation theory by presenting a number of numerical examples where such methods are applicable, employing for this purpose the Hamiltonian model (3). However, this model has a number of important limitations. In the present section we focus on one such limitation whose consequences are necessary to discuss, i.e., the fact that the perturbation term in (3) contains only a *finite number of Fourier harmonics*. Namely, in the original Hamiltonian we only have the terms $e^{\pm i\psi}$, $e^{\pm i(\psi+\phi)}$ and $e^{\pm i(\psi-\phi)}$. It has been discussed already that even with few terms initially, a whole spectrum of new Fourier terms are generated in the course of any of the normalization schemes discussed in section 2. However, in the sequel we are interested in a more general case, in which many, or even *all possible Fourier harmonics are present already in the original Hamiltonian.*

It should be made clear that the above situation occurs in almost all problems of practical interest encountered in dynamical astronomy. Consider, for example, the study of a quite common class of problems in galactic dynamics, referring to galaxies with a non-axisymmetric distribution of matter. Such is, for instance, the case of the study of motions in the galactic plane of a spiral galaxy. Using polar coordinates (r, θ) on the plane, the gravitational potential $V(r, \theta)$ can be written in the form of a sum of an axisymmetric term $V_0(r)$, which accounts for the gravitational effects of the disc, and a non-axisymmetric perturbation $\epsilon V_1(r, \theta)$ yielding the gravitational effects of the spiral arms (and/or a bar). The term V_1, in turn, can be expressed in terms of its Fourier decomposition (see subsection 3.5 for details):

$$V_1(r, \theta) = \sum_{k=-\infty}^{\infty} V_k(r) e^{ik\theta} \quad .$$

As discussed in subsection 3.5, the Fourier coefficients $V_k(r)$ can be analyzed in terms of the so-called 'radial' (or epicyclic) action angle variables (I_r, θ_r) as

$$V_k(r) = \sum_{k_r=-\infty}^{\infty} \tilde{V}_{k_r,k}(I_r) e^{ik_r\theta_r} \quad .$$

Then, the gravitational potential of a disc spiral galaxy is a sum of Fourier terms over all possible wavenumbers k_r, k, a fact implying that the original Hamiltonian describing stellar motions in the galaxy contains the whole possible spectrum of Fourier harmonics $\exp(i(k_r\theta_r + k\theta))$.

It is reasonable to expect that the Fourier coefficients of the higher order Fourier terms (i.e. the ones for which $|k_r| + |k|$ is high) are smaller in size. This question, of how the size of the Fourier terms decreases with Fourier order, plays an essential role in the development of almost all perturbative schemes dealing with problems of dynamical astronomy, because it crucially affects the way by which we can choose to implement *book-keeping* in the Hamiltonian normalization. To show this, consider a generic form of Hamiltonian given by

$$H = H_0 + \epsilon(\ldots \text{infinitely many harmonics} \ldots) = H_0 + \epsilon H_1 \quad . \qquad (97)$$

The whole term ϵH_1 can be considered as a quantity 'of order ϵ'. If we now choose to book-keep according to powers of ϵ, [29], we should write:

$$H = \lambda^0 H_0 + \lambda^1 \epsilon(\ldots \text{infinitely many harmonics} \ldots) \tag{98}$$

But in this way, Eq.(98) implies that infinitely many terms have to be normalized already at the first order of perturbation theory.

There is nothing fundamentally inconsistent in the above method of doing book-keeping in a Hamiltonian of the form (97). However there are a number of issues rendering the method rather problematic in practice. Let us mention the most important ones:

i) *Memory requirements:* in the computer we have to introduce a maximum order r_{max} in the book-keeping parameter up to which terms can be stored. Following Eq.(98), r_{max} represents also the maximum order in ϵ up to which terms are stored. However, at every order of ϵ we have terms of all Fourier orders. Thus, we must introduce also a maximum Fourier order K_{max}, up to which terms can be stored. The total memory requirements then depend on the size of the integer lattice (r_{max}, K_{max}). We can now see the following: if (r_0, K_0) denotes a so-called *domain of interest*, i.e. a domain in which we are interested in storing all possible terms arising in the *final* normal form series, then, this is only possible if allowance is made to store terms arising in *intermediate* normalization steps within a domain much larger than (r_0, K_0), namely

$$(r_{max}, K_{max}) = (r_0, K_0 r_0) \quad . \tag{99}$$

A detailed proof is given in Efthymiopoulos (2008). [30] One can see that in most applications the memory requirements due to Eq.(99) become prohibitive. In fact, we have the estimate

$$\frac{\text{number of terms that need to be stored}}{\text{number of terms in domain of interest}} \approx \left(\frac{r_0+1}{2}\right)^{2n}$$

where n is the number of degrees of freedom. Since r_0 is usually a number of order ~ 10, the memory requirements at intermediate normalization steps are orders of magnitude bigger than those for storing the final Hamiltonian.

---

[29] This is the most common suggestion in textbooks regarding the application of canonical perturbation theory, namely, to normalize first terms of order ϵ, then ϵ^2, etc.

[30] In summary: the worst memory requirements are caused by the operation $H^{(1)} = \exp(L_{\chi_1}) H^{(0)}$. The generating function χ_1 contains terms of the form $\epsilon a(J) \exp(ik\cdot\phi)$, for some of which we have $|k| = K_0$. The Hamiltonian $H^{(0)}$ contains also terms of the form $\epsilon a'(J) \exp(ik\cdot\phi)$, but for some terms we now have $|k| = K_{max}$. Then, the Poisson bracket operation between such terms yields terms of the form $\epsilon^2 [a(J) k\cdot\nabla_J a'(J) - a'(J) k'\cdot\nabla_J a(J)] \exp(i(k+k')\cdot\phi)$. Since the components of k and k' are added algebraically, it is possible that $|k+k'| = K_{max} - K_0$. In the same way, the s-th Poisson bracket contained in $L^s_{\chi_1} H^{(0)}$ can produce Fourier terms of order ϵ^{s+1} and Fourier order $K_{max} - sK_0$. The maximum s is then defined by $s+1 = r_0$, or $s = r_0 - 1$. But then, we must have $K_{max} - (r_0 - 1)K_0 = K_0$, or $K_{max} = r_0 K_0$.

(Non-)validity of some normal forms in open domains of the action space: Let us assume, again a book-keeping of the form (98), and, furthermore, that the zeroth order term H_0 has a nonlinear dependence on the action variables $\mathbf{I}$. A possible way to perform normal form computations is now the following: writing

$$H_1(\mathbf{I},\phi) = \sum_{all\ \mathbf{k}} H_{1,\mathbf{k}}(\mathbf{I}) \exp(i\mathbf{k}\cdot\phi)$$

and choosing any type of resonant module $\mathcal{M}$, we define a Lie generating function χ_1 by solving a homological equation similar to Eq.(36), namely:

$$\{H_0,\chi_1\} + h_1^{(0)} = 0 \tag{100}$$

where

$$h_1^{(0)}(\mathbf{I},\phi) = \sum_{\mathbf{k}\notin\mathcal{M}} H_{1,\mathbf{k}}(\mathbf{I}) \exp(i\mathbf{k}\cdot\phi) \quad .$$

However, the solution of (100)

$$\chi_1 = \sum_{\mathbf{k}\notin\mathcal{M}} \frac{H_{1,\mathbf{k}}(\mathbf{I}) \exp(i\mathbf{k}\cdot\phi)}{i\mathbf{k}\cdot\omega(\mathbf{I})} \tag{101}$$

where

$$\omega(\mathbf{I}) = \nabla_I H_0(\mathbf{I}) \tag{102}$$

is the frequency vector of the unperturbed Hamiltonian at the point $\mathbf{I}$ of the action space, has an important difference from the solution (50) of the homological equation (36). Namely, the denominators of Eq.(101) *depend explicitly on the action variables* $\mathbf{I}$. This fact has deep consequences regarding the definition of domains where such a normal form computation is valid [31]. In fact, provided that the functions $\omega(\mathbf{I})$ have at least a linear dependence on $\mathbf{I}$, we can readily prove the following: if we consider any (small whatsoever) open domain $\mathcal{W}$ in the action space, there are infinitely many wavevectors $\mathbf{k}$ for which the corresponding *resonant manifolds*, i.e. the surfaces defined by relations of the form

$$\mathbf{k}\cdot\omega(\mathbf{I}) = 0 \tag{103}$$

pass through $\mathcal{W}$. This is just a consequence of the fact that the set of all resonant manifolds of the form (103) is a dense set in action space [32]. Then, we conclude that if the coefficients $H_{1,\mathbf{k}}(\mathbf{I})$ in Eq.(101) are different from zero, a

---

[31] In fact, there are also many practical consequences rendering the whole approach of this type quite problematic. The most important problem is that, from the point of view of computer-algebraic operations, it is difficult to handle expressions involving rational functions in the action variables, as required by the form of the solutions given in Eq.(101). In conclusion, a method of normalization like in subsections 2.4 and 2.5, i.e. where we expand H_0 around some fixed values of the actions and push everything beyond linear terms to a higher book-keeping order, is preferable in practice over a method retaining H_0 in its original form.

[32] To give a simple example, let us consider the 'convex' case $H_0 = (I_1^2 + I_2^2)/2$. The frequencies are $\omega_1 = I_1$, $\omega_2 = I_2$, thus the resonant manifolds are just straight lines passing through the origin, defined by $k_1 I_1 + k_2 I_2 = 0$. Consider any point (I_{1*}, I_{2*}) of the action space, with

generating function of the form (101) cannot be defined in any open domain $\mathcal{W}$ of the action space, because some terms of χ_1 (and, similarly, in all subsequent generating functions) would have divisors *becoming equal to zero exactly* at some points within $\mathcal{W}$.

A 'remedy' to this problem, used already by Poincaré (1892), is to introduce a 'cut-off' in Fourier space, i.e. a maximum order K beyond which Fourier terms are not normalized. In this case, however, it is required to make a so-called optimal choice of the value of K, ensuring that the un-normalized terms with $|k| > K$ sum to a contribution smaller in size than the remainder terms produced during the normalization process (see Morbidelli and Giorgilli (1997) for a quantitative analysis of this problem). In fact, basic theory (see, for example, Morbidelli and Guzzo (1997)) yields an estimate $K \sim 1/\epsilon^p$, for some exponent p depending on the exact form of the resonant module $\mathcal{M}$. However, such estimates are not very useful in practice, because in the real computation we would need to know precisely the coefficient of proportionality between K and $1/\epsilon^p$.

It is now possible to see that both problems mentioned above are solved in a natural way by choosing a way of book-keeping different from Eq.(98), recognizing[33] the fact that, in a Hamiltonian like (97), the set of all Fourier harmonics can be split into *subsets of different order of smallness*, each subset containing only a *finite number* of harmonics. This immediately suggests a book-keeping of the form

$$\begin{aligned} H = H_0 + \epsilon[&\lambda^1(\text{group of Fourier terms of first order of smallness}) \\ &+\lambda^2(\text{group of Fourier terms of second order of smallness}) + \ldots] \end{aligned} \tag{104}$$

In subsection 3.2 we will see how to split the Hamiltonian in groups of Fourier terms of different smallness, taking into account a basic property of analytic Hamiltonian functions, namely the *exponential decay* of Fourier coefficients with increasing Fourier order $|k|$. For the moment, however, let us assume that such a splitting has been accomplished. Under the book-keeping (104), we now observe that only a finite number of harmonics are to be eliminated in every normalization step. For example, instead of the generating function of Eq.(101), such a book-keeping would result in a generating function of the form:

$$\chi_1 = \sum_{\mathbf{k}\in \text{ (group 1)}, \mathbf{k}\notin\mathcal{M}} \frac{H_{1,\mathbf{k}}(\mathbf{I})\exp(i\mathbf{k}\cdot\phi)}{i\mathbf{k}\cdot\omega(\mathbf{I})} \quad . \tag{105}$$

$I_{1*} > 0$ and $I_{2*} > 0$, and a ball $B_{\delta*}$ of radius δ around I_1*, I_2*. Then, all lines of the form $I_2 = gI_1$, with

$$\frac{I_{2*}/I_{1*} - \delta/\sqrt{I_{1*}^2 + I_{2*}^2 - \delta^2}}{1 + I_{2*}\delta/(I_{1*}\sqrt{I_{1*}^2 + I_{2*}^2 - \delta^2})} \leq g \leq \frac{I_{2*}/I_{1*} + \delta/\sqrt{I_{1*}^2 + I_{2*}^2 - \delta^2}}{1 - I_{2*}\delta/(I_{1*}\sqrt{I_{1*}^2 + I_{2*}^2 - \delta^2})}$$

cross the ball $B_{\delta*}$. Since the set of rational numbers is dense within the set of real numbers, it follows that there are infinitely many rational numbers $g = q/p$ within the above interval. Thus, for arbitrarily small δ, there are infinitely many lines of the form $I_2 = (q/p)I_1$, or $k_1 I_1 + k_2 I_2 = 0$ with $k_1 = q$, $k_2 = -p$, passing through $B_{\delta*}$.

[33] as, already, in the works of Poincaré (1892), and Arnold (1963)

It follows that generating functions of the form (105) can now be defined in *open sets* of the action space. A set of this form results from excluding, from an initial open domain $\mathcal{W}$, a finite number of resonant manifolds corresponding to those wavevectors $\mathbf{k}$ in Eq.(103) which i) belong to the group 1 and ii) cross $\mathcal{W}$. In practice, we exclude also some neighborhoods of the above manifolds, in order to avoid non-zero, but extremely small divisors in the series. But even after such an exclusion, we are left with an open set where all definitions are possible.

It has been stated that the easiest way to perform the splitting of Fourier terms in groups of different smallness stems from *Fourier theorem*, namely the fact that the Fourier coefficients of an analytic function decay exponentially with increasing Fourier order $|k|$. To this we now turn our attention.

3.2. Exponential decay of the Fourier coefficients

It is well known that the convergence properties of a series representing a certain function f are determined by the location and structure of the *singularities* of f in a *complex domain* of its arguments. For example, consider the series expansion of the function $f(x) = 1/(1+x^2)$ around $x_0 = 0$:

$$f(x) = \frac{1}{1+x^2} = 1 - x^2 + x^4 - x^6 + ..., \quad x \in \mathbf{R} \tag{106}$$

Applying, e.g., D'Alembert's criterion, it follows that the interval of convergence of the series (106) in the real axis around $x_0 = 0$ is given by $|x| < 1$, despite the fact that f can be defined for all $x \in \mathbf{R}$. This is because the domain of convergence of a series like (106) is defined by the position of singularities of the represented function f in the complex plane $x \in \mathbf{C}$. In our example, f has poles at $x = \pm i$, thus there is a disc of convergence around $x_0 = 0$ with radius $R = |i - x_0| = |i - 0| = 1$. This disc contains the interval $-1 < x < 1$ of the real axis, and this determines the restriction of the domain of convergence of the series (106) for real values of x.

Consider, now, the function

$$F(\phi_1, \phi_2) = \frac{1}{3 + \cos\phi_1 + \cos\phi_2} \quad . \tag{107}$$

Clearly, F has no poles on the real torus $[0, 2\pi) \times [0, 2\pi)$. However, if ϕ_1 and ϕ_2 are considered to be complex valued quantities, $\phi_j = \phi_{j,R} + i\phi_{j,I}$, $j = 1, 2$, fixing any two values of $\phi_{1,R}$ and $\phi_{2,R}$ we have a singularity at any solution for $(\phi_{1,I}, \phi_{2,I})$ of the set of equations

$$\cos\phi_{1,R}\cosh\phi_{1,I} + \cos\phi_{2,R}\cosh\phi_{2,R} + 3 = 0$$

$$\sin\phi_{1,R}\sinh\phi_{1,I} + \sin\phi_{2,R}\sinh\phi_{2,R} = 0 \quad .$$

The *closest* singularity to the real 2-torus is found if we set $\phi_{1,R} = \phi_{2,R} = \pi$, and $\cosh(\phi_{1,I}) = \cosh(\phi_{2,I}) = 3/2$, or $\phi_{1,I} = \pm\phi_{2,I} = \pm\sigma$, where $\cosh(\sigma) = 3/2$, or

$$\sigma = 0.962424...$$

How will the above singularity be manifested in a series representing $F(\phi_1, \phi_2)$? We first note that since (ϕ_1, ϕ_2) are angular variables, the series representation associated with F is a Fourier series

$$\frac{1}{3 + \cos\phi_1 + \cos\phi_2} = \sum_{k_1=-\infty}^{\infty} \sum_{k_2=-\infty}^{\infty} h_{k_1,k_2} \exp\big(i(k_1\phi_1 + k_2\phi_2)\big) \tag{108}$$

where the coefficients h_{k_1,k_2} are given by

$$h_{k_1,k_2} = \frac{1}{4\pi^2} \int_0^{2\pi} \int_0^{2\pi} \frac{\exp\big(-i(k_1\phi_1 + k_2\phi_2)\big) d\phi_1 d\phi_2}{3 + \cos\phi_1 + \cos\phi_2} \tag{109}$$

and satisfy the relation $h_{k_1,k_2} = h_{-k_1,-k_2}$ by virtue of the even parity of F with respect to both angles ϕ_1 and ϕ_2. Due to the position of the closest singularity, this series cannot be absolutely convergent beyond a so-called complexified torus domain given by

$$\mathbf{T}_\sigma = \Big\{ \phi \in \mathbf{C} : Re(\phi) \in [0, 2\pi), Im(\phi) \in (-\sigma, \sigma) \Big\} \tag{110}$$

with $\sigma = 0.962424....$ But now, suppose that we assign ϕ_1 and ϕ_2 with the imaginary values $\phi_1 = \phi_2 = -iu$ for some positive $u < \sigma$. Then, considering, without loss of generality, only the subsequence of all positive wavenumbers k_1, k_2 in the series (108), this subsequence is bounded by the majoring series

$$\sum_{k_1>0,k_2>0}^{\infty} |h_{k_1,k_2}| e^{(k_1+k_2)u} \quad .$$

This series should be absolutely convergent for all $u < \sigma$. However, this is only possible if the coefficients $|h_{k_1,k_2}|$ are bounded by an exponentially decaying function of $|k| = k_1 + k_2$. This is indeed the case, as proven by the so-called *Fourier theorem* on analytic functions (see, for example, Pinsky (2002)), which states that for all $\sigma' < \sigma$ one has:

$$|h_{k_1,k_2}| < A_{\sigma'} e^{-\sigma'|k|}, \quad \text{for } A_{\sigma'} = \sup_{\mathbf{T}'_\sigma} |F(\phi_1, \phi_2)| \quad . \tag{111}$$

Thus, choosing any value of σ' in the interval $u < \sigma' < \sigma$ provides an exponentially decaying bound on the size of the coefficients $|h_{k_1,k_2}|$.

In practice, we find optimal bounds if we set σ' to values very close to σ. Figure 9 shows the exponential decay of the coefficients h_{k_1,k_2} defined by Eq.(109). The coefficients are computed using the equations

$$\begin{aligned} h_{k_1,k_2} &= \sum_{n=N}^{\infty} \sum_{j=0}^{n-N} \frac{(-1)^{2n}(2n)!}{2^{2n}3^{2n+1}(|k_1|+j)!j!(|k_2|+n-j-N)!(n-j-N)!} \\ &\quad \text{with } N = \tfrac{|k_1|+|k_2|}{2} \text{ if } |k_1| + |k_2| \text{ even} \\ h_{k_1,k_2} &= \sum_{n=N}^{\infty} \sum_{j=0}^{n-N} \frac{(-1)^{2n+1}(2n+1)!}{2^{2n+1}3^{2n+2}(|k_1|+j)!j!(|k_2|+n-j-N)!(n-j-N)!} \\ &\quad \text{with } N = \tfrac{|k_1|+|k_2|-1}{2} \text{ if } |k_1| + |k_2| \text{ odd} \end{aligned} \tag{112}$$

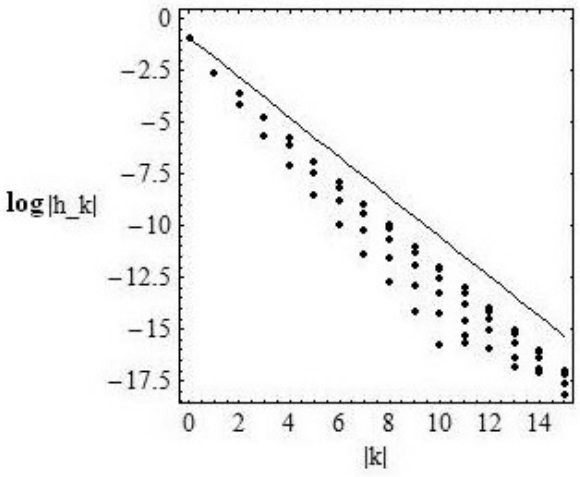

Figure 9. The logarithm of the absolute value of all coefficients h_{k_1,k_2} given by Eq.(109) as a function of the Fourier order $|k| = |k_1| + |k_2|$. The straight line corresponds to an upper bound law of the form (114), with $A = 0.4$, and $\sigma = 0.96$.

which follow directly after computing the Taylor expansion

$$\frac{1}{3+x} = \frac{1}{3} - \frac{x}{9} + \frac{x^2}{27} - ..., \tag{113}$$

and substituting x by $\cos\phi_1 + \cos\phi_2$. In Fig.9, the value of every coefficient h_{k_1,k_2} is computed approximately, by truncating the corresponding sum in Eq.(112) up to the order $n = |k_1| + |k_2| + 20$. The upper bound for the size of all coefficients is given by a straight line in Fig.9, which corresponds to the exponential law

$$|h_k| < A \exp(-|k|\sigma) \tag{114}$$

where, σ, now, denotes a numerical value set slightly below the value of the singularity, namely $\sigma = 0.96$, while $A = 0.4$.

The property of the exponential decay of Fourier coefficients provides the basis for a splitting of the Fourier harmonics of a Hamiltonian function in groups of different orders of smallness, i.e., for implementing a book-keeping of the form suggested in Eq.(104). In fact, based on Eq.(114), for any positive integer K', we can define the following groups of terms, of different smallness, according to the Fourier order $|k|$ of each term (see Giorgilli 2002, p.90-91, for details):

$$\text{terms of order} \quad 0 \le |k| < K' \qquad \text{smallness} \ = O\left(A(e^{-K'\sigma})^0\right)$$

$$\text{terms of order} \quad K' \le |k| < 2K' \qquad \text{smallness} \ = O\left(A(e^{-K'\sigma})^1\right)$$

$$\text{terms of order} \quad 2K' \le |k| < 3K' \qquad \text{smallness} \ = O\left(A(e^{-K'\sigma})^2\right)$$

$$\dots$$

We observe that the various groups are in *ascending powers of the quantity* $e^{-\sigma K'}$, which can thus be regarded as a *natural small quantity* appearing in a Hamiltonian with exponentially decaying Fourier coefficients.

How to choose K'? The simplest (and in many aspects optimal, see Giorgilli 2002) choice is to set $K' \sim 1/\sigma$, implying that the grouping is done in powers of the quantity $1/e$. An alternative choice is to determine K' so that the 'natural' (due to the exponential decay) small parameter $e^{-\sigma K'}$ becomes equal to the other small parameter of the Hamiltonian (97), i.e. ϵ. We thus require that $e^{-\sigma K'} \sim \epsilon$, or:

$$K' = \left[-\frac{\log(\epsilon)}{\sigma} \right] \quad . \tag{115}$$

In practice, due to the logarithmic dependence of K' on ϵ, as well as the fact discussed already, namely that we have a certain flexibility in defining a book-keeping, we find the following rule for practical normal form computations:

Practical rule for choosing K': set K' constant and equal to an average of the values found by Eq.(115) within the range of values of ϵ encountered in the particular problem under study.

This leads to the following

Practical rule for book-keeping in Hamiltonians of the form (97):

$$\begin{aligned} &\epsilon(\text{terms of order} \quad 0 \le |k| < K') \quad \to \lambda^1 \\ &\epsilon(\text{terms of order} \quad K' \le |k| < 2K') \quad \to \lambda^2 \\ &\epsilon(\text{terms of order} \quad 2K' \le |k| < 3K') \quad \to \lambda^3 \\ &\qquad\qquad\qquad\qquad\qquad\qquad\qquad\qquad \dots \end{aligned} \tag{116}$$

Further implications arise by the fact that the Fourier coefficients of a Hamiltonian expansion usually exhibit explicit dependence on the action variables of the problem under study. However, it is possible to see that this dependence takes place via rules which essentially allow to reproduce a book-keeping of the form (116) with a small modification, examples of which are given below.

3.3. Application 1: Width of resonances in a simple model

As an application of the book-keeping rules discussed in subsection 3.2, we consider now a simple Hamiltonian system of two degrees of freedom, depending on a small parameter ϵ, in which an appropriate form of resonant normal form theory yields the size of the islands of stability corresponding to various resonances, for small enough values of ϵ.

We consider the Hamiltonian function

$$H \equiv H_0 + \epsilon H_1 = \frac{I_1^2 + I_2^2}{2} + \epsilon \left(\frac{1 + I_1 + 2I_2 + I_1^2 - 3I_2^2 + 2I_1 I_2}{3 + \cos\phi_1 + \cos\phi_2} \right) \quad . \tag{117}$$

The Hamiltonian (117) is a 2D variant of a 3D Hamiltonian model introduced in Froeschlé et al. (2000) and used in subsequent studies of diffusion in the so-called Arnold web in the weakly chaotic regime (see section 4).

The Hamiltonian flow under the unperturbed part of the Hamiltonian, i.e. H_0, is quite simple: we have $\dot{I}_i = 0$, or $I_i = const.$, and $\dot{\phi}_i = I_i = \omega_i$, $i = 1, 2$. Thus, both actions I_i, $i = 1, 2$ are integrals of the flow of H_0, corresponding to motions under constant frequencies $\omega_i = I_i$.

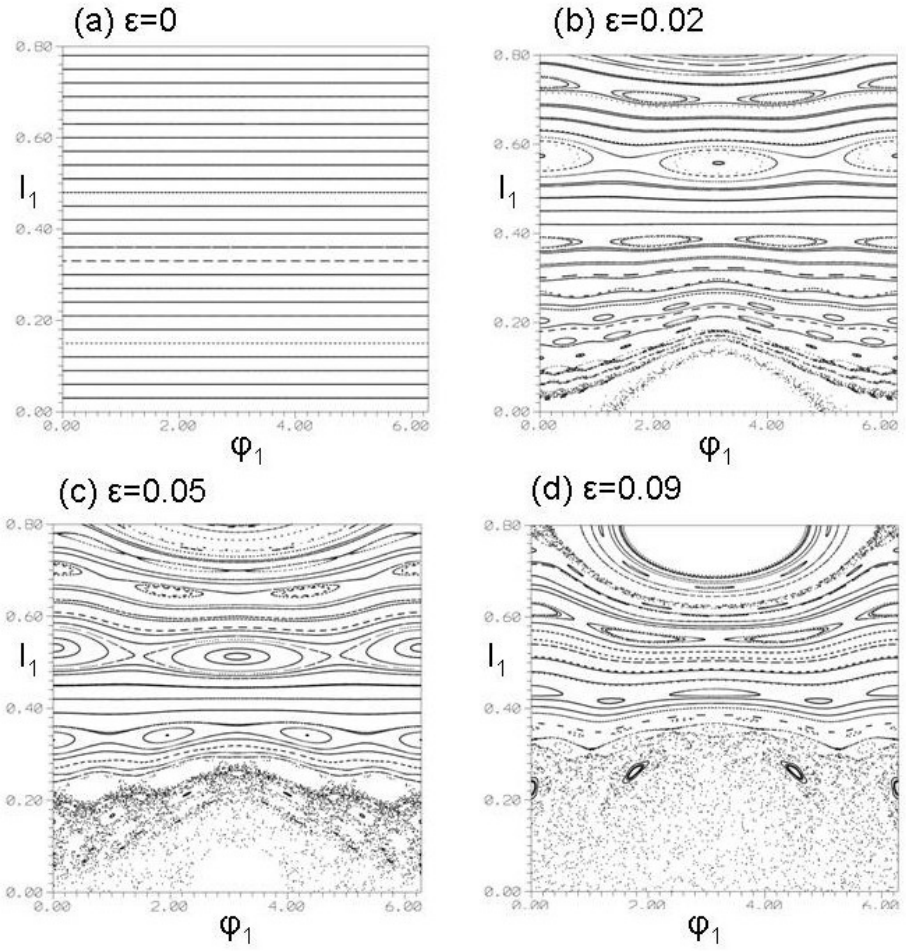

Figure 10. Phase portraits (surfaces of section (ϕ_1, I_1) for $mod(\phi_2, 2\pi) = 0$, $\dot{\phi}_2 > 0$), in the Hamiltonian model (117), for the energy $E = 1$, and (a) $\epsilon = 0$, (b) $\epsilon = 0.02$, (c) $\epsilon = 0.05$, and (d) $\epsilon = 0.09$.

As in Fig.1, we will use a surface of section, defined by the condition $\phi_2 mod 2\pi = 0$, $\dot{\phi}_2 > 0$, to provide phase portraits of the dynamics of the system (117) for various values of ϵ. Figure 10a corresponds to the motion in the unperturbed case $\epsilon = 0$, for a constant energy $H = E = 1$. Since, for $\epsilon = 0$ the actions remain constant in time for any pair of initial conditions $(I_1(0), I_2(0)) = (I_{1*}, I_{2*})$, the surface of section (ϕ_1, I_1) (Fig.10a) yields a set of straight lines $I_1 = I_{1*}$, representing the intersection, with the surface of section, of a foliation of *invariant tori* of the system under study.

The set of all invariant tori of Fig.10a can be divided in two distinct sets, of so-called *non-resonant*, or *resonant* tori. A non-resonant torus is one for which the frequencies $(\omega_{1*}, \omega_{2*}) = (I_{1*}, I_{2*})$ satisfy no commensurability relation, i.e no relation of the form:

$$k_1\omega_{1*} + k_2\omega_{2*} = 0, \quad (k_1, k_2) \in \mathbf{Z}, \quad |k| = |k_1| + |k_2| \neq 0 \ . \tag{118}$$

Conversely, if (118) is satisfied for some integer vector (k_1, k_2), the torus is called resonant. In the surface of section of Fig.10a, any initial condition on a resonant torus yields a distinct set of points along the corresponding straight line of Fig.10a. For example, in the case of the resonance

$$2\omega_{1*} - \omega_{2*} = 2I_{1*} - I_{2*} = 0$$

we have $\phi_1 - \phi_1(0) = \omega_{1*}t = (1/2)\omega_{2*}t = (1/2)(\phi_2 - \phi_2(0))$. Thus, whenever ϕ_2 completes two periodic circles, ϕ_1 completes one full circle, returning to the initial condition $\phi_1(0)$. Thus, in the surface of section we obtain two distinct points along the straight line $I_1 = I_{1*}$, i.e. one point for each of the two periodic circles of ϕ_2. After completion of the second circle, the motion is repeated periodically, thus yielding always a repetition of the same two consequents in the surface of section. This is called *a periodic orbit* of multiplicity two.

On the other hand, if the actions I_{1*}, I_{2*} are chosen so that the associated frequencies ω_{1*}, ω_{2*} satisfy no commensurability relation of the form (118), the associated non-resonant torus in Fig.10a is filled densely by the consequents of a single orbit produced by taking any initial condition on the torus.

For a fixed energy (e.g. $E = 1$, as in Fig.10), we can find precisely the values of I_{1*} for which the motion is on a resonant torus, by solving simultaneously the equations

$$k_1 I_{1*} + k_2 I_{2*} = 0, \quad \frac{I_{1*}^2 + I_{2*}^2}{2} = E$$

for any pair of integers (k_1, k_2) with $|k_1| + |k_2| \neq 0$. The positive solutions for I_1^* are given by:

$$\begin{aligned} I_{1*} &= 0 && \text{if } k_2 = 0 \\ I_{1*} &= \sqrt{\frac{2E}{1 + \frac{k_1^2}{k_2^2}}} && \text{if } k_2 \neq 0 \ . \end{aligned} \tag{119}$$

Eq.(119) can be used to find approximately the position of resonances also if $\epsilon \neq 0$, but small. The evolution of the phase portrait with increasing ϵ is shown in Fig.10. These portraits exemplify the well known phenomenon of transition to large scale chaos via the mechanism of *resonance overlap*. Namely, we see that, as ϵ increases, various resonant zones containing islands of stability occupy a larger and larger part of the phase space. For ϵ small, however, nearly every island chain appears delimited by a thin separatrix-like border, which is delimited, in turn, by two rotational tori, one below and one above the resonance. Nevertheless, beyond some critical ϵ (see below) the size of some resonant zones becomes so great that the zones start *overlapping*, thus forming an extended chaotic domain. In Fig.10, the first resonances to overlap as ϵ increases are

those closer to the $I_1 = 0$ axis. In fact, as ϵ increases, the formation of the chaotic domain due to resonance overlapping appears to progress from the lower part of the phase portrait upwards.

We describe now the main steps of construction of a resonant normal form enabling us to explain some of the above features of the phase portraits of Fig.10. We are interested, in particular, in: i) estimating by analytical means the size of the resonant zones, or, the so-called *separatrix width*, for various islands of Fig.10, and ii) making estimates about the critical value of ϵ where we have the onset the resonance overlapping regime leading to the appearance of extended chaos in Fig.10.

Let us start with the example of an important resonance appearing in the phase portraits of Figs.10b,c for values of I_1 roughly in the interval $0.50 \leq I_1 \leq 0.60$. This resonance corresponds to the choice $k_1^{(1)} = 2$, and $k_2^{(1)} = -1$ (otherwise called a '2:1 resonance') [34]. In the phase portraits of Figs.10b,c, we see the formation of two islands of stability within the corresponding resonant zone (one of the islands appears broken due to the modulo 2π evaluation of the angle ϕ_1).

As explained already, for $\epsilon = 0$ we have no islands but simply a resonant torus (straight line in Fig.10a) corresponding to the 2:1 resonance. The associated action value I_{1*} is found via Eq.(119), for $E = 1$, while the value of I_{2*} is found by the equation $k_1^{(1)} I_{1*} + k_2^{(1)} I_{2*} = 0$, for $(k_1^{(1)}, k_2^{(1)}) = (2, -1)$. We find

$$I_{1*} = 0.632456, \quad I_{2*} = 1.264912 \quad . \tag{120}$$

For $\epsilon \neq 0$ but relatively small (Fig.10b, $\epsilon = 0.02$), we observe that the whole resonant zone moves downwards, although it remains relatively close to the value of I_{1*} given by Eq.(120). Furthermore, as ϵ increases, the width of the resonant zone increases also. By numerical calculations we find that this tendency is maintained up to a value of $\epsilon \simeq 0.06$. However, for higher values of ϵ the size of the 2:1 islands starts decreasing, and at $\epsilon = 0.09$ (Fig.10d), the 2:1 island chain disappears all together.

The implementation of resonant normal form theory allows to interpret these phenomena, both qualitatively and quantitatively. The construction of a resonant normal form is done in nearly the same way as in the example examined in subsection 2.9, the main difference being in the book-keeping of the Hamiltonian, which in the present case follows the practical rules developed in subsection 3.2. We have the following steps:

Shift of center and expansion of the Hamiltonian (117) in the action variables with respect to the values I_{1*}, I_{2*}. This is analogous to the expansion of the Hamiltonian (3) around a resonant value p_*. In the present case, we introduce

[34] Use is made here of the same notation as in subsection 2.9. Namely, the superscript (1) means 'the first resonance condition'. Similarly to subsection 2.9, in the present case as well the use of the superscript (1) to enumerate a resonant vector is rather redundant, since in two degrees of freedom there can be no more than one linearly independent resonance conditions. However, this notation is consistent and actually allows one to more easily follow the analysis of resonant dynamics in the next section, where we pass from examining systems of two degrees of freedom to examining systems of three degrees of freedom

the canonical transformation:

$$I_1 = I_{1*} + I'_1, \quad I_2 = I_{2*} + I'_2 \quad . \tag{121}$$

Substituting (121) into (117), dropping a constant term, and substituting the numerical values of Eq.(119), the Hamiltonian takes the form:

$$\begin{aligned} H(\phi_1, \phi_2, I'_1, I'_2) &= 0.632456 I'_1 + 1.264912 I'_2 + \frac{I'^2_1 + I'^2_2}{2} \\ + \quad & \frac{\epsilon \left(1.36228 + 4.79473 I'_1 - 4.32456 I'_2 + I'^2_1 + 2 I'_1 I'_2 - 3 I'^2_2\right)}{3 + \cos\phi_1 + \cos\phi_2} \quad . \end{aligned} \tag{122}$$

Action rescaling: In subsection 2.9 it was shown that the separatrix width of a resonance scales proportionally to $\epsilon^{1/2}$. As shown below, this is a generic property, maintained also in systems of the form (97). Such a property can be 'a priori' taken into account in the normalization algorithm by introducing a *scaling* transformation $I'_1, I'_2 \to J_1, J_2$ defined by:

$$J_i = \epsilon^{1/2} I'_i, \quad i = 1, 2 \quad . \tag{123}$$

The transformation (123) is not canonical. However, it is straightforward to check that if we substitute (123) in the Hamiltonian (122), the equations of motion take the correct form in the new variables (ϕ, J) under a new Hamiltonian, given by:

$$H'(\phi, J) = \epsilon^{-1/2} H(\phi, J) \quad . \tag{124}$$

In the case of the Hamiltonian (122) we find:

$$\begin{aligned} H'(\phi_1, \phi_2, J_1, J_2) &= 0.632456 J_1 + 1.264912 J_2 + \epsilon^{1/2} \frac{J_1^2 + J_2^2}{2} \\ + \quad & \frac{\epsilon^{1/2} \left(1.36228 + \epsilon^{1/2} (4.79473 J_1 - 4.32456 J_2) + \epsilon (J_1^2 + 2 J_1 J_2 - 3 J_2^2) \right)}{3 + \cos\phi_1 + \cos\phi_2} \quad . \end{aligned} \tag{125}$$

A careful inspection of the new Hamiltonian (125) shows an essential feature: the fact that the terms quadratic in the actions are of order at least $O(\epsilon^{1/2})$ allows us to use only linear terms in the kernel of the homological equations computed at subsequent steps. This is analogous to the introduction of the book-keeping factor λ in front of the term $I_\psi^2/2$ in the example of subsection 2.3 (Eq.(24)).

Book-keeping: In the Hamiltonian (125) all terms (apart from the first two linear in the actions) are multiplied by some power of the quantity $\epsilon^{1/2}$. Thus, in order to split the terms in the Fourier series of (125) in groups of different orders of smallness compatible with powers of the quantity $\epsilon^{1/2}$, we use Eq.(115), but with $\epsilon^{1/2}$ instead of ϵ, i.e. we set

$$K' = \left[- \frac{\log(\epsilon^{1/2})}{\sigma} \right] \tag{126}$$

with $\sigma = 0.96$. The mean value of K' when, as in Fig.10, ϵ is varied in the interval $0.01 \leq \epsilon \leq 0.1$, is $K' = 2$. Finally, we implement the book-keeping rule of Eq.(116), again with $\epsilon^{1/2}$ instead of ϵ. In fact, since in (125) we have the appearance of terms with factors depending explicitly on a power of $\epsilon^{1/2}$, the book-keeping rule (116) is supplemented by the requirement to introduce an additional factor λ^p in front of any of the terms in Eq.(125) which appears multiplied by some factor $(\epsilon^{1/2})^p$.

In summary:

$$
\begin{aligned}
& H'(\phi_1,\phi_2,J_1,J_2) = 0.632456 J_1 + 1.264912 J_2 + \lambda\epsilon^{1/2}\frac{J_1^2+J_2^2}{2} \\
+ \quad & \frac{\lambda\epsilon^{1/2}\Big(1.36228 + \lambda\epsilon^{1/2}(4.79473 J_1 - 4.32456 J_2) + \lambda^2\epsilon(J_1^2 + 2J_1J_2 - 3J_2^2)\Big)}{3+\cos\phi_1+\cos\phi_2} =
\end{aligned}
$$

$$
\begin{aligned}
& 0.632456 J_1 + 1.264912 J_2 + \lambda\epsilon^{1/2}\frac{J_1^2+J_2^2}{2} \\
+ \quad & \lambda\epsilon^{1/2}\Big(1.36228 + \lambda\epsilon^{1/2}(4.79473 J_1 - 4.32456 J_2) + \lambda^2\epsilon(J_1^2 + 2J_1J_2 - 3J_2^2)\Big) \\
\times \quad & \sum_{k_1=-\infty}^{\infty}\sum_{k_2=-\infty}^{\infty} \lambda^{[\frac{|k_1|+|k_2|}{K'}]} h_{k_1,k_2} \exp\big(i(k_1\phi_1 + k_2\phi_2)\big)
\end{aligned}
\tag{127}
$$

with h_{k_1,k_2} given by (109), and $K' = 2$.

Computing the Fourier coefficients as in Eqs.(112), the Hamiltonian up to Fourier order 5 reads:

$$
\begin{aligned}
& H'(\phi_1,\phi_2,J_1,J_2) = 0.632456 J_1 + 1.264912 J_2 + \lambda\epsilon^{1/2}\frac{J_1^2+J_2^2}{2} \\
+ \quad & \lambda\epsilon^{1/2}\Big(1.36228 + \lambda\epsilon^{1/2}(4.79473 J_1 - 4.32456 J_2) + \lambda^2\epsilon(J_1^2 + 2J_1J_2 - 3J_2^2)\Big) \\
\times \Big[\quad & 0.384023 - 0.0760351(e^{i\phi_1} + e^{-i\phi_1} + e^{i\phi_2} + e^{-i\phi_2}) \\
& +0.016008\lambda(e^{2i\phi_1} + e^{-2i\phi_1} + e^{2i\phi_2} + e^{-2i\phi_2}) \\
& +0.0280895\lambda(e^{i\phi_1+i\phi_2} + e^{-i\phi_1+i\phi_2} + e^{i\phi_1-i\phi_2} + e^{-i\phi_1-i\phi_2}) \\
& -0.00354632\lambda(e^{3i\phi_1} + e^{-3i\phi_1} + e^{3i\phi_2} + e^{-3i\phi_2}) \\
& -0.00823336\lambda(e^{i\phi_1+2i\phi_2} + e^{-i\phi_1+2i\phi_2} + e^{i\phi_1-2i\phi_2} + e^{-i\phi_1-2i\phi_2} \\
& \qquad +e^{2i\phi_1+i\phi_2} + e^{-2i\phi_1+i\phi_2} + e^{2i\phi_1-i\phi_2} + e^{-2i\phi_1-i\phi_2}) \\
& +0.000817397\lambda^2(e^{4i\phi_1} + e^{-4i\phi_1} + e^{4i\phi_2} + e^{-4i\phi_2})
\end{aligned}
\tag{128}
$$

$$
\begin{aligned}
&+0.00222626\lambda^2(e^{i\phi_1+3i\phi_2}+e^{-i\phi_1+3i\phi_2}+e^{i\phi_1-3i\phi_2}+e^{-i\phi_1-3i\phi_2}\\
&\qquad +e^{3i\phi_1+i\phi_2}+e^{-3i\phi_1+i\phi_2}+e^{3i\phi_1-i\phi_2}+e^{-3i\phi_1-i\phi_2})\\
&+0.00307641\lambda^2(e^{2i\phi_1+2i\phi_2}+e^{-2i\phi_1+2i\phi_2}+e^{2i\phi_1-2i\phi_2}+e^{-2i\phi_1-2i\phi_2})\\
&-0.000194075\lambda^2(e^{5i\phi_1}+e^{-5i\phi_1}+e^{5i\phi_2}+e^{-5i\phi_2})\\
&-0.000581994\lambda^2(e^{i\phi_1+4i\phi_2}+e^{-i\phi_1+4i\phi_2}+e^{i\phi_1-4i\phi_2}+e^{-i\phi_1-4i\phi_2}\\
&\qquad +e^{4i\phi_1+i\phi_2}+e^{-4i\phi_1+i\phi_2}+e^{4i\phi_1-i\phi_2}+e^{-4i\phi_1-i\phi_2})\\
&-0.000995866\lambda^2(e^{2i\phi_1+3i\phi_2}+e^{-2i\phi_1+3i\phi_2}+e^{2i\phi_1-3i\phi_2}+e^{-2i\phi_1-3i\phi_2}\\
&\qquad +e^{3i\phi_1+2i\phi_2}+e^{-3i\phi_1+2i\phi_2}+e^{3i\phi_1-2i\phi_2}+e^{-3i\phi_1-2i\phi_2})+...\Big]
\end{aligned}
$$

Hamiltonian normalization. We now implement the usual resonant normal form procedure, in precisely the same way as in subsection 2.9. The resonant module is:

$$\mathcal{M}=\{k \text{ such that } k\cdot m=0\}, \quad \text{where } m=(1,2) \quad . \tag{129}$$

We give below the form of the generating functions χ_1 and χ_2 arising in the first two normalization steps:

$$\chi_1=\lambda i\Big[0.163776\epsilon^{1/2}(e^{i\phi_1}-e^{-i\phi_1})+0.0818879\epsilon^{1/2}(e^{i\phi_2}-e^{-i\phi_2})\Big]$$

$$
\begin{aligned}
\chi_2=\lambda^2 i\Big[&-0.0172402\epsilon^{1/2}(e^{2i\phi_1}-e^{-2i\phi_1})-0.0086201\epsilon^{1/2}(e^{2i\phi_2}-e^{-2i\phi_2})\\
&+0.0605033\epsilon^{1/2}(e^{i(\phi_1-\phi_2)}-e^{-i(\phi_1-\phi_2)})-0.0201678\epsilon^{1/2}(e^{i(\phi_1+\phi_2)}-e^{-i(\phi_1+\phi_2)})\\
&+0.0025462\epsilon^{1/2}(e^{3i\phi_1}-e^{-3i\phi_1})+0.0012731\epsilon^{1/2}(e^{3i\phi_2}-e^{-3i\phi_2})\\
&+0.0035468\epsilon^{1/2}(e^{i(\phi_1+2\phi_2)}-e^{-i(\phi_1+2\phi_2)})-0.0059114\epsilon^{1/2}(e^{i(\phi_1-2\phi_2)}-e^{-i(\phi_1-2\phi_2)})\\
&+0.0044336\epsilon^{1/2}(e^{i(2\phi_1+\phi_2)}-e^{-i(2\phi_1+\phi_2)})+(0.317480J_1-0.519907J_2)\epsilon(e^{i\phi_1}-e^{-i\phi_1})\\
&+(0.288216J_1-0.324691J_2)\epsilon(e^{i\phi_2}-e^{-i\phi_2})\Big] \quad .
\end{aligned}
$$

After two normalization steps, the Hamiltonian reads (omitting a constant)

$$
\begin{aligned}
H^{(2)}=&\,0.632456J_1+1.264912J_2+\lambda 0.5\epsilon^{1/2}(J_1^2+J_2^2)\\
&+\lambda^2\Big[1.84129\epsilon J_1-1.66073\epsilon J_2-0.011216\epsilon^{1/2}(e^{i(2\phi_1-\phi_2)}+e^{-i(2\phi_1-\phi_2)})\Big]+O(\lambda^3) \quad .
\end{aligned}
$$

In order to give $H^{(2)}$ the usual 'pendulum' form, we pass, again as in subsection 2.9, to resonant variables (ϕ_R, J_R), introducing also a pair of 'fast' canonical variables (ϕ_F, J_F). The fast angle will be ignorable, implying that J_F is a second

integral of the normal form flow. The transformation from the original to resonant variables is exactly the same as in Eq.(70) (with J_1 in the place of I_ψ and J_2 in the place of I), setting $k^{(1)} = (2, -1)$ and $m = (1, 2)$. We find $J_1 = 2J_R + J_F$, $J_2 = -J_R + 2J_F$, and $\phi_R = 2\phi_1 - \phi_2$. Substituting these expressions to $H^{(2)}$, transforming back to trigonometric functions, and setting $\lambda = 1$, we find the following expression of the resonant normal form in the variables (ϕ_R, J_R, J_F) (apart from constant terms):

$$\begin{aligned} Z_{res} &= 3.16228 J_F + 2.5\epsilon^{1/2} J_F^2 \\ &+ \epsilon^{1/2}\left(2.5 J_R^2 - 0.022432\cos\phi_R\right) \\ &+ \epsilon(5.34331 J_R - 1.48017 J_F) \quad . \end{aligned} \tag{130}$$

Eq.(130) clearly shows that, neglecting terms of order ϵ or higher, the resonant normal form takes the form of a pendulum Hamiltonian. This, in turn, can be used to estimate the size of the 2:1 islands by computing the *separatrix half-width* of the associated pendulum. Neglecting terms of order ϵ, from the second line of Eq.(130) we can estimate the separatrix half-width using the same method as in subsection 2.9. We find:

$$\Delta J_R = \sqrt{\frac{2 \cdot 0.022432}{2.5}} \simeq 0.134 \quad . \tag{131}$$

Since $J_1 = 2J_R + J_F$, and taking into account that J_F is an integral of the Hamiltonian (130) and hence exhibits no variations along the resonance separatrix, we have $\Delta J_1 = 2\Delta J_R \simeq 0.268$. Finally, passing back to the original variable I_1 before the re-scaling of Eq.(123), we have

$$\Delta I_1 = \Delta I_1' \simeq 0.268\epsilon^{1/2} \quad . \tag{132}$$

We recover here the well known result that the separatrix half-width scales proportionally to $\epsilon^{1/2}$. It should be noted that all the above estimates refer to the new canonical variables, obtained after the Lie transformations with the generating functions χ_1 and χ_2. However, these estimates remain precise when transforming back to the old variables, since the corrections induced by such transformation can be only of higher order, i.e. $O(\epsilon)$. In fact, for $\epsilon = 0.02$, $\epsilon = 0.05$, or $\epsilon = 0.09$ we find $\Delta I_1 \simeq 0.038$, $\Delta I_1 \simeq 0.06$ and $\Delta I_1 \simeq 0.08$ respectively. The first two of these values compare quite well with the size of the 2:1 island as found in the corresponding phase portraits of Figs.10b and c respectively. However, in Fig.10d it appears that the 2:1 island chain has been destructed. This is due to the resonance overlap mechanism examined below.

Another relevant phenomenon that can be predicted by the above resonant theory concerns the shift, downwards, of the position of the stable periodic orbit at the center of the 2:1 islands of stability, as ϵ increases. Considering, for definiteness, the island intersecting the axis $\phi_1 = 0$, in Fig.10 we see that the vertical position of the central periodic orbit, which, for $\epsilon = 0$ corresponds to the value $I_1 = I_{1*} = 0.632456$ has shifted to $I_1 \simeq 0.57$ for $\epsilon = 0.02$, and $I_1 \simeq 0.53$ for $\epsilon = 0.05$. This downward shift can be predicted theoretically as follows. From Eq.(130), the position of the stable periodic orbit in the surface of section

corresponds to $\phi_1 = 0$, $\phi_2 = 0$, as well as to the value $J_R = J_{R0}$ for which the condition

$$\frac{\partial Z_{res}}{\partial J_R} = 0$$

is satisfied. We find

$$J_{R0} = -1.06866\epsilon^{1/2} + \ldots \tag{133}$$

On the other hand, in evaluating the resonant normal form, we have started from the Hamiltonian (122), which originates from the original Hamiltonian (117) after dropping a constant term equal to $(I_{1*}^2 + I_{2*}^2)/2$. However, I_{1*} and I_{2*} themselves are chosen so that $E = (I_{1*}^2 + I_{2*}^2)/2$, where E is the numerical value of the energy. Thus, for the numerical value of Z_{res} we have

$$E_{Z_{res}} = \frac{1}{\epsilon^{1/2}} \left(E - \frac{I_{1*}^2 + I_{2*}^2}{2} \right) = 0 \quad .$$

Setting $Z_{res} = 0$ in (130), and substituting (133), we find an equation for J_F, whose solution $J_F = J_{F0}$ can be given in form of series in powers of $\epsilon^{1/2}$. We find

$$J_{F0} = 0.007\epsilon^{1/2} + \ldots \tag{134}$$

We finally have

$$J_{10} = 2J_{R0} + J_{F0} \simeq -2.13\epsilon^{1/2} + \ldots \tag{135}$$

Passing back to the non-scaled variable $I_1 = I_{1*} + \epsilon^{1/2} J_1$, we find

$$I_{10} \simeq 0.63 - 2.13\epsilon + \ldots \tag{136}$$

It should be noted, again, that these values refer to the *new* canonical variables, after the transformation by the generating functions χ_1 and χ_2. However, only a small change (of order $O(\epsilon^{3/2})$) takes place by passing back from (136) to the corresponding equation for the old variable I_1. In fact, if we set $\epsilon = 0.02$, or $\epsilon = 0.05$ in Eq.(136) we find $I_{10} = 0.59$ and $I_{10} = 0.52$ respectively, in good agreement with the numerical values.

On the other hand, for $\epsilon = 0.09$ we have $I_{10} = 0.44$. However, we will see that at this perturbation level, the resonance overlapping mechanism is effective, thus significantly altering all estimates based on a resonant normal form theory of the above form. To this we now turn our attention.

Resonance overlapping criterion. The resonance overlapping mechanism (Contopoulos (1966), Rosenbluth et al. (1966), Chirikov (1979)) stems from the following remark: we observe (e.g. via Eq.(136)) that the position of a stable periodic orbit changes, as a function of ϵ by a $O(\epsilon)$ quantity, while the size of the associated islands of stability increases as a function of ϵ by a much larger, i.e. $O(\epsilon^{1/2})$, quantity. Thus, if we consider the resonant zones around *two different* periodic orbits, there is a critical ϵ beyond which the zones necessarily overlap. However, the interaction of two or more resonances introduces chaos. Thus, by using the resonance overlapping criterion we can estimate the value of the perturbation ϵ beyond which we have the onset of a substantial degree of chaos in the system.

In the case of the system (117), we can invoke the resonance overlapping criterion in order to estimate the value of ϵ at which the chaotic domain in the lower part of the surfaces of section of Fig.10 extends up to covering the 2:1 resonance. To this end, we note first that the most important island in the lower part of Figs.10b,c,d corresponds to the resonance $\omega_{1*} = I_{1*} = 0$. For that resonance, the resonant wave-vector is $k^{(1)} = (1, 0)$, implying $m = (0, 1)$.The value of I_{2*} is given by $I_{2*} = \sqrt{2E}$.

In order to estimate the size of the island formed by this resonance, we implement again resonant normal form theory by exactly the same steps as in the case of the 2:1 resonance, using, however, the parameters stated above for the 1:0 resonance. [35] The reader is invited to accomplish him/herself all necessary calculations, which, in the present case, are sufficient to carry on up to order $O(\lambda)$. We give the final result. The generating function χ_1 is given by:

$$\chi_1 = \lambda 0.116754 i \epsilon^{1/2} (e^{i\phi_2} - e^{-i\phi_2})$$

while the Hamiltonian $H^{(1)} = \exp L_{\chi_1} H^{(0)}$ is given by (apart from constants):

$$H^{(1)} = 1.41421 J_2 + \lambda \epsilon^{1/2} \left[0.5(J_1^2 + J_2^2) + 0.16511(e^{i\phi_1} + e^{-i\phi_1}) \right] + O(\lambda^2) \quad .$$

The variables (ϕ_1, J_1) form a pair of resonant canonical variables. Following the same procedure as in the case of the 2:1 resonance, we find the separatrix half-width, which, in the present case, is given by

$$\Delta I_1 \simeq 1.15 \epsilon^{1/2} \quad . \tag{137}$$

For $\epsilon = 0.02$ or $\epsilon = 0.05$ we find $\Delta I_1 \simeq 0.16$, and $\Delta I_1 \simeq 0.26$ respectively, which are, again, in good agreement with the corresponding island sizes estimated numerically in Figs.10b,c.

The position of the stable periodic orbit in this approximation is at $I_{10} = 0$.

We can now implement the resonance overlap criterion: we estimate that an extended chaotic domain is formed between the two resonances at values of ϵ beyond the value at which *the sum of the half-widths of the two resonances becomes equal to the separation between the two central periodic orbits.* This corresponds to the value of ϵ at which the theoretical separatrices of the two resonances become tangent one to the other.

In our example, in view of Eq.(136), the separation ΔI_{per} between the two periodic orbits 2:1 and 1:0 is equal to the position of the 2:1 periodic orbit itself, i.e.

$$\Delta I_{per} = 0.63 - 2.13\epsilon$$

Setting this equal to the sum of the two separatrix half-widths (Eqs.(132) and (137) respectively), we arrive at the equation defining the critical ϵ for the overlapping of the two resonances, namely:

$$0.63 - 2.13\epsilon_c \simeq 1.42\epsilon_c^{1/2} \quad . \tag{138}$$

[35] This is also called an 'adiabatic' resonance, since one of the frequencies is zero, or, in higher order approximation, very close to zero.

The smallest root is $\epsilon_c = 0.09$. In fact, this value is an *overestimate* of the critical value for resonance overlapping, since, for $\epsilon = 0.09$ (Fig.10d), the 2:1 island chain has already disappeared. This overestimation is due to the fact that we neglected the effect of all other resonances between 2:1 and 1:0, i.e. the resonances 3:1, 4:1, etc. More accurate estimates are found by taking these resonances into account. However, even with a simple calculation based on the overlapping of the most conspicuous resonances, we are lead to a relevant and useful theoretical estimate for the critical value ϵ_c.

3.4. Kolmogorov normal form in analytic hamiltonian functions

In subsection 2.8 we discussed the implementation of Kolmogorov's algorithm used in proofs of the KAM theorem, in the case of a simple Hamiltonian model like (3). In the present subsection, we give the general form of Kolmogorov's algorithm for Hamiltonian systems of the form (97) for which the following conditions hold:

i) The Hamiltonian is analytic in a complexified domain of the action - angle variables, and
ii) The determinant of the Hessian matrix of the 'unperturbed part' H_0 is different from zero.

As an application, we compute the Kolmogorov normal form in the example of the Hamiltonian (117). We emphasize again the practical aspects of the construction of the Kolmogorov normal form, and in particular the way by which we introduce book-keeping in order to properly take into account the size of the various terms appearing in the Fourier expansion of the Hamiltonian.

The **general algorithm of construction of the Kolmogorov normal form** can be stated as follows:

Step 1: torus fixing. In a Hamiltonian of the form:

$$H(\phi, I; \epsilon) = H_0(I) + \epsilon H_1(\phi, I; \epsilon)$$

analytic in all its arguments, where (ϕ, I) are n-dimensional action-angle variables, we fix a frequency vector $\omega_* \equiv (\omega_{1*}, \ldots, \omega_{n*})$ such that the frequencies ω_{1*}, ..., ω_{n*} satisfy no commensurability relation. Then, we compute the actions I_* for which $\omega_* = \nabla H_0(I_*)$.

Step 2: shift of center. We define new action variables $J \equiv (J_1, J_2, \ldots, J_n)$ by the 'shift' transformation $I = I_* + J$. We substitute in the Hamiltonian, and expand around I_*. We perform the book-keeping rule (116), with K' given by the rule of Eq.(115). Then, the Hamiltonian takes the form (apart from a

constant): [36]

$$H^{(0)} = \omega_* \cdot J + \frac{1}{2}\left(J \cdot M \cdot J^T\right) + H_0^{>2}(J)$$
$$+\sum_{s=1}^{\infty} \lambda^s \sum_{k \in G_s} \left(h^{(0)}_{s,k,0}(\epsilon, I_*) e^{ik\cdot\phi} + (h^{(0)}_{s,k,1}(\epsilon, I_*) \cdot J) e^{ik\cdot\phi} + h^{(0)}_{s,k,\geq 2}(\epsilon, I_*, J) e^{ik\cdot\phi} \right)$$

where:

i) M is the $n \times n$ Hessian matrix of H_0 computed at I_*

$$M_{ij} = \frac{\partial^2 H_0(I_*)}{\partial I_i \partial I_j} \quad .$$

ii) $H_0^{>2}$ is a series in powers of the action variables J, starting with terms of degree 3.

iii) G_s means the set of wavevectors whose associated Fourier terms should be book-kept at the order s according to the chosen book-keeping rules.

iv) $h^{(0)}_{s,k,0}(\epsilon, I_*)$ are constants given as functions of the (also constant) indicated arguments.

v) $h^{(0)}_{s,k,1}(\epsilon, I_*)$ are n-component constant vectors, depending on the indicated arguments. The notation $(\ \cdot\ )$ means inner product.

vi) $h^{(0)}_{s,k,\geq 2}(\epsilon, I_*, J)$ are functions of the actions (and of the other indicated arguments), given as polynomial series which contain terms of degree 2 or higher in the actions.

Step 3: recursive normalization algorithm. Suppose r normalization steps have been accomplished. The Hamiltonian has the form:

$$H^{(r)} = \omega_* \cdot J + \frac{1}{2}\left(J \cdot M \cdot J^T\right) + H_0^{>2}(J)$$
$$+\lambda Z_1(\phi, J; \epsilon) + +\lambda^2 Z_2(\phi, J; \epsilon) + \ldots + \lambda^r Z_r(\phi, J; \epsilon)$$
$$+ \sum_{s=r+1}^{\infty} \lambda^s \sum_{k \in G_s} \left(h^{(r)}_{s,k,0}(\epsilon, I_*) + (h^{(r)}_{s,k,1}(\epsilon, I_*) \cdot J) + h^{(r)}_{s,k,\geq 2}(\epsilon, I_*, J) \right) e^{ik\cdot\phi}$$

where the functions Z_i, $i = 1, \ldots, r$ are *in Kolmogorov normal form, i.e. their dependence on the actions is in terms of degree 2 or higher.* Then:

Substep 3.1: eliminate the $O(\lambda^{r+1})$ terms depending on the angles and independent of the actions. To this end, define $\chi_{r+1,0}$ by solving the homological equation:

$$\{\omega_* \cdot J, \chi_{r+1,0}\} + \lambda^{r+1} \sum_{k \in G_{r+1}, |k| \neq 0} h^{(r)}_{r+1,k,0}(\epsilon, I_*) e^{ik\cdot\phi} = 0$$

[36] Once again, the reader is invited not to be discouraged by the apparent complexity of the formulae below. In in simple words: H_0 must be decomposed in three parts: i) linear in J, ii) quadratic in J, and iii) all the rest. Also, after performing the book-keeping, all Fourier coefficients of H_1 must be decomposed also in three parts, namely: i) terms independent of the actions, ii) terms linear in the actions, and iii) all the rest.

and compute

$$H^{(r+1,0)} = \exp(L_{\chi_{r+1,0}}) H^{(r)} \quad .$$

The hamiltonian takes the form

$$H^{(r+1,0)} = \omega_* \cdot J + \frac{1}{2}\left(J \cdot M \cdot J^T\right) + H_0^{>2}(J)$$

$$+\lambda Z_1(\phi, J; \epsilon) + \lambda^2 Z_2(\phi, J; \epsilon) + \ldots + \lambda^r Z_r(\phi, J; \epsilon)$$

$$+\lambda^{r+1} \sum_{k \in G_{r+1}} \left((h_{r+1,k,1}^{(r+1,0)}(\epsilon, I_*) \cdot J) + h_{r+1,k,\geq 2}^{(r+1,0)}(\epsilon, I_*, J) \right) e^{ik\cdot\phi}$$

$$+ \sum_{s=r+2}^{\infty} \lambda^s \sum_{k \in G_s} \left(h_{s,k,0}^{(r+1,0)}(\epsilon, I_*) + (h_{s,k,1}^{(r+1,0)}(\epsilon, I_*) \cdot J) + h_{s,k,\geq 2}^{(r+1,0)}(\epsilon, I_*, J) \right) e^{ik\cdot\phi} \quad .$$

Substep 3.2 (frequency fixing): eliminate the $O(\lambda^{r+1})$ terms linear in the actions and independent of the angles. To this end, define $\chi_{r+1,c}$ by

$$\chi_{r+1,c} = C \cdot \phi, \qquad C = (M^{-1}) h_{r+1,0,1}^{(r+1,0)}(\epsilon, I_*)$$

and compute

$$H^{(r+1,c)} = \exp(L_{\chi_{r+1,c}}) H^{(r+1,0)} \quad .$$

The hamiltonian takes the form

$$H^{(r+1,c)} = \omega_* \cdot J + \frac{1}{2}\left(J \cdot M \cdot J^T\right) + H_0^{>2}(J)$$

$$+\lambda Z_1(\phi, J; \epsilon) + \lambda^2 Z_2(\phi, J; \epsilon) + \ldots + \lambda^r Z_r(\phi, J; \epsilon)$$

$$+\lambda^{r+1} \sum_{k \in G_{r+1}, |k| \neq 0} \left((h_{r+1,k,1}^{(r+1,c)}(\epsilon, I_*) \cdot J) + h_{r+1,k,\geq 2}^{(r+1,c)}(\epsilon, I_*, J) \right) e^{ik\cdot\phi}$$

$$+ \sum_{s=r+2}^{\infty} \lambda^s \sum_{k \in G_s} \left(h_{s,k,0}^{(r+1,c)}(\epsilon, I_*) + (h_{s,k,1}^{(r+1,c)}(\epsilon, I_*) \cdot J) + h_{s,k,\geq 2}^{(r+1,c)}(\epsilon, I_*, J) \right) e^{ik\cdot\phi} \quad .$$

At this step, precisely, use is made of the required property that *the Hessian matrix M should have a determinant different from zero*, i.e. it should be an invertible matrix. This is required in order that the vector $C = (M^{-1}) h_{r+1,0,1}^{(r+1,0)}(\epsilon, I_*)$ can be computed. In fact, the generating function $\chi_{r+1,c}$ has the same property as encountered in subsection 2.8, namely it is a function linear rather than trigonometric in the angles. However, again as in the example of subsection 2.8, we can see that the linear dependence of $\chi_{r+1,c}$ on the angles introduces no formal issues in the algorithm, i.e. only terms of trigonometric dependence on the angles survive in the transformed Hamiltonian $H^{(r+1,c)}$.

Substep 3.3: eliminate the $O(\lambda^{r+1})$ terms linear in the actions and depending on the angles. To this end, define $\chi_{r+1,1}$ by solving the homological equation:

$$\{\omega_* \cdot J, \chi_{r+1,1}\} + \lambda^{r+1} \sum_{k \in G_{r+1}, |k| \neq 0} (h^{(r+1,c)}_{r+1,k,1}(\epsilon, I_*) \cdot J) e^{ik\cdot\phi} = 0$$

and compute

$$H^{(r+1)} = \exp(L_{\chi_{r+1,1}}) H^{(r+1,c)} \quad .$$

The hamiltonian takes the form

$$H^{(r+1)} = \omega_* \cdot J + \frac{1}{2}\left(J \cdot M \cdot J^T\right) + H_0^{>2}(J)$$

$$+\lambda Z_1(\phi, J; \epsilon) + \lambda^2 Z_2(\phi, J; \epsilon) + \ldots + \lambda^{r+1} Z_{r+1}(\phi, J; \epsilon)$$

$$+ \sum_{s=r+2}^{\infty} \lambda^s \sum_{k \in G_s} \left(h^{(r+1)}_{s,k,0}(\epsilon, I_*) + (h^{(r+1)}_{s,k,1}(\epsilon, I_*) \cdot J) + h^{(r+1)}_{s,k,\geq 2}(\epsilon, I_*, J) \right) e^{ik\cdot\phi}$$

i.e. it has been brought in Kolmogorov normal form up to terms of order $O(\lambda^{r+1})$. This completes one full step of the recursive algorithm of computation of the Kolmogorov normal form.

Example: We will construct the Kolmogorov normal form in the case of the Hamiltonian system (117), for a torus located in between the resonances considered in subsection 2.3, namely for the frequency ratio $\omega_{1*}/\omega_{2*} = I_{1*}/I_{2*} = q = 1/\gamma^2$, where $\gamma = (\sqrt{5}+1)/2$. To this end, we implement the steps of the general algorithm exposed above as follows:

Torus fixing: We have $q = 0.381966$, where $q = I_{1*}/I_{2*}$. Setting (for $\epsilon = 0$) $E = H_0$, we find $I_{2*} = \sqrt{2E/(1+q^2)}$. Hence, for $E = 1$, we have $I_{1*} = 0.504623$, and $I_{2*} = 1.32112$.

Shift of center: We set

$$I_1 = I_{1*} + J_1, \quad I_2 = I_{2*} + J_2 \quad . \tag{139}$$

Substituting (139) into (117), and omitting a constant, the Hamiltonian takes the form:

$$H = 0.504623 J_1 + 1.32112 J_2 + \frac{J_1^2 + J_2^2}{2}$$

$$+\epsilon \left(\frac{0.49877 + 4.65148 J_1 - 4.91747 J_2 + J_1^2 + 2 J_1 J_2 - 3 J_2^2}{3 + \cos\phi_1 + \cos\phi_2} \right) \quad .$$

Following now the general book-keeping rule of Eq.(116), we compute a constant K' from the average of Eq.(115) in the considered range of values of ϵ. Within the interval $0.01 \leq \epsilon \leq 0.1$, we find $K' = 3$.

In summary:

$$
\begin{aligned}
& H^{(0)}(\phi_1,\phi_2,J_1,J_2) = 0.504623J_1 + 1.32112J_2 + \frac{J_1^2+J_2^2}{2} \\
+ \quad & \lambda\epsilon\Big(0.49877 + 4.65148J_1 - 4.91747J_2 + J_1^2 + 2J_1J_2 - 3J_2^2\Big) \\
\times \Big[\quad & 0.384023 - 0.0760351(e^{i\phi_1} + e^{-i\phi_1} + e^{i\phi_2} + e^{-i\phi_2}) \\
& +0.016008(e^{2i\phi_1} + e^{-2i\phi_1} + e^{2i\phi_2} + e^{-2i\phi_2}) \\
& +0.0280895(e^{i\phi_1+i\phi_2} + e^{-i\phi_1+i\phi_2} + e^{i\phi_1-i\phi_2} + e^{-i\phi_1-i\phi_2}) \\
& -0.00354632\lambda(e^{3i\phi_1} + e^{-3i\phi_1} + e^{3i\phi_2} + e^{-3i\phi_2}) \\
& -0.00823336\lambda(e^{i\phi_1+2i\phi_2} + e^{-i\phi_1+2i\phi_2} + e^{i\phi_1-2i\phi_2} + e^{-i\phi_1-2i\phi_2} \\
& \qquad +e^{2i\phi_1+i\phi_2} + e^{-2i\phi_1+i\phi_2} + e^{2i\phi_1-i\phi_2} + e^{-2i\phi_1-i\phi_2}) \\
& +0.000817397\lambda(e^{4i\phi_1} + e^{-4i\phi_1} + e^{4i\phi_2} + e^{-4i\phi_2}) \\
& +0.00222626\lambda(e^{i\phi_1+3i\phi_2} + e^{-i\phi_1+3i\phi_2} + e^{i\phi_1-3i\phi_2} + e^{-i\phi_1-3i\phi_2} \\
& \qquad +e^{3i\phi_1+i\phi_2} + e^{-3i\phi_1+i\phi_2} + e^{3i\phi_1-i\phi_2} + e^{-3i\phi_1-i\phi_2}) \\
& +0.00307641\lambda(e^{2i\phi_1+2i\phi_2} + e^{-2i\phi_1+2i\phi_2} + e^{2i\phi_1-2i\phi_2} + e^{-2i\phi_1-2i\phi_2}) \\
& -0.000194075\lambda(e^{5i\phi_1} + e^{-5i\phi_1} + e^{5i\phi_2} + e^{-5i\phi_2}) \\
& -0.000581994\lambda(e^{i\phi_1+4i\phi_2} + e^{-i\phi_1+4i\phi_2} + e^{i\phi_1-4i\phi_2} + e^{-i\phi_1-4i\phi_2} \\
& \qquad +e^{4i\phi_1+i\phi_2} + e^{-4i\phi_1+i\phi_2} + e^{4i\phi_1-i\phi_2} + e^{-4i\phi_1-i\phi_2}) \\
& -0.000995866\lambda(e^{2i\phi_1+3i\phi_2} + e^{-2i\phi_1+3i\phi_2} + e^{2i\phi_1-3i\phi_2} + e^{-2i\phi_1-3i\phi_2} \\
& \qquad +e^{3i\phi_1+2i\phi_2} + e^{-3i\phi_1+2i\phi_2} + e^{3i\phi_1-2i\phi_2} + e^{-3i\phi_1-2i\phi_2}) + ... \Big]
\end{aligned}
\tag{140}
$$

Normalization: We are now ready to perform the first recursive step of the normalization algorithm, separated in the three sub-steps. We give the corresponding formulae for the generating functions and for the final Hamiltonian after the first normalization step. We have:

$$
\begin{aligned}
\chi_{1,0} = \lambda\epsilon i \Big[& 0.0751533(e^{i\phi_1} - e^{-i\phi_1}) + 0.028706(e^{i\phi_2} - e^{-i\phi_2}) \\
& -0.0079112(e^{2i\phi_1} - e^{-2i\phi_1}) - 0.0030218(e^{2i\phi_2} - e^{-2i\phi_2}) \\
& -0.0076737(e^{i(\phi_1+\phi_2)} - e^{-i(\phi_1+\phi_2)}) + 0.0171589(e^{i(\phi_1-\phi_2)} - e^{-i(\phi_1-\phi_2)}) \Big] \quad .
\end{aligned}
$$

$$
\chi_{1,c} = \lambda\epsilon(1.78628\phi_1 - 1.88842\phi_2)
$$

$$
\begin{aligned}
\chi_{1,1} = \lambda\epsilon i \Big[& (0.551942J_1 - 0.74095J_2)(e^{i\phi_1} - e^{-i\phi_1}) \\
& +(0.267709J_1 - 0.304746J_2)(e^{i\phi_2} - e^{-i\phi_2})
\end{aligned}
$$

$$+(-0.0581015J_1 + 0.0779978J_2)(e^{2i\phi_1} - e^{-2i\phi_1})$$
$$+(-0.028181J_1 + 0.0320798J_2)(e^{2i\phi_2} - e^{-2i\phi_2})$$
$$+(0.181038J_1 - 0.190188J_2)(e^{i(\phi_1-\phi_2)} - e^{-i(\phi_1-\phi_2)})$$
$$+(-0.0673611J_1 + 0.0798595J_2)(e^{i(\phi_1+\phi_2)} - e^{-i(\phi_1+\phi_2)})\Big] \quad .$$

The Hamiltonian, after the first normalization step is given by

$$H^{(1)} = \exp(L_{\chi_{1,1}}) \exp(L_{\chi_{1,c}}) \exp(L_{\chi_{1,0}}) H^{(0)} \quad .$$

We find:

$$H^{(1)} = \lambda\epsilon\Big[1.78498 + 0.384023J_1^2 + 0.768047J_1J_2 - 1.15207J_2^2$$
$$(0.475907J_1^2 - 0.89302J_1J_2 + 0.228105J_2^2)(e^{i\phi_1} + e^{-i\phi_1})$$
$$+(-0.0760351J_1^2 + 0.115639J_1J_2 - 0.0766411J_2^2)(e^{i\phi_2} + e^{-i\phi_2})$$
$$+(-0.100195J_1^2 + 0.188012J_1J_2 - 0.048024J_2^2)(e^{2i\phi_1} + e^{-2i\phi_1})$$
$$+(0.016008J_1^2 - 0.024346J_1J_2 + 0.0161356J_2^2)(e^{2i\phi_2} + e^{-2i\phi_2})$$
$$+(0.209127J_1^2 - 0.315047J_1J_2 + 0.10592J_2^2)(e^{i(\phi_1-\phi_2)} + e^{-i(\phi_1-\phi_2)})$$
$$+(-0.0392716J_1^2 + 0.0686773J_1J_2 - 0.00440891J_2^2)(e^{i(\phi_1+\phi_2)} + e^{-i(\phi_1+\phi_2)})\Big] \quad .$$

We close this subsection with a note on the convergence of the Kolmogorov normal form. The accumulation of divisors in the present scheme follows nearly the same pattern as exposed in subsection 2.8. In fact, it turns out that the accumulation of divisors is the same whether one progresses by normalizing according to the quadratic scheme (i.e. in groups of terms $O(\lambda)$, then $O(\lambda^2)$, $O(\lambda^3)$, then $O(\lambda^4)$, $O(\lambda^5)$, $O(\lambda^6)$, $O(\lambda^7)$, etc.), or according to a linear scheme (Giorgilli and Locatelli 1997). Using the same heuristic notation as in subsection 2.8, the situation is summarized with the help of a figure (Fig.11). The arrows indicate the most important Poisson brackets formed by the generating functions $\chi_{r,0}$ and $\chi_{r,1}$ in one example, of, say, the order $r = 5$. The terms specified on top of each arrow indicate the Hamiltonian terms with which the most important repetitions of Poisson brackets take place, either by the generating function $\chi_{5,0}$, or by $\chi_{5,1}$. The symbol (X) denotes a path produced by repeated Poisson brackets of the generating functions $\chi_{r,0}$ or $\chi_{r,1}$, leading to terms that *stop being normalized* at subsequent normalization steps. In fact, this can happen for two reasons: i) a repeated Poisson bracket leads eventually to zero new terms (this can happen if both functions in a bracket are independent of the actions), or it leads to terms depending quadratically on the actions. A careful inspection of Fig.11 shows now that the worst possible accumulation of divisors in Kolmogorov's scheme is quadratic. For example, starting from the normalization order $r = 5$ we have an accumulation of the form:

$$a_5 \to a_5^2 a_{10} \to a_5^4 a_{10}^2 a_{20} \to \ldots$$

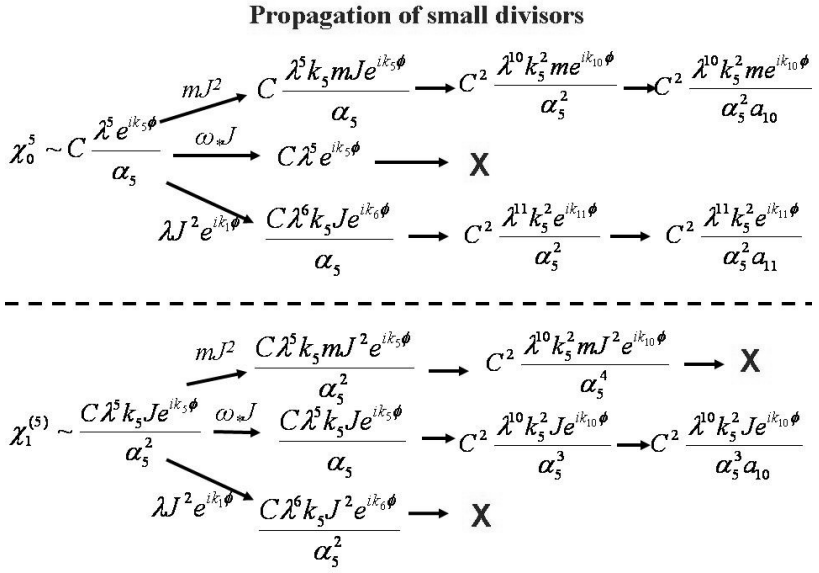

Figure 11. Propagation of divisors in the Kolmogorov normal form construction. Using the heuristic notation introduced in subsections 2.7 and 2.8, the figure shows the most important chains of terms produced in the Kolmogorov series by the repeated Poisson brackets of the generating functions $\chi_{r,0}$ and $\chi_{r,1}$ at the normalization order $r = 5$ (see text for details).

Using the same arguments as in subsection 2.8, we can show that such an accumulation ensures the convergence of the Kolomogorov normal form for sufficiently small values of ϵ. This, in turn, proves the existence of an invariant torus with the given frequencies for sufficiently small ϵ. In fact, a numerical convergence test shows that the convergence in the present example persists up to $\epsilon \simeq 0.06$. This is about 70% of the maximum perturbation value up to which the torus is found to exist by purely numerical means.

4. THREE DEGREES OF FREEDOM: DIFFUSION IN THE ARNOLD WEB

In the present section, we consider nearly-integrable Hamiltonian systems of three degrees of freedom of the form $H = H_0 + \epsilon H_1$, exhibiting a phenomenon of diffusion of weakly chaotic orbits in the web or resonances, otherwise called *Arnold diffusion* (Arnold (1964), Arnold and Avez (1968)).

In nearly integrable systems of two degrees of freedom, the presence of two-dimensional invariant tori, whose existence is a consequence of the Kolmogorov - Arnold - Moser theorem, poses topological restrictions to the possible excursions that a chaotic orbit can undergo within any hypersurface of constant energy $H = E$ embedded in the system's phase space. In fact, in systems of two degrees of freedom the maximal dimension of invariant tori is two, while the hypersurface $H = E$ has dimension three. Thus, in such a hyper-surface the maximal

tori do not allow communication between chaotic domains in their interior and in their exterior. [37]. However, in systems of three degrees of freedom, the invariant KAM tori can no longer act as absolute barriers to the communication of the various chaotic domains co-existing in the same hyper-surface of constant energy. This is because the latter's dimension (equal to five) exceeds by two the maximal dimension of invariant tori (equal to three). The non-existence of topological restrictions renders *a priori* possible, in turn, that a chaotic orbit started at a certain point of a constant energy hyper-surface undergoes a long excursion, hence visiting (possibly after a quite long time) the neighborhood of any other point in a connected chaotic domain within the same hyper-surface. This topological possibility exists even if the perturbation ϵ is infinitesimally small, and the so-resulting diffusion of chaotic orbits is called Arnold diffusion.

It should be stressed that besides topological arguments, a demonstration that the Arnold diffusion really takes place in a concrete system requires establishing the existence of a *mechanism of transport* of the chaotic orbits within the Arnold web (see Lochak (1999) for a detailed discussion of the distinction between the terms 'Arnold diffusion' and 'Arnold's mechanism'). In fact, Arnold (1964) gave an example of such mechanism, whose existence, however, is guaranteed only in a rather special type of Hamiltonian model of three degrees of freedom. As shown in subsection 4.5, Arnold's model shares some common features with models arising from the implementation of *resonant normal form theory* in systems of three degrees of freedom satisfying some so-called *convexity conditions* (see subsection 4.3 below). However, there is also a crucial difference between the two types of models, discussed in subsection 4.5, which renders difficult (and non-existent, to date) a generalization of the proof of whether Arnold's mechanism exists in generic Hamiltonian systems of three or more degrees of freedom (see Simó and Valls (2001), and Mather (2004)).

On the other hand, following some early works in systems of three degrees of freedom or 4D symplectic mappings (Froeschlé (1970a,b, 1972), Froeschlé and Scheidecker (1973), Tennyson (1982), weakly-chaotic diffusion in the web of resonances has been observed numerically in an extended list of works in recent years referring to model Hamiltonian systems or mappings. Indicative references are: Kaneko and Konishi (1989), Wood et al. (1990), Laskar (1993) Dumas and Laskar (1993), Skokos et al. (1997), Efthymiopoulos et al. (1998), Lega et al. (2003), Giordano and Cincotta (2004), Froeschlé et al. (2005), Guzzo et al. (2005, 2006), Lega et al. (2009, 2010a, 2010b), Cincotta and Giordano (2012), Mestre et al. (2012), Mestre (2012), Efthymiopoulos and Harsoula (2012). Also, various aspects of the problem of diffusion have been studied in concrete astronomical dynamical models, as for example, the motion of asteroids in solar system dynamics (e.g. Holman and Murray (1996), Murray and Holman (1997), Levison et al. (1997), Nesvorny and Morbidelli (1998), Morbidelli and Nesvorny (1999), Marzari et al. (2003), Tsiganis et al. (2005), Cordeiro and Mendes de Souza (2005), Cordeiro (2006), Robutel and Gabern (2006), Lhotka et al. (2008),

[37] This property is manifested also when considering Poincaré surfaces of section. For example, in Figs.1a,b any chaotic orbit started in a domain surrounded by a closed invariant curve cannot find itself in another chaotic domain outside the curve. Thus, two chaotic domains, one in the interior and the other in the exterior of the closed KAM curve, do not communicate. Likewise, two domains above and below a rotational KAM curve do not communicate.

Tsiganis (2008, 2010), Cachucho et al. 2010), or the motion along resonances in galactic dynamics (e.g. Papaphilippou and Laskar, (1996, 1998), Wachlin and Ferraz-Mello (1998), Muzzio et al. (2005), Kalapotharakos and Voglis (2005), Cincotta et al. (2006), Aquilano et al. (2007), Valluri et al. (2012)). In fact, there is evidence that such a diffusion takes place in systems satisfying a variety of different convexity (or, more generally *steepness*) conditions, as well as conditions of so-called *a priori stability* (or instability). Thus, not all diffusion phenomena appearing in works as the above should be characterized as Arnold diffusion. Also, an important comment is in order at this point, regarding the *slowness* of Arnold diffusion, as observed in most numerical experiments. In fact, a comparison of the timescale of Arnold diffusion with the timescales of interest in astronomical systems renders often quite questionable whether this type of diffusion is relevant in realistic applications (see also a discussion of this point in the article by Cincotta et al. (2012) in the present volume of proceedings). For example, the orbits of stars in galaxies evolve in a timescale of 10^2 – 10^4 periods, which is quite a small time compared to the timescale in which Arnold diffusion produces observable effects (10^6 – 10^{11} periods for perturbation values as those encountered in Table 1). Thus, it appears that Arnold diffusion plays a small role in galaxies, except perhaps for orbits passing very close to the galactic center. However, the time scale of Arnold diffusion is quite relevant to applications in solar system dynamics, where the characteristic timescales are of order 10^8 – 10^{10} periods.

It should be noted also that in most applications we find that the distinction between the so-called *Nekhoroshev regime* (see below), where the rate of diffusion becomes exponentially small in the inverse of a small parameter, and the *resonance overlap* regime, where the diffusion speed is given by a power-law of ϵ, is not so sharp in practice. However, it is important to emphasize that normal form theory can be applied to some extent in both regimes. In fact, as shown below the most relevant quantity characterizing the speed diffusion turns to be the *size of the remainder R_{opt} at the optimal normalization order*. Thus, one can obtain realistic estimates of the speed of diffusion using R_{opt} in both regimes, i.e. independently on whether R_{opt} depends on $1/\epsilon$ exponentially or algebraically.

In the remaining part of this section we present the main elements of resonant normal form theory as well as some of its applications in describing weakly-chaotic diffusion in the web of resonances in systems of three degrees of freedom. This implementation allows one to derive useful tools for describing, both qualitatively and quantitatively, the *geometric* properties of diffusion. In particular, by the resonant normal form theory we can explain why the diffusion progresses preferentially in some directions of the phase space, and what invariant objects (like periodic orbits or low-dimensional tori) are responsible for such preference. Furthermore, via normal forms we can compute quantitative estimates of the diffusion rate, which are found to compare well with the results of numerical experiments.

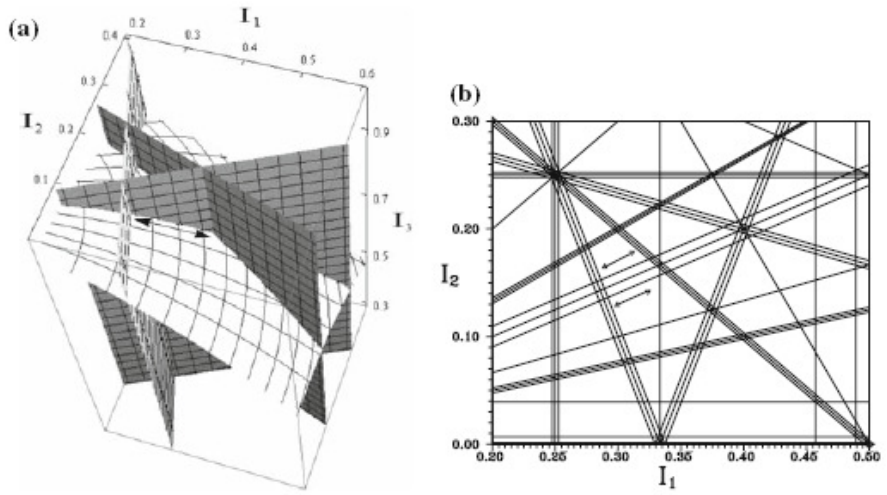

Figure 12. (a) A part of the paraboloid of constant energy condition $I_1^2 + I_2^2 + 2I_3 = 2E$ in the action space for the model (141) with $\epsilon = 0$, and for the value of the energy $E = 1$. Gray-shaded planes indicate some resonant manifolds in this model. The intersection of all the resonant planes with the paraboloid of constant energy produces a set of parabolic curves which is the 'web of resonances'. (b) The projection of the web of resonances $k_1 I_1 + k_2 I_2 + k_3 = 0$ for $|k| \leq 5$ on the (I_1, I_2) plane. Single or triple lines correspond to resonances whose corresponding coefficient in the Fourier series of H_1 is positive or negative respectively (after Efthymiopoulos (2008)).

4.1. Diffusion along resonances: a numerical example

As a tool serving to introduce basic concepts, let us consider a simple example of a Hamiltonian model of three degrees of freedom (Froeschlé et al. (2000)):

$$H = H_0 + \epsilon H_1 = \frac{I_1^2 + I_2^2}{2} + I_3 + \frac{\epsilon}{4 + \cos\phi_1 + \cos\phi_2 + \cos\phi_3} \quad . \tag{141}$$

The integrable part H_0 produces a simple dynamics. All the orbits lie on invariant tori, and we have $\dot{I}_i = 0$, while $\dot{\phi}_1 = \omega_{0,1} = I_1$, $\dot{\phi}_2 = \omega_{0,2} = I_2$, $\dot{\phi}_3 = \omega_{0,3} = 1$.

The surface of constant energy $H_0 = E$ is a paraboloid in the action space given by $I_1^2 + I_2^2 + 2I_3 = 2E$. Part of this paraboloid is shown as a grid-lined inclined surface in Fig.12a.

We define the *resonant manifolds* corresponding to the integrable Hamiltonian H_0 as the set of all two-dimensional manifolds defined by relations of the form:

$$k_1\omega_{0,1} + k_2\omega_{0,2} + k_3\omega_{0,3} = k_1 I_1 + k_2 I_2 + k_3 = 0 \tag{142}$$

with $k \equiv (k_1, k_2, k_3) \in \mathbf{Z}^3$, $|k| \equiv |k_1| + |k_2| + |k_3| \neq 0$. In fact, we see that for any choice of k, Eq.(142) implies that the invariant manifolds in this example are just planes, which are always normal to the plane (I_1, I_2).

Consider now the intersections of all the resonant planes with a surface of constant energy $E = H_0$. These form a set of parabolic curves, which form a *web* on the surface $E = H_0$ (see Fig.12a). This is called a *web of resonances*.

Viewed from the top of Fig.12a, the projection of the resonance web on the plane (I_1, I_2) is a set of straight lines (Fig. 12b). It will be shown below that, when $\epsilon \neq 0$, a small *resonant domain*, of thickness $O(|h_k\epsilon|^{1/2}))$, is formed around each resonant manifold, where h_k is the coefficient of the term $\exp(ik\cdot\phi)$ in the Fourier development of the perturbation H_1. The intersections of the resonant domains with the surface of constant energy form *resonant zones*, also of thickness $O(|h_k\epsilon|^{1/2})$. As a result, when projected on the plane (I_1, I_2), the web of resonances along with the resonant zones looks like in Fig.12b. In fact, in this figure some resonances are represented by a single line, while other by a triple line, i.e. a line corresponding to the central resonance and two nearly parallel lines on either side of it, representing the border of the resonant zone. This difference reflects a real phenomenon encountered when using a numerical method in order to depict the resonance web, that will be explained below.

The main phenomenon, of chaotic diffusion in the Arnold web, is now shown with the example of Fig.13. In both panels, the color (or grayscale) background corresponds to a so-called *FLI map* (Froeschlé et al. (2000)), allowing to clearly see the resonant structure of the system in the action space when (a) $\epsilon = 0.01$, and (b) $\epsilon = 0.015$. The *Fast Lyapunov Indicator* (Froeschlé et al (1997)) is a numerical index of the degree of chaotic behavior of individual orbits, computed via a numerical integration of the linearized equations of motion together with the full equations of motion. The reader is deferred to the original article (Froeschlé et al (1997)), as well as to Maffione et al. (2011) for a review of numerical methods of chaos detection and/or quantification in conservative dynamical systems. For our purpose in the present tutorial, it suffices to note that a dark (blue or green) color in Fig.12 indicates ordered orbits, while a light (yellow) color means chaotic orbits. By the FLI map, we are able to clearly see the network formed by the projection of different resonant manifolds on the plane I_1, I_2, as well as the form of one conspicuous (and other, smaller) *resonance junctions*, i.e. the chaotic domains formed at the loci where the manifolds of different resonances intersect each other.

Using normal form theory, in subsequent subsections it will be shown that the possibility to distinguish the various resonances in Fig.13 is due to the fact that *in the neighborhood of any resonant domain the dynamics can be locally approximated by the dynamics of the perturbed pendulum.* Namely, we will show that the resonant normal form for a Hamiltonian like (141) can be written as:

$$\begin{aligned} H_{res} &= Z(I_{R_2}, I_F) + \frac{1}{2}\beta I_R^2 + 2\epsilon g_k \cos\phi_R + \ldots \\ &+ R(\phi_R, \phi_{R_2}, \phi_F, I_R, I_{R_2}, I_F) \end{aligned} \tag{143}$$

where the variables $(\phi_R, \phi_{R_2}, \phi_F, I_R, I_{R_2}, I_F)$ are resonant action-angle variables derived from the original canonical variables by a linear canonical transformation. The derivation of Eq.(143) (see subsection 3.4) follows from a quite similar analysis as in subsection 3.3 for the corresponding 2D problem. We observe that the Hamiltonian (143) is split in three parts: a part depending only on the

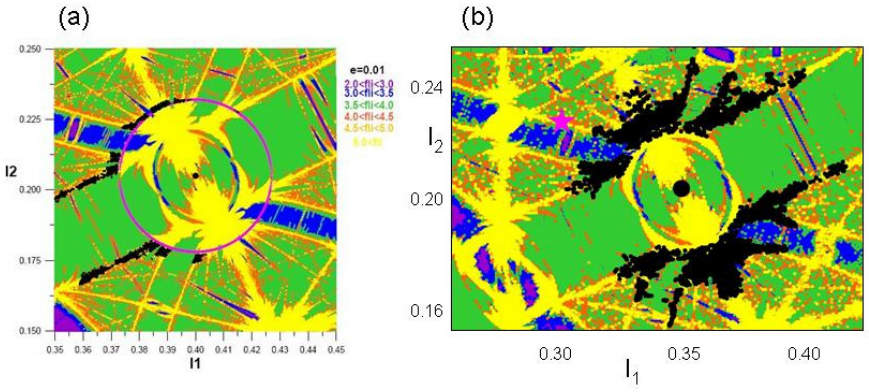

Figure 13. (a) Arnold diffusion in the model (141) for $\epsilon = 0.01$. An orbit with initial conditions in the chaotic separatrix-like layer of the 2:1 resonance slowly diffuses along the resonance, until reaching a doubly-resonant domain. The motion along the simple resonance, as well as the circular motion within the doubly-resonant domain are both interpreted by resonant normal form theory (see subsections 4.3 and 4.4 respectively). (b) Chaotic diffusion for $\epsilon = 0.015$. The same chaotic orbit visits several parts of the Arnold web.

actions I_{R_2}, I_F, a second part given by the pendulum Hamiltonian:

$$H_{pend} = \frac{1}{2}\beta I_R^2 + 2\epsilon g_k \cos\phi_R \tag{144}$$

where β and g_k are constants, and finally, a third part, i.e. the remainder $R(\phi_R, \phi_F, \phi_3, I_R, I_F, I_3)$. The coefficient g_k is nearly equal to the coefficient h_k of the term $\exp(ik\cdot\phi)$ in the Fourier series representing H_1 in the original Hamiltonian, where k is the wave-vector corresponding to the particular resonance considered.

If we neglect the remainder effect, the actions I_{R_2} and I_F are integrals of the Hamiltonian H_{res}. This allows to calculate the separatrix half-width of the resonance in the same way as in subsection 3.3. We find

$$\Delta I_{R,sep} = \sqrt{\frac{8|g_k\epsilon|}{\beta}} \quad . \tag{145}$$

In reality, however, there is no true separatrix at the border of each resonance, since *the effect of the remainder is to introduce chaos in the system.* Thus, instead of a separatrix, we have the formation of a separatrix-like layer at the border of any resonance [38]. Any initial condition started within such a chaotic layer yields a large value of the FLI. Thus, computing many such orbits allows to obtain a clear picture of the structure of all chaotic layers, and hence of the whole

[38] This is similar to the effect shown in Fig.6 for the simple perturbed pendulum model (3). Namely, the theoretical invariant curves computed by a normal form in that example yield a separatrix curve, while, in reality, we have instead a thin separatrix-like chaotic layer as revealed by a numerical integration of orbits.

resonance web. In fact, when the resonance web is visualized numerically in the action space, e.g. by the FLI method, one has to make an appropriate choice of Poincaré surface of section in order to fix the angles at which the FLI maps are computed. In Fig.12, we make the choice $\phi_3 = 0$, $|\phi_1| + |\phi_2| \leq 0.05$. This corresponds essentially to setting the resonant angle $\phi_R = k_1\phi_1 + k_2\phi_2 + k_3\phi_3$ to a value very close to zero, i.e., $\phi_R \approx 0$. We then see that this means to plot two sets of points in the plane (I_1, I_2), corresponding to a chaotic orbit passing close to the maxima or minima of the theoretical separatrices, when $g_k < 0$, or one set of points on the plane (I_1, I_2), corresponding to passing close to the X-point of each separatrix, when $g_k > 0$. Consequently, the thin chaotic borders of the resonances appear as a pair of thick lines in the surface of section if $g_k < 0$, or as a single line if $g_k > 0$. This rule is used for plotting the resonances and their borders in Fig.12b.

Returning to Fig.13, the black points show now the excursion traveled in the action space along the resonance web by *one* chaotic orbit, when (a) $\epsilon = 0.01$ and (b) $\epsilon = 0.015$. In both cases, the orbit starts in the left part of the corresponding plots, within the separatrix layer of the resonance $I_1 - 2I_2 = 0$. In Fig.13a, the orbit undergoes a phase of diffusion along a simple resonance. This phase lasts for a quite long time ($t \sim 10^8$), while, afterwards, the orbit enters a so-called doubly-resonant domain formed by the intersection of many resonances. The orbit remains in that domain up to the end of the numerical integration ($t = 2 \times 10^8$). We observe that despite the fact that the central part of the doubly resonant domain appears quite chaotic, the motion of the chaotic orbit in this domain appears confined in a nearly circular arc, while the diffusion rate is quite slow in the direction normal to the arc. In Fig.13b, on the other hand, for somewhat larger ϵ ($\epsilon = 0.015$) we observe that the orbit, within a similar timescale, covers a much more extended part of the resonance web, passing via more than one doubly-resonant domains and undergoing also changes of direction from along one resonance to along another.

Both phenomena, of diffusion along simple resonances, or within doubly resonant domains, as well as the geometric properties of the motion in either case, are explained by an appropriate form of resonant perturbation theory. Furthermore, it is possible to obtain quantitative estimates regarding the *rate of diffusion* (or the value of the diffusion coefficient, assuming, as a first approximation, that the diffusion has a normal character)[39], in terms of the *size of the remainder* of the normal form series computed either in the simply resonant, or doubly resonant case. We will now give the general theory of resonant normal form dynamics referring to both cases. However, we will return to a specific numerical example concerning the Hamiltonian model (141) in subsection 4.4, illustrating Arnold diffusion in a concrete calculation where an appropriate set of resonant canonical variables, produced via a normal form computation, are used.

[39]There has been some numerical evidence (see e.g. the review article of Lega et al. (2008)), that the diffusion along simple resonances has a normal character. However, counter-examples can be found (see e.g. Giordano and Cincotta (2004)).

4.2. Resonant normal form theory: Exponential estimates and the role of convexity.

We hereafter focus on systems of three degrees of freedom of the form

$$H = H_0 + \epsilon H_1$$

which satisfy necessary conditions for the holding of the *theorem of Nekhoroshev* (Nekhoroshev (1977), Benettin et al. (1985), Benettin and Galavotti (1986), Lochak (1992), Pöschel (1993)). The Nekhoroshev theorem ensures that for any initial datum in the action space, the speed of diffusion is bounded by a quantity *exponentially small* in the inverse of the small parameter ϵ, namely one has:

$$|I(t) - I(0)| < \epsilon^a, \quad \text{for all } t < T = O\left(\exp\left(\frac{\epsilon_0}{\epsilon}\right)^b\right) \tag{146}$$

where a, b, ϵ_0 are positive constants.

The basic formulation of the Nekhoroshev theorem relies on a number of assumptions relevant to the phenomenon of Arnold diffusion. In particular, the so-called *geometric part* of Nekhoroshev theorem examines the question of whether there are allowable directions left in the action space along which a chaotic orbit can undergo a fast drift, after all restrictions due to resonant conditions have been properly taken into account in any local domain within the action space. It is then found that additional restrictions to the diffusion are posed if some so-called *convexity* (or, more generally, *steepness*) conditions are fulfilled by the unperturbed part H_0 of the Hamiltonian. We now present a simple form of such conditions.

Analyticity and convexity conditions. We assume that the Hamiltonian function satisfies the following conditions:

Analyticity: We assume that:

i) there is an open domain $\mathcal{I} \subset \mathbf{R}^3$ and a positive number ρ such that for all points $I_* \equiv (I_{1*}, I_{2*}, I_{3*}) \in \mathcal{I}$ and all complex quantities $I_i' \equiv I_i - I_{i*}$ satisfying the inequalities $|I_i'| < \rho$, the function H_0 can be expanded as a convergent Taylor series

$$H_0 = H_{0*} + \omega_* \cdot I' + \sum_{i=1}^{3}\sum_{j=1}^{3} \frac{1}{2} M_{ij*} I_i' I_j' + \ldots \tag{147}$$

where $\omega_* = \nabla_I H_0(I_*)$, while M_{ij*} are the entries of the Hessian matrix of H_0 at I_*, denoted by M_*.

ii) For all $I \in \mathcal{I}$, H_1 admits an absolutely convergent Fourier expansion

$$H_1 = \sum_k h_k(I) \exp(ik \cdot \phi) \tag{148}$$

in a domain where all three angles satisfy $0 \leq Re(\phi_i) < 2\pi$, $|Im(\phi_i)| < \sigma$ for some positive constant σ. We recall that, exactly as in subsection 3.2, the latter condition implies that the size of the Fourier coefficients h_k is bounded by a quantity decaying exponentially with $|k|$, i.e. the inequality (114) is satisfied.

iii) We finally assume that all coefficients h_k can be expanded around I_*

$$h_k = h_{k*} + \nabla_{I_*} h_k \cdot I' + \frac{1}{2} \sum_{i=1}^{3} \sum_{j=1}^{3} h_{k,ij*} I'_i I'_j + \dots \tag{149}$$

and that the series (149) are convergent in the same union of domains as the series (147) for H_0. [40]

Convexity: We assume that for all $I_* \in \mathcal{I}$ either two of the (real) eigenvalues of the Hessian matrix M_* have the same sign and one is equal to zero, or all three eigenvalues have the same sign. It is noted that the fact that the eigenvalues are real follows from the property that M_* is a symmetric matrix.

Multiplicity of resonances: We now give some definitions allowing to characterize the multiplicity of resonant dynamics. As in subsection 3.3, we define a *resonant manifold* (denoted hereafter by $\mathcal{R}_k$) associated with a non-zero wavevector k with co-prime integer components $k \equiv (k_1, k_2, k_3)$ as the two-dimensional surface in the action space defined by the relation

$$\mathcal{R}_k = \{I \in \mathcal{I} : k_1\omega_1(I) + k_2\omega_2(I) + k_3\omega_3(I) = 0\} \quad , \tag{150}$$

where $\omega_i(I) = \partial H_0/\partial I_i$.

Let $I_* \in \mathcal{I}$ be such that all three frequencies $\omega_i(I_*)$, $i = 1, 2, 3$ are different from zero. We distinguish the following three cases:

i) *Non-resonance:* no resonant manifold $\mathcal{R}_k$ contains I_*.

ii) *Simple resonance:* one resonant manifold $\mathcal{R}_k$ contains I_*.

iii) *Double resonance:* more than one resonant manifolds contain I_*. In the latter case, it is possible to choose two linearly independent vectors $k^{(1)}, k^{(2)}$ such that all resonant manifolds $\mathcal{R}_k$ containing I_* are labeled by vectors k which are linear combinations of the chosen vectors $k^{(1)}, k^{(2)}$ with rational coefficients. The intersection of these manifolds forms a one-dimensional *resonant junction*. A doubly-resonant point I_* corresponds to the intersection of a resonant junction with a constant energy surface $H_0(I_*) = E$.

Normal form computation

In computing a resonant normal form for a system with the above properties, we follow a similar method as in subsection 3.3. Namely:

i) We define an *expansion center*, i.e. a point I_* in the action space around which all quantities are expanded. The point I_* must be chosen so that:

a) the orbits whose study we are interested in should reside in a neighborhood of I_*, and

b) This neighborhood should belong to the domain of analyticity of the *optimal* normal form series.

---

[40] Actually, a more precise statement is that we assume that the intersection of all the domains where the series (147) and (149) are convergent is a non-empty open set $\mathcal{I}$.

Both conditions require some further clarification:

a) Let us consider the left part of Fig.13a. The plotted chaotic orbit undergoes a diffusion within the separatrix chaotic layer along the resonance $I_1 - 2I_2 = 0$. We seek to properly choose a value for the actions I_* in order to compute a resonant normal form in this domain, i.e., well before the orbit approaches the resonant junction at the center of the same figure. For many practical reasons, it proves convenient to choose I_* in such a way that the corresponding frequencies ω_* *always satisfy a doubly-resonant condition*, i.e. there are two linearly independent conditions of the form $k^{(i)} \cdot \omega_* = 0$, $i = 1, 2$. For reasons clarified immediately below, we can see that, provided that $|k^{(2)}| >> |k^{(1)}|$, i.e. that the second resonant wave-vector $k^{(2)}$ corresponds to a resonance of order *much higher* than the order of the first resonant wave-vector $k^{(1)}$, the so-resulting normalization will effectively correspond to a simply resonant normal form, even if, formally, I_* is a doubly-resonant point (see subsection 4.3 below). On the other hand, if $|k^{(2)}|$ and $|k^{(1)}|$ are of similar order, the so resulting normal form is found to represent all features of dynamics in a doubly-resonant domain (subsection 4.4).

Let us give an example: in the case of the Hamiltonian (141) we have $\omega_{1*} = I_{1*}$ and $\omega_{2*} = I_{2*}$, while $\omega_{3*} = 1$. Returning to Fig.13a, if, looking to the leftmost part of the plot, we choose $I_{1*} = 0.355$, $I_{2*} = 0.1775$, we find that the two independent resonance conditions satisfied for this choice, and corresponding to the minimum possible $|k^{(1)}|$ and $|k^{(2)}|$ are: a) $I_{1*} - 2I_{2*} = 0$, corresponding to $k^{(1)} = (1, -2, 0)$, $|k^{(1)}| = 3$, and b) $200I_{1*} - 71 = 0$, corresponding to $k^{(2)} = (200, 0, -71)$, $|k^{(2)}| = 271$. Hence, we have $|k^{(2)}| >> |k^{(1)}|$. In subsection 4.3 we will see that the normal form constructed by such a choice of expansion center effectively describes simply resonant dynamics, despite the fact that the point I_* is formally doubly-resonant, because trigonometric terms of only the resonant angle $k^{(1)} \cdot \phi$ are present in the final normal form formula. On the other hand, as the orbit moves along the resonance in the right direction in Fig.13a, we find that at some later time the orbit passes from the neighborhood of the point $I_{1*} = 4/11 = 0.3636...$, $I_{2*} = 2/11 = 0.1818....$ Now, this is also a doubly-resonant point with $k^{(1)} = (1, -2, 0)$, and $k^{(2)} = (4, 3, -2)$. Thus, $|k^{(2)}| = 9$, i.e. $|k^{(2)}|$ is now much smaller than in the previous example (although still larger than $|k^{(1)}|$). When computing the normal form, we find that for ϵ sufficiently small the so resulting formula contains trigonometric terms of both resonant angles $k^{(1)} \cdot \phi$ and $k^{(2)} \cdot \phi$, thus, it accounts for phenomena due to the double resonance condition. In fact, in this case the effect of the second resonance is visible even numerically, since in Fig.13a we distinguish a thin chaotic layer intersecting transversally the basic (2:1) the main guiding resonance. Finally, as the orbit continues to move rightwards, the orbit approaches, and eventually enters into the conspicuous doubly-resonant domain at the center of Fig.(13a). Then, the orbit exhibits the most prominent effects due to the double resonance. Such effects can be accounted for by a third choice of expansion center, namely $I_{1*} = 0.4$, $I_{2*} = 0.2$, leading to $k^{(2)} = (2, 1, -1)$ and $|k^{(2)}| = 4$ (while $|k^{(1)}| = 3$ always). We observe that both resonant vectors are now of quite low order. Then, it turns out that the resulting normal form contains always trigonometric terms of both resonant angles $k^{(1)} \cdot \phi$ and $k^{(2)} \cdot \phi$ independently of the value of ϵ. In fact, the so resulting normal form can explain the features of the chaotic

motion within the doubly resonant domain seen e.g. in the example of the orbit of Fig.13a.

b) In the above discussion, we saw that different choices of I_* must be made in order to describe the dynamics locally and in different time intervals, i.e. as the orbit gradually drifts from left to right along the resonance $I_1 - 2I_2 = 0$. However, a question arises: in order that the normal form associated with each choice of I_* provides a valid description for the numerical data set of an orbit, we must guarantee that all data points of the orbit considered are contained within the analyticity domain of the normalized Hamiltonian $H^{(r)}$ around I_*, where r is the maximum normalization order considered in the normal form calculation. The question is how to perform this check. A precise description of the techniques by which we specify the analyticity domains of a normal form construction at successive normalization steps is too technical to be presented here. However, we can mention some basic tools used in such specification (the reader may consult Giorgilli (2002) for a more advanced but still quite pedagogical presentation). Briefly, in order to check that a function $f(\phi, J)$ is analytic in a complexified domain of its arguments

$$\mathcal{W}_{\rho,\sigma} = \{(\phi, J) : J \in \mathbf{C}^n : |J_i| < \rho, \phi \in \mathbf{T}^n_\sigma\}$$

where n is the number of degrees of freedom, we compute the so-called *Fourier-weighted norm*

$$||f(\phi, J)||_{\rho,\sigma} = \sum_k \sup |f_k(J)|_\rho e^{|k|\sigma} \tag{151}$$

were f_k are the coefficients of the Fourier development of $f(\phi, J)$, i.e.

$$f_k(J) = \frac{1}{(2\pi)^n} \int_0^{2\pi} \int_0^{2\pi} \dots \int_0^{2\pi} f(\phi, J) e^{-ik\cdot\phi} d^n\phi$$

and $\sup |\cdot|_\rho$ denotes the supremum of a quantity in the union of the domains $|J_i| < \rho$. The criterion whether the function $f(\phi, J)$ is analytic in a domain $\mathcal{W}_{\rho,\sigma}$ is that Fourier-weighted norm (151) should have a finite upper bound, i.e. $||f(\phi, J)||_{\rho,\sigma} < \infty$.

It is now possible to show that in normal form theory, at every normalization step, the size of the domain of analyticity of both the transformed Hamiltonian and the normalizing transformation series in general *decreases* with respect to the previous step. As a consequence, we have to check that the points of any particular orbit that we intend to study via a normal form continue to remain within the domain of analyticity of these functions at least until a calculation up to the so-called optimal order (see below, and also subsection 2.7), where the normalization can stop. In fact, since at every step we pass from old to new canonical variables, one has to find also the canonical transformations allowing to see how a final domain of analyticity, computed in the new variables, transforms when mapped back to the old variables at which the numerical orbits are computed. Without giving more details, we mention that these tests are necessary ingredients of any study and/or computer-algebraic program in the framework of normal form calculations.

ii) *Resonant module:* After choosing the resonant vectors $k^{(1)}$ and $k^{(2)}$ so that $|k^{(1)}| + |k^{(2)}|$ is minimal, the resonant module can be defined by

$$\mathcal{M} \equiv \left\{ k \in \mathcal{Z}^3 : k \cdot m = 0 \right\} \tag{152}$$

where the vector $m \equiv (m_1, m_2, m_3)$ is defined by the relations

$$m_1 = k_2^{(1)} k_3^{(2)} - k_2^{(2)} k_3^{(1)},\ m_2 = k_3^{(1)} k_1^{(2)} - k_3^{(2)} k_1^{(1)},\ m_3 = k_1^{(1)} k_2^{(2)} - k_1^{(2)} k_2^{(1)}\ . \tag{153}$$

If m_1, m_2, m_3 are not co-prime integers, we re-define m by dividing the m_i by their maximal common divisor. One sees immediately that by the above definition m is a vector parallel to ω_* (m is sometimes called the 'pseudo-frequency' vector).

Action re-scaling and book-keeping: We implement the same action rescaling as in subsection 3.3, namely

$$J_i = \epsilon^{-1/2}(I_i - I_{i*}) = \epsilon^{-1/2} I'_i, \quad i = 1, 2, 3 \tag{154}$$

and work with the Hamiltonian function $h(J, \phi) = \epsilon^{-1/2} H(I_* + \epsilon^{1/2} J, \phi)$ producing the correct equations of motion in the re-scaled action variables. Also, in order to separate the Fourier terms in groups of different order of smallness we use again Eq.(115) rewritten here as

$$K' = \left[-\frac{1}{2\sigma} \ln(\epsilon) \right] \tag{155}$$

to define an average value for K' in the domain of interest for the values of ϵ under consideration.

After all previous steps, we finally implement the book-keeping formula

$$\begin{aligned} h &= \omega_* \cdot J + \lambda \epsilon^{1/2} \sum_{i=1}^{3} \sum_{j=1}^{3} \frac{1}{2} M_{ij*} J_i J_j + \ldots + \sum_k \Bigg(\lambda^{1+[|k|/K']} \epsilon^{1/2} h_{k*} \\ &+ \lambda^{2+[|k|/K']} \epsilon \nabla_I h_k \cdot J + \lambda^{3+[|k|/K']} \frac{\epsilon^{3/2}}{2} \sum_{i=1}^{3} \sum_{j=1}^{3} h_{k,ij*} J_i J_j + \ldots \Bigg) \exp(ik \cdot \phi)\ . \end{aligned} \tag{156}$$

Setting $Z_0 = \omega_* \cdot J$, the Hamiltonian (156) takes the form

$$h = H^{(0)}(J, \phi) = Z_0 + \sum_{s=1}^{\infty} \lambda^s H_s^{(0)}(J, \phi; \epsilon^{1/2}) \tag{157}$$

where the superscript (0) denotes, as usually, the original Hamiltonian, and the functions $H_s^{(0)}$ are given by

$$H_s^{(0)} = \sum_{\mu=1}^{s} \epsilon^{\mu/2} \sum_{k=K'(s-\mu)}^{K'(s-\mu+1)-1} H_{\mu,k}^{(0)}(J) \exp(ik \cdot \phi) \tag{158}$$

where $H^{(0)}_{\mu,k}(J)$ are polynomials containing terms of degree $\mu-1$ or μ in the action variables J. Precisely, we have:

$$H^{(0)}_{\mu,k}(J)=\sum_{\mu_1=0}^{\mu-1}\sum_{\mu_2=0}^{\mu-1-\mu_1}\sum_{\mu_3=0}^{\mu-1-\mu_1-\mu_2}\frac{1}{\mu_1!\mu_2!\mu_3!}\frac{\partial^{\mu-1}h_{1,k}(I_*)}{\partial^{\mu_1}I_1\partial^{\mu_2}I_2\partial^{\mu_3}I_3}J_1^{\mu_1}J_2^{\mu_2}J_3^{\mu_3}$$

if $|k|>0$, or

$$H^{(0)}_{\mu,k}(J)=\sum_{\mu_1=0}^{\mu}\sum_{\mu_2=0}^{\mu-\mu_1}\sum_{\mu_3=0}^{\mu-\mu_1-\mu_2}\frac{1}{\mu_1!\mu_2!\mu_3!}\frac{\partial^{\mu}H_0(I_*)}{\partial^{\mu_1}I_1\partial^{\mu_2}I_2\partial^{\mu_3}I_3}J_1^{\mu_1}J_2^{\mu_2}J_3^{\mu_3}$$

$$+\sum_{\mu_1=0}^{\mu-1}\sum_{\mu_2=0}^{\mu-1-\mu_1}\sum_{\mu_3=0}^{\mu-1-\mu_1-\mu_2}\frac{1}{\mu_1!\mu_2!\mu_3!}\frac{\partial^{\mu-1}h_{1,0}(I_*)}{\partial^{\mu_1}I_1\partial^{\mu_2}I_2\partial^{\mu_3}I_3}J_1^{\mu_1}J_2^{\mu_2}J_3^{\mu_3}$$

if $k=0$.

Hamiltonian normalization: The Hamiltonian normalization is performed by the usual recursive equation:

$$H^{(r)}=\exp(L_{\chi_r})H^{(r-1)} \tag{159}$$

where χ_r is the r-th step generating function defined by the homological equation

$$\{\omega_*\cdot J^{(r)},\chi_r\}+\lambda^r\tilde{H}_r^{(r-1)}(J^{(r)},\phi^{(r)})=0 \tag{160}$$

and $\tilde{H}_r^{(r-1)}(J^{(r)},\phi^{(r)})$ denotes all terms of $H^{(r-1)}$ which do not belong to the resonant module $\mathcal{M}$.

Remainder and optimal normalization order: After r normalization steps, the transformed Hamiltonian $H^{(r)}$ has the form

$$H^{(r)}(\phi,J)=Z^{(r)}(\phi,J;\lambda,\epsilon)+R^{(r)}(\phi,J;\lambda,\epsilon) \tag{161}$$

where $Z^{(r)}(J^{(r)},\phi^{(r)};\lambda,\epsilon)$ and $R^{(r)}(J^{(r)},\phi^{(r)};\lambda,\epsilon)$ are the normal form and the remainder respectively. The normal form is a finite expression which contains terms up to order r in the book-keeping parameter λ, while the remainder is a convergent series containing terms of order λ^{r+1} and beyond.

In a similar way as in subsection 2.7, where we discussed the asymptotic character of the series for the simple model (3), it is now possible to see that the above normalization process has also an asymptotic character. Namely, i) the domain of convergence of the remainder series $R^{(r)}$ shrinks as the normalization order r increases, and ii) the size $||R^{(r)}||$ of $R^{(r)}$, where $||\cdot||$ is a properly defined norm in the space of trigonometric polynomials, initially decreases, as r increases, up to an optimal order r_{opt} beyond which $||R^{(r)}||$ increases with r. In the so-called *Nekhoroshev regime*, one has $||Z^{(r_{opt})}|| >> ||R^{(r_{opt})}||$. Thus, stopping at r_{opt} best unravels the dynamics, which is given essentially by the Hamiltonian flow of $Z^{(r_{opt})}$ slightly perturbed by $R^{(r_{opt})}$.

A basic result, now, of Nekhoroshev theory is that the optimal normalization order r_{opt} depends on ϵ via an inverse power-law namely

$$r_{opt} \sim \epsilon^{-a} \quad , \tag{162}$$

for some positive exponent a. A heuristic derivation of this basic result is given in the Appendix. Taking into account that the leading terms in the remainder are $O(\lambda^{r_{opt}+1})$, while, due to Eq.(155), the book-keeping itself was determined so as to split terms in groups corresponding to powers of the quantity $e^{-\sigma K'} \sim \epsilon^{1/2}$, we conclude that the size of the remainder can be estimated as of order $O(\epsilon^{(r_{opt}+1)/2})$, implying (viz.Eq.(155)):

$$||R^{(r_{opt})}|| \sim \epsilon^{1/2} \exp\left(\frac{-K'\sigma}{\epsilon^a}\right) \tag{163}$$

i.e. *the remainder at the optimal normalization order is exponentially small in* $1/\epsilon$.

The Fourier order

$$K_{opt}(\epsilon) = K' r_{opt}(\epsilon) \tag{164}$$

is called the optimal K–truncation order. All the normal form terms of $H^{(r_{opt})}$ are of Fourier order $0 \leq |k| < K_{opt}(\epsilon)$.

The role of convexity in resonant dynamics

We now examine in detail the dynamics induced by the combined effects of the normal form and of the remainder in the above resonant normal form construction.

To this end, let us recall, first, that the normal form at the optimal normalization order r_{opt} is a function of the new canonical variables $\phi^{(r_{opt})}$,$J^{(r_{opt})}$, which are near-identity transformations of the old canonical variables (ϕ, J). [41] The most important terms in the normalized Hamiltonian are i) the lowest order terms independent of the angles, and ii) the resonant terms, depending on the angles via linear combinations of the resonant arguments $k^{(1)} \cdot \phi^{(r_{opt})}$, or $k^{(2)} \cdot \phi^{(r_{opt})}$. The Hamiltonian takes the form

$$\begin{aligned} h(J^{(r_{opt})}, \phi^{(r_{opt})}) = \omega_* \cdot J^{(r_{opt})} + \epsilon^{1/2} \sum_{i=1}^{3} \sum_{j=1}^{3} \frac{1}{2} M_{ij*} J_i^{(r_{opt})} J_j^{(r_{opt})} + \ldots \\ + \epsilon^{1/2} \sum_{n_1,n_2 \in Z^2} g_{n_1,n_2}(J^{(r_{opt})}) \exp(i(n_1 k^{(1)} + n_2 k^{(2)}) \cdot \phi^{(r_{opt})}) + \ldots \\ + R_{nonres}(J^{(r_{opt})}, \phi^{(r_{opt})}) \quad . \end{aligned} \tag{165}$$

[41] The reader should be reminded at this point of the convention used throughout this tutorial, that was mentioned in subsection 2.4, namely that we drop superscripts of the form (r) from all symbols referring to canonical variables just for the purpose of simplifying notation, bearing, however, in mind, that in any Hamiltonian function denoted as $H^{(r)}(\phi, J)$ the arguments are the transformed variables, i.e. $(\phi, J) \equiv (\phi^{(r)}, J^{(r)})$ after r consecutive normalization steps. Here, however, we restore the original notation because both the original and the transformed variables appear in some formulae.

The term $R_{nonres}(J^{(r_{opt})}, \phi^{(r_{opt})}))$, called the *non-resonant remainder*, contains all terms depending on the angles via combinations different from the resonant ones, i.e. $k^{(1)} \cdot \phi^{(r_{opt})}$, or $k^{(2)} \cdot \phi^{(r_{opt})}$.

As in subsection 3.3, let us introduce, now, resonant canonical action - angle variables. We consider the canonical transformation

$$(J_1^{(r_{opt})}, J_2^{(r_{opt})}, J_3^{(r_{opt})}, \phi_1^{(r_{opt})}, \phi_2^{(r_{opt})}, \phi_3^{(r_{opt})}) \to (J_{R_1}, J_{R_2}, J_F, \phi_{R_1}, \phi_{R_2}, \phi_F)$$

defined by

$$\begin{aligned}
J_1^{(r_{opt})} &= k_1^{(1)} J_{R_1} + k_1^{(2)} J_{R_2} + m_1 J_F \\
J_2^{(r_{opt})} &= k_2^{(1)} J_{R_1} + k_2^{(2)} J_{R_2} + m_2 J_F \\
J_3^{(r_{opt})} &= k_3^{(1)} J_{R_1} + k_3^{(2)} J_{R_2} + m_3 J_F \\
\phi_{R_1} &= k_1^{(1)} \phi_1^{(r_{opt})} + k_2^{(1)} \phi_2^{(r_{opt})} + k_3^{(1)} \phi_3^{(r_{opt})} \\
\phi_{R_2} &= k_1^{(2)} \phi_1^{(r_{opt})} + k_2^{(2)} \phi_2^{(r_{opt})} + k_3^{(2)} \phi_3^{(r_{opt})} \\
\phi_F &= m_1 \phi_1^{(r_{opt})} + m_2 \phi_2^{(r_{opt})} + m_3 \phi_3^{(r_{opt})}
\end{aligned} \tag{166}$$

where $m \equiv (m_1, m_2, m_3)$ has been defined in Eq.(153). The Hamiltonian takes the form

$$\begin{aligned}
&h(J_{R_1}, J_{R_2}, J_F, \phi_{R_1}, \phi_{R_2}) = (\omega_* \cdot m) J_F \\
&+\epsilon^{1/2} \sum_{i,j=1}^{3} \frac{1}{2} M_{ij*} (k_i^{(1)} J_{R_1} + k_i^{(2)} J_{R_2} + m_i J_F)(k_j^{(1)} J_{R_1} + k_j^{(2)} J_{R_2} + m_j J_F) \\
&+\epsilon^{1/2} \sum_{n_1, n_2 \in Z^2} g_{n_1,n_2}(J_{R_1}, J_{R_2}, J_F) \exp(i(n_1 \phi_{R_1} + n_2 \phi_{R_2})) + \dots \\
&+R_{nonres}(J_{R_1}, J_{R_2}, J_F, \phi_{R_1}, \phi_{R_2}) \quad .
\end{aligned} \tag{167}$$

If we neglect the remainder term R_{nonres}, the constant-valued action J_F is an integral of motion of the Hamiltonian flow of (167). On the other hand, the terms

$$\begin{aligned}
&Z_0(J_{R_1}, J_{R_2}; J_F) = (\omega_* \cdot m) J_F \\
&+\epsilon^{1/2} \sum_{i,j=1}^{3} \frac{1}{2} M_{ij*} (k_i^{(1)} J_{R_1} + k_i^{(2)} J_{R_2} + m_i J_F)(k_j^{(1)} J_{R_1} + k_j^{(2)} J_{R_2} + m_j J_F) \\
&+\dots
\end{aligned} \tag{168}$$

define an 'integrable part' of the Hamiltonian (167), while the remaining terms depending on the resonant angles, which are of order at least $\epsilon^{1/2}$, can be considered as a perturbation. It is now possible to show the following: *Due to the convexity conditions satisfied by the original Hamiltonian, the constant energy condition $Z_0 = E_Z$, for various values of E_Z, defines a set of invariant ellipses on the plane of the variables J_{R_1}, J_{R_2}.* Furthermore, it will be shown that *if the effects of the remainder are omitted, any chaotic orbit in the considered resonant*

domain, moving under the normal form Hamiltonian flow alone, stays confined on one ellipse defined for a particular value of E_Z (which remains constant under the normal form dynamics).

This last remark is of crucial importance for understanding the geometric consequences of the convexity condition on the way by which the diffusion of the chaotic orbits proceeds in the action space. In fact, the existence of an invariant ellipse of the normal form Hamiltonian flow (neglecting the remainder effects) prevents the chaotic orbits from diffusing in directions of the action space normal to the ellipse. For instance, when reaching the doubly resonant chaotic domain at the center of Fig.13a, the chaotic orbit appears for a long time to be nearly completely confined along a circular arc. This arc is part of an invariant ellipse of the form $Z_0 = E_Z$ corresponding to the particular resonances into play in this example. In fact, as shown below the orbit can only escape from this type of motion due to remainder effects, as will be shown below. Thus, *the size of the remainder determines the rate at which the diffusion of chaotic orbits can proceed.* This property holds in the neighborhood of every resonance junction in the action space of a system satisfying convexity conditions similar to the one set at the beginning of the present subsection. But since the doubly resonant points are dense in the action space, the entire chaotic motion in the resonance web can be modeled as a sequence of crossings of different resonant junctions, where, in each junction, a local resonant normal form construction can be made leading to a set of invariant ellipses as above.

We now show why the convexity conditions of the original Hamiltonian imply that the relation of the form $Z_0 = E_Z = const$ defines an invariant ellipse in the plane (J_{R_1}, J_{R_2}). This is equivalent to showing that the quadratic form

$$\zeta_{0,2} = \frac{1}{2} \sum_{i,j=1}^{3} M_{ij*}(k_i^{(1)} J_{R_1} + k_i^{(2)} J_{R_2})(k_j^{(1)} J_{R_1} + k_j^{(2)} J_{R_2}) \tag{169}$$

is positive definite. The latter can be written as

$$\zeta_{0,2} = (J_{R_1}, J_{R_2}) \cdot k^{(1,2)} \cdot M_* \cdot (k^{(1,2)})^T \cdot (J_{R_1}, J_{R_2})^T \tag{170}$$

where $k^{(1,2)}$ is a 2×3 matrix whose first and second line are given by $(k_1^{(1)}, k_2^{(1)}, k_3^{(1)})$ and $(k_1^{(2)}, k_2^{(2)}, k_3^{(2)})$ respectively. Since the matrix M_* is real symmetric, it can be written in the form $M_* = X \cdot \mu_* \cdot X^T$, where $\mu_* = diag(\mu_1, \mu_2, \mu_3)$, with $\mu_i =$ the eigenvalues of M_*, while X is an orthogonal matrix with columns equal to the normalized eigenvectors of M_*. Using the above expression for M_*, Eq.(170) resumes the form

$$\zeta_{0,2} = (J_{R_1}, J_{R_2}) \cdot Y \cdot \mu_* \cdot Y^T (J_{R_1}, J_{R_2})^T$$

where $Y = k^{(1,2)} \cdot X$ is a 2×3 matrix. Writing Z_{02} as $Z_{02} = QJ_{R_1}^2 + VJ_{R_1}J_{R_2} + PJ_{R_2}^2$, and denoting by y_{ij} the elements of Y, the discriminant $\Delta = 4QP - V^2$ is given by:

$$\begin{aligned} \Delta &= -[(y_{11}y_{22} - y_{12}y_{21})^2\mu_1\mu_2 + (y_{11}y_{23} - y_{13}y_{21})^2\mu_1\mu_3 \\ &+ (y_{12}y_{23} - y_{13}y_{22})^2\mu_2\mu_3] \ . \end{aligned} \tag{171}$$

However, by the convexity condition assumed at the beginning of this subsection, we have that either all three eigenvalues μ_i have the same sign, or two of them have the same sign and one is zero, by Eq.(171) we have that $\Delta < 0$. That is, the quadratic form $\zeta_{0,2}$ is positive definite.

After demonstrating the geometric consequences of convexity for the chaotic motion along resonances, we now examine separately the chaotic diffusion in the case of *simple resonance*, i.e. when as discussed above, $|k^{(2)}| >> |k^{(1)}|$, and in the case of *double resonance*, i.e. when $|k^{(2)}|$ and $|k^{(1)}|$ are of comparable size.

4.3. Diffusion along simple resonances. Comparison with Chirikov's estimates

In order to implement resonant normal form theory in the case of simply resonant dynamics, we define first local resonant canonical variables around the center of the ellipses $Z_0 = E_Z$, which is given by:

$$\begin{aligned} J_{R_1,0} &= \frac{\left(k^{(1)} \cdot M_* k^{(2)}\right)\left(m \cdot M_* k^{(2)}\right) - \left(k^{(2)} \cdot M_* k^{(2)}\right)\left(m \cdot M_* k^{(1)}\right)}{\left(k^{(1)} \cdot M_* k^{(1)}\right)\left(k^{(2)} \cdot M_* k^{(2)}\right) - \left(k^{(1)} \cdot M_* k^{(2)}\right)^2} J_F \\ J_{R_2,0} &= \frac{\left(k^{(1)} \cdot M_* k^{(2)}\right)\left(m \cdot M_* k^{(1)}\right) - \left(k^{(1)} \cdot M_* k^{(1)}\right)\left(m \cdot M_* k^{(2)}\right)}{\left(k^{(1)} \cdot M_* k^{(1)}\right)\left(k^{(2)} \cdot M_* k^{(2)}\right) - \left(k^{(1)} \cdot M_* k^{(2)}\right)^2} J_F \end{aligned} \tag{172}$$

We then define:

$$\Delta J_{R_i} = J_{R_i} - J_{R_{i,0}}, \quad a_{ij} = k^{(i)} \cdot M_* k^{(j)}, \quad i,j = 1,2 \ .$$

The key remark is that, if we have $|k^{(2)}| >> |k^{(1)}|$, for all values of ϵ of practical interest we also find $|k^{(2)}| > K_{opt}(\epsilon) > |k^{(1)}|$, i.e. *for all values of ϵ of practical interest, all resonant terms containing the angle ϕ_{R_2} are of Fourier order higher than the optimal K–truncation order.* This implies that such terms can be considered as *part of the remainder.* [42]

[42] A concrete example is here in order. Let as consider again, as at the beginning of the previous subsection, the resonant normal form construction for $I_{1*} = 0.355$, $I_{2*} = 0.1775$. We saw that in that case $|k^{(1)}| = 3$, while $|k^{(2)}| = 271$. However, if we roughly set $K_{opt} = K' r_{opt} = K'(\epsilon_0/\epsilon)^a$ (in view of Eq.(163)), then we see that if we take $a = 0.25$ (simple resonance, see Eq.(240)), giving some typical values to K' and ϵ_0, e.g. $K' = 3$, $\epsilon_0 \sim 0.1$ we have $K_{opt} < 10^2$ in the range $10^{-4} \leq \epsilon \leq 10^{-1}$. Thus, in the same range, we have $|k^{(2)}| > K_{opt}$, implying that the construction can be considered simply resonant in practically the entire range of values of ϵ that would be encountered in realistic applications (cf. Table 1). We note also that the latter result is not sensitive to the choice of the constants K' and ϵ_0.

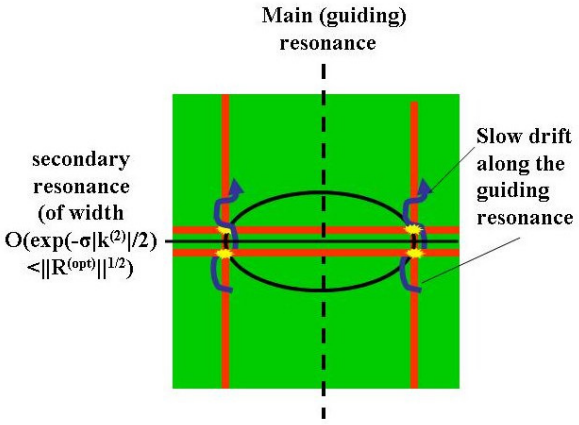

Figure 14. Schematic representation of the diffusion along a simple resonance. Any resonance crossing transversally the main (guiding) resonance has an exponentially small width and acts as a 'driving' resonance for diffusion.

With the above considerations, the transformed Hamiltonian reads:

$$\begin{aligned} h(J^{(r_{opt})},\phi^{(r_{opt})}) &= Z(J^{(r_{opt})},\phi^{(r_{opt})}) + R(J^{(r_{opt})},\phi^{(r_{opt})}) \\ &= \omega_* \cdot J^{(r_{opt})} + \epsilon^{1/2}\sum_{i=1}^{3}\sum_{j=1}^{3}\frac{1}{2}M_{ij*}J_i^{(r_{opt})}J_j^{(r_{opt})} + \dots \\ &+\epsilon^{1/2}\sum_{n\in\mathcal{Z}^*} g_n(J^{(r_{opt})})\exp(i(nk^{(1)}\cdot\phi^{(r_{opt})}) + \dots \\ &+R(J^{(r_{opt})},\phi^{(r_{opt})}) \quad . \end{aligned} \tag{173}$$

Taking into account the canonical transformations (166), after some algebra the Hamiltonian (173) takes the form

$$\begin{aligned} h \;\approx\; & (m\cdot\omega_*)J_F + \epsilon^{1/2}\left[\frac{1}{2}a_{11}\Delta J_{R_1}^2 + a_{12}\Delta J_{R_1}\Delta J_{R_2} + \frac{1}{2}a_{22}\Delta J_{R_2}^2\right. \\ + \;& \left. 2f_{R_1}\cos(\phi_{R_1}) + \dots + \sum_{|k|\geq K^{(opt)}} f_{k*}\exp[ik\cdot(\kappa_1\phi_{R_1}+\kappa_2\phi_{R_2}+\kappa_3\phi_F)] + \dots\right] \end{aligned} \tag{174}$$

where i) the (non-integer) vectors κ_i, $i = 1, 2, 3$ come from the solution of the right set of Eqs.(166) for the angles $\phi_i^{(r_{opt})}$ in terms of the angles ϕ_{R_1}, ϕ_{R_2}, and ϕ_F, and ii) we approximate all the Fourier coefficients in the remainder series by their constant values f_{k*} at the points $\Delta J_{R_1} = \Delta J_{R_2} = 0$ (we set $f_{R_1} = f_{k*}$ for $k = k^{(1)}$).

We note that, neglecting the non diagonal term $a_{12}\Delta J_{R_1}\Delta J_{R_2}$, the Hamiltonian (174) is of the form discussed at the beginning of the present section, i.e. the Hamiltonian (143).

The 'pendulum' part of the above Hamiltonian is given by

$$\begin{aligned} Z_{res} &= \frac{1}{2}a_{11}\Delta J_{R_1}^2 + a_{12}\Delta J_{R_1}\Delta J_{R_2} + \frac{1}{2}a_{22}\Delta J_{R_2}^2 + ... \\ &+ \epsilon^{1/2}\left(g_n e^{in\phi_{R_1}} + g_{-n}e^{-in\phi_{R_1}}\right) + \dots \end{aligned} \tag{175}$$

Since the angle ϕ_{R_2} is ignorable, the action J_{R_2} (or ΔJ_{R_2}) is an integral of the flow of Z_{res}, in addition to J_F. Thus, Z_{res} defines an integrable Hamiltonian. A pair of constant values $J_F = c_1$, $\Delta J_{R_2} = c_2$ defines a straight line

$$\Delta J_{R_1} = -\frac{a_{12}}{a_{11}}c_2 \tag{176}$$

which corresponds to the unique resonance $\omega_{R_1}(J^{(r_{opt})}) = k^{(1)} \cdot \omega(J^{(r_{opt})}) = 0$. This will be called 'main resonance' (= the 'guiding resonance' in Chirikov's theory; see Chirikov (1979), Cincotta (2002)).

In Figure 14 (schematic), the domain of the main resonance is delimited by two vertical thick red lines corresponding to the separatrix-like thin chaotic layers at the boundary of the resonance similarly to Fig.15.

Under the normal form dynamics, motions are allowed only across the resonance, i.e. in the direction $\Delta J_{R_2} = const.$ In Fig.14 this is the horizontal direction. The thin strip delimited by two horizontal red lines corresponds to the resonance with resonant wavevector $k^{(2)}$, which, since $k^{(2)} > K(\epsilon)$, is now of width exponentially small ($O(\epsilon^{1/2}e^{-\sigma|k^{(2)}|/2})$. Thus, it will be called a 'secondary' resonance.

We now ask the following question: since the diffusion along the resonance is only possible because of the remainder influence on dynamics, can we estimate the *speed* of diffusion (or the value of the diffusion coefficient), by knowing the *size of the remainder of the optimal normal form construction*?

We can see that the approximation of Eq.(174) is sufficient for estimates regarding the speed of diffusion. The key remark is that for all the coefficients f_{k*} the bound $|f_{k*}| < ||R_{opt}||$ holds, while, for the leading Fourier term $\exp(ik_l \cdot \phi^{(r_{opt})})$ in the remainder we have $|f_{k_l*}| \sim ||R_{opt}||$. In fact, we typically find that the size of the leading term is larger from the size of the remaining terms by several orders of magnitude, since this term contains a repeated product of small divisors of the form $k_l \cdot \omega_*$ (see Appendix). Furthermore, using an analysis as in Efthymiopoulos et al. (2004), we readily find $|k_l| = (1-d)K_{opt}$, where $0 < d < 1$ is a so-called (in Efthymiopoulos et al. (2004)) 'delay' constant. We note in passing that the Fourier terms of the form $\exp(ik_l \cdot \phi^{(r_{opt})})$ are called 'resonant' in Morbidelli and Giorgilli (1997).

The value of the diffusion coefficient can now be estimated by applying the basic theory of Chirikov (1979). This theory is reviewed for the purpose of applications in dynamical astronomy by Cincotta (2002), and a recent application in the so-called three body resonance problem in solar system dynamics was given in Cachucho et al. (2010). Briefly, the theory uses the Arnold-Melnikov integral technique to estimate the speed of diffusion along simple resonances by examining the so-called variations in the pendulum energy as a chaotic orbit moves in the separatrix-like chaotic layer of a simply resonant domain. It is found that

the following estimate holds for the diffusion coefficient:

$$D \sim \frac{\epsilon}{2\Omega_G^2 T}|f_{k_l *}|^2 A(|\kappa_l|)^2 \quad . \tag{177}$$

In Eq.(177):

i) $\Omega_G = \epsilon^{1/4} f_{R_1}^{1/2}$, where $T = ln(32e/w)/\Omega_G$ is an average period of motion within the main resonance separatrix-like thin chaotic layer, of width w.

ii) A is the *Melnikov function* with argument $|\kappa_l|$ (see Appendix B of Ferraz-Mello (2007)). The vector κ_l is defined by the relation

$$\kappa_{l,1}\phi_{R_1} + \kappa_{l,2}\phi_{R_2} + \kappa_{l,3}\phi_F = k_l \cdot \phi^{(r_{opt})}$$

and the estimate

$$A(|\kappa_l|) \sim 8\pi|\kappa_l|e^{-\pi|\kappa_l|/2}$$

holds.

The key point in connecting Chirikov's formula (177) with the estimates based on the optimal remainder function is that, in view of Eq.(166), we have that

$$|\kappa_l| = O((1-d)K^{(opt)}/|k^{(1)}|) \quad . \tag{178}$$

However, it was pointed out in subsection 4.2 that the optimal K–truncation order K_{opt} depends on ϵ as an inverse power, i.e. we have $K_{opt} \sim \epsilon^{-1/4}$ in simply resonant domains (see Appendix), yielding also $||R_{opt}|| \sim e^{-\sigma K^{(opt)}}$. Substituting these expressions into Eq.(178) it follows that

$$A(|\kappa_l|) \sim \epsilon^{3/4}||R_{opt}||^b$$

for an exponent $b > 0$. Putting, finally, these estimates together in Eq.(177), we arrive at an estimate of the dependence of the diffusion coefficient D on the optimal remainder $||R_{opt}||$ in the case of simple resonances, namely:

$$D \sim \frac{\epsilon}{2\Omega_G^2 T}\epsilon^{3/4}||R_{opt}||^{2(1+b)} \quad . \tag{179}$$

We emphasize that the precise value of b is an open issue, which appears to be hardly tractable to address on the basis exclusively of the behavior of the Melnikov integrals discussed above. We note, however, that the quantity $A(\kappa_l)$ yields the size of the 'splitting' S of the separatrix of the main (guiding) resonance due to the effects of the leading term in the remainder function. The relation between the separatrix splitting and the size of the optimal remainder has been examined in Neishtadt (1984), and later in Morbidelli and Giorgilli (1997). In the latter work, the estimate $S \sim \mu^{1/2}$ was predicted and probed by numerical experiments, where μ (in the notation of Morbidelli and Giorgilli 1997) is the effective size of the perturbation to the normal form pendulum dynamics caused by the remainder. Setting thus $\mu \sim ||R_{opt}||$ suggests the scaling $A(\kappa_l) \sim S \sim ||R_{opt}||^{1/2}$, whereby the constant b can be estimated as $b \simeq 1/2$. Hence (in view of Eq.(179)) we find

$$D \sim ||R_{opt}||^3$$

in simply resonant domains. In Efthymiopoulos (2008) the diffusion coefficient D along a simple resonance was compared directly to the size of the optimal normal form remainder in a concrete example referring to the numerical data reported in the work of Lega et al. (2003). It was found that $D \propto ||R_{opt}||^{2.98}$, essentially confirming that $p = 2(1 + b) \simeq 3$, or $b \simeq 0.5$. However, in Lega et al. (2010a) a different exponent was found $p \simeq 2.56$ regarding the same resonance, while it was found that $p = 2.1$ in the case of a very low order simple resonance (with $|k^{(1)} < K'$). These numerically defined exponents, however, depend on the chosen definition of numerical measure used to estimate both S and $||R_{opt}||$. Thus, a detailed quantitative comparison of the various estimates given in the literature is an open problem.

4.4. Diffusion along double resonances

We now pass to analyzing, via a resonant normal form, the properties of weakly-chaotic diffusion when double resonance condition is fulfilled, the latter being defined by the requirement that $|k^{(2)}| < K_{opt}(\epsilon)$, ensuring that both resonances due to $k^{(1)}$ and $k^{(2)}$ are important.

In order to analyze the normal form dynamics in double resonances, we first write the normal form constant energy condition as:

$$E' = (Z_0 - (\omega_* \cdot m)J_F) = const. \tag{180}$$

If higher order terms in the action variables of the development of Eq.(168) are taken into account, the constant energy condition of Eq.(180) yields deformed ellipses on the plane (J_{R_1}, J_{R_2}). If $J_{R_1} \neq J_{R_{1,0}}$ or $J_{R_2} \neq J_{R_{2,0}}$, we can define two slow frequencies for the resonant angles, namely $\dot{\phi}_{R_1} \equiv \omega_{R_1}$, $\dot{\phi}_{R_2} \equiv \omega_{R_2}$. We have

$$\begin{aligned} \omega_{R_1} &= \left(k^{(1)} \cdot M_* k^{(1)}\right)(J_{R_1} - J_{R_{1,0}}) + \left(k^{(1)} \cdot M_* k^{(2)}\right)(J_{R_2} - J_{R_{2,0}}) + \ldots \\ \omega_{R_2} &= \left(k^{(1)} \cdot M_* k^{(2)}\right)(J_{R_1} - J_{R_{1,0}}) + \left(k^{(2)} \cdot M_* k^{(2)}\right)(J_{R_2} - J_{R_{2,0}}) + \ldots \end{aligned} \tag{181}$$

On the other hand, due to the definition (166) one has

$$\omega_{R_1} = k^{(1)} \cdot \omega(J^{(r_{opt})}), \quad \omega_{R_2} = k^{(2)} \cdot \omega(J^{(r_{opt})}), \quad \omega_F = m \cdot \omega(J^{(r_{opt})})$$

which is valid for any value of (J_{R_1}, J_{R_2}, J_F) in the domain of convergence of the series (168). It follows that all the resonant manifolds defined by relations of the form $(n_1 k^{(1)} + n_2 k^{(2)}) \cdot \omega(J^{(r_{opt})}) = 0$ intersect any of the planes (J_{R_1}, J_{R_2}) corresponding to a fixed value of J_F. Using again the notation

$$\Delta J_{R_i} = J_{R_i} - J_{R_{i,0}}, \quad a_{ij} = k^{(i)} \cdot M_* k^{(j)}, \quad i, j = 1, 2$$

the intersection of one resonant manifold with the plane (J_{R_1}, J_{R_2}) is a curve given, in the linear approximation, by

$$(n_1 a_{11} + n_2 a_{12})\Delta J_{R_1} + (n_1 a_{12} + n_2 a_{22})\Delta J_{R_2} + \ldots = 0 \quad .$$

The above equation defines a 'resonant line', which is the local linear approximation to a 'resonant curve'. All resonant lines (or curves) pass through the point $(J_{R_{1,0}}, J_{R_{2,0}})$, which, therefore, belongs to the resonant junction defined by the wavevectors $k^{(1)}, k^{(2)}$. To each resonant curve we can associate a resonant strip in action space whose width is proportional to the separatrix width for that resonance. If, for a single pair of integers (n_1, n_2), we only isolate the resonant terms $g_{\pm n_1,\pm n_2} e^{\pm i(n_1\phi_{R_1}+n_2\phi_{R_2})}$ in the normal form Z (Eq.(165)), we obtain a simplified resonant normal form $Z_{res(n_1,n_2)}$ corresponding to the limiting case of a single resonance. In a strict sense, Z_{res} describes well the dynamics far from the resonant junction. However, it can also be used in order to obtain estimates of the resonance width along the whole resonant curve defined by the integer pair (n_1, n_2). To this end, the leading terms of $Z_{res(n_1,n_2)}$ are (apart from constants):

$$\begin{aligned} Z_{res(n_1,n_2)} &= \epsilon^{1/2}\Bigg[\frac{1}{2}a_{11}\Delta J_{R_1}^2 + a_{12}\Delta J_{R_1}\Delta J_{R_2} + \frac{1}{2}a_{22}\Delta J_{R_2}^2 + ... \qquad (182)\\ &+ \left(g_{n_1,n_2}e^{i(n_1\phi_{R_1}+n_2\phi_{R_2})} + g_{-n_1,-n_2}e^{-i(n_1\phi_{R_1}+n_2\phi_{R_2})}\right)\Bigg] + \dots \end{aligned}$$

The coefficients $g_{\pm n_1,\pm n_2}$ satisfy the estimate

$$|g_{n_1,n_2}| \approx A e^{-(|n_1||k^{(1)}|+|n_2||k^{(2)}|)\sigma} \quad . \qquad (183)$$

After still another transformation $\Delta J_{R_1} = n_1 J_R + n_2 J_F$, $\Delta J_{R_2} = n_2 J_R - n_1 J_F$, $\phi_R = n_1\phi_{R_1} + n_2\phi_{R_2}$, J_F becomes a second integral of motion of $Z_{res(n_1,n_2)}$, which takes the form

$$\begin{aligned} Z_{res(n_1,n_2)} &= \epsilon^{1/2}\Bigg[c(J_F) - \frac{1}{2}(a_{11}n_{11}^2 + 2a_{12}n_1n_2 + a_{22}n_2^2)(J_R - J_{R,0}(J_F))^2\\ &+ \left(g_{n_1,n_2}e^{i\phi_R} + g_{-n_1,-n_2}e^{-i\phi_R}\right) + \dots\Bigg] \qquad (184) \end{aligned}$$

where $c(J_F)$ and $J_{R,0}(J_F)$ are constants of the Hamiltonian flow of (184). Combining (183) and (184), the separatrix width can be estimated as

$$\Delta J_R \approx \sqrt{\frac{32Ae^{-(|n_1||k^{(1)}|+|n_2||k^{(2)}|)\sigma}}{a_{11}n_{11}^2 + 2a_{12}n_1n_2 + a_{22}n_2^2}} \quad . \qquad (185)$$

Eq.(185) allows to estimate the width of a resonant strip in the direction normal to a resonant curve on the plane (J_{R_1}, J_{R_2}). Using the relations $\Delta(\Delta J_{R_i}) = n_i\Delta J_R$ (for $\Delta J_F = 0$), this estimate takes the form

$$\Delta J_{R,width} =\approx \left(\frac{32A(n_1^2+n_2^2)}{a_{11}n_{11}^2 + 2a_{12}n_1n_2 + a_{22}n_2^2}\right)^{1/2} e^{-\frac{1}{2}(|n_1||k^{(1)}|+|n_2||k^{(2)}|)\sigma} \quad . \qquad (186)$$

The outcome of the above analysis can be visualized with the help of Figure 15 (schematic). The left panel shows the structure of a doubly-resonant domain

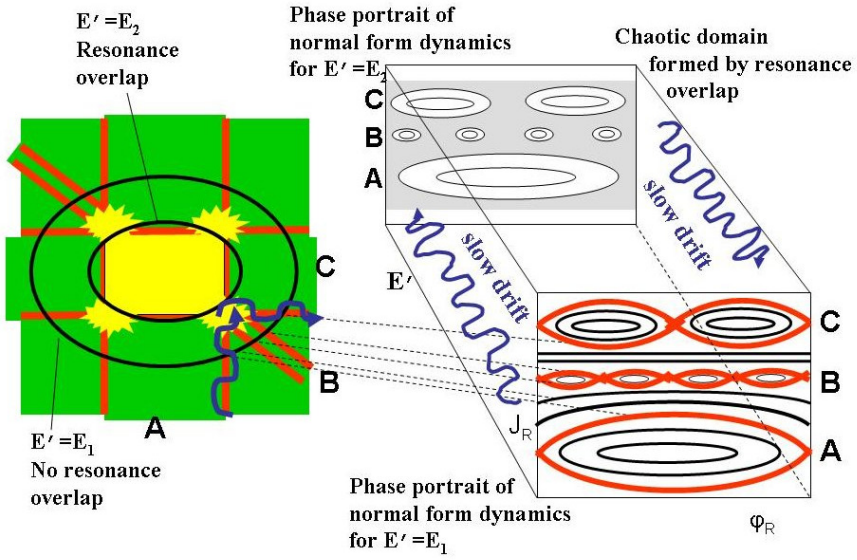

Figure 15. Schematic representation of the normal form and remainder dynamics in a domain of double resonance. Left panel: the resonant structure formed in the action plane of the variables (J_{R_1}, J_{R_2}) by the overlapping of various resonant strips whose limits (pairs of parallel red lines) correspond to separatrix-like thin chaotic domains around each resonance. Two constant normal form energy ellipses $E' = E_1$ and $E' = E_2$ are also shown. Right: The front and back panels show the phase portraits corresponding to a surface of section (in one of the pairs (ϕ_{R_1}, J_{R_1}) or (ϕ_{R_2}, J_{R_2})) under the normal form dynamics alone, for the energies $E' = E_1$ (front panel) and $E' = E_2$ (back panel). The blue curly arrows in both panels indicate the directions of a possible 'drift' motion (=slow change of the value of E') due to the influence of the remainder on dynamics.

in the plane of the resonant action variables (J_{R_1}, J_{R_2}). The two bold ellipses correspond to the constant energy condition for two different values of E', namely $E' = E_1$ and $E' = E_2$ with $E_1 > E_2$. Their common center is the point $(J_{R_{1,0}}, J_{R_{2,0}})$ defined in Eq.(172). The three pairs of parallel red lines depict the borders of the separatrix-like thin chaotic layers of three resonances passing through the center. Infinitely many such resonances exist, corresponding to different choices of integer vectors $n \equiv (n_1, n_2)$; however, their width decreases as $|n|$ increases, according to Eq.(186). We thus show schematically only three resonances with a relatively low value of $|n|$, named by the letters 'A', 'B' and 'C'.

With the help of Figure 15, the influence of the normal form terms on dynamics, by considering the Hamiltonian flow under the approximation $H \simeq Z$, can now be understood as follows:

- For any fixed value of E', and a fixed section in the angles, the motion is confined on one ellipse.

- For E' large enough ($E' = E_1$, outermost ellipse in the left panel of Fig.15), the various resonant strips intersect the ellipse $E' = E_1$ at well distinct arcs, i.e. there is no resonance overlap. The right front panel in Fig.15 shows schematically the expected phase portrait, which can be obtained by evaluating an appropriate Poincaré surface of section, e.g. in the variables (J_{R_1}, ϕ_{R_1}) or (J_{R_2}, ϕ_{R_2}). The dashed lines show the correspondence between the limits of various resonant domains depicted in the left and right panels. In particular, the intersection of each resonant strip in the left panel with the ellipse $E' = E_1$ corresponds to the appearance of an associated *island chain* in the right panel. The size of islands is given essentially by the separatrix width estimate of Eq.(186). Hence, the size of the islands decreases exponentially with the order of the resonance $n = |n_1| + |n_2|$. However, the main effect to note is that, since all resonant strips are well separated on the ellipse, the thin separatrix-like chaotic layers marking the borders of each of their respective island chains do not overlap. As a result the local chaos around one resonance is isolated from the local chaos around the other resonances. In fact, the normal form dynamics induces the presence of rotational KAM tori which, in this approximation ($H \simeq Z$), completely obstruct the communication among the resonances.

- While the size of the islands is nearly independent of the energy E', their separation is reduced as the energy *decreases*. Thus, below a critical energy E'_c, significant resonance overlap takes place, leading to the communication of the chaotic layers of the various resonances and an overall increase of chaos. This is shown in the left panel of Fig.15 for an ellipse $E' = E_2 < E'_c$, with the corresponding phase portrait shown in the right back panel. We note in particular the 'melting' of all three resonant domains one into the other, which produces a large connected chaotic domain surrounding all three island chains (and many other smaller chains, not visible in this scale).

The value of the critical energy E'_c marking the onset of large scale resonance overlap can be estimated as follows: Each resonant strip intersects one fixed energy ellipse on one arc segment. Also, Eq.(186) can be replaced by the estimate

$$\Delta J_{R,width} \approx \frac{(32A)^{1/2}}{M_h k_{1,2}} e^{-\frac{1}{2} n k_{1,2} \sigma} \tag{187}$$

where $n = |n_1| + |n_2|$, $k_{1,2} = (|k^{(1)}| + |k^{(2)}|)/2$, and M_h is a measure of the size of the eigenvalues of the Hessian matrix M_*. The total length S_{res} of all segments can be now estimated by summing, for all n, the estimate (187), namely

$$S_{res} \approx \frac{(32A)^{1/2}}{M_h k_{1,2}} \sum_{n=1}^{\infty} e^{-\frac{1}{2} n k_{1,2} \sigma} \approx \frac{(128A)^{1/2}}{M_h k_{1,2} \sigma} e^{-\frac{1}{2} k_{1,2} \sigma} \quad . \tag{188}$$

On the other hand, the total circumference of the ellipse for the energy E' is estimated as $S_{E'} = \pi R(E')^2$ where $R(E')$ is the geometric mean of the ellipse's major and minor semi-axes. For $R(E')$ one has the obvious estimate $R(E') \sim (2E'/(\epsilon^{1/2} M_h))^{1/2}$, whence

$$S_{E'} \sim \frac{2\pi E'}{\epsilon^{1/2} M_h} \quad . \tag{189}$$

The critical energy $E' = E'_c$ can now be estimated as the value where $S(E') \approx S_{res}$, implying that the associated ellipse is fully covered by segments of resonant strips. Thus

$$E'_c \approx \frac{32(\epsilon A)^{1/2}}{\pi k_{1,2}\sigma} e^{-\frac{1}{2}k_{1,2}\sigma} \quad . \tag{190}$$

Eq.(190) implies that E'_c is a $O(\epsilon^{1/2} e^{-\frac{1}{2}k_{1,2}\sigma})$ quantity.

So far, we have neglected the role of the remainder in dynamics. In Fig.15, the drift in action space caused by the remainder is shown schematically by the blue curly curves in both the left and right panels. Their significance is the following: The energy $E = h$ corresponding to the total Hamiltonian $h = Z + R^{(r_{opt})}$ of Eq.(227) is an exactly preserved quantity. Thus, the doubly-resonant normal form energy E' as well as J_F cannot be preserved exactly, but they are approximate integrals, i.e. they undergo time variations bounded by an $O(||R^{(r_{opt})}||)$ quantity. In Fig.15, such variations will in general lead to a very slow change of the value of E', i.e. a very slow drift of the chaotic orbits from one ellipse to another. We seek to estimate the time required for the remainder to induce a transition between two ellipses with an energy difference of the same order as E'_c, namely

$$E'_2 - E'_1 = O(\epsilon^{1/2} e^{-\frac{1}{2}k_{1,2}\sigma}) \tag{191}$$

assuming that this effect can be described as a *random walk* in the value of E'. Let T be an average period of the oscillations of the resonant variables. By Eqs.(182) and (183), the estimate $T \sim (\epsilon A)^{-1/2} e^{n_{eff} k_{1,2}\sigma/2}$ holds, for a constant $n_{eff} \sim 1$ marking the order of the most important resonances in (182). In consecutive steps, dE' can be either positive or negative, while its typical size is $|dE'| \sim ||R_{opt}||$. Then, after N steps of a random walk (in the values of E'), we find an rms spread of these values given by

$$\Delta E \approx N^{1/2} ||R_{opt}|| \tag{192}$$

Using (191) and (192), the number of steps required for the spread ΔE to become equal to $E'_2 - E'_1$ (given by (191) is $N \sim \epsilon e^{-n_{eff} k_{1,2}\sigma} ||R_{opt}||^{-2}$. The diffusion coefficient can be estimated as

$$D \sim \frac{\Delta E^2}{NT} \sim \left(\epsilon A e^{-n_{eff} k_{1,2}\sigma}\right)^{1/2} ||R_{opt}||^2 \tag{193}$$

i.e. the diffusion coefficient scales as the square of the size of the optimal remainder function.

Visualization of Arnold diffusion using normal forms

The possibility to use the resonant variables (ϕ_{R_1}, J_{R_1}), as well as the normal form energy E' in order to study the phenomenon of Arnold diffusion in systems satisfying the necessary conditions for the holding of the Nekhoroshev theorem, was first pointed out in the work of Benettin and Gallavotti (1986). Recently, however, it has become possible to obtain *real* (non-schematic) examples of this visualization, by computing a doubly-resonant normal form at a quite high order. More precisely, in Efthymiopoulos and Harsoula (2012) we have given a detailed

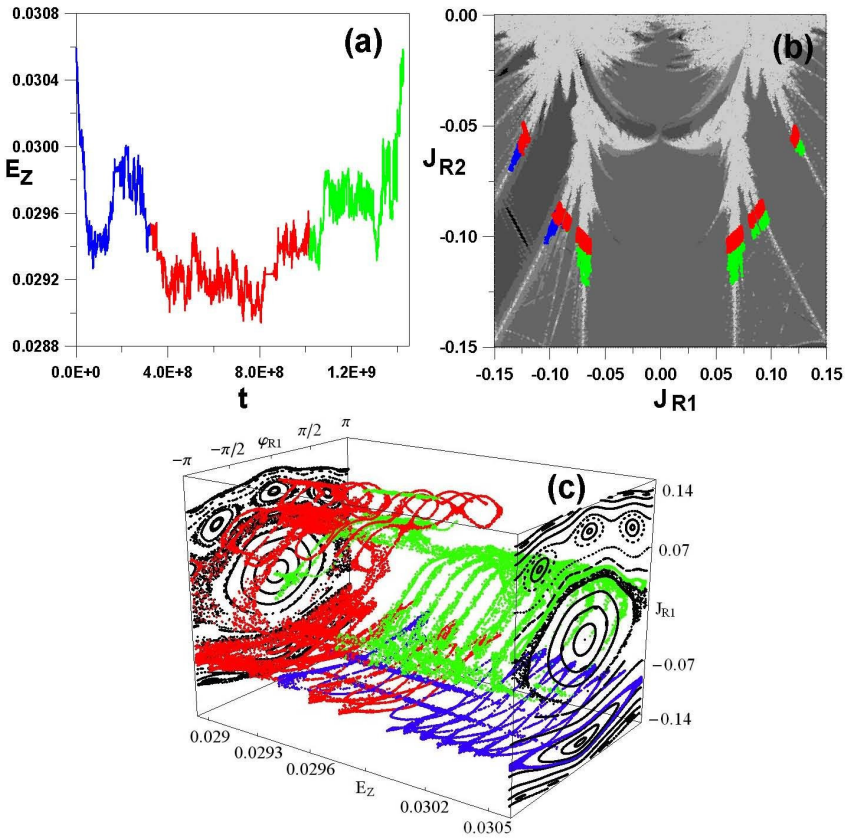

Figure 16. Visualization of Arnold diffusion in a numerical example of high-order doubly resonant normal form computation in the Hamiltonian model (141) (After Efthymiopoulos and Harsoula (2012), see text for details).

numerical example of the above, using the Hamiltonian model (141) in the case of the double resonance defined by $I_{1*} = 0.4$, $I_{2*} = 0.2$. Figure 16 shows the visualization of Arnold diffusion in the above model in appropriate variables of the doubly-resonant normal form, for a numerical orbit in the Hamiltonian (141) for $\epsilon = 0.008$. After computing the optimal normal form, we find, via the Lie canonical transformations, the values of all transformed variables $J_{R_1}(t), J_{R_2}(t), J_F(t)$ and $\phi_{R_1}(t), \phi_{R_2}(t), \phi_F(t)$ corresponding to particular values of the old variables $J_1(t), J_2(t), J_3(t)$ and $\phi_1(t), \phi_2(t), \phi_3(t)$ stored at many different times t within an interval $0 \leq t \leq 1.5 \times 10^9$ along the numerical run. Using the numerical values of the computed transformed variables, (a) shows the variation of the normal form energy $E_Z(t)$ as a function of t in the intervals $0 \leq t \leq 3 \times 10^8$ (blue), $3 \times 10^8 \leq t \leq 10^9$ (red), and $10^9 \leq t \leq 1.5 \times 10^9$ (green). The initial and final values are equal to $E_Z(t = 0) = E_Z(t = 1.5 \times 10^9) = 0.0306$, while the minimum value, occurring around $t = 8 \times 10^8$ is $E_Z = 0.029$. On the other hand, the evolution of the orbit in the action space (J_{R_1}, J_{R_2}), using the same colors as in Fig.16a for the corresponding time intervals, is shown in Fig.16b. In the first time interval (blue), the orbit wanders in the thin chaotic layer of the resonance $\omega_1 + 3\omega_2 - \omega_3 = 0$. In the second time interval (red) it jumps first to the resonance $3\omega_1 - \omega_2 - \omega_3 = 0$, and then to the resonance $\omega_1 - 2\omega_2 = 0$. In the third time interval (green) the orbit recedes from the doubly-resonant domain along the resonance $\omega_1 - 2\omega_2 = 0$.

The main result, now, is shown in Fig.16c representing a 3D plot in the variables $(\phi_{R_1}, J_{R_1}, E_Z)$, which visualizes Arnold diffusion for the same orbit. Taking 20 equidistant values of $E_{Z,i}$, $i = 1, 2, \ldots 20$ in the interval $0.029 \leq E_Z \leq 0.0306$, we first find the times t_i in the interval $0 \leq t \leq 9 \times 10^8$ when the normal form energy value $E_Z(t)$ of the numerical orbit approaches closest to the values $E_{Z,i}$. For each i, starting with the momentary values of all resonant variables at t_i, we then compute 1000 Poincaré consequents of the normal form flow on a surface of section defined by $(\phi_2 mod 2\pi) = 0$. The same procedure is repeated in a second interval $9 \times 10^8 \leq t \leq 1.5 \times 10^9$. As a net result, the orbit at the beginning and end of the calculation is found on the same section (corresponding to $E_Z = 0.0306$), but in a different resonant layer, having bypassed the barriers (invariant tori of the normal form dynamics) via a third dimension (here parameterized by the time-varying value of E_Z).

As an overall conclusion, we see that high order normal form calculations lead to practically useful results, i.e. the possibility to obtain good canonical variables in which the phenomenon of Arnold diffusion can be conveniently studied, but also visualized. In fact, the use of good canonical variables obtained via a normal form is crucial for a proper study of all main structures of the phase space that play a role in diffusion phenomena. Such structures are, for example, the unstable periodic orbits of the normal form flow, whose asymptotic manifolds (and their heteroclinic intersections) have been conjectured to provide the mechanism by which the diffusion progresses over the entire Arnold web.

4.5. Arnold's example and its relation to normal forms

We close this section with some reference to the fundamental work of Arnold (1964), in which the topological features of diffusion along resonances in systems of three degrees of freedom were first discussed. The Hamiltonian model

considered by Arnold has the form:

$$H = \frac{I_1^2}{2} + \epsilon(\cos\phi_1 - 1) + \frac{I_2^2}{2} + \mu(\cos\phi_1 - 1)(\sin\phi_2 + \cos t) \quad . \tag{194}$$

A review of the properties of this model is given in Lega et al. (2008). Notice in particular Fig.2.1 of that review, showing a chain of the invariant manifolds corresponding to a set of *foliated pendula* along the axis I_2, for $\mu = 0$. Using Melnikov's theory, when $\mu \neq 0$, Arnold demonstrates that there are heteroclinic connections between the stable and unstable manifolds (called 'whiskers') of the chain of unstable 2D tori existing for different values of I_2. These connections can then cause long excursions of the chaotic orbits along the I_2 axis, even if ϵ is infinitesimally small.

We now show that the motivation for choosing a Hamiltonian model of the form (194) for the study of Arnold diffusion stems from a similarity with the optimal Hamiltonian arising in resonant normal form theory developed in the previous subsections. In fact, one can see that Arnold's model is a simplified version of the *simply-resonant* normal form (174). A comparison of the Hamiltonians (174) and (194) shows that the action angle pair (I_1, ϕ_1) in Arnold's model corresponds to the resonant pair $(\Delta J_{R_1}, \phi_{R_1})$ in the Hamiltonian (174), while I_2 corresponds to action ΔJ_{R_2}. Finally, the time t in Arnold's model corresponds to the angle ϕ_F in the Hamiltonian (174), since, neglecting the appearance of J_F in the remainder of Eq.(174), the angle ϕ_F varies essentially linearly in time and independently of the initial datum, i.e. we have $\phi_F = (m \cdot \omega)t$.

Finally, we notice that the term $\mu(\cos\phi_1 - 1)(\sin\phi_2 + \cos t)$ in Arnold's model provides a simplified model for the *remainder term* $R(\Delta J_{R_1}, \Delta J_{R_2}, J_F, \phi_{R_1}, \phi_{R_2}, \phi_F)$ in the Hamiltonian (174). It follows that *the parameter μ in Arnold's model (194) should have a value reflecting the size of the optimal remainder in a generic simply resonant normal form construction* of the type discussed in subsections 3.3 to 3.5.

However, at this point, precisely, lies the difficulty in generalizing Arnold's results in a generic Hamiltonian of the type considered above. The difficulty is the following: in Arnold's example, the possibility to implement Melnikov's theory in order to establish the existence of the whiskers' heteroclinic intersections referred to above is based on the fact that *the parameter μ is allowed to vary independently of the parameter ϵ*. However, in a generic model, *the optimal remainder size depends on* ϵ, i.e. one should consider a model in which $\mu \sim ||R_{opt}(\epsilon)||$. This is a theoretical difficulty, due to which a demonstration of Arnold's result in more general Hamiltonian systems of three degrees of freedom still remains an important open problem of Hamiltonian dynamical systems' theory.

5. HAMILTONIAN FORMALISM FOR BASIC SYSTEMS IN DYNAMICAL ASTRONOMY

In the present section, we present some basic Hamiltonian models in action - angle variables which find applications in the two main fields of dynamical astronomy, namely celestial mechanics and galactic (or stellar) dynamics. In every case considered, we give the basic starting formulae as well as some hints on how

to implement book-keeping in these models. Finally, in subsection 5.4 we present a 'case study', i.e. the resonant theory at the Inner Lindblad Resonance in spiral galaxies. In fact, using a technique analogous to the one used in subsection 3.3, in order to locate the position of a periodic orbit in this resonance, we are lead to a main conclusion regarding the orientation of these periodic orbits, which forms the basis for the orbital version of the so-called density wave theory of spiral structure in galaxies.

5.1. Action - angle variables in the restricted three body problem. The Hamiltonian at mean motion resonances

A basic formalism of Celestial Mechanics regards the derivation of a Hamiltonian function in action-angle variables describing the so-called *restricted three body problem* (RTBP). This refers to the dynamics of a small body (e.g. an asteroid or a small planet) under the combined gravitational effects of a star (Sun) and a giant planet (Jupiter) in orbit around the star. In fact, various extensions of this formalism (also to more than three bodies) can be used to study problems of greater complexity, such as the stability of planetary and/or satellite systems.

The definition of action angle variables in Hamiltonian models of Celestial Mechanics is based on the use of the so-called *elements* (of a Keplerian elliptic orbit). The elements are quantities allowing to fit the instantaneous motion of a test particle to a temporary ellipse, which is the ellipse that the particle would constantly move on if, at a certain time t, all interactions except for the one with the central star were instantaneously 'turned off'. Since in the real problem, however, these interactions always exist, it is the values of the elements that change in time, i.e. the elements are *osculating*. However, in many cases the use of canonical perturbation theory allows one to define approximate action integrals for the Hamiltonian under study. These are quite useful, since they serve as labels for the motions of small bodies in the solar system. Such integrals are called *proper elements* (see e.g. Milani and Knežević (1990), Knežević et al. (2002)). Their computation for an extended catalogue of minor bodies has been a central subject in studies of asteroidal dynamics, since they allow to identify the so-called *families* of asteroids, i.e. present-day groups of asteroids which are assumed to have originated from one bigger body through, e.g., some past collision event. Finally, the diffusion of such bodies in the action space, i.e. the space of proper elements, allows one to deduce information on the history, or even the *chronology* of a family (Milani and Farinella (1994), Nesvorny et al. (2002, 2003), Tsiganis et al. (2007)). In fact, the study of the long-term evolution of the various asteroidal zones (like the main or Kuiper's belt in our solar system) provides clues to restructuring *the history of the solar system itself*, and it is a quite modern subject of study (see, for example, Knežević and Milani 2005, Lazzaro et al. 2006).

The derivation of the Hamiltonian formulation of the RTBP is a classical topic discussed in all books of Celestial Mechanics (see, for example, Murray and Dermott (1999), Morbidelli (2002), or Ferraz-Mello (2007) for some modern expositions). Here, we only give some basic formulae, in order to demonstrate that this formalism is amenable to the usual book-keeping approach discussed in sections 3.1 and 3.2 for analytic Hamiltonian systems containing a perturbation with infinitely many Fourier harmonics.

The starting formula for the description of a test particle's motion in the combined gravitational potential of a star of mass M and a planet of mass m moving around the star is

$$H = \frac{\mathbf{p}^2}{2} - \frac{GM}{r} - Gm\left(\frac{1}{|\mathbf{r}-\mathbf{r}'|} - \frac{\mathbf{r}\cdot\mathbf{r}'}{\mathbf{r}'^{\mathbf{3}}}\right) \tag{195}$$

where $\mathbf{p}$ is the momentum per unit mass, $\mathbf{r}$, $\mathbf{r}'$ are the positions of the test body and of the planet respectively in a fixed heliocentric (=centered around the star) system of reference, r is the modulus of $\mathbf{r}$, and G is Newton's gravitational constant. In this formula, the terms $-GM/r$ and $-Gm/|\mathbf{r}-\mathbf{r}'|$ give the contribution to the gravitational potential due to the star and to the planet respectively. On the other hand, the term $-Gm\mathbf{r}\cdot\mathbf{r}'/\mathbf{r}'^{\mathbf{3}}$ describes the effects caused by considering a frame of reference is fixed on the star, which, however, itself moves around the common barycenter of the star-planet system.

The elements are now defined as follows: we consider a fixed Cartesian frame (x, y, z) with origin on the star, as well as the plane of the temporary ellipse along which on which the test body would constantly move in the Keplerian approximation (i.e. if $m = 0$ in Eq.(195)). The plane of the ellipse intersects the plane (x, y) along a line. This is called *line of nodes*. The nodes (ascending and descending) are the points where the ellipse intersects the line of nodes. The oriented angle Ω between the positive direction of the x-axis and the direction of the line of nodes pointing to the ascending node, is called the *longitude of the nodes*. The angle ω formed between the direction of the ascending node and a line starting from the origin and directed to the perihelion of the ellipse is called *argument of the perihelion*, while the angle $\varpi = \omega + \Omega$ is called *longitude of the perihelion*. Finally, the angle u formed between the direction from the origin to the perihelion and the direction pointing to the actual position of the moving testing particle on the ellipse is called *true anomaly*, while the angle $M = n(t - t_0)$, where $n = 2\pi/T$ is the *mean motion* frequency corresponding to the period T of motion on the ellipse, and t_0 is a time when the test body passes from the perihelion, is called the *mean anomaly*. We define also the *mean longitude* $\lambda = \varpi + M$. The relation allowing to pass from the true to the mean anomaly is:

$$\begin{aligned} \cos(u) &= \frac{2(1-e^2)}{e}\left(\sum_{\nu=1}^{\infty} J_\nu(\nu e)\cos(\nu M)\right) - e \\ \sin(u) &= 2\sqrt{1-e^2}\sum_{\nu=1}^{\infty}\frac{1}{2}[J_{\nu-1}(\nu e) - J_{\nu+1}(\nu e)]\sin(\nu M) \end{aligned} \tag{196}$$

where J_ν are Bessel functions, while e is the *eccentricity* of the ellipse defined by $(1-e)/(1+e) = r_p/r_a$, where r_p/r_a is the ratio of the distances to the perihelion and to the aphelion. On the other hand, the distance from the origin to the test body is given by:

$$r = a\left(1 + \frac{e^2}{2} - 2e\sum_{\nu=1}^{\infty}\frac{[J_{\nu-1}(\nu e) - J_{\nu+1}(\nu e)]\cos(\nu M)}{2\nu}\right) \tag{197}$$

where a is the *major semi-axis* of the ellipse, [43] i.e. the distance from the center of the ellipse to the aphelion. The set of elements is completed by the *inclination* i, i.e the angle formed between the plane (x, y) and the plane of the ellipse.

The set of *modified Delaunay action-angle variables* (Λ, Γ, Z) (actions) and (λ, γ, ζ) (angles) is now defined by:

$$\begin{aligned} \Lambda &= \sqrt{(1-\mu)a}, & \lambda \\ \Gamma &= \sqrt{(1-\mu)a}(1-\sqrt{1-e^2}), & \gamma = -\varpi \\ Z &= \sqrt{(1-\mu)a}(1-\sqrt{1-e^2})(1-\cos i), & \zeta = -\Omega \end{aligned} \tag{198}$$

where $\mu = m/M$ is the *mass parameter*. The action variables (Λ, Γ, Z) are a measure of the major semi-axis, the eccentricity and the inclination respectively.

In order to find the form of the Hamiltonian (195) in the modified Delaunay action-angle variables, we use Eqs.(196), (197), (198) for the test body and for the perturbing planet, as well as an equation relating the angle ϕ between the position vectors $\mathbf{r}$ and $\mathbf{r}'$, namely

$$\cos(\phi) = (u - u' + \varpi - \varpi') \quad .$$

After all substitutions in Eq.(195), and a number of algebraic manipulations (described in every detail, e.g. in Murray and Dermott (1999)), we arrive at:

$$H = -\frac{(1-\mu)^2}{2\Lambda^2} + n'\Lambda' - \mu R(\Lambda, \Gamma, Z, \lambda, \gamma, \zeta; a', e', i', \lambda', \gamma', \zeta') \tag{199}$$

where the function R is called the *disturbing function* of the RTBP and n' is the mean motion of the disturbing planet.

The form of the disturbing function, as well as the question of the existence of efficient methods to compute its coefficients, is a classical subject in Celestial Mechanics. Briefly, the disturbing function has the form

$$\begin{aligned} R &= \sum_{k_1,k_1',k_2,k_2',k_3,k_3'} \Big(R_{k_1,k_1',k_2,k_2',k_3,k_3'}(\Lambda, \Gamma, Z; a', e', i') \\ &\times \cos(k_1\lambda + k_1'\lambda' + k_2\gamma + k_2'\gamma' + k_3\zeta + k_3'\zeta') \Big) \end{aligned} \tag{200}$$

where the integers $(k_1, k_1', k_2, k_2', k_3, k_3')$ satisfy the following so-called *D'Alembert rules*: i) k_3, k_3' are even, and ii) $k_1 + k_1' + k_2 + k_2' + k_3 + k_3' = 0$. Furthermore, we have that the coefficient $R_{k_1,k_1',k_2,k_2',k_3,k_3'}$ is of the form:

$$\begin{aligned} &R_{k_1,k_1',k_2,k_2',k_3,k_3'}(\Lambda, \Gamma, Z; a', e', i') = \\ &\sum_{s_2 \geq |k_2|, s_2' \geq |k_2'|, s_3 \geq |k_3|, s_3' \geq |k_3'|} Y(\Lambda; a')\Gamma^{s_2/2}(e')^{s_2'} Z^{s_3/2}(i')^{s_3'} \end{aligned} \tag{201}$$

[43] Called, sometimes, also 'semi-major axis'. But an axis of an ellipse cannot be 'semi-major', either it is the major or the minor one.

where the coefficients $Y(\Lambda; a')$ are determined in terms of the so-called *Laplace coefficients* (see Murray and Dermott 1999).

A case of particular interest that can be studied with the help of the Hamiltonian model (199) is the case of *mean motion resonance* (MMR). This refers to a resonance between the periods T, T', or the mean motions $n = 2\pi/T$, $n' = 2\pi/T'$ of an asteroid and of Jupiter respectively. The main elements of dynamics in mean motion resonances are reviewed e.g. in Tsiganis (2008). The basic formulae are as follows: If we consider an asteroid moving on a Keplerian ellipse, according to third Kepler's law we have a mean motion resonance

$$kn - (k+q)n' = 0 \tag{202}$$

with k, q positive integers when the asteroid's ellipse has major semi-axis:

$$a_{k,q} = a' \left(\frac{k}{k+q} \right)^{2/3} (1-\mu)^{1/3} \quad .$$

The integer k is called the order of the resonance. The value of $a_{k,q}$ corresponds to a distance (from the Sun) which defines the region of a particular MMR. If we define the *resonant* action-angle variables by:

$$\psi = k\lambda - (k+q)\lambda', \quad \Lambda = k\Psi \tag{203}$$

the Hamiltonian can be shown to take the form (assuming the inclination of Jupiter equal to zero, and averaging over short period terms):

$$\begin{aligned} H_{MMR} &= -\frac{(1-\mu)^2}{2k^2\Psi^2} - n'(k+q)\Psi \\ &- \mu \left[c_1(\Psi)\Gamma + c_2(\Psi) e' \Gamma^{1/2} \cos(\gamma) + c_3(\Psi) Z \right] \\ &- \mu \sum_{m_1,m_2,m_3} C_{m_1,m_2,m_3}(\Psi, \Gamma, Z; e') \cos(m_1\psi + m_2\gamma + m_3\zeta) \quad . \end{aligned} \tag{204}$$

Under this basic form, the Hamiltonian (204) has been used in many classical studies of e.g. the origin of the Kirkwood gaps or diffusion in the main asteroidal belt (e.g. Wisdom (1980), (1983), Murray and Holman (1997), Neishtadt (1987), Nesvorny et al. (2002)). From the Hamiltonian (204) we see immediately that the major semi-axis of the asteroid does not vary significantly, since $\dot{\Lambda} = k\dot{\Psi} = O(\mu)$. Thus, in simplified models we quite often substitute Ψ in the coefficients c_1, c_2, c_3 as well as in the disturbing function by the constant value $\Psi_{k,q} = (1/k)\sqrt{(1-\mu)a_{k,q}}$.

Under this latter form, the Hamiltonian (204) represents a case of the second fundamental resonance model (see footnote 7). In particular, denoting $c_1^* = c_1(\Psi_{k,q}), c_2^* = c_2(\Psi_{k,q})$, the term $c_1^*\Gamma$ can be thought of as representing a harmonic oscillator Hamiltonian. However, due to the presence of also a term $\sim \Gamma^{1/2}$, the 'equilibrium' position of this oscillator is shifted with respect to the value $\Gamma = 0$. This is seen most easily if we pass to the so-called 'Poincaré' (or cartesian) variables $X = \sqrt{2\Gamma}\cos\gamma$, $Y = \sqrt{2\Gamma}\sin\gamma$, in view of which the oscillator part of the Hamiltonian takes the form

$$H_\Gamma = -\mu \left[\frac{c_1^*}{2}(X^2 + Y^2) + \frac{c_2^* e'}{\sqrt{2}} X \right]$$

implying that the equilibrium point is at $X_0 = -c_2^* e'/(c_1^*\sqrt{2})$. This non-zero equilibrium position represents now a 'forced eccentricity', i.e. the orbit of the asteroid at the equilibrium position has a certain eccentricity induced essentially by the effect of Jupiter's eccentricity. The value of the forced eccentricity is $e_f \simeq |X_0|/((1-\mu)a_{k,q})^{1/4}$.

It is now possible to define book-keeping rules for a treatment of the Hamiltonian (204). The key point is that the analyticity properties of the Hamiltonian result in that the coefficients C_{m_1,m_2} exhibit exponential decay with respect to the modulus $|m| = |m_1| + |m_2| + |m_3|$. In fact, one can see that trigonometric terms of the form $\cos(m_1\psi + m_2\gamma + m_3\zeta)$ can only contain powers $\Gamma^{s/2}Z^{p/2}$ with $s \geq |m_2|$, $p \geq |m_3|$. Thus, in the former case we have powers of a small quantity proportional to the asteroid's eccentricity, while in the latter case we have powers of a small quantity proportional to the asteroid's inclination. In summary, a simple book keeping rule for the Hamiltonian (204) is:

Book-keeping rule for the MMR Hamiltonian: i) Introduce a factor λ^0 in the first two lines of Eq.(204). ii) introduce a book-keeping factor λ^{1+s+p} in front of any trigonometric term of the third line of Eq.(204) with a monomial coefficient $\Gamma^{s/2}Z^{p/2}$.

5.2. Hamiltonian models of axisymmetric galaxies (or other axisymmetric gravitating bodies)

The gravitational field generated by a number of different astronomical or astrophysical objects can be well approximated by an *axisymmetric* gravitational potential, i.e., a potential of the form $V \equiv V(r,z)$ in cylindrical coordinates (r,ϕ,z) (z =axis of symmetry). Examples of such bodies are: i) axisymmetric galaxies, and ii) oblate stars or planets. The orbits around such bodies can, to some extent, be described by common forms of canonical perturbation theory.

We will refer, in particular, to the case of the orbits of stars in an axisymmetric galaxy. The orbits in the equatorial plane are described by a Hamiltonian of the form

$$H_0 = \frac{p_r^2}{2} + \frac{p_\theta^2}{2r^2} + V_0(r) \tag{205}$$

where $V_0(r) = V(r, z=0)$, and $p_\theta = L_z = \text{const}$ is the component of the angular momentum along the axis of symmetry, which is a preserved quantity. Due to this, the Hamiltonian (205) can be considered as of one degree of freedom, with $p_\theta = L_z$ as a parameter. All the orbits are *rosettes* moving in an annulus between a pericentric and an apocentric radius (see Efthymiopoulos et al. (2008) for a review of the various types of orbits in axisymmetric galaxies). The quantity

$$V_{eff}(r; L_z^2) = L_z^2/2r^2 + V_0(r)$$

is called effective potential. For a fixed energy E, the pericenter and apocenter radii (r_p, r_a respectively) are defined by the two roots for r of $E = V_{eff}(r, L_z^2)$. These are joined at the radius r_c of the circular orbit which corresponds to the minimum of the effective potential, i.e. the root, for r_c of the equation

$$-\frac{L_z^2}{r_c^3} + \frac{dV_0(r_c)}{dr} = 0 \quad . \tag{206}$$

The radial period (= time it takes to go from pericenter to apocenter and back to pericenter) is given by $T_r(E, L_z^2) = 2\int_{r_p(E,L_z^2)}^{r_a(E,L_z^2)} [2(E - V_0(r)) - L_z^2/r^2]^{-1/2} dr$. The quantity $\kappa = 2\pi/T_r$ is called epicyclic frequency. For orbits not far from circular, κ is the frequency of (harmonic) radial oscillation close to the minimum of the effective potential at $r = r_c$. Then

$$\kappa = \sqrt{\frac{d^2 V_{eff}(r_c)}{dr_c^2}} = \sqrt{\frac{d^2 V_0(r_c)}{dr_c^2} + \frac{3}{r_c}\frac{dV_0(r_c)}{dr_c}} \quad . \tag{207}$$

On the other hand, the angular velocity of circular orbits is given by

$$\Omega(r_c) = \left(\frac{1}{r_c}\frac{dV_0(r_c)}{dr}\right)^{1/2} \quad . \tag{208}$$

The frequencies $\Omega(r_c)$ and $\kappa(r_c)$ are the basic frequencies of the so-called 'epicyclic theory' of orbits. In this theory, nearly circular orbits are described as the composition of two independent motions, namely a circular motion of the *guiding center*, with frequency $\Omega(r_c)$, and an oscillation in *both* the radial and angular directions, with frequency $\kappa(r_c)$.

If we now consider orbits off the equatorial plane, the Hamiltonian takes the form

$$H = \frac{p_z^2}{2} + \frac{p_r^2}{2} + \frac{L_z^2}{2r^2} + V(r, z) \quad . \tag{209}$$

A basic form of canonical perturbation theory arises from developing the Hamiltonian (209) around the coordinates $r = r_c$, $z = 0$ characterizing the circular orbit with given angular momentum L_z. We introduce the variables $q_1 = r - r_c$, $q_2 = z$, and notice that

$$-\frac{L_z^2}{r_c^3} + \frac{\partial V(r_c, 0)}{\partial r} = 0$$

(condition (206) of the circular orbit), and

$$\frac{\partial V(r_c, 0)}{\partial z} = 0$$

(condition of zero perpendicular force on stars whose orbits lie in the equatorial plane). The series expansion of (209) around $r = r_c$, $z = 0$ now yields (apart from a constant)

$$H = \frac{p_1^2}{2} + \frac{p_2^2}{2} + \frac{1}{2}\omega_1^2 q_1^2 + \frac{1}{2}\omega_2^2 q_2^2 + \sum_{s=3}^{\infty}\sum_{d=0}^{s} V_{s,d} q_1^d q_2^{s-d} \tag{210}$$

$$V_{s,d} = \frac{1}{(s-d)!d!}\frac{\partial^s}{\partial^{s-d} r \partial^d z}\left(\frac{L_z^2}{2r^2} + V(r, z)\right)\Bigg|_{r=r_c, z=0}$$

where $\omega_1 = \kappa$ as given by Eq.(207), and $\omega_2 = (\partial^2 V(r_c, 0)/\partial z^2)^{1/2}$. The Hamiltonian (210) is a *polynomial series* in the variables (q_1, q_2). In fact, the third

order truncation of the Hamiltonian (210) has a special place in the historical development of galactic dynamics, since it is the Hamiltonian function for which a 'third integral' (besides the energy and the angular momentum) was computed by Contopoulos (1960). Also, after a linear transformation this Hamiltonian reduces to the celebrated Hénon - Heiles model, on which the applicability of the 'third integral' was checked for the first time by numerical integrations (Hénon and Heiles, (1964)).

We can show now that the Hamiltonian (210), when transformed into action - angle variables, displays exponential decay of its associated Fourier coefficients. In order to introduce action - angle variables, we observe that the lowest order approximation of the Hamiltonian (210) corresponds to a 2D harmonic oscillator motions with frequencies ω_1 and ω_2. The harmonic oscillator action - angle variables are introduced via the canonical transformation

$$q_i = \sqrt{\frac{2I_i}{\omega_i}} \sin\phi_i, \quad p_i = \sqrt{2\omega_i I_i} \cos\phi_i, \quad , i = 1, 2 \tag{211}$$

in view of which the Hamiltonian (210) takes the form

$$\begin{aligned} H &= \omega_1 I_1 + \omega_2 I_2 \\ &+ \sum_{s=3}^{\infty} \sum_{d=0}^{s} V_{s,d} \left(\sqrt{\frac{2I_1}{\omega_1}} \frac{(e^{i\phi_1} - e^{-i\phi_1})}{2i} \right)^d \left(\sqrt{\frac{2I_2}{\omega_2}} \frac{(e^{i\phi_2} - e^{-i\phi_2})}{2i} \right)^{s-d} . \end{aligned} \tag{212}$$

Consider a Fourier term $e^{i(k_1\phi_1 + k_2\phi_2)}$. It is straightforward to see that in the sum of the r.h.s. of Eq.(212) such a term appears first at the order $s = |k_1| + |k_2|$, with coefficient $V_{|k_1|+|k_2|,|k_1|}(1/2^{3/2})^{|k_1|+|k_2|}\omega_1^{-|k_1|/2}\omega_2^{-|k_2|/2} I_1^{|k_1|/2} I_2^{|k_2|/2}$. Since higher order contributions are smaller in size, we may use the above expression as an estimate of the total size of the coefficient of the Fourier term $e^{i(k_1\phi_1 + k_2\phi_2)}$. For further simplification, we may consider the two frequencies ω_1, ω_2 of similar size and substitute them by their mean ω. Finally, we note that the original Hamiltonian expansion (210) is, in general, valid within a domain of convergence given by the inequalities $|q_i| < \rho_0$, $|p_i| < \rho_0$, $i = 1, 2$, for some constant $\rho_0 > 0$. Thus, there is a positive constant A such that

$$\sum_{s=3}^{\infty} \sum_{d=0}^{s} |V_{s,d}||q_1|^d |q_2|^{s-d} < A \sum_{s=3}^{\infty} \sum_{d=0}^{s} \frac{|q_1|^d |q_2|^{s-d}}{\rho_0^s} .$$

This implies that for the Fourier coefficient H_{k_1,k_2} of the term $e^{i(k_1\phi_1 + k_2\phi_2)}$ in the Hamiltonian (212) we have an upper bound estimate

$$|H_{k_1,k_2}| < G_{k_1,k_2}$$

with

$$G_{k_1,k_2} \sim A \left(\frac{1}{\rho_0 (8\omega)^{1/2}} \right)^{|k|} I_1^{|k_1|/2} I_2^{|k_2|/2}$$

where $|k| = |k_1| + |k_2|$. However, recalling that the action variables themselves represent oscillations with respect to an equilibrium point of the Hamiltonian

(212) (which corresponds to the equatorial circular orbit), the expansion in this Hamiltonian is valid for orbits whose action variables I_1 and I_2 remain always small enough so that the original canonical variables q_1,q_2,p_1,p_2 remain within the domain or convergence defined by ρ_0. This happens in a polydisc defined by two inequalities of the form $|I_i| < I_{0,i}$, $i = 1, 2$, where $I_{0,i}$ are positive constants. Thus, defining $I_0 = \min\{I_{0,1}, I_{0,2}\}$ we arrive at

$$G_{k_1,k_2} \sim A \left(\frac{I_0}{8\rho_0^2 \omega} \right)^{|k|/2}$$

or

$$|H_{k_1,k_2}| < A e^{-\sigma|k|} \quad \text{with} \quad \sigma \sim \frac{1}{2} \ln \left(\frac{8\rho_0^2 \omega}{I_0} \right) \quad . \tag{213}$$

Eq.(213) clearly shows that the exponential decay of the Fourier coefficients of the Hamiltonian (212) is steeper in *smaller* polydiscs in the action space, i.e. for smaller values of I_0. As a result, the most natural choice of book-keeping in the Hamiltonian (212) is in ascending powers of the action variables, namely:

$$\begin{aligned} H &= \omega_1 I_1 + \omega_2 I_2 \qquad (214) \\ &+ \sum_{s=3}^{\infty} \lambda^{s-2} \sum_{d=0}^{s} V_{s,d} \left(\sqrt{\frac{2I_1}{\omega_1}} \frac{(e^{i\phi_1} - e^{-i\phi_1})}{2i} \right)^d \left(\sqrt{\frac{2I_2}{\omega_2}} \frac{(e^{i\phi_2} - e^{-i\phi_2})}{2i} \right)^{s-d} . \end{aligned}$$

We note that the terms of degree $s/2$ in the actions (or s in the original 'Poincaré' variables (q, p)) acquire a book-keeping factor λ^{s-2}. The reduction of the exponent by two is done for algorithmic convenience, i.e., in this way the harmonic oscillator terms are of order 0 in λ, the cubic terms of order 1, etc. In fact, the same rule can be applied in more general polynomial Hamiltonian models appearing in various contexts besides galactic dynamics.

5.3. Hamiltonian models in barred-spiral galaxies

Consider a disc galaxy with a rotating 'pattern' figure, i.e. a set of spiral arms, or a bar, rotating with uniform angular speed Ω_p. In cylindrical coordinates (r, θ, z), the gravitational potential on the disc plane takes the form

$$V(r, \theta, z = 0) = V_0(r) + V_1(r, \theta) \tag{215}$$

where V_0 accounts for the gravitational effects of the axisymmetric disc component, and $V_1(r, \theta)$ for the gravitational effects of all non axisymmetric features in the disc (i.e. the spiral arms or the bar) of the galaxy. The reader is deferred to (Efthymiopoulos (2010)) for a tutorial presentation of how, starting from observations of a disc galaxy, the decomposition of the potential in components of the form (215) can be realized in practice.

It is convenient to express the component $V_1(r, \theta)$ in terms of its Fourier decomposition

$$V_1(r, \theta) = \sum_{m=-\infty}^{\infty} V_m(r) e^{im\theta} \quad . \tag{216}$$

One has $Im(V_m) = -Im(V_{-m})$ for V_1 to be a real-valued function of its (real-valued) arguments.

Let r_c be a fixed radius. We consider epicyclic motions around r_c as viewed in a rotating frame with angular speed Ω_p, when a non-axisymmetric 'pattern' rotates on the disc with the same speed. In the rotating frame, the pattern appears always at the same place. Thus, the time-dependence of the gravitational potential disappears at the cost of introducing centrifugal and Coriolis forces. The total Hamiltonian can be written as:

$$H(r,\theta,p_r,p_\theta) = \frac{p_r^2}{2} + \frac{p_\theta^2}{2r^2} - \Omega_p p_\theta + V_0(r) + \sum_{m=-\infty}^{\infty} V_m(r) e^{im\theta} \quad . \tag{217}$$

In (217), θ denotes the angular position of an orbit with respect to a fixed axis ($\theta_0 = 0$) in the *rotating frame*, i.e. the axis co-rotates with the pattern. However, p_θ is the angular momentum per unit mass along an orbit (with respect to the center) as measured in the *rest frame* (this, despite the fact that (217) describes motions in the rotating frame; p_θ defined as such preserves its canonical conjugate relation with θ).

We now define action-angle variables for the above Hamiltonian to describe local motions around r_c. The pair (θ, p_θ) in (217) is already an angle-action pair. As in subsection 3.4, a second pair (θ_r, J_r) can be defined for epicyclic oscillations via the canonical transformation $(r, p_r) \to (\theta_r, J_r)$ given by

$$r - r_c = \left(\frac{2J_r}{\kappa(r_c)}\right)^{1/2} \sin\theta_r, \qquad p_r = (2\kappa(r_c)J_r)^{1/2}\cos\theta_r \quad . \tag{218}$$

Setting $J_\theta = p_\theta - \Omega(r_c) r_c^2$, the variables (θ, J_θ) are still canonically conjugated.

Substituting the above expressions into Eq.(217), and Taylor-expanding with respect to r_c brings the Hamiltonian to the form (apart from a constant)

$$\begin{aligned} H(\theta_r,\theta,J_r,J_\theta) &= \kappa_c J_r + \frac{1}{2r_c^2} J_\theta^2 + (\Omega_c - \Omega_p) J_\theta \\ &+ \sum_{m=-\infty}^{\infty} \sum_{n=-\infty}^{\infty} F_{m,n}(J_r, J_\theta) e^{i(n\theta_r + m\theta)} \end{aligned} \tag{219}$$

where $\kappa_c \equiv \kappa(r_c)$, $\Omega_c \equiv \Omega(r_c)$. It is readily seen that the coefficients $F_{m,n}$ are of the form

$$F_{m,n}(J_r, J_\theta) = F_{0,m,n}(r_c; J_r) + F_{1,m,n}(r_c; J_r) J_\theta + F_{2,m,n}(r_c; J_r) J_\theta^2$$

where

$$F_{j,0,0} = 0, \quad j = 0, 1, 2$$

$$F_{0,0,n} = \sum_{k=0}^{\infty} \mathcal{B}_{nk} \left[\frac{d^{|n|+2k} V_0(r_c)}{dr_c^{|n|+2k}} + \frac{(-1)^{|n|+2k}(|n|+2k+1)!\Omega_c^2}{2r_c^{|n|+2k-2}} \right] \left(\frac{2J_r}{\kappa_c}\right)^{\frac{|n|}{2}+k}$$

$$F_{1,0,n} = \sum_{k=0}^{\infty} \mathcal{B}_{nk} \left[\frac{(-1)^{|n|+2k}(|n|+2k+1)!\Omega_c}{r_c^{|n|+2k}} \right] \left(\frac{2J_r}{\kappa_c}\right)^{\frac{|n|}{2}+k}, \qquad n \neq 0$$

$$F_{2,0,n} = \sum_{k=0}^{\infty} \mathcal{B}_{nk} \left[\frac{(-1)^{|n|+2k}(|n|+2k+1)!}{2r_c^{|n|+2k+2}} \right] \left(\frac{2J_r}{\kappa_c} \right)^{\frac{|n|}{2}+k}, \qquad n \neq 0$$

$$F_{1,m,n} = F_{2,m,n} = 0, \quad n \neq 0, \quad m \neq 0$$

$$F_{0,m,n} = \sum_{k=0}^{\infty} \mathcal{B}_{nk} \left[\frac{d^{|n|+2k} V_m(r_c)}{dr_c^{|n|+2k}} \right] \left(\frac{2J_r}{\kappa_c} \right)^{\frac{|n|}{2}+k}, \quad n \neq 0, \quad m \neq 0$$

and the coefficients $\mathcal{B}_{nk}$ are

$$\mathcal{B}_{nk} = \frac{(-1)^k}{(sgn(n)2i)^{|n|+2k} k!(|n|+k)!} \quad .$$

The key point to notice in Eq.(219) is that the basic frequencies κ_c and $\Omega_c - \Omega_p$ depend on the reference radius r_c in a continuous way. Thus, as r_c increases, infinitely many different resonant combinations $k_1\kappa_c + k_2(\Omega_c - \Omega_p) = 0$ are encountered.

In subsection 5.4 we will examine an example of implementation of resonant normal form theory in the Hamiltonian (219), in the case of the so-called *inner Lindblad resonance*, where $\Omega(r_c) - \Omega_p = \kappa(r_c)/2$. We will see that the theory is able to predict the form and orientation of a family of elliptic-like periodic orbits, whose superposition provides the basis of the so-called orbital *density wave theory* (Kalnajs (1971), Contopoulos (1975)).

Regarding the book-keeping rules for the Hamiltonian (219), following an analogous procedure as in subsection 5.2 it is straightforward to show that the coefficients of the Fourier development in the second line of Eq.(219) exhibit exponential decay with respect to the Fourier order $|k| = |n| + |m|$. It follows that the most natural choice of book keeping in (219) goes with powers of the action variables, i.e. we have the following book-keeping rule:

Book-keeping rule for the Hamiltonian 219: introduce a factor λ^{1+s+p} in front of any Fourier term in the second line of Eq.(219) with coefficient depending on the monomial $J_\theta^s J_r^{p/2}$.

The term $J_\theta^2/2r_c^2$, on the other hand, can be book-kept either as $O(\lambda^0)$ or as $O(\lambda^1)$, according to whether or not, depending on the application, we want its inclusion in the Hori kernel of the corresponding homological equation.

In a number of applications, and in particular in the investigation of the so-called 'edge-on' profiles of disc galaxies, we are interested also in examining motions perpendicularly to the disc. The 3D motion of stars is accounted for by the Hamiltonian:

$$H(r,\theta,z,p_r,p_\theta,p_z) = \frac{p_z^2}{2} + \frac{p_r^2}{2} + \frac{p_\theta^2}{2r^2} - \Omega_p p_\theta + V_0(r,z) + \sum_{m=-\infty}^{\infty} V_m(r,z) e^{im\theta} \quad . \tag{220}$$

We assume the potential to have an even symmetry above and below the disc plane and to be smooth at $z = 0$.

The starting point for the study of 3D orbits is the set of circular equatorial orbits under the axisymmetric potential $V_0(r,z)$. Let r_c be the radius of a circular orbit. Proceeding as in the 2D case, we Taylor-expand (220) around $r = r_c$, $z = 0$. Defining

$$\kappa_z(r_c) = \left(\frac{\partial^2 V_0(r_c, z=0)}{\partial z^2} \right)^{1/2} \tag{221}$$

as well as an action-angle pair of variables for vertical oscillations via

$$p_z = (2\kappa_z(r_c) J_z)^{1/2} \cos\theta_z, \quad z = \left(\frac{2J_z}{\kappa_z(r_c)} \right)^{1/2} \sin\theta_z, \tag{222}$$

the Hamiltonian (220) resumes the form

$$\begin{aligned} H(\theta_r, \theta, \theta_z, J_r, J_\theta, J_z) &= \kappa_c J_r + (\Omega_c - \Omega_p) J_\theta + \kappa_{zc} J_z + \frac{1}{2r_c^2} J_\theta^2 \\ &+ \sum_{|m|+|n|+|q|=0}^{\infty} F_{m,n,q}(J_r, J_\theta, J_z) e^{i(n\theta_r + m\theta + q\theta_z)} \end{aligned} \tag{223}$$

where $\kappa_{zc} \equiv \kappa_z(r_c)$.

Similarly to the 2D case, the coefficients $F_{m,n,q}$ are polynomial up to second degree in J_θ, while they are semi-polynomial, i.e. of half-integer powers $s/2$, $s'/2$ in J_r and J_z respectively. Expressions similar to Eq.(219) hold, while the book-keeping is implemented by the same rules as for the Hamiltonian (219).

5.4. An example: Resonant dynamics in the inner Lindblad resonance and the density wave theory of spiral arms

The stellar dynamics of disc galaxies is a classical topic of dynamical astronomy (see Contopoulos (2002) for a review). Here, we will discuss one particular aspect of this topic, namely the study of the motions of stars in the neighborhood of the so-called *inner Lindblad resonance*. This study is essential in understanding the form and structure of rotating spiral arms in normal disc galaxies, or of the inner parts of a rotating bar in barred galaxies.

In the previous subsection we presented the main features of the Hamiltonian formalism of the so-called epicyclic theory of motions in a disc galaxies. The epicyclic approximation is justified when the motions of stars in a disc galaxy are not very far from circular motions. If we assume that a galaxy contains a rotating figure, like a set of spiral arms, revolving with constant angular speed Ω_p, then we can define *disc resonances* by commensurability relations between the basic frequencies of the epicyclic theory. In a frame rotating with speed Ω_p, the disc resonances are defined by

$$\Omega - \Omega_p = \frac{n}{m} \kappa \quad , \tag{224}$$

where Ω and κ are the angular velocity of the circular orbit and the epicyclic frequency respectively, defined in subsection 3.6.

The following are the most important disc resonances: for $n = 1$, and $m = 2$ we have the *inner Lindblad resonance (ILR)*. For $n = -1$ and $m = 2$ we have the *outer Lindblad resonance* (OLR). Finally, for $n = 1$ and $m \to \infty$ we have *corotation*, otherwise defined by $\Omega = \Omega_p$. It is important to recall that: i) Ω and κ are functions of the radial distance r on the disc, thus, these resonances occur at particular distances from the center (plus or minus some 'width' Δr associated with resonance width, see subsection 3.3). ii) The location of all resonances depends on the pattern speed Ω_p. However, the pattern speed is one of the most difficult quantities to determine observationally. Thus, one may use information from resonant theory in order to proceed the other way around, i.e., *estimate the pattern speed* from other observable features of resonances. This is one of the central questions of research in galactic dynamics regarding disc galaxies.

In the basic formulation of resonant perturbation theory for disc galaxies (see e.g. Contopoulos (1975, 1978) and (2002, pp.436-460)) we start from a Hamiltonian of the form (219) and aim to transform it into a *resonant normal form* using a procedure of canonical transformations similar to those examined in subsection 2.9 and 3.3. The new Hamiltonian $Z(\theta'_r, \theta', I'_r, I'_\theta)$ contains only terms which are either independent of the angles, or depending on them through trigonometric terms with arguments of the form $k_1\theta_r + k_2\theta$ (or multiples), where (k_1, k_2) is a resonant wave-vector corresponding to the particular resonance under study. Under the form of the new Hamiltonian it is possible to explain the main features of the orbits in the associated resonant domain by analytical means.

In the case of the Inner Lindblad resonance, using resonant theory we can find the form and orientation of the basic *stable* periodic orbits existing in a large domain of the disc. In the case of spiral galaxies, we find that the main periodic orbits have a shape of *elongated ellipses* with a major axis changing orientation when considering orbits further and further away from the center. Then, the superposition of these orbits creates a *response density* which accounts for the observed spiral arms. This configuration, of 'precessing ellipses', conceived in the early works of Lindblad (1940, 1956, 1961), was given a concrete form by Kalnajs (1973), and serves as the basis of the orbital version of the so-called *density wave theory* (Lin and Shu (1964), see Bertin (2000) and Binney and Tremaine (2008)).

A numerical example of this mechanism is shown in Figure (17a). The details of this figure are explained in (Efthymiopoulos (2010)), and a brief summary is given below. Essentially, the figure shows the predictions of resonant normal form theory regarding the shape of the periodic orbits in a particular model (see Efthymiopoulos (2010)). We see that the orientation of the orbits changes in a way so as to support a density wave, i.e. a local enhancement of the density traveling within the disc (when viewed in a fixed frame). In fact, the stars go in and out of the wave as they move with much higher angular velocities than the pattern itself. However, as there are many stars distributed all along any of the periodic orbits of Fig.(17a), the pattern is maintained invariant in time, being at every snapshot composed by different stars.

The main question regards the so-called *self-consistency* of such a mechanism, namely whether the response density produced by the combination of

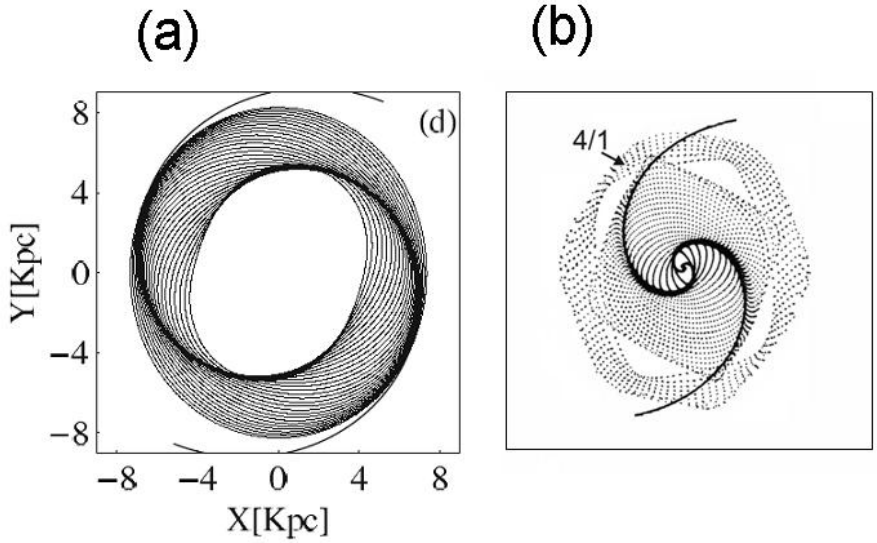

Figure 17. (a) Spiral density wave formed by periodic orbits beyond the Inner Lindblad Resonance in the model considered in Efthymiopoulos (2010). (b) Termination of spirals at the 4:1 resonance due to nonlinear effects which imply that the periodic orbits do not support the spiral arms beyond this resonance (after Contopoulos and Grosbol 1986).

'precessing ellipses' can match the imposed density upon which the calculation of periodic orbits was based. This question was examined in (Contopoulos (1985), Contopoulos and Grosbol (1986), and Patsis et al. (1991)). The main conclusion is that a self-consistent model of the above type can be maintained up to a distance a little before corotation, i.e. up to the 4/1 resonance, (see Fig.17b).

We now give the main features of the resonant normal form theory leading to a figure like Fig.17a. Our purpose will now be to compute a resonant normal form, and employ it in order to identify periodic orbits which are the *continuations of circular orbits* of the axisymmetric problem in the 2:1 resonant domain. We implement the following steps:

i) *Hamiltonian expansion.* We fix first a value of the radius r_c of a circular orbit of the axisymmetric problem near the ILR. The main features of the orbits are found by Taylor-expanding the Hamiltonian around r_c up to fourth degree in $r - r_c$, and by using the expressions (218). Then, starting from (219), the following Hamiltonian is arrived at:

$$\begin{aligned} H &= H_c + \omega_r J_r + \omega J_\theta + c_{20} J_r^2 + c_{11} J_r J_\theta \\ &+ c_{02} J_\theta^2 + c_{21} J_r^2 J_\theta + c_{22} J_r^2 J_\theta^2 + \ldots + H_{0F}(J_\theta; J_r, \theta_r) \\ &+ \left(d_{c1} J_r^{1/2} + d_{c3} J_r^{3/2} + \ldots \right) \cos(\theta_r - 2\theta) \\ &+ \left(d_{s1} J_r^{1/2} + d_{s3} J_r^{3/2} + \ldots \right) \sin(\theta_r - 2\theta) \\ &+ H_{1F}(J_r; \theta, \theta_r) \quad . \end{aligned} \tag{225}$$

The first two lines in (225) are produced by the 'unperturbed' part of the original Hamiltonian $p_r^2/2 + p_\theta^2/2r^2 - \Omega_p p_\theta + V_0(r)$. In fact, they come from the Taylor expansion of this part around r_c (see formulae after Eq.(219)). The function H_{0F} contains all terms from this Taylor expansion which depend on the epicyclic angle θ_r. The subscript 'F' stands for 'fast', since under the dynamics induced by this Hamiltonian term all angles rotate with a fast frequency.

An important remark is that the linear term $(r - r_c) \propto J_r^{1/2}$ appears in H_{0F} only as a combined product with J_θ or J_θ^2. This is because the linear term $[-\Omega_c^2 r_c + V_0'(r_c)](r - r_c)$ in the Taylor expansion is exactly equal to zero by the circular orbit condition. This implies that no 'low order', i.e. $O(J_r^{1/2})$, terms can appear in the first two lines of (225).

By contrast, such terms do appear in the next two lines which are produced by Taylor expanding the spiral potential, which is of the form $V_s = A_s(r)\cos(2\theta - \phi_2(r))$, around r_c. In particular

$$\begin{aligned} d_{c1} &= \frac{1}{(2\kappa_c)^{1/2}}[A_s'(r_c)\sin\phi_2(r_c) + A_s(r_c)\phi_2'(r_c)\cos\phi_2(r_c)] \qquad (226) \\ d_{s1} &= \frac{1}{(2\kappa_c)^{1/2}}[A_s'(r_c)\cos\phi_2(r_c) - A_s(r_c)\phi_2'(r_c)\sin\phi_2(r_c)] \end{aligned}$$

and we notice that the coefficients d_{c1} and d_{s1} are non-zero only if the non-axisymmetric perturbation is non-zero. We note here, in passing, that due to the form of Eq.(225), the dynamics in the inner Lindblad resonance represent a case of the 'second fundamental resonance model' (see footnote 7 and references therein).

Finally, similarly to H_{0F}, The function H_{1F} contains all terms due to the spiral perturbation which do not contain resonant ('slow') trigonometric arguments, but also some higher order resonant terms that are included in the normal form at higher normalization orders.

The presence of the $O(J_r^{1/2})e^{i(2\theta-\theta_r)}$ terms in the hamiltonian (225) produces an important physical effect, namely the fact that the periodic orbits arising as a continuation of the circular orbit in the perturbed case necessarily have a 'forced' ellipticity, caused by a forced epicyclic oscillation. As explained in Efthymiopoulos (2010), this phenomenon of 'forced ellipticity' (a term introduced first by Kalnajs (1973)) is analogous to the phenomenon of 'forced eccentricity' in motions at mean motion resonances in the restricted elliptic three body problem.

In the case of the Hamiltonian (225), a measure of the 'forced ellipticity' is the value of the epicyclic action J_r for periodic orbits in the resonant domain. This is found by an analogous procedure as above, namely by the subsequent steps:

ii) *Hamiltonian normalization.* By performing a canonical transformation (using e.g. the Lie method) we eliminate in the transformed Hamiltonian all terms included in H_{0F} and H_{1F} which are not in normal form. The new canonical variables are $O(A_0)$ deformations of the old ones, where A_0 is the amplitude of the spiral perturbation. Since A_0 is assumed small, we will refer to the new canonical variables using the same symbols as for the old ones. In numerical simulations, we often neglect the $O(A_0)$ corrections and replace numerical values

of the old variables as if they were the same with those of the new variables. With these simplifications, the resonant Hamiltonian takes the form (apart from a constant H_c)

$$\begin{aligned} H_{res} &= \omega_r J_r + \omega J_\theta + c_{20} J_r^2 + c_{11} J_r J_\theta + c_{02} J_\theta^2 + c_{21} J_r^2 J_\theta + c_{22} J_r^2 J_\theta^2 + \dots \\ &+ \left(d_{c1} J_r^{1/2} + d_{c3} J_r^{3/2} + \dots \right) \cos(\theta_r - 2\theta) \\ &+ \left(d_{s1} J_r^{1/2} + d_{s3} J_r^{3/2} + \dots \right) \sin(\theta_r - 2\theta) \quad . \end{aligned} \tag{227}$$

Since H_c was omitted, the numerical value of H_{res} for a circular orbit when the coefficients d_c, d_s are zero, i.e., the spiral perturbation is 'turned off', is equal to zero. We will look for periodic orbits in the full Hamiltonian (227) for the same value of the energy (Jacobi constant) i.e. $H_{res} = 0$. Introducing the resonant variables $\psi = \theta_r - 2\theta$, $J_F = J_\theta + 2J_r$ (the index F stands for 'fast'), the pairs (ψ, J_r), (θ, J_F) are canonical (it is useful to remember the correct ordering of variables in this canonical transformation, namely $(\theta_r, \theta, J_r, J) \to (\psi, \theta, J_r, J_F)$). The resonant Hamiltonian in new variables reads:

$$\begin{aligned} H_{res} &= (\omega_r - 2\omega) J_r + \omega J_F + (c_{20} - 2c_{11} + 4c_{02}) J_r^2 + (c_{11} - 4c_{02}) J_r J_F \\ &+ c_{02} J_F^2 - 2c_{21} J_r^3 + c_{21} J_r^2 J_F + 4c_{22} J_r^4 + c_{22} J_r^2 J_F^2 - 4c_{22} J_r^3 J_F \\ &+ \left(d_{c1} J_r^{1/2} + d_{c3} J_r^{3/2} \right) \cos\psi + \left(d_{s1} J_r^{1/2} + d_{s3} J_r^{3/2} \right) \sin\psi \quad . \end{aligned} \tag{228}$$

iii) *Position of the periodic orbits.* Setting the numerical value $H_{res} = 0$, and considering a constant value $J_F = \text{const}$, the Hamiltonian H_{res} can be considered as describing the evolution of the one degree of freedom system of the canonical pair (ψ, J_r). Periodic orbits correspond to the equilibria of this system, since then the motion takes place on the 'one-torus' ($\equiv$ periodic orbit) defined by $J_F = \text{const}$. The periodic orbits are then found by the roots for J_F, J_r, ψ of

$$H_{res} = 0, \quad \dot{\psi} = \frac{\partial H_{res}}{\partial J_r} = 0, \quad \dot{J}_r = -\frac{\partial H_{res}}{\partial \psi} = 0 \quad . \tag{229}$$

The following simplifications allow to analytically approximate the roots J_r^*, J_F^*, ψ^* of the system (229):

1) to estimate J_{F*} we use the lowest order terms of the first of equations (229). That is

$$(\omega_r - 2\omega) J_r^* + \omega J_F^* + J_r^{*1/2} \left(d_{c1} \cos\psi^* + d_{s1} \sin\psi^* \right) \simeq 0$$

or

$$J_F^* \simeq -\frac{1}{\omega} \left[(\omega_r - 2\omega) J_r^* + J_r^{*1/2} \left(d_{c1} \cos\psi^* + d_{s1} \sin\psi^* \right) \right] \quad . \tag{230}$$

2) We substitute the above expression into the second and third of equations (229) and solve simultaneously for J_r^*, ψ^*. It can be shown (Contopoulos (1975)) that, depending on the model and examined value of r_c, one or three roots (ψ^*, J_r^*) can be found. If one root can be found, this defines a periodic orbit called x_1 (this nomenclature follows from the Poincaré canonical coordinate $x_1^* =$

$\sqrt{2J_r^*}\cos\psi^*$ corresponding to the unique fixed point). In this case, varying r_c so as to cross the radius of one ILR changes the number of roots from one to three. The two new roots generated at such a transition are called $x_1(2)$ (stable) and $x_1(3)$ (unstable). We use a different nomenclature in cases where there are two ILRs and r_c is in the interval between them, in which case the new periodic orbits are called x_2 (stable) and x_3 (unstable). In either case, if we neglect the terms of order $O(J_r^{3/2})$ or higher in (228), the roots for ψ^* are defined by:

$$\tan\psi^* = \frac{d_{s1}}{d_{c1}} = \frac{A_s'(r_c)\cos\phi_2(r_c) - A_s(r_c)\phi_2'(r_c)\sin\phi_2(r_c)}{A_s'(r_c)\sin\phi_2(r_c) + A_s(r_c)\phi_2'(r_c)\cos\phi_2(r_c)} \tag{231}$$

where we recall that $\phi_2(r_c) = 2\ln(r_c/a)/\tan(i_0)$ in our model. Now, we have

$$\left|\frac{A_s(r_c)\phi_2'(r_c)}{A_s'(r_c)}\right| = \left|\frac{1}{\tan i_0(1-r_c\epsilon_s)}\right| >> 1$$

for i_0 equal to a few degrees, thus the second terms in both the numerator and denominator of the r.h.s. of (231) are more important than the first order terms. Thus $\sin[\psi^* + \phi_2(r_c)] \simeq 0$. The error in this relation is, again, $O(A_0)$. The final result is that $\psi^* \simeq -\phi_2(r_c)$ or $\psi^* \simeq -\phi_2(r_c)+\pi$, i.e., as r_c increases, the angle ψ^* 'precesses' by closely following the same law as the phase of spiral arms $\phi_2(r_c)$. It should be stressed that this is not a precession in time of one orbit, but a geometric shift of the apsides of *different* orbits belonging to the same family, which arise by implementation of the above theory for different values of the 'reference radii' r_c.

To accomplish the task of determining periodic orbits, Eq.(231) has two solutions, which differ by π. Substituting one of them into the third of Eqs.(229), and ignoring terms of order $O(J_r^2)$ or higher, we obtain a cubic equation for $\sqrt{J_r}$. In our case, this equation has three real roots if r_c is beyond the outermost ILR. For one of the angles ψ^*, the three roots are one positive and two negative, while, for the other, two roots are positive and one negative. In total, there are three positive roots for $\sqrt{J_r}$, yielding three distinct positive values J_r^* for which the resulting orbit is periodic. The key point is that we must always focus on the value of ψ^* for which the stable orbit generated after the outermost ILR is closest to the circular orbit of the axisymmetric case. For this orbit the epicyclic action J_r^* is an increasing function of the spiral amplitude A_0. For J_r^* we have the estimate $J_r^{*1/2} \sim A_0/(\omega_r - 2\omega)$. This scaling law quantifies the 'forced ellipticity'. In fact, the ellipticity of the periodic orbit is due to the fact that its non-zero value of the epicyclic action J_r^*, which enforces an in-and-out motion of the orbit from the circle $r = r_c$, is induced by the spiral amplitude A_0. Furthermore, as r_c increases, the difference $(\omega_r - 2\omega)$ also increases, thus the ellipticity of the periodic orbits decreases as we move away from the ILR. It should be stressed also that this simplified analysis breaks down also very close to the ILR, where the denominator of the previous scaling law tends to zero. However, it is possible to obtain the form of the periodic orbits by an alternative way, namely by computing a local *non-resonant* normal form, setting $J_{r*} = 0$ and $J_{\theta*}$ equal to the value of the angular momentum corresponding to the circular orbit in the axisymmetric case. Then, the form of the periodic orbits in the perturbed problem is found directly from the canonical transformation

connecting the action variables before and after the computation of the non-resonant normal form.

Figure 17a shows the combined effect of all previous phenomena, which will be called the 'precessing ellipses' mechanism of generation of spiral density waves. This figure shows a precise calculation of periodic orbits as described in the above steps for the model introduced in Efthymiopoulos (2010), and for the adopted parameter set in Fig. 4c of that reference. The theoretical periodic orbits are described by the equation (in polar coordinates) $r - r_c = (2J_r^*/\kappa_c)\sin(\psi^* + 2\theta)$, where ψ^* and J_r^* are calculated on a grid of values of r_c in the range $r_{ILR} < r_c \leq 1.6 r_{ILR}$. We see that the gradual variation of ψ^* essentially follows the phase of the imposed spirals. This fact causes a gradual re-orientation of the elliptical periodic orbits in a way so as to produce a 'response density' appearing enhanced exactly on the locus of the imposed spiral arms.

Regarding the termination of spiral arms supported by the above mechanism, the main effect is due to the presence of higher order terms in the expansions of the resonant Hamiltonian (227). Due to such terms, it turns that the shape of the so-resulting periodic orbits is no longer elliptic, but follows essentially the shape imposed by the kind of epicyclic resonance $n : 1$, where n increases as r_c approaches corotation. The most important nonlinear effect is produced close to the 4:1 resonance (Contopoulos and Grosbol (1986, 1988), Patsis et al (1991). A numerical calculation shows that the resulting periodic orbits should have a rectangular shape (Fig.17b). This fact prevents the response density from supporting the self-consistency of the spiral arms beyond the 4:1 resonance, and the conclusion from this type of approach is that main bisymmetric open spiral arms in normal galaxies should terminate at the 4:1 resonance (only weak extensions can survive up to corotation, see Patsis et al. (1991)).

6. SUMMARY

The present article deals with some topics of canonical perturbation theory, as well as with applications of the latter in problems of stability and (weakly) chaotic diffusion in systems appearing in the framework of dynamical astronomy. The focus is on giving concrete examples of implementation of various normal form techniques, stressing the practical and/or computational aspects, and providing (in most examples) sufficient detail in order to facilitate self-study. We summarize below, in form of a 'practical guideline list', the main methods, techniques, and applications of normal forms discussed in the present text.

1) In subsection 2.3 we introduced the main algebraic technique used throughout this tutorial for performing near-identity canonical transformations needed in normal form computation. This is the technique of *Lie series*, whose merits are explained in the same subsection.

In subsection 2.4 we discussed an algorithmic technique, called *book-keeping* which greatly facilitates the practical computation of normal forms and the development of computer-algebraic programs for this purpose. It was explained how the book-keeping process, which reflects an evaluation of the importance

of various terms in the original Hamiltonian to the dynamics, influences also purely algorithmic aspects of a normal form construction. It was discussed how to develop book-keeping schemes maximizing algorithmic convenience.

2) In subsections 2.4 to 2.7 we presented the main elements of a *Birkhoff normal form*, using , as an example, the theoretical computation of rotational tori in a perturbed pendulum model. We described (subsection 2.6) the practical aspects of this computation, which allows to find i) approximate integrals of motion, and ii) the form of the invariant tori (or invariant curves) in *open domains* of the action space. We stressed however (subsection 2.7) the asymptotic character of the Birkhoff series, implying that there is an optimal normalization order beyond which the method yields worse instead of better results. We then introduced the notion of the *remainder* of a normal form Hamiltonian, which gives a measure of the deviations of the true dynamics from the theoretical dynamics computed via a normal form.

3) In subsection 2.8 we presented the *Kolmogorov normal form*, making again reference to a concrete example. We demonstrated that, contrary to the Birkhoff normal form, the Kolmogorov normal form is convergent for sufficiently small values of the perturbation parameter. This convergence forms, in fact, the basis for proving Kolmogorov theorem for the existence of invariant tori in nearly-integrable Hamiltonian systems. We explained how this convergence arises by examining the effects of the accumulation of small divisors in this case. Finally, we emphasized that in practical computations the Kolmogorov normal form can be used in order to find a convergent series representation of the motion on *just one* invariant torus (for some fixed choice of frequencies), instead of an open domain, as in the case of the Birkhoff normal form. This limitation notwithstanding, the Kolmogorov normal form allows to recover the form of quasi-periodic solutions on a torus with an arbitrary accuracy, while Birkhoff's method cannot have an accuracy better than the size of the remainder at the optimal normalization order, which is finite.

4) In subsection 2.9 we examined the construction of a *resonant normal form*. This was used in order to obtain the local phase portraits in domains containing *islands of stability*. Also, the resonant normal form was used to estimate how the size of an island scales with ϵ.

5) In subsection 2.10 we introduced the *hyperbolic normal form* due to Moser (1958), using again a concrete example. It was shown that by this normal form it is possible to compute the position and a periodic series representation of an *unstable* periodic orbit, and also to compute (up to some extent) the stable and unstable invariant manifolds of the same orbit. We then discussed an extension of the method, allowing to compute the position of homoclinic points where the stable and unstable manifolds intersect each other. We finally explained why the method continues to be successful in the regime of strong chaos.

6) Section 3 deals with systems whose Hamiltonian contains infinitely many Fourier harmonics already at first order in the small parameter ϵ. In this case, it was explained how to perform book-keeping, by splitting the Fourier series of the

original Hamiltonian in groups of Fourier terms of different order of smallness. It was shown that such a splitting is naturally suggested by the consequences of the Fourier theorem on analytic functions, which implies that the Fourier coefficients decay exponentially with increasing Fourier order. Finally, we gave two concrete examples of how to implement book-keeping in this case, one for a resonant normal form, and one for the Kolmogorov normal form. As an application, in the former case we computed a critical value of ϵ at which a *resonance overlap* criterion is fulfilled for the system under study.

7) Section 4 presents the relation between resonant normal form theory in systems of three degrees of freedom and the phenomenon called Arnold diffusion. This includes a discussion of the role of convexity in the relevant phenomena, as well as some reference to the relation between the original model introduced by Arnold (1964) and the Hamiltonians found by resonant normal form theory. However, we also give a concrete example of visualization of Arnold diffusion using appropriate variables constructed via a resonant normal form.

8) Finally, in section 5 we provide some basic formulations of Hamiltonian functions in action-angle variables for three problems of central interest in dynamical astronomy. These are i) the restricted three body problem (with a particular application in the case of mean motion resonances in the solar system), ii) the Hamiltonian in axisymmetric non-rotating galaxies, and iii) the Hamiltonian in rotating barred-spiral galaxies. In all cases we give explicit formulae for the corresponding Hamiltonian functions, supplemented by a discussion of how to perform book-keeping in normal form computations in each case. The section closes with one example from resonant normal form theory in the inner Lindblad resonance in disc galaxies, which leads to the derivation of a theoretical model for the orbits supporting a 'density wave' form of spiral arms.

References

Aquilano, R.O., Muzzio, J.C., Navone, H.D., & Zorzi, A.F. 2007, Cel. Mech. Dyn. Astron. 99, 307

Arnold, V.I. 1963, Russ. Math. Surveys, 18, 9

Arnold, V.I. 1964, Sov. Math. Dokl., 6, 581

Arnold, V.I., & Avez, A. 1968, Ergodic Problems in Classical Mechanics, Benjamin, New York.

Arnold, V.I. 1978, Mathematical Methods of Classical Mechanics, Springer-Verlag, Berlin.

Arnold, V.I., Kozlov, V.V., & Neishtadt, A.I. 1993, Mathematical Aspects of Classical and Celestial Mechanics (2rd Edition), Springer, Berlin - Heidelberg.

Benest, D., Froeschlé, C., & Lega, E. 2008, Topics in Gravitational Dynamics, Lect. Notes Phys., 729, Springer.

Benest, D., Froeschlé, C., & Lega, E. 2010, Diffusion and Dissipation in Quasi-Integrable Systems. Theory and Application to Gravitational Systems, Eur. Phys. J. Spec. Topics, 186.

Benettin, G., Galgani, L., & Giorgilli, A. 1985, Cel. Mech., 37, 1.

Benettin, G., & Gallavotti, G. 1986, J. Stat. Phys., 44, 293.

Benettin, G. 1999, in A. Giorgilli (Ed.) Hamiltonian Dynamics. Theory and Applications, *Lect. Notes Math.* 1861, 1.

Bertin, G. 2000, Dynamics of Galaxies, Cambridge Univ. Press, Cambridge.

Binney, J., & Tremaine, S. 2008, Galactic Dynamics (2nd edition), Princeton University Press, New Jersey.

Boccaletti, D. & Pucacco, G. 1996, Theory of Orbits, Springer, Berlin.

Cachucho, F., Cincotta, P.M., & Ferraz-Mello, S. 2010, Cel. Mech. Dyn. Astron., 108, 35.

Celletti, A., Giorgilli, A., & Locatelli, U. 2000, Nonlinearity, 13, 397.

Cherry, T.M. 1924, Proc. Camb. Phil. Soc. 22, 510.

Chierchia, L. 2008, Reg. Cha. Dyn., 13, 130.

Chirikov, B.V. 1979, Phys. Rep., 52, 263.

Cincotta, P. 2002, New Astronomy Reviews, 46, 13.

Cincotta, P., Giordano, C., & Pérez, M.J. 2006, Astron. Astrophys. 455, 499.

Cincotta, P., & Giordano, C. 2012, in Cincotta, P., Giordano, C., & Efthymiopoulos, C. (eds), Proceedings of the Third La Plata School on Astronomy and Geophysics, AAA.

Contopoulos, G. 1960, Z. Astrophys., 49, 273.

Contopoulos, G. 1963, Astron. J., 68, 763.

Contopoulos, G., & Moutsoulas, M. 1965, Astron. J., 70, 817.

Contopoulos, G. 1966, Bull. Astron. CNRS, 2, 223.

Contopoulos, G, 1975, Astrophys. J, 201, 566.

Contopoulos, G, 1978, Astron. Astrophys., 64, 323.

Contopoulos, G., & Grosbol, P. 1986, Astron. Astrophys., 155, 11.

Contopoulos, G. & Grosbol, P. 1988, Astron. Astrophys., 197, 83.

Contopoulos, G. & Polymilis, H. 1993, Phys. Rev. E, 47, 1546.

Contopoulos, G. 2002, Order and Chaos in Dynamical Astronomy, Springer, Berlin.

Cordeiro, R.R., & Mendes de Souza, L.A. 2005, Astron. Astrophys. 439, 375.

Cordeiro, R.R. 2006, Astron. J., 132, 2114.

Da Silva Ritter, G.I., Ozorio de Almeida, A.M., & Douady, R. 1987, Physica D, 29, 181.

Delshams, A., & Gutiérrez, P. 1996, J. Diff. Eq., 128, 415.

Deprit, A., 1969, Cel. Mech., 1, 12.

Dumas, H.S., & Laskar, J. 1993, Phys. Rev. Lett., 70, 2975.

Efthymiopoulos, C., Contopoulos, G., & Voglis, N. 1998, in Benest, D., and Froeschlé, C. (Eds), Discrete Dynamical Systems, Gordon and Breach Science Publishers, pp.91-106.

Efthymiopoulos, C., Giorgilli, A., & Contopoulos, G. 2004, J. Phys. A Math. Gen., 37, 10831.

Efthymiopoulos, C. 2008, Cel. Mech. Dyn. Astron., 102, 49.

Efthymiopoulos, C., Voglis, N., & Kalapotharakos, C. 2008, in D. Benest, C. Froeschlé and E. Lega (eds), Topics in Gravitational Dynamics, Lect. Notes Phys., 729, Springer, Berlin, pp.297-389.

Efthymiopoulos, C. 2010, Eur. Phys. J. Spec. Topics, 186, 91.

Efthymiopoulos, C., & Harsoula, M. 2012, "The speed of Arnold diffusion", submitted.

Ferraz-Mello, S. 2007, Canonical Perturbation Theories. Degenerate Systems and Resonance, Springer (New York).

Froeschlé, C. 1970a, Astron. Astrophys. 4, 115.

Froeschlé, C. 1970b, Astron. Astrophys. 5, 177.

Froeschlé, C. 1972, Astron. Astrophys. 16, 172.

Froeschlé, C., & Scheidecker, J.P. 1973, Astron. Astrophys. 22, 431.

Froeschlé, C., Lega, E., & Gonczi, R. 1997, Cel. Mech. Dyn. Astron., 67, 41.

Froeschlé, C., Guzzo, M., & Lega, E. 2000, Science, 289, (5487), 2108.

Froeschlé, C., Guzzo, M., & Lega, E. 2005, Cel. Mech. Dyn. Astron., 92, 243.

Giordano, C.M., & Cincotta, P.M. 2004, Astron. Astrophys., 423, 745.

Giorgilli A., & Locatelli, U. 1997, ZAMP, 48, 220.

Giorgilli, A., & Locatelli, U. 1999, in C. Simó (ed.), Hamiltonian Systems with Three or More Degrees of Freedom, NATO ASI Series C, 533, Kluwer, Dordrecht, pp. 72 - 89.

Giorgilli, A 2001, Disc. Cont. Dyn. Sys., 7, 855.

Giorgilli, A 2002, Notes on exponential stability of Hamiltonian systems, in Dynamical Systems. Part I: Hamiltonian Systems and Celestial Mechanics, Pubblicazioni della Classe di Scienze, Scuola Normale Superiore, Pisa.

Giorgilli, A., Locatelli, U., & Sansoterra, M.: 2009, Cel. Mech. Dyn. Astron., 104, 159.

Gómez, G., & Barrabés, E. 2011, Scholarpedia 6(2), 10597.

Grobman, D.M. 1959, Dokl. Akad. Nauk SSSR, 128, 880.

Gustavson, F., 1966, Astron. Astrophys., 71, 670.

Guzzo, M., Lega, E., & Froeschlé, C. 2005, Discr. Con. Dyn. Sys. B, 5, 687.

Guzzo, M., Lega, E., & Froeschlé, C. 2006, Nonlinearity, 19, 1049.

Hartman, P. 1960, Proc. Amer. Math. Soc., 11, 610.

Hénon, M., & Heiles, C. 1964, Astron. Astrophys., 69, 73.

Hénon, M. 1966, Bulletin Astronomique 1, 3eme série.

Henrard, J., & Lemaitre, A. 1983, Cel.Mech., 30, 218.

Holman, M., & Murray, N. 1996, Astron. J. 112, 1278.

Hori, G.I. 1966, Publ. Astron. Soc. Japan, 18, 287.

Kalnajs, A. 1971, Astrophys. J., 166, 275.

Kalnajs, A. 1973, Proc. Astron. Soc. Australia, 2, 174.

Kaneko, K., & Konishi, T. 1989, Phys. Rev. A, 40, 6130.

Knežević, Z., Lemaitre, A., & Milani, A. 2002, in Bottke, W.F. et al. (eds), Asteroids III, University of Arizona Press, Tucson, pp. 603-612.

Knežević, Z., & Milani, A. 2005, Dynamics of Populations of Planetary Systems, Proceedings of the IAU Colloquium 197, Cambridge University Press.

Kolmogorov, A.N. 1954, Dokl. Akad. Nauk SSSR, 98, 527.

Laskar, J. 1993, Physica D, 67, 257.

Lazzaro, D., Ferraz-Mello, S., & Fernandez, J.A. 2006, Asteroids, Comets and Meteors, Proceedings of the IAU Symposium 229, Cambridge University Press.

Lega, E., Guzzo, M., & Froeschlé, C. 2003, Physica D, 182, 179.

Lega, E., Froeschlé, C., & Guzzo, M. 2008, Lect. Notes Phys., 729, 29.

Lega, E., Guzzo, M., & Froeschlé, C. 2009, Cel. Mech. Dyn. Astron., 104, 191.

Lega, E., Guzzo, M., & Froeschlé, C. 2010a, Cel. Mech. Dyn. Astron., 107, 129.

Lega, E., Guzzo, M., & Froeschlé, C. 2010b, Cel. Mech. Dyn. Astron., 107, 115.

Levison, H.F., Shoemaker, E.M., & Shoemaker, C.S. 1997, Nature 385, 42.

Lhotka, Ch., Efthymiopoulos, C., & Dvorak, R. 2008, Mon. Not. R. Astron. Soc., 384, 1165.

Lin, C.C., & Shu, F.H. 1964, Astrophys. J., 140, 646.

Lindblad, B. 1940, Astrophys. J., 92, 1.

Lindblad, B. 1956, Stockholm Obs. Ann., 19, 1.

Lindblad, B., Stockholm Obs. Ann. 1961, 21, 8.

Lochak, P. 1992, Russ. Math. Surv., 47, 57.

Lochak, P. 1999, in C. Simó (ed.), Hamiltonian Systems with Three or More Degrees of Freedom, NATO ASI Series C, 533, Kluwer, Dordrecht, 168.

Maffione, N.P., Darriba, L.A., Cincotta, P.M., & Giordano, C.M. 2011, Cel. Mech. Dyn. Astron. 111, 285.

Marzari, F., Tricarico, P., & Scholl, H. 2003, Mon. Not. Royal. Astron. Soc. 345, 1091.

Mather, J. 2004, J. Math. Sci., 124, 5275.

Mestre, M.F., Cincotta, P., & Giordano, C. 2012, in Cincotta, P., Giordano, C., & Efthymiopoulos, C. (eds), Proceedings of the Third La Plata School on Astronomy and Geophysics, AAA.

Mestre, M.F. 2012, Difusión caótica en sistemas Hamiltonianos casi-integrables, Ph.D Thesis, Universidad Nacional de La Plata.

Milani, A., & Knežević, Z. 1990, Cel. Mech. Dyn. Astron. 49, 347.

Milani, A., & Farinella, P. 1994, Nature 370, 40.

Morbidelli, A., & Guzzo, M. 1997, Cel. Mech. Dyn. Astron., 65, 107.

Morbidelli, A., & Giorgilli, A. 1997, Physica D, 102, 195.

Morbidelli, A., & Nesvorny, D 1999, Icarus 139, 295.

Morbidelli, A. 2002, Modern Celestial Mechanics. Aspects of Solar System Dynamics, Taylor and Francis, London.

Moser, J 1958,Commun. Pure Applied Math., 11, 1958.

Moser, J 1962, Nachr. Akad. Wiss. Göttingen, Math. Phys. Kl II, 1-20.

Murray, C.D., & Dermott, S.F. 1999, Solar System Dynamics, Cambridge University Press.

Murray, N., & Holman, M. 1997, Astron. J. 114, 1246.

Murray, N., Holman, M., & Potter, M. 1998, Astron. J. 116, 2583.

Muzzio, J.C., Carpintero, D.D., & Wachlin, F.C. 2005, Cel. Mech. Dyn. Astron. 91, 173.

Neishtadt, A.I. 1984, J. Appl. Math. Mech., 48, 133.

Nekhoroshev, N.N. 1977, Russ. Math. Surv., 32(6), 1.

Nesvorny, D., & Morbidelli, A. 1998, Astron. J. 116, 3029.

Nesvorny, D., Bottke, W.F., Dones, L. et al. 2002, Nature 417, 720.

Nesvorny, D., Bottke, W.F., Levison, H. et al. 2003, Astrophys. J. 591, 486.

Ozorio de Almeida, A.M. 1988, Hamiltonian Systems: Chaos and Quantization, Cambridge University Press.

Ozorio de Almeida, A.M., & Viera, W.M. 1997, Phys. Lett. A, 227, 298.

Patsis, P.A., Contopoulos, G., & Grosbol, P. 1991, Astron. Astrophys., 243, 373.

Perozzi, E., & Ferraz-Mello, S. 2010, Space Manifold Dynamics, Springer.

Pinsky, M. 2002, Introduction to Fourier Analysis and Wavelets, Grad. Studies Math., Am. Math. Soc.

Poincaré, H 1892, Méthodes Nouvelles de la Mécanique Céleste, Gautier-Vilard, Paris.

Pöshel, J. 1993, Math. Z., 213, 187.

Robutel, P., & Gabern, F. 2006, Mon. Not. Royal Astron. Soc. 372, 1463.

Romero-Gomez, M., Masdemont, J.J., Athanassoula, E.M., & Garcia-Gomez, C., 2006, Astron. Astrophys, 453, 39.

Romero-Gomez, M., Athanassoula, E.M., Masdemont, J.J., & Garcia-Gomez, C. 2007, Astron. Astrophys., 472, 63.

Rosenbluth, M., Sagdeev, R., Taylor, J., & Zaslavskii, M. 1966, Nucl. Fusion, 6, 217.

Sansottera, M., Locatelli, U., & Giorgilli, A. 2011, Cel. Mech. Dyn. Astron. 111, 337.

Siegel, C.L., & Moser, J. 1991, Lectures on Celestial Mechanics, Springer, Heidelberg, 1991.

Simó, C., & Valls, C. 2001, Nonlinearity, 14, 1707.

Skokos, C., Contopoulos, G., & Polymilis, C. 1997, Cel. Mech. Dyn. Astr., 65, 223.

Tennyson, J. 1982, Physica D, 5, 123.

Tsiganis, K., Varvoglis, H., & Dvorak, R. 2005, Cel. Mech. Dyn. Astron. 92, 71.

Tsiganis, K., knežević, Z., & Varvoglis, H. 2007, Icarus, 186, 484.

Tsiganis, K. 2008, Lect. Notes Phys. 729, 111.

Tsiganis, K. 2010, Eur. Phys. J. Special Topics 186, 67.

Tsoutsis, P., Efthymiopoulos, C., & Voglis, N. 2008, Mon. Not. R. Astr. Soc., 387, 1264.

Tsoutsis, P., Kalapotharakos, C., Efthymiopoulos, C., & Contopoulos, G. 2009, Astron. Astrophys., 495, 743.

Valluri, M., Debattista, V.P., Quinn, T.R., Roškar, R., & Wadsley, J. 2012, Mon. Not. Royal Astron. Soc. 419, 1951.

Vieira, W.M., and A.M. Ozoiro de Almeida 1996, Physica D, 90, 9.

Voglis, N., Tsoutsis, P., & Efthymiopoulos, C. 2006, Mon. Not. R. Astr. Soc., 373, 280.

Whittaker, E.T. 1916, Proc. Roy Soc. Edinburgh, Sect. A, 37, 95.

Wisdom, J. 1980, Astron. J. 85, 1122.

Wisdom, J. 1983, Icarus 56, 51.

Wood, B.P., Lichtenberg, A.J., & Lieberman, M.A. 1990, Phys. Rev. A, 42, 5885.

Appendix: Optimal normalization order

In Efthymiopoulos et al. (2004) a method was proposed on how to practically estimate the growth of the size of the remainder function in a Birkhoff normalization procedure with Lie generating functions. This method relies upon carefully examining the accumulation of small divisors in the series terms; see also classical "constructive" proofs of either the Kolmogorov or the Nekhoroshev theorems (e.g. Giorgilli 1999, and references therein for a review, or Giorgilli and Locatelli 1997) based on a similar approach. We now examine how the same method applies in the case of the normalization algorithm developed in subsection 2.2.

We start by defining first the sequence a_r of smallest divisors appearing at any normalization order r. This is given by:

$$a_r = \min\{|k \cdot \omega_*| : \ |k| < K'r, \ k \notin \mathcal{M}\} \tag{232}$$

where K' is given by Eq.(155) and $\mathcal{M}$ is the resonant module defined in Eq.(152). In view of the homological equation defined in Eq.(160, the generating function χ_r acquires a term with divisor $k \cdot \omega_*$ for any Fourier term $\exp(ik \cdot \phi)$ of $\tilde{H}_r^{(r-1)}$. Then the bound

$$||\chi_r|| \leq \frac{||\tilde{H}_r^{(r-1)}||}{a_r} \tag{233}$$

holds, where norms are defined as explained in subsection 4.2.

We now examine how a divisor a_r appearing first at the normalization order r propagates at subsequent orders. The propagation of divisors is due to Eq.(159), implying that the divisor a_r appears also in $H^{(r+1)}$, since

$$H^{(r+1)} = H^{(r)} + \{H^{(r)}, \chi_r\} + \frac{1}{2}\{\{H^{(r)}, \chi_r\}, \chi_r\} + \ldots \tag{234}$$

By repeating the two previous steps, we then find that a_r propagates at all subsequent orders after r. This, in turn, implies that $\tilde{H}_{r+1}^{(r+1)}$ contains divisors accumulated along all previous steps, i.e. by contributions from the generating functions χ_r, χ_{r-1},... via Poisson brackets like in Eq.(234). The same holds true for χ_{r+1} defined via the homological equation $\{\omega_* \cdot J, \chi_r\} + \tilde{H}_{r+1}^{(r+1)} = 0$. Define now the operators $\mathcal{G}_{j_{r,s}}^{(r)}$ acting on analytic functions f in the domains considered in subsection 2.1 via the recursive formulae

$$\begin{aligned} \mathcal{G}_{j_{r,s}}^{(r)} f &= \left(\prod_{q=1}^{r} \frac{1}{j_q!} \mathcal{L}_{\psi_q}^{j_q} \right) f, \quad j_{r,s} \equiv (j_1, j_2, \ldots, j_r) \text{ with } j_q \geq 0, \quad \sum_{q=1}^{r} j_q = s \\ \psi_q &= -\mathcal{L}_{\omega_* \cdot J}^{-1} < \mathcal{G}_{j_{q-1,s}}^{(q-1)} f >_q \end{aligned} \tag{235}$$

where $< \cdot >_q$ denotes the terms of order q in the book-keeping parameter of the included function belonging to the range of the operator $\mathcal{L}_{\omega_* \cdot J}$. The product in the first of Eqs.(235) is considered to be normally ordered, i.e. the operators

$\mathcal{L}_{j_q}$ are ordered from right to left for increasing q. The hamiltonian after r normalization steps is then given by

$$H^{(r)} = \exp \mathcal{L}_{\chi_r} \circ \exp \mathcal{L}_{\chi_{r-1}} \circ \ldots \exp \mathcal{L}_{\chi_1} H^{(0)} = \sum_{s=0}^{\infty} \sum_{\text{all possible } j_{r,s}} \mathcal{G}^{(r)}_{j_{r,s}} H^{(0)} \tag{236}$$

Let $\nu(w; j_{r,s})$ represent the number of times that an integer j_q in $j_{r,s}$ is equal to w. The key remark is that the asymptotic character of the normalization process is only due to sequences of terms generated by operators $\mathcal{G}^{(r)}_{j_{r,s}}$ for which $\nu(1; j_{r,s}) \neq 0$. In fact, it can be shown that for any fixed positive integer u, all sequences $b^{(r)}_u$, $r = 2, 3, ...$ of the form:

$$b^{(r)}_u = \sum_{\substack{\text{all possible } j_{r,r+u} \\ \text{with}_{\nu(w;j_{r,s})=0 \text{ if } w<2}}} ||\mathcal{G}^{(r)}_{j_{r,r+u}} H^{(0)}|| \tag{237}$$

are absolutely convergent in a sub-domain of the original domain of analyticity of f. The proof follows the same arguments as in subsection 3.4. Namely, one shows that the accumulation of divisors in sequences of the form (237) is at worst quadratic, and this suffices to establish an upper bound for the terms $b_{r,u}$ given by a geometric series. However, this is no longer guaranteed for operations in Eq.(236) involving $\mathcal{G}^{(r)}_{j_{r,s}}$ $\nu(1; j_{r,s}) \neq 0$, because among the latter there are cases leading to asymptotic rather than absolutely convergent sequences. In particular, the worst accumulation of divisors appears in the sequence:

$$d^{(r)} = ||\mathcal{G}^{(r)}_{j_1=j_2=\ldots=j_r=1} H^{(0)}|| \quad . \tag{238}$$

Similarly to what was observed in Efthymiopoulos et al. (2004), this particular sequence causes *repetitions* of small divisors that eventually lead to an asymptotic growth of the series coefficients. Starting from any Fourier term $h_{k,r_0} = c_k(J) \exp(ik \cdot \phi)$ in the Hamiltonian (156), this term is first encountered at the normalization order $r_0 = [|k|/K'] + 1$. The repetitions are found by considering the terms produced in the generating functions χ_{r_0}, χ_{r_0+1}, ... due to Poisson brackets with the $O(\lambda)$ normal form terms. If I_* is such that both resonant vectors satisfy the inequalities $|k^{(1)}| \geq K'$ and $|k^{(2)}| > K'$ (this excludes only some very low order resonances), the only $O(\lambda)$ normal form terms are given by $Z_1 = \epsilon^{1/2} \sum_{i,j=1}^{3} (1/2) M_{ij} J_i J_j$. Taking the successive normalization steps after the order r_0 we find the terms

In χ_{r_0}:
$\xi_{k,r_0} = \frac{h_{k,r_0}}{ik \cdot \omega_*}$ whereby $||\xi_{k,r_0}||_{\mathcal{W}_{I_*,B}} \leq \frac{||h_{k,r_0}||_{\mathcal{W}_{I_*,B}}}{a_{r_0}}$
In $H^{(r_0)}_{r_0+1}$:
$h_{k,r_0+1} \equiv \{Z_1, \xi_{k,r_0}\}$ whereby $||h_{k,r_0+1}||_{\mathcal{W}_{I_*,B}} \leq ||\xi_{k,r_0}||_{\mathcal{W}_{I_*,B}} \epsilon^{1/2} |M| B |k|$
$\leq \frac{||h_{k,r_0}||_{\mathcal{W}_{I_*,B}} K' \epsilon^{1/2} |M| B r_0}{a_{r_0}}$

In χ_{r_0+1}:
$\xi_{k,r_0+1} = \frac{h_{k,r_0+1}}{ik\cdot\omega_*}$ whereby $||\xi_{k,r_0+1}||_{\mathcal{W}_{I_*,B}} \leq \frac{||\xi_{k,r_0}||_{\mathcal{W}_{I_*,B}} K'\epsilon^{1/2}|M|Br_0}{a_{r_0}}$
etc., where $|M| = \max|M_{ij}|$. In general, the following inequalities are satisfied:

$$\frac{||\xi_{k,r_0+u}||_{\mathcal{W}_{I_*,B}}}{||\xi_{k,r_0+u-1}||_{\mathcal{W}_{I_*,B}}} \leq \frac{K'\epsilon^{1/2}|M|Br_0}{a_{r_0}}, \quad \frac{||h_{k,r_0+u}||_{\mathcal{W}_{I_*,B}}}{||h_{k,r_0+u-1}||_{\mathcal{W}_{I_*,B}}} \leq \frac{K'\epsilon^{1/2}|M|Br_0}{a_{r_0}}$$

whereby it follows that both sequences $||\xi_{k,r_0+u}||_{\mathcal{W}_{I_*,B}}$ and $||h_{k,r_0+u}||_{\mathcal{W}_{I_*,B}}$, $u = 1, 2, \ldots$ are bounded by a geometric series with ratio $K'\epsilon^{1/2}|M|Br_0/a_{r_0}$. That is, after being first encountered at order r_0, the same term h_{k,r_0} causes a sequence of repetitions of the same Fourier terms in all orders after r_0, the size of the term growing essentially by a geometric factor $\sim (K'\epsilon^{1/2}|M|Br_0/a_{r_0})^u$ at the order $r_0 + u$. Since, now, the original terms $h_{k,r}$ are of order $\sim Ae^{-\sigma|k|} \sim A\epsilon^{r_0/2}$, we finally arrive at an estimate for the size of the terms $d^{(r)}$ of the sequence (238), which itself represents an estimator of the size of the remainder $R^{(r)}$, namely:

$$||d^{(r)}||_{\mathcal{W}_{I_*,B}} \sim ||R^{(r)}||_{\mathcal{W}_{I_*,B}} \sim A\epsilon^{r/2} \sum_{r_0=2}^{r} \left(\frac{K'\epsilon^{1/2}|M|Br_0}{a_{r_0}} \right)^{r-r_0} . \qquad (239)$$

Eq.(239) implies an asymptotic growth of the size of $||R^{(r)}||_{\mathcal{W}_{I_*,B}}$ with r, since, e.g. close to the median of the summation values of r_0, i.e. $r_0 \simeq r/2$, one has terms of size $\sim (\epsilon^{1/2}Br/(2a_{r/2}))^{r/2} \sim [(\epsilon^{1/2}Be/(2a_{r/2}))^r r!]^{1/2}$, which grow at least as fast as $(B\epsilon^{1/2})^r r!$. The exact growth rate depends on whether $\mathcal{W}_{I_*,B}$ is a doubly, simply, or non-resonant domain with respect to a high enough K-truncation, since one has, $a_r = \min|\omega_*|_i$ in doubly-resonant domains, while $a_r \sim \gamma/r^\tau$ with γ a positive constant $\gamma = O(\min|\omega_*|_i)$, and $\tau = 1$ for simple resonance or $\tau = 2$ for non-resonance (in three degrees of freedom, assuming diophantine behavior of the frequencies). Accordingly, we arrive at the remainder estimate $||R^{(r)}||_{\mathcal{W}_{I_*,B}} \sim (B\epsilon^{1/2})^r r!^{1+\tau}$, whence, using standard approximations (e.g. Stirling's formula), we finally find

$$\begin{aligned}
&\text{Double resonance:} && r_{opt} \sim \frac{1}{\epsilon^{1/2}}, && ||R^{(r_{opt})}|| \sim \exp\left((\epsilon_0/\epsilon)^{-1/2}\right) \\
&\text{Simple resonance:} && r_{opt} \sim \frac{1}{\epsilon^{1/4}}, && ||R^{(r_{opt})}|| \sim \exp\left((\epsilon_0/\epsilon)^{-1/4}\right) \\
&\text{Non-resonance:} && r_{opt} \sim \frac{1}{\epsilon^{1/6}}, && ||R^{(r_{opt})}|| \sim \exp\left((\epsilon_0/\epsilon)^{-1/6}\right)
\end{aligned} \qquad (240)$$

that is, we recover Eq.(163), and its associated exponential estimates for the size of the remainder, with exponent a as indicated in Eq.(240).